


MA3D1 – Fluid Dynamics and
MA4L0 – Advanced Topics in Fluids
Lecture notes

Shreyas Mandre

`shreyas.mandre@warwick.ac.uk`

©2020 Shreyas Mandre

CC-BY-NC-ND 

with contribution from

Thomasina Ball

(Chapter 9: Stokes Flow,

Chapter 10: Lubrication theory,

Chapter 11: Complex Fluids and Non-Newtonian Rheology and

Chapter 12: Hydrodynamic Instability)

Last updated: Mon Apr 8 17:16:44 BST 2024

Contents

1 Preliminaries	9
1.1 Newtonian mechanics	9
1.2 Units and dimensions	10
1.3 Cartesian tensors	11
1.4 Tensor Calculus	12
2 Mathematical Modelling of Fluid Flow	15
2.1 Definition of a fluid	15
2.2 Fluids in Continuum Mechanics	16
2.3 Material properties of fluids	16
2.4 Lagrangian and Eulerian Descriptions	17
2.4.1 Lagrangian description	17
2.4.2 Eulerian description	18
2.4.3 Eulerian versus Lagrangian descriptions	18
2.4.4 The Material Derivative and Acceleration	19
2.4.5 Reynolds transport theorem	20
2.5 Flow Visualisation	20
2.6 Deformation of infinitesimal fluid elements	23
2.7 Conservation Laws in Continuum Mechanics	27
2.7.1 The dimensional inconsistency of the surface source term	28
2.7.2 Cauchy's tetrahedron argument	29
2.8 Conservation of Mass a.k.a. Mass Balance	30
2.9 Conservation of Momentum a.k.a. Momentum Balance	31
2.10 Conservation of Angular Momentum a.k.a. Torque Balance	32
2.11 Constitutive laws	32
2.11.1 General considerations	33
2.11.2 An Ideal or Inviscid fluid	33
2.11.3 A Newtonian Fluid	34
2.11.4 Navier-Stokes in cylindrical coordinates	34
2.12 Boundary and initial conditions	35
2.12.1 Initial conditions	35

2.12.2	Boundary conditions	35
3	One-dimensional flows	37
3.1	Steady flows	37
3.1.1	One-dimensionality	37
3.1.2	The driving force	38
3.2	Select solutions of Navier-Stokes	38
3.2.1	Plane Poiseuille flow	38
3.2.2	Hagen-Poiseuille	39
3.3	Unsteady flows	40
3.3.1	Stokes first problem	40
4	Dimensional Analysis	43
4.1	Reducing parameters in a set of equations	43
4.2	Deducing dependence on parameters	44
5	Hydrostatics and Bernoulli equation	47
5.1	Hydrostatics	47
5.1.1	Archimedes principle	47
5.2	Bernoulli equation	47
5.2.1	Steady incompressible inviscid flow	48
5.2.2	Unsteady incompressible potential flow	48
5.3	Applications and examples	48
5.3.1	Flow through an opening in a tank	49
5.3.2	A wind turbine	49
5.3.3	A water wave	53
6	Potential flow	55
6.1	Conditions for and implications of potential flow	55
6.2	Incompressible and irrotational flow in two-dimensions	55
6.2.1	Stream function and streamlines	56
6.2.2	Stream function and velocity potential	56
6.3	Elementary complex potentials	56
6.3.1	Uniform flow	57
6.3.2	Point source	57
6.3.3	Point vortex	58
6.3.4	Point dipole	59
6.3.5	Higher multipoles	59
6.4	Potential flow past immersed bodies	59
6.4.1	Rankine half-body	59

6.4.2	Rankine oval	59
6.4.3	Circle	60
6.5	Force on a immersed body	61
6.5.1	Force in a steady potential flow	61
6.5.2	Added mass from the unsteady term	63
6.6	Flow around an airfoil	63
7	Boundary layers	67
7.1	Flow next to a flat plate	67
7.1.1	Qualitative description of the flow	67
7.1.2	Derivation of the Prandtl boundary layer equations	69
7.1.3	Self-similar flow past a semi-infinite flat plate	71
7.1.4	Drag on the plate	74
8	Acoustics and Incompressibility	75
8.1	Acoustic limit of Navier-Stokes equations	75
8.1.1	The Acoustic limit	76
8.2	Incompressible approximation	77
8.2.1	Variations in density due to pressure	77
8.2.2	The finite propagation-speed of sound	78
9	Stokes Flow	79
9.1	Recap: Governing Equations	79
9.1.1	Navier-Stokes Equations	79
9.1.2	Reynolds number	79
9.1.3	Energy and Dissipation	80
9.1.4	Additional comments	81
9.2	Properties of Stokes Flows	81
9.3	Stokes Flow Solutions	84
9.3.1	Representation as Harmonic Functions	84
9.3.2	Papkovich-Neuber Solutions	85
9.3.3	Spherical Harmonic Solutions	85
9.3.4	Tensors and Pseudotensors	86
9.3.5	Point Force and Source Flow	86
9.3.6	Motion of a rigid particle	88
9.3.7	Translating Rigid Sphere	88
10	Lubrication Theory	91
10.1	Lubrication approximation for flow in a thin layer	91
10.2	Squeeze flow	92

10.2.1	Thrust bearing	92
10.2.2	Cylinder approaching a wall	94
10.3	Free surface flow	95
10.3.1	Surface Tension	95
10.3.2	Bond number	97
10.3.3	Capillary number	97
10.3.4	Capillary drop	97
10.3.5	Gravitational spreading	98
10.3.6	Gravitational spreading down an inclined plane	102
11	Complex Fluids and Non-Newtonian Rheology	105
11.1	Constitutive laws	105
11.1.1	Newtonian fluid	105
11.1.2	Generalised Newtonian fluid	106
11.2	Poiseuille flow	107
11.3	Taylor-Couette flow	108
11.4	Viscoelastic fluids	110
11.4.1	Maxwell fluid	110
11.4.2	Oldroyd B fluid	111
11.4.3	Shear flow	112
11.4.4	Extensional flow	113
11.4.5	Weakly non-linear viscoelastic fluids	114
11.4.6	Rod climbing for a second-order fluid	115
11.4.7	Words of caution	115
12	Hydrodynamic Instability	117
12.1	The Kelvin-Helmholtz Instability	117
12.2	The Rayleigh-Plateau Instability	119
12.3	The Rayleigh Instability	121
13	Linear waves and instabilities	125
13.1	Interfacial waves and instabilities	125
13.1.1	The governing equations	125
13.1.2	Steady state and linearization	126
13.1.3	Fourier transform	127
13.1.4	Solution to Laplace equation	129
13.2	Waves and instabilities	129
13.2.1	Deep water gravity waves	129
13.2.2	Capillary and gravity-capillary waves	131
13.2.3	Rayleigh-Taylor instability	132

13.2.4 Kelvin-Helmholtz instability 134

Chapter 1

Preliminaries

The theory of fluid dynamics rests on the developments in some greater disciplines such as mathematics and physics, especially mechanics. In this chapter, let us summarize and revise some of these topics.

1.1 Newtonian mechanics

While it is not possible to do justice to Newtonian mechanics here, we present the basic tenets.¹ Newtonian mechanics, at its core, describes physical laws governing the motion of point material particles. Consider a point material object of mass m moving through empty space. Let us say that the objects location is given by $\mathbf{x}(t)$ as a function of time t . The velocity of the body is $\mathbf{v}(t) = d\mathbf{x}/dt$. The three laws of motion according to Newtonian mechanics are:

1. **First law:** In an inertial reference frame, every body continues in its state of rest or uniform motion until and unless acted upon by an external unbalanced force. Essentially, this law defines the notion of an inertial reference frame, i.e. one in which a free body moves uniformly.
2. **Second law:** When an external unbalanced force, \mathbf{F} , acts on a body it must equal the rate of change of momentum of this body. The momentum (also known as the linear momentum) of this point mass is defined as $\mathbf{p} = m\mathbf{v}$. Therefore, the mathematical statement of the second law is:

$$\mathbf{F} = \frac{d\mathbf{p}}{dt}. \quad (1.1)$$

Noting that the acceleration of the particle, $\mathbf{a} = d\mathbf{v}/dt$, if the mass of the body does not change with time, then this law is also written as $\mathbf{F} = m\mathbf{a}$. This law describes the motion of the particle.

3. **Third law:** Every action has an equal and opposite reaction. In other words, if a body A exerts a force \mathbf{F} on a body B , then the body B must exert a force of $-\mathbf{F}$ on body A . This law describes the interaction between particles.

As a consequence of Newton's laws of motion for point particles, it is possible to derive the following "conservation laws" of momentum and angular momentum for extended deformable bodies. A common terminology used in physics is the moment of a quantity, which is obtained by making a cross product of the position vector \mathbf{x} of a point particle with that quantity. Suppose that an extended material object at time t occupies a region of space given by Ω . Then its total momentum is obtained by breaking it up into infinitesimal pieces of mass dm , determining the momentum of these individual pieces, and summing the momentum. Mathematically, this amounts to integrating as

$$\mathbf{p} = \int_{\Omega} dm \mathbf{v}(\mathbf{x}, t), \quad (1.2)$$

where \mathbf{v} is the velocity of the piece at position $\mathbf{x} \in \Omega$. The total mass m of the body is simply $m = \int_{\Omega} dm$. The moment of momentum, also known as the angular momentum \mathbf{l} , is then

$$\mathbf{l} = \int_{\Omega} dm \mathbf{x} \times \mathbf{v}. \quad (1.3)$$

¹For more detailed treatments, refer to a book on undergraduate mechanics, e.g., Halliday and Resnick, Physics - I, or, if you prefer the economy of Soviet authors, I. E. Irodov, Fundamental Laws of Mechanics.

These conservation laws invoke the “centre of mass” \mathbf{x}_c of this object, defined as

$$\mathbf{x}_c = \frac{\int_{\Omega} dm \mathbf{x}}{\int_{\Omega} dm} = \frac{1}{m} \int_{\Omega} dm \mathbf{x}. \quad (1.4)$$

Suppose that the external forces \mathbf{F}_i , $i = 1, 2, \dots, n$ act on this object at locations \mathbf{x}_i . The net torque $\boldsymbol{\tau}$ on this body is the moment of the external forces,

$$\boldsymbol{\tau} = \sum_{i=1}^n \mathbf{x}_i \times \mathbf{F}_i. \quad (1.5)$$

So long as the object does not exchange material with anything outside it, the laws of conservation state that:

1. **Conservation of (linear) momentum:** The rate of change of total momentum must equal the total external unbalanced force on the object, i.e.

$$\frac{d\mathbf{p}}{dt} = \sum_{i=1}^n \mathbf{F}_i. \quad (1.6)$$

Noting the relation between \mathbf{p} and \mathbf{x}_c , this law is also stated as

$$m \frac{d^2 \mathbf{x}_c}{dt^2} = \sum_{i=1}^n \mathbf{F}_i, \quad (1.7)$$

which means that the mass times the acceleration of the centre of mass must equal the external unbalanced force.

2. **Conservation of angular momentum:** The rate of change of angular momentum must equal the net torque on the body. Mathematically,

$$\frac{d\mathbf{l}}{dt} = \boldsymbol{\tau}. \quad (1.8)$$

While the momentum and angular momentum are not constants of motion, here the term “conservation law” is used in the sense that it is possible to keep an account of these quantities in relation to their respective sources.

1.2 Units and dimensions

Units are used to describe the values of physical quantities. For example, Dr. Shreyas Mandre is 170 cm tall, weigh 10 stones and consume about 100 Watts when resting. The choice of the unit is arbitrary, as reflected in the plethora of units available for the same quantity, e.g. 170 cm \approx 68 inches \approx 1.8×10^{-16} light-years. The SI system is popular for the purpose of standardization (and that purpose alone).

The fundamental nature of a quantity attributes it with a unique dimension. Example of dimensions are length L , mass M , time T , force F , etc. Many different units are associated with each dimension, as described above. The basic rules for analysis based on dimensions are as follows. The dimension of product of physical quantities is the product of the dimensions of the individual multiplicands. It is an error to add quantities of different dimensions, i.e. lengths may be added with lengths but not mass. For an equation in physics to be dimensionally consistent, the dimensions on both sides of the equation must be identical.

Dimensions of quantities are not necessarily independent of each other. For example, the dimensions of volume L^3 depend on the dimensions of length. This dependence is best expressed in systems of dimensions. In the MLT system, the dimensions M , L and T are considered basic, from which all other dimensions are derived, e.g. $F = ML/T^2$. There is some arbitrariness in constructing systems of dimensions, for example, equally valid is the FLT system where $M = FT^2/L$ is a derived dimension.

Exercise: Construct a ρVL system, where ρ is the dimension of density and V of velocity. Express the dimensions of mass and time in terms of ρ , V and L .

Exercise: What are the dimensions of p , μ and ν ?

This arbitrariness in the nature of physical quantities underlies some of the most powerful theoretical tools in physics. It was on the basis of such considerations that Sir G. I. Taylor estimated the yield of the atomic bomb, a heavily guarded American secret at the time, from publicly available images. Ignore dimensions at your own peril!

1.3 Cartesian tensors

Vectors and tensors offer a compact representation to tackle the large number of variables whilst accounting for the relationship between them. Vectors are quantities that, in the colloquial sense, have a magnitude and a direction. Mathematically, vectors are elements of \mathbb{R}^3 , where the components commonly represent Cartesian components. Tensors are generalization of vectors which have more than three components in 3-dimensions. An n^{th} rank tensor has 3^n components in 3 dimensions. In this way, a vector is a first-rank tensor. Examples of second rank tensors include moment of inertia of a solid body. Here the nine Cartesian components of the moment-of-inertia tensor are

$$\begin{aligned} I_{xx} &= \int_V x^2 dm, & I_{yy} &= \int_V y^2 dm, & I_{zz} &= \int_V z^2 dm, \\ I_{yx} = I_{xy} &= \int_V xy dm, & I_{zy} = I_{yz} &= \int_V yz dm, & I_{zx} = I_{xz} &= \int_V xz dm, \end{aligned}$$

where dm represents an infinitesimal mass element spanning the extent of the body V .

Tensors of rank zero are scalars.

Two different notations are available to represent vector and tensor expressions, they are called the vector notation and the index notation. Depending on the circumstance, one notation may be preferred to the other either for clarity or compactness.

We will use boldface symbols to represent vectors and tensors in vector notation. In this notation, it is crucial to declare the rank of the tensor a symbol represents, e.g., let \mathbf{u} represent first-rank velocity tensor, and let \mathbf{T} represent the second rank stress tensor. The operations on these symbols are understood as a matter of convention, e.g., $\mathbf{a} + \mathbf{b}$ is the sum of two tensors \mathbf{a} and \mathbf{b} of equal rank. Vector notation is not equipped to unambiguously represent dot products and cross products, but it is denoted as $\mathbf{a} \cdot \mathbf{b}$ and $\mathbf{a} \times \mathbf{b}$, respectively, when no ambiguity exists. Examples will be abundant in the rest of the notes. The advantage of this notation is that it treats tensors in their abstraction without reference to any specific coordinate system.

The index notation explicitly invokes (for this module Cartesian) coordinate system. The Cartesian coordinates are themselves written as $x_1 = x$, $x_2 = y$ and $x_3 = z$. Let $\hat{\mathbf{e}}_1$, $\hat{\mathbf{e}}_2$ and $\hat{\mathbf{e}}_3$ be the unit vectors along x_1 , x_2 and x_3 coordinates, respectively. Then the components u_1 , u_2 and u_3 of the tensor a first rank tensor (i.e., a vector) \mathbf{u} are written as u_i , where the index i ranges from 1 to 3. The components of a second rank tensor are represented using two indices, e.g., the components of the moment-of-inertia tensor are represented as I_{ij} , where

$$I_{ij} = \int_V x_i x_j dm, \quad \text{and } i \text{ and } j \text{ both independently range from 1 to 3.}$$

It is customary to omit the range of the indices in this notation. In general, n^{th} rank tensors have n indices.

The summation convention: Expressions, such as the dot product between two vectors are written as a sum in index notation, e.g.

$$\mathbf{a} \cdot \mathbf{b} = a_1 b_1 + a_2 b_2 + a_3 b_3 = \sum_{i=1}^3 a_i b_i. \quad (1.9)$$

As a matter of convention due to Einstein, it is customary to also omit the summation sign over an index which appears twice in any product. Hence, $\mathbf{a} \cdot \mathbf{b} = a_i b_i$, with an implied sum over i from 1 to 3. When a sum on an index appearing twice is not implied, this must be stated explicitly. Similarly, whether a sum is implied on an index that repeats more than two times must be explicitly stated.

Two special tensors: Let us introduce two special and basic tensors. The first is called the Kronecker delta, defined as

$$\delta_{ij} = \begin{cases} 0 & \text{for } i \neq j \\ 1 & \text{for } i = j \end{cases}. \quad (1.10)$$

The second is the third-rank alternating tensor, also known as the Levi-Civita, which is defined as

$$\epsilon_{ijk} = \begin{cases} 0 & \text{if } i = j, j = k \text{ or } i = k, \\ 1 & \text{for } (i, j, k) = (1, 2, 3), (2, 3, 1) \text{ or } (3, 1, 2), \\ -1 & \text{for } (i, j, k) = (1, 3, 2), (2, 1, 3) \text{ or } (3, 2, 1). \end{cases} \quad (1.11)$$

Tensor algebra: Using these rules, the notation for tensor algebra is as follows. Here w is a scalar, \mathbf{a} , \mathbf{b} and \mathbf{c} are vectors, \mathbf{T} , \mathbf{S} , \mathbf{A} and \mathbf{B} are second rank tensors.

	Vector notation	Index notation	Tensorial rank
Sum of vectors:	$\mathbf{c} = \mathbf{a} + \mathbf{b}$	$c_i = a_i + b_i$	1
Dot product of vectors:	$w = \mathbf{a} \cdot \mathbf{b}$	$w = a_i b_i$	0
Dot product of tensors:	$\mathbf{T} = \mathbf{A} \cdot \mathbf{B}$	$T_{ij} = A_{ik} B_{kj}$	2
Outer product of vectors	$\mathbf{A} = \mathbf{a}\mathbf{b}$	$A_{ij} = a_i b_j$	2
Outer product of tensors:	$\mathbf{A}\mathbf{B}$	$A_{ij} B_{km}$	4
Contraction:	$\text{tr}(\mathbf{A})$	A_{ii}	0
Scalar triple product:	$\mathbf{a} \cdot (\mathbf{b} \times \mathbf{c})$	$\epsilon_{ijk} a_i b_j c_k$	0
Vector triple product:	$\mathbf{a} \times (\mathbf{b} \times \mathbf{c})$	$\epsilon_{ijk} \epsilon_{kmn} a_j b_m c_n$	1

A combination of the above operations is a contraction between two second rank tensors denoted by $\mathbf{A} : \mathbf{B}$ defined as $A_{ik} B_{ki}$. Note that $\mathbf{A} : \mathbf{B} = \text{tr}(\mathbf{A} \cdot \mathbf{B})$.

A symmetric second-rank tensor is one that satisfies $S_{ij} = S_{ji}$ for all combinations of i and j . An anti-symmetric one is that satisfies $A_{ij} = -A_{ji}$.

Components of vectors transform in a predictable way when represented in a different coordinate system. In other words, if a vector \mathbf{u} has components u_i , i.e. $\mathbf{u} = u_i \hat{\mathbf{e}}_i$ (note: sum implied), then the components of \mathbf{u} change when the basis vectors change to $\hat{\mathbf{e}}'_i$. Similarly, tensor components also change in a predictable way under coordinate transformations. This can be seen using the representation of tensors in terms of the Cartesian basis vectors as $\mathbf{T} = T_{ij} \hat{\mathbf{e}}_i \hat{\mathbf{e}}_j$ (sum implied). Note that $\hat{\mathbf{e}}_i \hat{\mathbf{e}}_j$ is the outer product between $\hat{\mathbf{e}}_i$ and $\hat{\mathbf{e}}_j$, and just like $\hat{\mathbf{e}}_i$ is a unit vector, the term $\hat{\mathbf{e}}_i \hat{\mathbf{e}}_j$ is one of the nine unit second-rank tensors.

The reason to introduce the Kronecker delta and the alternating tensor are that they are special second and third rank tensors. They are the so-called “unit isotropic” tensors, i.e. the Cartesian components of these tensors do not change under coordinate transformations. (We shall take it for granted here without proof.) By extension, any algebraic expressions constructed using these unit isotropic tensors are also isotropic. In fact, the most general second, third, and fourth rank isotropic tensors are

$$I_{ij}^2 = \lambda \delta_{ij} \quad (1.12a)$$

$$I_{ijk}^3 = \lambda \epsilon_{ijk} \quad (1.12b)$$

$$I_{ijkl}^4 = \lambda \delta_{ij} \delta_{kl} + \alpha \delta_{ik} \delta_{jl} + \beta \delta_{il} \delta_{jk}, \quad (1.12c)$$

where λ , α and β are arbitrary scalars.

The so-called $\epsilon - \delta$ identity is useful in simplifying the inner products of two alternating tensors as

$$\epsilon_{ijk} \epsilon_{kmn} = \delta_{im} \delta_{jn} - \delta_{in} \delta_{jm}. \quad (1.13)$$

Here note that the left hand side is an isotropic fourth-rank tensor, which is expressed on the right-hand side as a special case of the most general isotropic fourth-rank tensor.

1.4 Tensor Calculus

Tensorial notation also aids in representing multivariate calculus of fields. Here are the basic elements in terms of scalar field $\phi(\mathbf{x}, t)$, vector field $\mathbf{u}(\mathbf{x}, t)$ and tensor fields $\mathbf{T}(\mathbf{x}, t)$. A special notation called the comma notation is used to denote derivatives with respect to Cartesian coordinates, $\partial\phi/\partial x_i = \phi_{,i}$, i.e. an index following a comma in the subscript of a symbol implies differentiation with respect to the corresponding Cartesian coordinate.

	Vector notation	Index notation	Tensorial rank
Gradient of a scalar:	$\nabla \phi$	$\frac{\partial \phi}{\partial x_i} = \phi_{,i}$	1
Divergence of a vector:	$\nabla \cdot \mathbf{u}$	$\frac{\partial u_i}{\partial x_i} = u_{i,i}$	0
Gradient of a vector:	$\nabla \mathbf{u}$	$\frac{\partial u_i}{\partial x_j} = u_{i,j}$	2
Divergence of a tensor:	$\nabla \cdot \mathbf{T}$	$\frac{\partial T_{ij}}{\partial x_j} = T_{i,j,j}$	1
Curl of a vector:	$\nabla \times \mathbf{u}$	$\epsilon_{ijk} \frac{\partial u_k}{\partial x_j} = \epsilon_{ijk} u_{k,j}$	1

Results in integral calculus may also be condensed using the index notation. Consider a volume Ω in space, with its unit normal oriented outwards denoted by $\hat{\mathbf{n}}$. The divergence theorem expressed in vector and index notation is

$$\int_{\partial\Omega} \mathbf{u} \cdot \hat{\mathbf{n}} \, dA = \int_{\Omega} \nabla \cdot \mathbf{u} \, d\Omega \quad \text{or} \quad \int_{\partial\Omega} u_i n_i \, dA = \int_{\Omega} u_{i,i} \, d\Omega, \quad (1.14)$$

where $\partial\Omega$ represents the bounding surface of Ω and dA is the infinitesimal area element on it. A generalization of this theorem for second-rank tensor is

$$\int_{\partial\Omega} \mathbf{T} \cdot \hat{\mathbf{n}} \, dA = \int_{\Omega} \nabla \cdot \mathbf{T} \, d\Omega \quad \text{or} \quad \int_{\partial\Omega} T_{ij} n_j \, dA = \int_{\Omega} T_{ij,j} \, d\Omega. \quad (1.15)$$

Stokes theorem applies to closed curves C , the unit tangent to it $\hat{\mathbf{t}}$, the surface it encloses S and the unit normal to the surface $\hat{\mathbf{n}}$. For vectors, it reads

$$\int_C \mathbf{u} \cdot \hat{\mathbf{t}} \, ds = \int_S (\nabla \times \mathbf{u}) \cdot \hat{\mathbf{n}} \, dA \quad \text{or} \quad \int_C u_i t_i \, ds = \int_S \epsilon_{ijk} u_{kj} n_i \, dA, \quad (1.16)$$

where ds is the infinitesimal arc-length element.

Chapter 2

Mathematical Modelling of Fluid Flow

In this chapter, we will derive the mathematical model governing the motion of fluids. In summary, these will be the Navier-Stokes equations, but on the way we will encounter the Eulerian and the Lagrangian descriptions of fluid motion, the deformation of infinitesimal fluid particles, Cauchy's notion of stress and his equation for motion of continuum, Euler's equations for motion of an ideal fluid, etc. We begin with the definition of a fluid.

2.1 Definition of a fluid

Definition

Fluid: A continuum substance that cannot withstand shear stress without continually deforming.

Consider a thin layer of material sandwiched between two plane walls, as shown in Figure 2.1. Under the action of the applied traction, σ , each layer of the material slides proportional to the distance from the lower wall, which is held fixed. The displacement is given by $\xi = \gamma(t)y$. The shear in this scenario is $d\xi/dy = \gamma(t)$. At long times, $\gamma(t)$ approaches a constant for a solid. But for a fluid, $\gamma(t)$ keeps increasing at a constant rate, i.e., $\gamma(t) = \dot{\gamma}t$, where $\dot{\gamma}$ is the rate of shear.

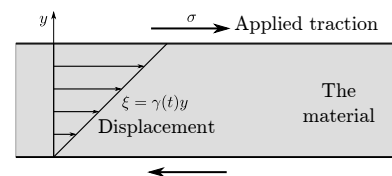


Figure 2.1: The deformation of a material under a constant applied traction.

There are other definitions of a fluid that, while appropriate to be used at more elementary treatments of fluid dynamics, are inadequate for the purposes of deriving mathematical models for describing their behaviour. One such definition is that a fluid is a substance that assumes the shape of its container. This definition is inadequate for our purpose because there is no mention of gravity, the driving force that makes some of those substances, namely liquids, conform to the shapes of their containers. But even for gases, this definition does not furnish the defining element instrumental in deriving the governing equations for fluid flow – the internal stress experienced by elements of the fluid and the resulting deformation.

While our definition addresses some of the shortcomings of the more elementary definitions, it has left some terms undefined. For instance, what is a continuum substance? What is a shear stress? How does one quantify continual deformation? Also note that the definition does not constrain the magnitudes of the shear stress or that of the deformation, nor does it specify any relation between the two.

Based on this guiding definition, we derive mathematical representations of the laws of conservation of mass, momentum and angular momentum in §2.8, §2.9 and §2.10, respectively. The concepts of deformation rate and stress will emerge in the process. A fluid is any substance that obeys the assumptions that go into the derivations of these mathematical representations. On the one hand, such an exercise rigorously constrains the materials to which the governing equations could be applied. And on the other hand it broadens the scope to include materials that are not commonly classified as fluids but whose mechanics are governed by the equations we derive because they satisfy the underlying assumptions. Understanding the significance of the assumptions that form the basis of the derivation of the governing equations is the objective of this chapter.

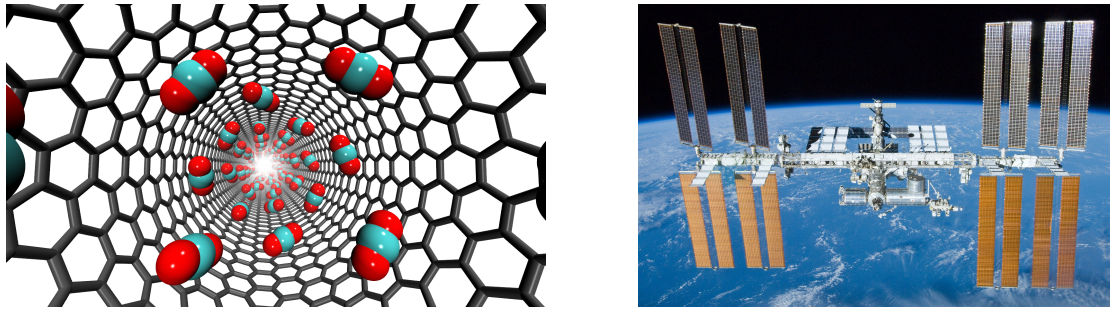


Figure 2.2: Left: An example where continuum mechanics is unlikely to work - a molecular dynamics simulation of a desalination membrane, where water molecules flow through a carbon nanotube (see www.micronanoflows.ac.uk). Right: The International Space Station (source: www.wikipedia.org/wiki/International_Space_Station).

2.2 Fluids in Continuum Mechanics

Matter on earth is made up of atoms and molecules, each obeying classical or quantum laws of physics. When dealing with a large collection of molecules, the granularity of molecular composition somehow is lost and/or becomes irrelevant. Properties of matter can then be considered to vary smoothly with location within the material. The emergence of thermodynamics is an example of this. Similarly, when describing motion of macroscopic matter on length scales much larger than molecular scales, it becomes possible to consider the material as a infinitely divisible continuum. The theory of mechanics that arises out of such a consideration is called continuum mechanics.

The continuum approach is accurate when the mean free path ℓ , which is the length a molecule of the medium travels between collisions with other molecules, is much smaller than the dimensions of the flow L , so that $\ell/L \ll 1$ (the continuum limit takes $\ell/L \rightarrow 0$). Note that ℓ/L is a ‘dimensionless number or parameter’, whose value does not depend on the system of units used. When $\ell/L \approx 1$ or $\ell \gg L$, microscopic methods (molecular dynamics for liquids and kinetic theory for gases) are required.

It is worthwhile to ponder briefly about cases where continuum hypothesis fails. Here are two situations:

1. **Flow of water through a carbon nanotube:** Nanotubes are modern materials consisting of a tube of diameter as small as 0.4 nm. Figure 2.2 shows the use of nanotubes made out of carbon for desalinating water. The basic idea is that while water can flow through the tube, the impurities do not. In this case, the water near the centre of the tube flows faster compared to that near the tube walls, where friction impedes the flow. Thus, the water speed changes over a distance compared to the diameter of the tube, so $L \approx 0.4$ nm. The molecular mean-free path is about 0.25 nm. In this case, $\ell/L \approx 0.25/0.4 = 0.625$, which is not small. Therefore, the continuum hypothesis is likely to fail.
2. **Motion of the International Space Station (ISS):** The ISS is about $79 \text{ m} \times 109 \text{ m}$, say approximately $L = 100$ m across and orbits the earth at an altitude of 400 km. The atmosphere there is so rarified that the mean free path of gas molecules is $\ell \approx 20$ km. The ratio $\ell/L = 20 \times 10^3/100 = 200$ is clearly not small, so the surrounding gas cannot be treated as a continuum.

In summary, the continuum approximation of the fluid may fail because (i) the length-scale over which the flow varies is too small, or (ii) the mean free path of the fluid molecules is too large. Both these cases are adequately encapsulated by the ratio ℓ/L .

In day-to-day situation, e.g. flow of water through ordinary pipes, continuum approximation does apply. In that case, every point in space is assigned physical properties such as density, pressure, velocity, stress, etc. Continuous functions of space and time, called fields, are used to represent these physical variables.

2.3 Material properties of fluids

There are five main properties that will be important for us in this module.

1. **Density (ρ):** The mass of the fluid per unit volume. Air has a density of about 1.2 kg/m^3 and water of 1000 kg/m^3 . Physically, the density of a fluid is determined by its thermodynamic state, and could thus change with pressure and temperature, for instance. If the conditions are such that the density of the fluid does not change appreciably in the flow then such a flow is termed “incompressible”. Under ordinary circumstances, flows of air and water are incompressible. For flow of air around a jet plane, the flow is compressible. And it is certainly so for flow around a supersonic plane.
2. **Pressure (p):** The force a fluid exerts on a wall per unit area. At sea level, air exerts a pressure of about 10^5 N/m^2 . In SI system, $\text{N/m}^2 = \text{Pa}$, a Pascal. Other common units of pressure, especially in atmospheric sciences, are the bar, $1 \text{ bar} = 10^5 \text{ Pa}$, and the atmosphere, $1 \text{ atm} = 101325 \text{ Pa}$. Pressure is also measured in terms of a height of a fluid column, where the fluid is commonly but not necessarily either water or mercury. Normal human blood pressure is purported to range from 80 to 120 mm of mercury.
3. **Dynamic Viscosity (μ):** Also known as Newtonian viscosity. It represents the resistance of a fluid to shear. The viscosity is the ratio of the traction applied to the shear rate generated in steady state. In the terminology used in Figure 2.1, $\mu = \sigma/\dot{\gamma}$. Dynamic viscosity has the SI units of Ns/m^2 or, equivalently, Pa s . An “ideal” fluid or an “inviscid” fluid is one with zero viscosity.
4. **Kinematic viscosity (ν):** The kinematic viscosity is the dynamic viscosity divided by fluid density, i.e. $\nu = \mu/\rho$. In the SI system, it has units of m^2/s (note the absence of kg in the units, hence the epithet kinematic).
5. **Surface tension (σ):** The surface of a liquid behaves like a stretched membrane. The tension in this “membrane”, measured as force per unit length, is called surface tension. Surface tension has SI units of N/m .

The conditions termed as incompressible and inviscid or ideal are idealizations of real conditions. They are never exactly realized.

2.4 Lagrangian and Eulerian Descriptions

Watch the video on ‘Lagrangian and Eulerian descriptions of fluid flow’ narrated by Prof. John Lumley of Cornell University from the National Committee for Fluid Mechanics. YouTube link: www.youtube.com/watch?v=mdN800kx2ko, duration: 27 mins.

The objective in developing the continuum theory of fluids is to decompose the fluid into an infinite number of infinitesimal fluid elements and impose Newton’s laws of motion on each one of them. To do so, it is necessary to label each infinitesimal element of a fluid. There are two common approaches historically employed for doing so. These approaches are called the Eulerian and the Lagrangian descriptions of fluid flow.

2.4.1 Lagrangian description

The Lagrangian description seeks to label and track infinitesimal material volumes of fluid. Their boundaries move with the average speed of the molecules composing the boundaries (only possible in the continuum limit, when there are a large number of molecules on the boundary). Consequently, these volumes always contains the same amount of mass within them. Intrinsic¹ material properties are attributed to the volume by virtue of the material contained in the volume. For example, the velocity, the acceleration, the density, the temperature, the pressure, the concentration of any dissolved species could be attributed to the material volumes. These infinitesimal fluid volumes are also called (Lagrangian) fluid particles or fluid parcels.

A convenient label is the position of an infinitesimal fluid volume, X_j , at some reference time t_0 . In the Lagrangian description, the fluid velocity is then given by the fields $U_i(X_j, t)$. This expression stands for the velocity of the Lagrangian fluid particle at time t , which was at position X_j at time t_0 . Similar interpretation is applied to the density $R(X_j, t)$, acceleration $A_i(X_j, t)$, pressure $P(X_j, t)$, etc. As an informal convention, we will use capital letters to denote Lagrangian fields.

Caution: It is a common misunderstanding that the fluid inside the material volume is composed of the same material throughout the flow. This is not true. Instead, the correct statement, as mentioned earlier, is that the

¹Here intrinsic quantities are those which do not depend on the total amount of material in the volume. Examples of intrinsic quantities are pressure, temperature, density, as opposed to *extrinsic* quantities such as mass, volume, etc, which are proportional to the mass of material in the volume.

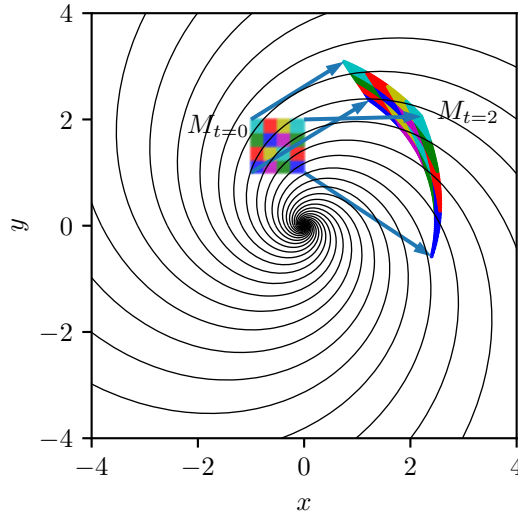


Figure 2.3: The motion and deformation of a Lagrangian fluid volume in a flow. The black curves denote streamlines of the flow spiralling outwards. The square coloured patch labelled $M_{t=0}$ shows the Lagrangian fluid volume at $t = 0$. The Lagrangian volume at $t = 2$ is shown as the deformed coloured patch labelled $M_{t=2}$. Blue arrows show the displacement of Lagrangian fluid particles forming the corners of the $M_{t=0}$. The colour of the sub-patches is preserved between $M_{t=0}$ and $M_{t=2}$.

fluid inside the volume always contains the same amount of mass. Molecules composing the fluid move in and out of the volume such that no net mass leaves or enters the volume.

2.4.2 Eulerian description

The Eulerian description seeks to label the fluid particles by their current location in space. A convenient and common label are the coordinates of the points in space. All physical properties of the fluid are then described as fields over these labels, i.e., the Cartesian coordinates, x_j . For example, the velocity of the fluid is described as a field $u_i(x_j, t)$, which is interpreted as the velocity of the Lagrangian fluid particle that is at location x_j at time t . Note that even in the Eulerian description, physical quantities are attributed to the fluid elements and not to the space. Similarly, the density is denoted $\rho(x_j, t)$, the pressure as $p(x_j, t)$, the acceleration as $a_i(x_j, t)$, the stress as $T_{ij}(x_k, t)$, etc.

Definition: A Steady Eulerian Field

A steady field is one for which $\partial/\partial t = 0$. One of the advantages of the Eulerian description of fluid flow is that in many cases and in properly chosen reference frames, the resulting fields of velocity and pressure are steady. This significantly simplifies the analysis of such flows.

2.4.3 Eulerian versus Lagrangian descriptions

The two descriptions are invoked in fluid dynamics because they simplify different stages of the analysis. Newton's laws of motion are formulated in the Lagrangian description. Later, we will write the acceleration of Lagrangian particles in terms of the forces they experience. In this formulation, we will need to represent the force exerted by the neighbouring fluid particle as it pushes against the one under consideration, or slides past it. This will require us to track the neighbouring fluid particles as well. Now, the nature of fluid flows is such that the Lagrangian fluid volumes deform significantly with time and so do their neighbours, see Figure 2.3.

The Eulerian description does not suffer from the deformation of volumes. The volume remains fixed because we have defined it to be so. Neighbouring particles also remain in place without deforming. However, the laws of mechanics have been formulated in Lagrangian description. Whilst in the Eulerian description one sits at a fixed position and watches the flow pass (like standing at the bank of a river), in the Lagrangian description we 'follow the fluid' (as in a boat flowing with the river or on a weather balloon).

To bridge this gap, we use an Eulerian-Lagrangian map. The most basic element of the map is the trans-

formation between the labels. Given the Eulerian labels \mathbf{x} and the Eulerian velocity field $\mathbf{u}(\mathbf{x}, t)$, the position of Lagrangian fluid particles labeled \mathbf{X} may be determined by solving for $\mathbf{F}(\mathbf{X}, t)$

$$\left. \frac{\partial \mathbf{F}}{\partial t} \right|_{\text{fixed } \mathbf{X}} = \mathbf{u}(\mathbf{F}(\mathbf{X}, t), t), \quad (2.1)$$

with $\mathbf{F}(\mathbf{X}, t_0) = \mathbf{X}$. In other words, the rate of change of position of a Lagrangian fluid particle is simply the Eulerian velocity at the current location of the fluid particle.

2.4.4 The Material Derivative and Acceleration

There is a section on ‘Material Derivative applied to the concentration of a pollutant in a river’ starting at 12:00 mins in the video on ‘Lagrangian and Eulerian descriptions of fluid flow’ by Prof. John Lumley of Cornell University from the National Committee for Fluid Mechanics. YouTube link: www.youtube.com/watch?v=mdN800kx2ko, starting 12:00 mins to the end.

We now use this relation to develop the most common Eulerian to Lagrangian conversion of an operation, differentiation with time. For a generic intrinsic fluid property $c(\mathbf{x}, t)$ of arbitrary tensorial rank, the partial derivative with time $\partial c / \partial t$ merely represents the rate of change of c at the Eulerian location \mathbf{x} . It does not account for the fact that at an infinitesimally later time, a different fluid particle now occupies the location \mathbf{x} . Since most physical laws are formulated in terms of the properties of the Lagrangian fluid particle, it is useful to instead derive an expression for the rate of change of c following the fluid particle.

To do so, note that $c(F_i(\mathbf{X}, t), t)$ is the property c evaluated at the position F_i of the Lagrangian particle labelled by \mathbf{X}^2 . The location of the particle itself changes with time. Therefore, the rate of change of c following the fluid particle is

$$\begin{aligned} \left. \frac{\partial c(F_i(\mathbf{X}, t), t)}{\partial t} \right|_{\text{fixed } \mathbf{X}} &= \left. \frac{\partial c}{\partial t} \right|_{\text{fixed } \mathbf{x}} + \left. \frac{\partial F_i}{\partial t} \frac{\partial c}{\partial x_i} \right|_{\text{fixed } t} \\ &= \left. \frac{\partial c}{\partial t} \right|_{\text{fixed } \mathbf{x}} + u_i \left. \frac{\partial c}{\partial x_i} \right|_{\text{fixed } t} \quad \dots \quad \text{using } \frac{\partial F_i}{\partial t} = u_i \text{ from (2.1)} \\ &= \left. \frac{\partial c}{\partial t} \right|_{\text{fixed } \mathbf{x}} + \mathbf{u} \cdot \nabla c \quad \dots \quad \text{in vector notation.} \end{aligned} \quad (2.2)$$

Definition: The Material Derivative a.k.a. The Lagrangian Derivative a.k.a. The Total Derivative a.k.a. The Substantial Derivative

The material derivative is the rate of change of an intrinsic property of a Lagrangian fluid particle expressed in terms of Eulerian quantities. It is symbolically denoted as $\frac{D}{Dt}$ and is given by the expression

$$\frac{D}{Dt} = \frac{\partial}{\partial t} + (\mathbf{u} \cdot \nabla). \quad (2.3)$$

Interpretation of the terms in the Material derivative:

1. The first term is the local rate of change at a fixed Eulerian position \mathbf{x} due to temporal changes.
2. The second is the ‘convective rate of change’ caused by the velocity \mathbf{u} driving fluid elements through spatial gradients in the quantity of interest. The next example illustrates how a steady (i.e. time independent) Eulerian field could imply a non-zero time-rate-of-change for Lagrangian properties because of the convective rate-of-change term.

Example: If there is a concentration of pollutant $c = c(x)$ in a river that flows steadily with constant speed $\mathbf{u} = (u_0, 0, 0)$ (see Figure 2.4), how does the concentration change in a fluid element that ‘follows the fluid’?

Note that (a) the concentration at a fixed point does not change with time $\partial_t c = 0$ but (b) the concentration inside a fluid element that ‘follows the fluid’ will change in time, at a rate given by the material derivative

$$\frac{Dc}{Dt} = \frac{\partial c}{\partial t} + u \frac{\partial c}{\partial x} + v \frac{\partial c}{\partial y} + w \frac{\partial c}{\partial z} = u_0 \frac{\partial c}{\partial x}, \quad (2.4)$$

which is non-zero if and only if there is flow $u_0 \neq 0$ and spatial gradients in $\partial_x c \neq 0$.

It is the material derivative which gives us the rate of change of velocity, i.e. the acceleration \mathbf{a} or a_i , of the fluid element

$$a_i = \frac{Du_i}{Dt} = \frac{\partial u_i}{\partial t} + u_j \frac{\partial u_i}{\partial x_j} \quad \text{or} \quad \mathbf{a} = \frac{D\mathbf{u}}{Dt} = \frac{\partial \mathbf{u}}{\partial t} + (\mathbf{u} \cdot \nabla)\mathbf{u}. \quad (2.5)$$

Notably, even when the flow is *steady* in the Eulerian frame, so that $\partial_t \mathbf{u} = 0$, the acceleration still has a component $(\mathbf{u} \cdot \nabla)\mathbf{u}$ due to the spatial variation of the velocity field—this is the convective acceleration.

Example: If we take a one-dimensional steady flow $\mathbf{u} = (u(x), 0, 0)$ (see Figure 2.5), then what is the acceleration of fluid particles?

$$a_1 = \frac{\partial u}{\partial t} + u \frac{\partial u}{\partial x} + v \frac{\partial u}{\partial y} + w \frac{\partial u}{\partial z} = u \frac{\partial u}{\partial x}, \quad a_2 = a_3 = 0, \quad (2.6)$$

so that where there is a spatial gradient in u there is an acceleration.

2.4.5 Reynolds transport theorem

To describe laws of physics in terms of continuum quantities, we also need the time-rate-of-change of a total quantity enclosed within a finite Lagrangian volume Ω . If the volumetric density of a property B is b , i.e., if the total amount of B in any volume Ω may written as

$$B = \int_{\Omega} b \, d\Omega, \quad (2.7)$$

then

$$\frac{D}{Dt} \left(\int_{\Omega(t)} b \, d\Omega \right) = \int_{\Omega} \frac{\partial b}{\partial t} \, d\Omega + \int_{\partial\Omega} b(\mathbf{u} \cdot \hat{\mathbf{n}}) \, dA, \quad (2.8)$$

where $\partial\Omega$ is the bounding surface of Ω and \mathbf{u} is the Eulerian velocity. The first term on the right hand side is simply the contribution that arises from the rate of change of b within the volume, even when the Lagrangian volume stays fixed. The second term arises from the motion of the Lagrangian volume under the Eulerian velocity \mathbf{u} . Here $(\mathbf{u} \cdot \hat{\mathbf{n}}) \, dA$ is the rate at which volume of fluid enters the surface $\partial\Omega$ through an infinitesimal area dA (as shown in Figure 2.6), and its product with b gives the amount of B entering the volume per unit time.

2.5 Flow Visualisation

Watch the video on ‘Flow Visualisation’ narrated by Prof. Stephen J. Kline from Stanford University. YouTube link: www.youtube.com/watch?v=nuQyKGuXJOs, duration: 31 mins.

²Here we mix index notation for \mathbf{F} with vector notation for \mathbf{X} .



Figure 2.4: Evolution of a fluid element through a spatial gradient in concentration $c = c(x)$ showing that the concentration inside the fluid element will change from $t = 0$ to $t = t_1$ even though the flow is steady $\partial_t \mathbf{u} = \mathbf{0}$.

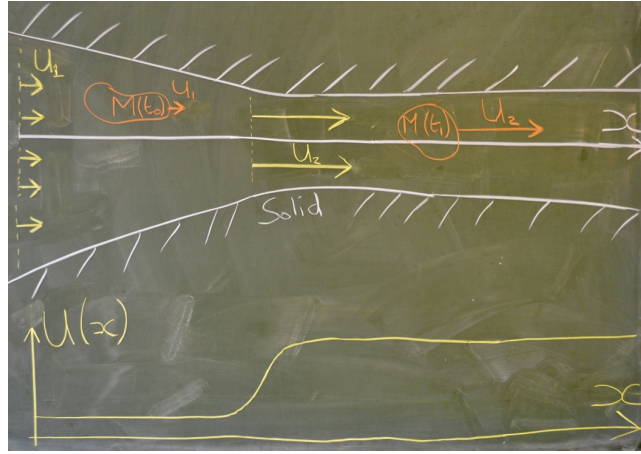


Figure 2.5: The acceleration of a fluid element M as it travels from an area of low speed (left) at time t_0 to a region of high speed (right) at $t = t_1$. Therefore, despite the flow being steady, so that at a fixed point $\partial_t u = 0$, the fluid inside M feels an acceleration due to its motion.

The most common way to visualise a flow, theoretically (once we have \mathbf{u}) or experimentally, is by drawing a set of curves. Four types of curves are commonly used in fluid dynamics. Some are purely theoretical concepts, while others are used for experimental convenience.

To visualise a flow field experimentally, one usually places illuminated passive tracers (e.g. dye, bubbles or beads that don't alter the flow) into the flow (e.g. Figure 2.7). The various curves are then realized by the choice of the initial release of the tracer particles and the visualization technique.

1. **Particle paths or pathlines:** The paths of fluid elements ('*particle paths*') $F_i(t)$, which are simply the locus of points traced by a Lagrangian fluid element. Equation (2.1) may be used to theoretically determine these from an Eulerian description of the velocity field. Typically a small amount of illuminated passive tracers are introduced in the flow, and the resulting images superimposed in post-processing to reveal the pathlines for a flow. Long exposures, if possible, also yield pathlines.
2. **Streaklines:** The instantaneous locus of all the Lagrangian fluid elements that have passed through or will pass through a fixed point in space is a 'streakline'. It is easier to visualize streaklines experimentally, which can be done by introducing a steady streak of a passive tracer in the fluid (hence the name). Theoretically, streakline at time t passing through a point \mathbf{X}_0 may be obtained by solving the equation

$$\mathbf{F}(\mathbf{X}, s) = \mathbf{X}_0, \quad t_i \leq s \leq t_f, \quad (2.9)$$

for $\mathbf{X}(s)$, where t_i and t_f are the initial and final times of interest, and then plotting $\mathbf{F}(\mathbf{X}(s), t)$ for fixed t while varying s as a parameter.

3. **Timelines:** A 'time line' is the subsequent shape of a curve made of Lagrangian fluid elements. It is more convenient to visualize a timeline experimentally than it is to calculate it theoretically. For the experimental visualization, a passive tracer is released at a time instance in the shape of a curve. The subsequent evolution of the curve naturally visualizes the timeline. To construct the timeline from an Eulerian velocity field, we start with a curve parameterized as $\mathbf{X}_0(s)$ by parameter s . The subsequent shape of the curve at time t is $\mathbf{F}(\mathbf{X}_0(s), t)$, which is the timeline at time t .

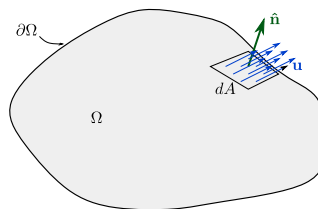


Figure 2.6: Schematic showing a motion of a small area element dA of $\partial\Omega$ of the surface bounding the volume Ω . Here \mathbf{u} is the Eulerian velocity field on the surface and $\hat{\mathbf{n}}$ is the unit normal. The quantity $(\mathbf{u} \cdot \hat{\mathbf{n}}) dA$ is the rate at which volume of fluid is entrained into Ω through dA .

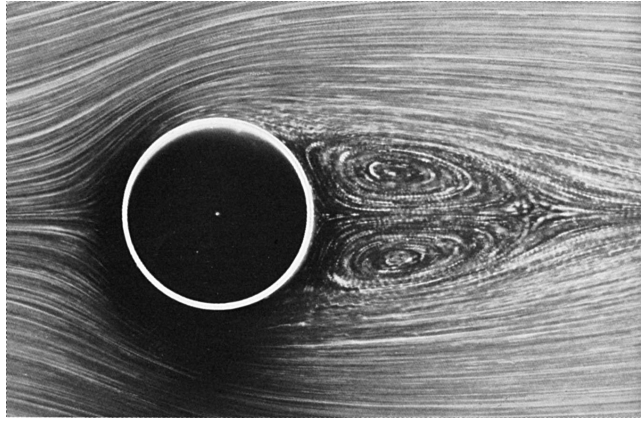


Figure 2.7: Steady laminar flow (from left to right) around a solid cylinder with streamlines/particle paths showing the trajectories of fluid elements

4. **Streamlines:** A ‘streamline’ is a curve which is everywhere tangent to the velocity vector of an Eulerian flow field. Streamlines are mathematical constructions, and, therefore, are easier to construct theoretically. Parameterized by an independent parameter s , the streamlines $(x, y, z) = (x(s), y(s), z(s))$ at time t are obtained by solving

$$\left. \frac{\partial x_i(s)}{\partial s} \right|_{\text{fixed } t} = u_i. \quad (2.10)$$

To visualize streamlines in an experiment, it is necessary to measure the Eulerian velocity field. This measurement can be accomplished using techniques such as particle image velocimetry (PIV).

Streamlines, although theoretical, have deep physical significance, especially for incompressible flows. Because the volume of a Lagrangian fluid element is conserved for an incompressible fluid, the only way a fluid element can move is by displacing the one ahead of it. At the same instance, the one ahead in turn displaces the one ahead of it, and so on. An incompressible fluid can flow only by forming such chains of instantaneous displacement of fluid elements. A streamline is nothing but one such chain.

Because of the aforementioned interpretation, streamlines cannot terminate in an incompressible fluid. They must extend all the way to infinity or form closed curves.

In general, the particle paths differ from the streamlines, which differ from streaklines. The following example illustrates that.

Example (from Acheson Ex 1.8): Consider the two-dimensional flow given by

$$\mathbf{u} = (u_0, kt, 0), \quad \text{with} \quad u_0, k > 0.$$

What are the pathlines, streamlines and streaklines?

The pathlines are obtained from solving

$$\frac{\partial F_1}{\partial t} = u_0, \quad \frac{\partial F_2}{\partial t} = kt \quad \frac{\partial F_3}{\partial t} = 0$$

for fixed initial position $(F_1, F_2, F_3) = (X, Y, Z)$ at $t = 0$. Therefore,

$$(F_1, F_2, F_3) = \left(u_0 t + X, \frac{1}{2} k t^2 + Y, Z \right)$$

which, notably, could be used to transform from Eulerian to Lagrangian coordinates (by expressing (x, y, z) in terms of (X, Y, Z)). We can eliminate t to find the particle paths

$$y = \frac{k}{2} \left(\frac{x - X}{u_0} \right)^2 + Y$$

which are parabolas with their minimum at (X, Y) and $k/2u_0^2$ as the coefficient of the quadratic term (see figure 2.8 for the pathline through the origin).

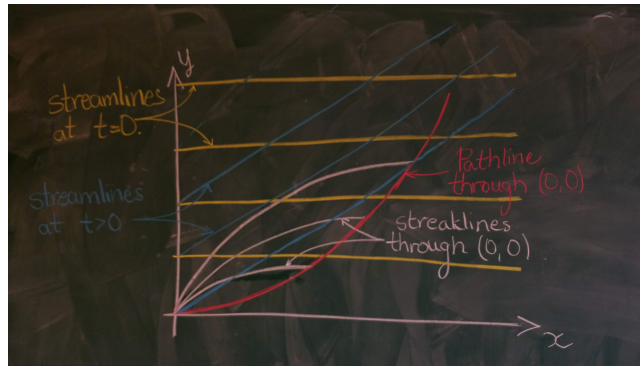


Figure 2.8: Sketch showing how streamlines change in time, differing at $t = 0$ and $t = t_1$, the particle path $y = \frac{k}{2}(x/u_0)^2$ of a fluid element starting from $X = Y = 0$ at $t = 0$, and streaklines for three different times passing through $X = Y = 0$.

The streamlines come from

$$\frac{\partial x}{\partial s} = u_0, \quad \frac{\partial y}{\partial s} = kt, \quad \frac{\partial z}{\partial s} = 0$$

for a fixed t . Therefore

$$(x, y, z) = (u_0 s + a, kts + b, c)$$

for a, b, c constant. Eliminating s we find that

$$y = \frac{kt}{u_0}x + (b - kta/u_0)$$

showing that the streamlines are straight lines whose slope will increase in time. The result is figure 2.8.

The streaklines are also easy to calculate. Upon solving equation (2.9), we get for $\mathbf{X}(s)$

$$X(s) = X_0 - us, \quad Y(s) = Y_0 - \frac{1}{2}ks^2, \quad Z(s) = Z_0.$$

The equation for the curve for the streakline is $\mathbf{F}(\mathbf{X}(s), t)$, which is

$$x = X_0 - us + ut, \quad y = Y_0 - \frac{1}{2}ks^2 + \frac{1}{2}kt^2, \quad z = Z_0.$$

These are to be plotted for fixed t while varying s as a parameter, which means that they are inverted parabolas through $(X_0 + ut, Y_0 + kt^2/2, Z_0)$. The one through the origin is plotted in figure 2.8.

2.6 Deformation of infinitesimal fluid elements

The study of the deformation of continuous media (including solid and fluid dynamics) is a course in its own right, so we will only consider the concepts we will require to formulate the equations of fluid mechanics. In particular, we will attempt to understand how flow deforms fluid elements; as it is this (rate of) deformation that is related to the internal stress (and hence forces) required for formulating Newton's second law for the fluid.

The velocity can be decomposed into fundamental components which specify the kinematics of the flow (the geometry of the motion), i.e. how small fluid elements are deformed by the flow. To do so, consider the flow at an infinitesimal distance δx_j from a reference point x_j , see figure 2.9.

The Taylor expansion of $u_i(x_j + \delta x_j)$, keeping only the terms up to the first power in δx_j inclusive, gives

$$u_i(x_j + \delta x_j, t) = u_i(x_j, t) + \frac{\partial u_i}{\partial x_j} \delta x_j = \underbrace{\underbrace{u_i(x_j)}_{\text{Translation}} + \underbrace{r_{ij} \delta x_j}_{\text{Rotation}}}_{\text{Rigid Body Motions}} + \underbrace{e_{ij} \delta x_j}_{\text{Shearing and Extension}} \quad (2.11)$$

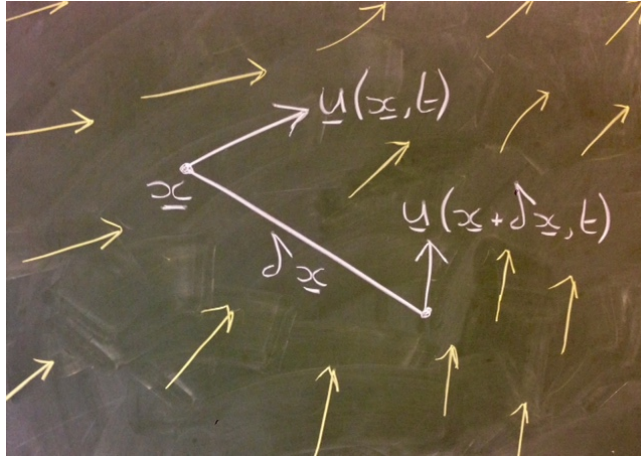


Figure 2.9: Flow kinematics - how the flow velocity varies in the vicinity of (a distance $\delta \mathbf{x}$ from) a point \mathbf{x} .

where we have decomposed $\partial_{x_j} u_i$ into an anti-symmetric ($r_{ij} = -r_{ji}$) *rate of rotation tensor*

$$r_{ij} = \frac{1}{2} \left(\frac{\partial u_i}{\partial x_j} - \frac{\partial u_j}{\partial x_i} \right) \quad \text{or in vector notation} \quad \mathbf{r} = \frac{1}{2} (\nabla \mathbf{u} - \nabla \mathbf{u}^T),$$

and the symmetric ($e_{ij} = e_{ji}$) *rate of strain tensor*

$$e_{ij} = \frac{1}{2} \left(\frac{\partial u_i}{\partial x_j} + \frac{\partial u_j}{\partial x_i} \right) \quad \text{or in vector notation} \quad \mathbf{e} = \frac{1}{2} (\nabla \mathbf{u} + \nabla \mathbf{u}^T).$$

Note that $\nabla \mathbf{u} = \mathbf{e} + \mathbf{r}$.

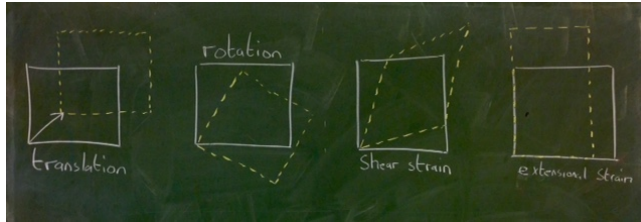


Figure 2.10: Different modes of deformation to a fluid element (in 2D).

Each of the terms contributing to the velocity

$$u_i(x_j + \delta x_j, t) = u_i^T + u_i^R + u_i^S, \quad \text{where} \quad u_i^T = u_i(x_j), \quad u_i^R = r_{ij} \delta x_j, \quad u_i^S = e_{ij} \delta x_j \quad (2.12)$$

can now be analysed. The first term in (2.11) is due to rigid body translation $u_i^T = u_i(x_j, t)$. If $r_{ij} = e_{ij} = 0$, then all fluid elements have the same velocity.

Rate of rotation OR Vorticity

Due to the antisymmetry of r_{ij} , there are only 3 independent components (all diagonal elements zero) and we can rewrite the term $u_i^R = r_{ij} \delta x_j$ as a cross product $u_i^R = \epsilon_{ijk} \Omega_j \delta x_k$ or $\mathbf{u}^R = \boldsymbol{\Omega} \times \delta \mathbf{x}$ (see figure 2.11), where $\boldsymbol{\Omega} = (r_{32}, r_{13}, r_{21})$ is the rate of rotation *vector* (you can check this). Thus we see that this term is associated with rigid body rotation about the reference point with rotational rate $\boldsymbol{\Omega}$.

Notably, the rate of rotation vector $\boldsymbol{\Omega}$ is equal to half the *vorticity* vector

$$\boldsymbol{\omega} = \nabla \times \mathbf{u} = 2\boldsymbol{\Omega}, \quad \text{so that} \quad \mathbf{u}^R = \frac{1}{2} \boldsymbol{\omega} \times \delta \mathbf{x} \quad (2.13)$$

which is an important fluid mechanical quantity we will repeatedly encounter - now we can recognise it as a measure of the local rate of rotation in the fluid. In Cartesian coordinates it is given by

$$\boldsymbol{\omega} = \begin{vmatrix} \mathbf{e}_x & \mathbf{e}_y & \mathbf{e}_z \\ \frac{\partial}{\partial x} & \frac{\partial}{\partial y} & \frac{\partial}{\partial z} \\ u & v & w \end{vmatrix} = \left(\frac{\partial w}{\partial y} - \frac{\partial v}{\partial z}, \frac{\partial u}{\partial z} - \frac{\partial w}{\partial x}, \frac{\partial v}{\partial x} - \frac{\partial u}{\partial y} \right).$$

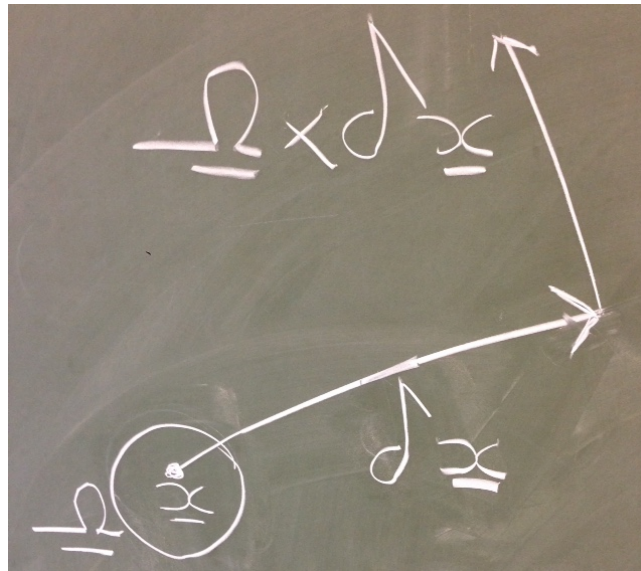


Figure 2.11: Sketch illustrating the rigid body rotation $\mathbf{u}^R = \boldsymbol{\Omega} \times \delta \mathbf{x}$ induced a distance $\delta \mathbf{x}$ away from a point \mathbf{x} by the rotation rate $\boldsymbol{\Omega}$. Here, $\boldsymbol{\Omega}$ points out of the paper.

Example: How many components of vorticity does a 2D flow have?

For a two-dimensional flow $\mathbf{u} = (u(x, y, t), v(x, y, t), 0)$, the vorticity has only one component $(0, 0, \omega)$ where $\omega = \frac{\partial v}{\partial x} - \frac{\partial u}{\partial y}$, with a rotation axis in the z -direction.

Strain rate:

As the first two terms in (2.11) are associated with rigid body motion, it is the third term $u_i^S = e_{ij} \delta x_j$ which represents the straining motions which distinguish the flow through the relative motion of adjacent fluid elements. The rate of strain tensor e_{ij} can be further decomposed into (a) diagonal elements which are associated with extensional motion and (b) off-diagonal elements give the shear rate of strain.

Consider how the components of e_{ij} deform an infinitesimal rectangular fluid element of size $\delta x \times \delta y$ (figure 2.12) in a two-dimensional flow $\mathbf{u} = (u(x, y, t), v(x, y, t), 0)$. For simplicity, we will remove translation of the fluid element by considering flow relative to the point A, so that a Taylor expansion gives the flow components at adjacent points to A shown in figure 2.12.

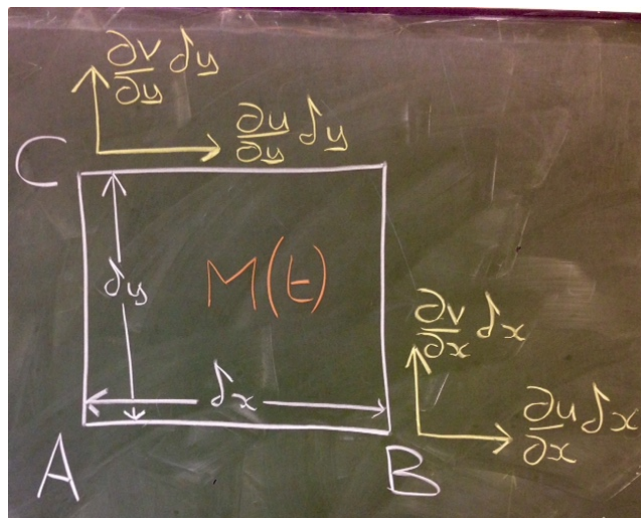


Figure 2.12: The velocity components relative to a point A in a material element M at time t .

From figure (2.13) we can see that *extensional rate of strain* acts to increase the lengths of the sides. For

example, taking the line AB , in a time δt the point B moves so that the new length of AB at time $t + \delta t$ is

$$\delta x(t + \delta t) = \delta x(t) + \underbrace{\frac{\partial u}{\partial x} \delta x}_{\text{speed}} \delta t. \quad (2.14)$$

Therefore, the (infinitesimal) strain (extension/original length)

$$\delta S_x = (\delta x(t + \delta t) - \delta x(t)) / \delta x(t) \stackrel{(2.14)}{=} \frac{\partial u}{\partial x} \delta t \quad \text{so the rate of strain is} \quad \frac{\partial S_x}{\partial t} = \frac{\partial u}{\partial x} = e_{11}$$

as expected.

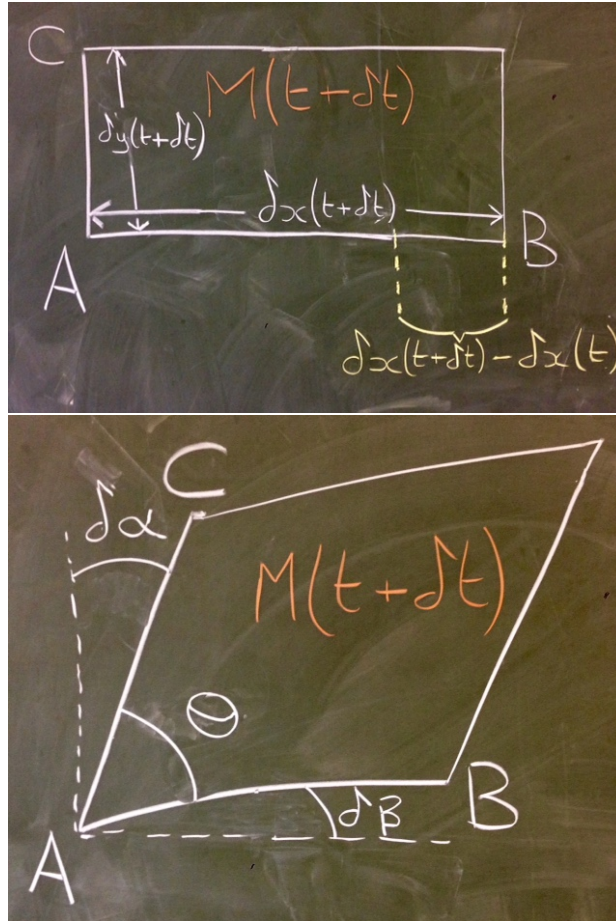


Figure 2.13: Left: deformation due to extensional strain on the material element at a time $t + \delta t$. Right: influence of shear strain on the material element at a time $t + \delta t$.

It can be shown that the extensional components change the volume V of the fluid element as

$$\frac{1}{V} \frac{DV}{Dt} = e_{kk} \quad \text{symbolically} \quad \frac{1}{V} \frac{DV}{Dt} = \nabla \cdot \mathbf{u} \quad (2.15)$$

so that for an incompressible fluid, where the volume of the fluid element does not change in time ($D_t V = 0$), we have $e_{kk} = e_{11} + e_{22} + e_{33} = 0$. In other words, extension of a fluid element in one direction must lead to contraction in one of the other directions.

The *shear* rate of strain acts to drive the element from its rectangular shape. This can be quantified by measuring the angle between the sides. It can be shown that (see Examples Sheet 2) the angle θ at CAB in figure 2.12 evolves according to

$$-\frac{\partial \theta}{\partial t} = 2e_{12}.$$

So we have seen that it is the vorticity and rate of strain that give us all of the information we require to understand how fluid elements are locally deformed, with the former telling us about the rotation of the flow and the latter about the relative motion of fluid elements (which is related to viscous stress).

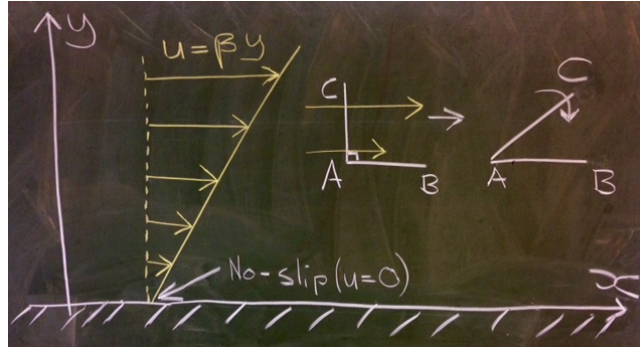


Figure 2.14: The deformation of two initially perpendicular fluid line element (i.e. they ‘follow the fluid’) in a shear flow showing how AC rotates - hence the flow contains vorticity.

Example (Adapted from Acheson §1.4): Consider the ‘shear flow’ $\mathbf{u} = (\beta y, 0, 0)$. How does this simple flow deform fluid elements? E.g., what is the contribution from deformation to (2.12)?

Let’s consider all the different contributions to (2.12).

- The translational term is just $u_i^T = (\beta y, 0, 0)$.
- The vorticity will only have a component in the z -direction $\boldsymbol{\omega} = (0, 0, \omega)$ which is

$$\omega = \frac{\partial v}{\partial x} - \frac{\partial u}{\partial y} = -\beta.$$

So there is rotation in the flow, despite the streamlines and particle paths being straight. This is because the velocity at the point C is greater than that at A so the line CA rotates clockwise (figure 2.14). The rate of rotation will be $\omega/2 = -\beta/2$.

Therefore, the contribution to (2.12) is

$$u_i^R = \frac{1}{2} \epsilon_{ijk} \omega_j \delta x_k = \frac{1}{2} (\beta dy, -\beta dx, 0)$$

- The only non-zero entries in the rate of strain tensor will be due to $\partial_y u = \beta$. Therefore, extensional strains are all zero (ensuring incompressibility) and the only non-zero entries are $e_{12} = e_{21} = \beta/2$. Consequently, the contribution to (2.12) is

$$u_i^S = \frac{1}{2} (\beta dy, \beta dx, 0).$$

- Therefore, even in this simple flow there are rigid body motions of translation and rotation as well as deformation.

2.7 Conservation Laws in Continuum Mechanics

In continuum mechanics, it is customary to refer to laws of nature as conservation laws. An obvious example is the law of conservation of mass. As the fluid flows, mass can neither be created nor could it disappear. A less obvious one is Newton’s second law of motion. While momentum is not “conserved”, the law constrains the rate of change of momentum to be equal to force. Thus, by considering forces to be “sources” of momentum, one may still use the language of “conservation laws” to describe Newton’s second law. Examples of quantities to develop conservation laws for include mass, (linear) momentum, angular momentum (or moment of momentum), internal energy, total energy, and entropy. We will limit ourselves to mass, momentum and angular momentum.

Three main concepts need to be introduced to develop the conservation law for an abstract quantity, which we will call B . These are the volumetric density of B , the volumetric rate of generation (also known as the source) of B , and the rate of exchange of B between neighbouring fluid volumes.

1. Volumetric density of B is the quantity b such that the total amount of B in any volume Ω could be written as

$$\int_{\Omega} b \, d\Omega.$$

Examples are presented in Table 2.1. The tensorial rank of b and B are identical. Furthermore, b is an Eulerian field, i.e., $b(\mathbf{x}, t)$.

B	b	Notes
Mass	ρ	ρ is the mass density
Momentum	$\rho \mathbf{u}$	\mathbf{u} is the Eulerian fluid velocity
Angular momentum	$\mathbf{x} \times \rho \mathbf{u}$	
Internal energy	ρe	e is the specific internal energy
Entropy	ρs	s is the specific entropy

Table 2.1: Examples of physical quantities B and their volumetric density.

2. Volumetric source term also known as **body source term**, q^B , is the volumetric density of the rate of generation of B . The rate of increase of B in any volume Ω due to the volumetric source is

$$\int_{\Omega} q^B \, d\Omega.$$

Examples include gravitational force as a source for momentum and ohmic generation of heat as an example for energy. The source $q^B(\mathbf{x}, t)$ is a field with its tensorial rank being equal to that of b .

3. Surface source term, h^B , originates from the fact that the volume Ω may gain the quantity B from the neighbouring fluid. For example, the force exerted on Ω by the neighbouring fluid contributes to the rate of change of momentum in Ω . By Newton's third law, the volume Ω exerts an equal and opposite force on the surrounding fluid. In this sense, the surface source may be interpreted as an exchange of B between neighbouring fluid volumes.

A concrete example of such a term is the action of fluid pressure to generate force, or rate of change of momentum, on a volume Ω . Due to the pressure, $h^B = -p\hat{\mathbf{n}}$ because the net force due to pressure is

$$\int_{\partial\Omega} -p\hat{\mathbf{n}} \, dA.$$

Generally, the strength of such a surface source term is proportional to area of the bounding surface, rather than volume as for the volumetric source term. In general, the contribution to the rate of change of B due to the surface source is written as

$$\int_{\partial\Omega} h^B \, dA.$$

The tensorial rank of h^B and of b are equal. Clearly, h^B must also be a field, i.e. $h^B(\mathbf{x}, t)$. One important way h^B differs from both b and q^B is that in addition to being a field, h^B also has dependency on the orientation of the surface $\partial\Omega$. In other words, if a point \mathbf{X} is on the boundary of two different volumes, h^B can have different values depending on the unit outward normal to their bounding surfaces. This is represented through an explicit dependence on the unit normal as $h_B(\mathbf{x}, t; \hat{\mathbf{n}})$.

The conservation law for B may now be written as

$$\frac{D}{Dt} \int_{\Omega} b \, d\Omega = \int_{\Omega} q^B \, d\Omega + \int_{\partial\Omega} h^B \, dA. \quad (2.16)$$

2.7.1 The dimensional inconsistency of the surface source term

Let us consider an arbitrary shape for Ω . Now consider the limit of (2.16) as Ω shrinks in size indefinitely, whilst retaining its shape. Let L be a length characterizing Ω . The volume of Ω scales a L^3 and the area as L^2 . Thus, the first two terms of (2.16) scale as proportional to L^3 , while the surface source term scales proportional to L^2 , i.e.,

$$\underbrace{\frac{D}{Dt} \int_{\Omega} b \, d\Omega}_{\propto L^3} = \underbrace{\int_{\Omega} q^B \, d\Omega}_{\propto L^3} + \underbrace{\int_{\partial\Omega} h^B \, dA}_{\propto L^2}. \quad (2.17)$$

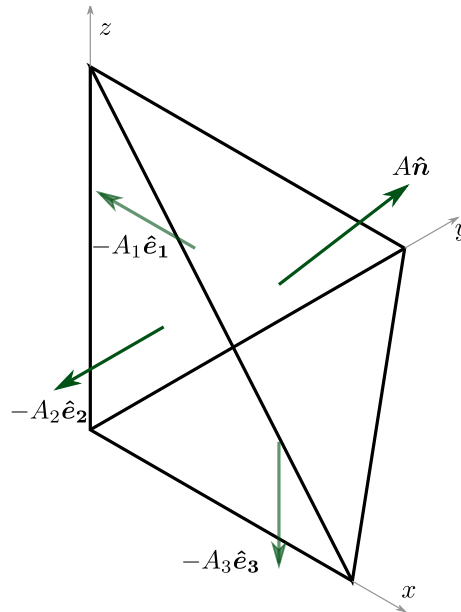


Figure 2.15: Cauchy's tetrahedron.

As the volume shrinks, L becomes successively smaller, and relative to the surface source term, the first two terms become smaller. In the limit $L \rightarrow 0$, the conservation law for B (2.16) reduces to

$$\int_{\partial\Omega} h^B(\mathbf{x}, t; \hat{\mathbf{n}}) dA = 0. \quad (2.18)$$

In other words, for *any* infinitesimal volume, the contribution of the surface source term that is proportional to the area of the bounding surface must vanish. The consequence of this condition is the basis for all continuum mechanics.

2.7.2 Cauchy's tetrahedron argument

Augustine-Louis Cauchy, a french mathematician, engineer and physicist, reasoned the compelling consequence of (2.18) by taking the shape of the volume Ω to be a tetrahedron, as shown in Figure 2.15. The tetrahedron has four faces; the area of the inclined face is given by the (vector³) $A\hat{\mathbf{n}}$, while the remaining three faces are $-A_1\hat{\mathbf{e}}_1$, $-A_2\hat{\mathbf{e}}_2$ and $-A_3\hat{\mathbf{e}}_3$, respectively, so that $A\hat{\mathbf{n}} = A_i\hat{\mathbf{e}}_i$. We will now evaluate the terms of the integral in (2.18), but note because of the infinitesimal size of the tetrahedron, we will not need the distribution of h_B over the areas. The value of h^B may be considered a constant with \mathbf{x} , and we will drop the dependence on \mathbf{x} in the notation here. But because we could choose a tetrahedron of any proportions, the dependence on $\hat{\mathbf{n}}$ remains, which we will explicitly write.

The contribution to the integral in (2.18) from the four face may now be written as

$$h^B(\hat{\mathbf{n}})A + h^B(-\hat{\mathbf{e}}_1)A_1 + h^B(-\hat{\mathbf{e}}_2)A_2 + h^B(-\hat{\mathbf{e}}_3)A_3 = 0. \quad (2.19)$$

By the principle of exchange of B , $h^B(-\hat{\mathbf{e}}_1) = -h^B(\hat{\mathbf{e}}_1)$, which arises from the fact that the amount of B gained by the tetrahedron is lost by the neighbouring fluid. Let's further define (in index notation) $T_{\dots j}^B = h^B(\hat{\mathbf{e}}_j)$, where the \dots on the indices of T^B accounts for the free indices of h^B , which may have a nonzero tensorial rank. In this way, T_B has a tensorial rank one higher than h^B . Furthermore, it follows from the geometry for tetrahedrons, $A_i = An_i$. With this notation, (2.19) becomes

$$h^B(\hat{\mathbf{n}}) = T_{\dots j}^B n_j. \quad (2.20)$$

This dependence of the surface source term on the surface normal helps satisfies the condition (2.18) not only for a tetrahedron but also for any Ω . This is so because

$$\int_{\partial\Omega} h^B(\mathbf{x}, t; \hat{\mathbf{n}}) dA = \int_{\partial\Omega} T_{\dots j}^B n_j dA = \int_{\Omega} \frac{\partial T_{\dots j}^B}{\partial x_j} d\Omega, \quad (2.21)$$

³Reminder: the direction of a planar area is normal to its face.

where the last step follows from the tensorial form of the divergence theorem. This step converts the surface integral to a volume integral, and in the limit of vanishing volume Ω , this term scales as L^3 and not as L^2 .

The conservation law for B now reads

$$\frac{D}{Dt} \int_{\Omega} b \, d\Omega = \int_{\Omega} q^B \, d\Omega + \int_{\partial\Omega} T^{\dots j} n_j \, dA = \int_{\Omega} q^B \, d\Omega + \int_{\Omega} \frac{\partial T^{\dots j}}{\partial x_j} \, d\Omega. \quad (2.22)$$

Applying the Reynolds transport theorem and the divergence to the left hand side yields two additional forms of this equation.

$$\int_{\Omega} \frac{\partial b}{\partial t} \, d\Omega + \int_{\partial\Omega} b u_j n_j \, dA = \int_{\Omega} q^B \, d\Omega + \int_{\partial\Omega} T^{\dots j} n_j \, dA = \int_{\Omega} q^B \, d\Omega + \int_{\Omega} \frac{\partial T^{\dots j}}{\partial x_j} \, d\Omega, \quad (2.23)$$

$$\int_{\Omega} \left(\frac{\partial b}{\partial t} + \frac{\partial(bu_j)}{\partial x_j} \right) \, d\Omega = \int_{\Omega} q^B \, d\Omega + \int_{\partial\Omega} T^{\dots j} n_j \, dA = \int_{\Omega} q^B \, d\Omega + \int_{\Omega} \frac{\partial T^{\dots j}}{\partial x_j} \, d\Omega, \quad (2.24)$$

Equation (2.22-2.24) are integral representations of the law of conservation of B . The term $bu_j - T^{\dots j}$ is the total flux of b and bu_j is the convective flux. (In general, the flux of b is the rate at which b crosses a surface per unit area.) Conservation laws also have a differential form. To derive it, note that (2.24) holds irrespective of the volume Ω . This is only possible if the integrand itself vanishes everywhere, i.e.,

$$\frac{\partial b}{\partial t} + \frac{\partial(bu_j)}{\partial x_j} = q^B + \frac{\partial T^{\dots j}}{\partial x_j}. \quad (2.25)$$

We will see that in the differential representation of general conservation laws, the rate of change of the density b is balanced by the divergence of the flux of b and the volumetric generation of b .

We now apply the result of this general analysis to specific quantities.

2.8 Conservation of Mass a.k.a. Mass Balance

Now we use the (classical) physical law that mass can neither be created or destroyed. This implies, when $b = \rho$, then $q^B = T^{\dots j} = 0$, and (2.22-2.24) becomes

$$\frac{D}{Dt} \int_{\Omega} \rho \, d\Omega = 0, \quad (2.26)$$

$$\int_{\Omega} \frac{\partial \rho}{\partial t} \, d\Omega + \int_{\partial\Omega} \rho u_j n_j \, dA = 0, \quad (2.27)$$

$$\int_{\Omega} \left(\frac{\partial \rho}{\partial t} + \frac{\partial(\rho u_j)}{\partial x_j} \right) \, d\Omega = 0. \quad (2.28)$$

Equations (2.26-2.28) are integral representations of the law of conservation of mass. The differential representation corresponding to (2.25)

$$\frac{\partial \rho}{\partial t} + \frac{\partial(\rho u_j)}{\partial x_j} = 0 \quad \text{or in vector notation} \quad \frac{\partial \rho}{\partial t} + \nabla \cdot (\rho \mathbf{u}) = 0. \quad (2.29)$$

We will now interpret the terms in some of representations of the law of conservation of mass, starting with (2.27). The first term in this equation is the rate of change of mass in a fixed (i.e. Eulerian) volume Ω . The second term is the rate at which mass exits the volume due to the Eulerian velocity \mathbf{u} . Conservation of mass implies that the two rates must balance, which is the statement of (2.27).

Next we will discuss the terms in (2.29). The first term is the Eulerian rate-of-change of density the second is the divergence of the convective mass flux $\rho \mathbf{u}$. Another form of (2.29), written using the expression

$$\frac{\partial \rho}{\partial t} + \mathbf{u} \cdot \nabla \rho + \rho \nabla \cdot \mathbf{u} = 0 \quad (2.30)$$

as

$$\frac{1}{\rho} \frac{D\rho}{Dt} = -\nabla \cdot \mathbf{u} = -\frac{1}{V} \frac{DV}{Dt}, \quad (2.31)$$

can be interpreted as the relative Lagrangian rate of change of density is balanced by the negative of the relative Lagrangian rate of change of volume. In other words, if volume of an infinitesimal Lagrangian element increases, its density must decrease.

If either the fluid or the flow is “incompressible”, that means that the density of infinitesimal Lagrangian fluid particles does not change with time, i.e., $D\rho/Dt = 0$. This implies

$$\nabla \cdot \mathbf{u} \equiv 0 \text{ everywhere.} \quad (2.32)$$

2.9 Conservation of Momentum a.k.a. Momentum Balance

The density of momentum is $\rho\mathbf{u}$, and its rate of change is a force as per Newton’s second law of motion. The volumetric source term is a force per unit volume that acts on the fluid and is termed a “body force”, e.g. the force of gravity. We will denote it by $q^B = \rho\mathbf{g}$, where \mathbf{g} is acceleration due to the body force. Here the density and the volumetric source of momentum are vectors. The second rank tensor resulting from the surface force $T^B = \mathbf{T}$ is the stress tensor, which when acting on an area element dA with normal n_j exerts the force $dF_i = T_{ij}n_j dA$.

The three different integral forms representing conservation of momentum are

$$\frac{D}{Dt} \int_{\Omega} \rho u_i d\Omega = \int_{\Omega} \rho g_i d\Omega + \int_{\partial\Omega} T_{ij}n_j dA = \int_{\Omega} \rho g_i d\Omega + \int_{\Omega} \frac{\partial T_{ij}}{\partial x_j} d\Omega. \quad (2.33)$$

$$\int_{\Omega} \frac{\partial(\rho u_i)}{\partial t} d\Omega + \int_{\partial\Omega} \rho u_i u_j n_j dA = \int_{\Omega} \rho g_i d\Omega + \int_{\partial\Omega} T_{ij}n_j dA = \int_{\Omega} \rho g_i d\Omega + \int_{\Omega} \frac{\partial T_{ij}}{\partial x_j} d\Omega, \quad (2.34)$$

$$\int_{\Omega} \left(\frac{\partial(\rho u_i)}{\partial t} + \frac{\partial(\rho u_i u_j)}{\partial x_j} \right) d\Omega = \int_{\Omega} \rho g_i d\Omega + \int_{\partial\Omega} T_{ij}n_j dA = \int_{\Omega} \rho g_i d\Omega + \int_{\Omega} \frac{\partial T_{ij}}{\partial x_j} d\Omega. \quad (2.35)$$

The differential form of momentum balance is

$$\frac{\partial(\rho u_i)}{\partial t} + \frac{\partial(\rho u_i u_j)}{\partial x_j} = \rho g_i + \frac{\partial T_{ij}}{\partial x_j}. \quad (2.36)$$

The left-hand side of (2.36) is $D(\rho\mathbf{u})/Dt$ can be simplified further by using the product rule and mass balance (2.29) as

$$\frac{\partial(\rho u_i)}{\partial t} + \frac{\partial(\rho u_i u_j)}{\partial x_j} = u_i \left(\frac{\partial\rho}{\partial t} + \frac{\partial(\rho u_j)}{\partial x_j} \right) \overset{0, \text{ mass balance}}{\rightarrow} + \rho \left(\frac{\partial u_i}{\partial t} + u_j \frac{\partial u_i}{\partial x_j} \right). \quad (2.37)$$

This simplifies the differential form of momentum balance (2.36) to the Cauchy momentum balance equation as

$$\rho \frac{Du_i}{Dt} \equiv \rho \left(\frac{\partial u_i}{\partial t} + u_j \frac{\partial u_i}{\partial x_j} \right) = \rho g_i + \frac{\partial T_{ij}}{\partial x_j}, \quad \text{or} \quad \rho \frac{D\mathbf{u}}{Dt} = \rho\mathbf{g} + \nabla \cdot \mathbf{T}. \quad (2.38)$$

The left-hand side of this equation is mass times acceleration per unit volume of an infinitesimal Lagrangian element. The right-hand side contains the net forces on this volume per unit volume. It is obvious that $\rho\mathbf{g}$ is the body force per unit volume. To see that $\nabla \cdot \mathbf{T}$ is the unbalanced surface force per unit volume, consider forces acting on a infinitesimal cubic fluid element with side d and bottom corner at $\mathbf{x} = (x_0, y_0, z_0)$; see figure 2.16. We will start with the x -component of this force which will involve us calculating $T_{1j}n_j \delta A$ (with $\delta A = d^2$) over all six sides of the cube.

$$\delta F_1 = d^2 (T_{11}(x_0 + d, y, z) - T_{11}(x_0, y, z)) \quad (2.39)$$

$$+ d^2 (T_{12}(x, y_0 + d, z) - T_{12}(x, y_0, z)) \quad (2.40)$$

$$+ d^2 (T_{13}(x, y, z_0 + d) - T_{13}(x, y, z_0)). \quad (2.41)$$

Taylor expanding this expression in small d and keeping the leading order only, we have:

$$\delta F_1 = d^3 \left[\frac{\partial T_{11}(x, y, z)}{\partial x} + \frac{\partial T_{12}(x, y, z)}{\partial y} + \frac{\partial T_{13}(x, y, z)}{\partial z} \right] = d^3 \frac{\partial T_{1j}(x, y, z)}{\partial x_j}$$

where we have used the summation convention (with j the repeated index).

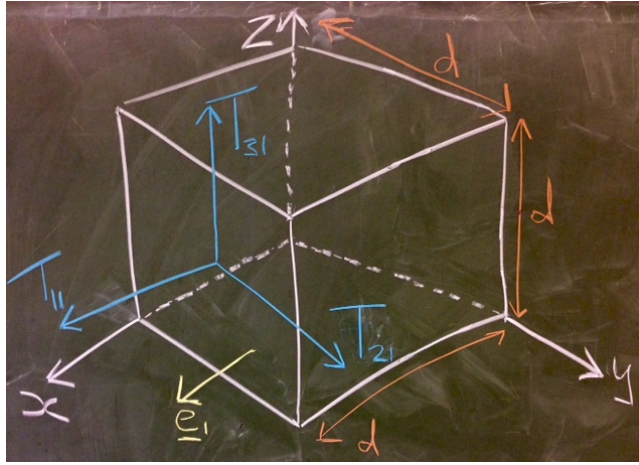


Figure 2.16: An infinitesimal cubic fluid element. Shown are the components of the stress tensor acting on one face whose normal aligns with the x-axis.

Generalising to the other force components, we have:

$$\delta F_i = d^3 \frac{\partial T_{ij}(x, y, z)}{\partial x_j}.$$

symbolically this is the divergence of the stress tensor $\delta \mathbf{F} = d^3 \nabla \cdot \mathbf{T}$.

2.10 Conservation of Angular Momentum a.k.a. Torque Balance

The angular momentum changes at a rate equal to the net external torque applied on a body. For angular momentum, $b = \mathbf{x} \times \rho \mathbf{u}$, $q^B = \mathbf{x} \times \rho \mathbf{g}$, and $h^B = \mathbf{x} \times (\mathbf{T} \cdot \hat{\mathbf{n}})$. Note that the sources of angular momentum are related to the sources of linear momentum. We will go straight to the differential form of the angular momentum balance, which reads

$$\frac{\partial(\epsilon_{ijk} x_j \rho u_k)}{\partial t} + \frac{\partial(\epsilon_{ijk} x_j \rho u_k u_m)}{\partial x_m} = \epsilon_{ijk} x_j \rho g_k + \frac{\partial(\epsilon_{ijk} x_j T_{km})}{\partial x_m}. \quad (2.42)$$

Differentiating each term using the product rule yields

$$\epsilon_{ijk} x_j \left(\frac{\partial(\rho u_k)}{\partial t} + \frac{\partial(\rho u_k u_m)}{\partial x_m} - \rho g_k - \frac{\partial(T_{km})}{\partial x_m} \right) + \epsilon_{ijk} \rho u_j u_k = \epsilon_{ijk} T_{jk}. \quad (2.43)$$

The first term is the cross product of \mathbf{x} with the linear momentum equation (2.36), and the second term is zero due to the anti-symmetry of ϵ_{ijk} in the indices j, k and the symmetry of $u_j u_k$. Thus the only remaining term is $\epsilon_{ijk} T_{jk} = 0$. A direct consequence of this is that $T_{jk} = T_{kj}$, or, in other words, \mathbf{T} is a symmetric second-rank tensor.

2.11 Constitutive laws

The differential equations governing a continuum material in an Eulerian description that we have derived so far are mass balance (2.29) and momentum balance (2.38). These equations are partial differential equations for determining the density and velocity by integrating in time, i.e., if suitable initial conditions are available for ρ and \mathbf{u} , and the volumetric forces \mathbf{g} and stress \mathbf{T} were known, then one may use these equations to find the rate of change of ρ and \mathbf{u} , which one then uses to determine the subsequent evolution of ρ and \mathbf{u} . The situation is similar to the use of Newton's second law of motion for describing the motion of rigid bodies; knowing the external forces one uses it to integrate for velocity and position. Here we think about integrating for ρ and \mathbf{u} . Let's examine quantities we do not know yet; viz. \mathbf{g} and \mathbf{T} .

The simplest one is \mathbf{g} : it must be prescribed as part of the problem.

The stress \mathbf{T} needs to be determined based on the fluid and the flow, so that the system of equations (2.29) and (2.38) is closed. The closure of this system is made by the constitutive law for the continuum material.

This constitutive law is what distinguishes between a solid and a fluid, and for that matter, between different kinds of “complex” fluids. Next we present some considerations for a constitutive law.

2.11.1 General considerations

An infinitesimal fluid element must continue to deform when a shear stress acts on it – this is the definition of a fluid. Therefore, we expect the components of the stress to be related to the components of the rate of shear tensor, i.e.,

$$T_{ij} = f_{ij}[e_{mn}; \rho]. \quad (2.44)$$

We will start with some simple models.

2.11.2 An Ideal or Inviscid fluid

In an ideal or inviscid fluid there is no friction between fluid elements, so that the stress is given by an isotropic pressure that acts normal to the surface and inward. Therefore, our particular form of the stress tensor (known as a constitutive relation) is

$$T_{ij} = -p\delta_{ij}. \quad (2.45)$$

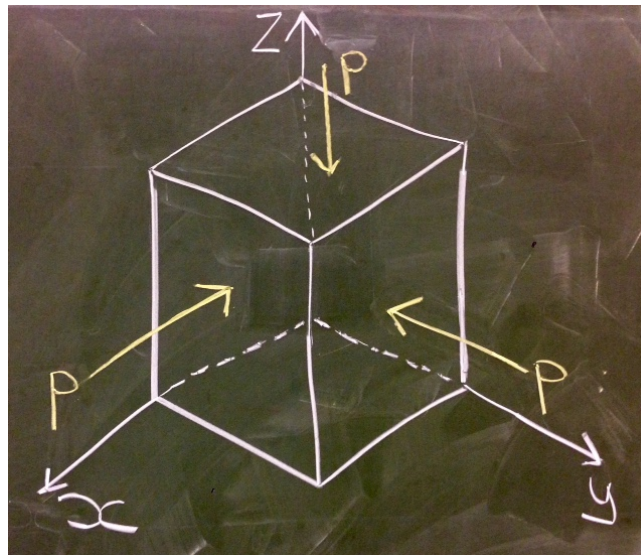


Figure 2.17: In an inviscid fluid the stress is generated entirely by the pressure, which acts with equal magnitude on all faces of our infinitesimal cubic fluid element. Clearly then, flow must be driven by this pressure changing from point to point, i.e. by spatial gradients in pressure.

Substituting into Cauchy’s equation (2.38), we arrive at the so-called Euler equation which describes inviscid fluid flow

$$\rho \frac{Du_i}{Dt} = -\frac{\partial p}{\partial x_i} + \rho g_i \quad \text{or in vector notation} \quad \rho \frac{D\mathbf{u}}{Dt} = -\nabla p + \rho \mathbf{g}. \quad (2.46)$$

This equation is named after Leonhard Euler, the celebrated Swiss mathematician.

Here the pressure p is a thermodynamic quantity, so an equation of state that relates p to other thermodynamic quantities would serve this purpose. The problem is that thermodynamic relations also introduce some other thermodynamic variable independent of density (say temperature) into consideration, which in itself could be non-uniformly distributed throughout the fluid. So an equation incorporating the law of conservation of thermal energy must be derived and treated for this new variable with mass and momentum balance. In some limited but practically useful circumstances, it is possible to eliminate the temperature and simply write $p(\rho)$. Examples include the propagation of sound waves. Under those circumstances, p is well-defined. A very singular special case of this scenario is for an incompressible flow, for which ρ is a constant, and, therefore, there is no explicit form for $p(\rho)$ but p must be deduced such that no changes in ρ occur.

We will see later that an ideal fluid has a zero Newtonian viscosity.

In the absence of fluid motion $D_t \mathbf{u} = 0$ we recover a hydrostatic balance $p = p_0 - \rho g z$.

2.11.3 A Newtonian Fluid

To describe a viscous fluid, we separate the pressure contribution to the stress tensor from the remaining terms — the latter will be associated with an internal friction or viscosity as

$$T_{ij} = -p\delta_{ij} + \sigma_{ij}, \quad (2.47)$$

where σ_{ij} is called the *deviatoric stress tensor*. For a Newtonian fluid, the deviatoric stress arises from viscosity, and therefore, σ_{ij} is also called the *viscous stress tensor*. An ideal fluid is characterized by $\sigma_{ij} \equiv 0$. For a general fluid the dependence on the rate-of-strain tensor in (2.44) is passed on to σ_{ij} as $\sigma_{ij} = s_{ij}[e_{mn}; \rho]$ for some tensorial function s_{ij} .

The Newtonian constitutive law corresponds to the relation where the relation between σ_{ij} and e_{mn} is linear and isotropic. Linearity means that

$$\sigma_{ij} = A_{ijmn} e_{mn}, \quad (2.48)$$

where A_{ijmn} is a constant fourth rank tensor. For the relation to be isotropic, A_{ijmn} must be isotropic, i.e., its components may not depend of the coordinate system used to represent the tensor. We saw in (1.12c) that the most general fourth rank isotropic tensor has the form $\lambda\delta_{ij}\delta_{kl} + \alpha\delta_{ik}\delta_{jl} + \beta\delta_{il}\delta_{jk}$, where λ , α and β are scalar constants. Substituting in (2.48) yields $\sigma_{ij} = (\alpha + \beta)e_{ij} + \lambda\delta_{ij}e_{mm}$. Here we learn that, in general, two constants are needed to specify the Newtonian constitutive law. However, for incompressible fluids (which Newton tacitly assumed), the term $e_{mm} = \nabla \cdot \mathbf{u}$ is identically zero, and setting $(\alpha + \beta)$ to 2μ , where μ is the coefficient of Newtonian viscosity, yields the tensorial form of the Newtonian constitutive law for an incompressible fluid⁴

$$\sigma_{ij} = 2\mu e_{ij} \quad \text{so that} \quad T_{ij} = -p\delta_{ij} + \mu \left(\frac{\partial u_i}{\partial x_j} + \frac{\partial u_j}{\partial x_i} \right). \quad (2.50)$$

Under a uniform shear flow, such as in Figure 2.1, the relation (2.50) reduces to the one-dimensional relation $\sigma = \mu\dot{\gamma}$.

Substituting (2.50) into Cauchy's equation (2.38), we have the *incompressible Navier-Stokes equations*:

$$\rho \frac{Du_i}{Dt} = -\frac{\partial p}{\partial x_i} + \mu \frac{\partial^2 u_i}{\partial x_j^2} + \rho g_i \quad \text{or symbolically} \quad \rho \frac{D\mathbf{u}}{Dt} = -\nabla p + \mu \nabla^2 \mathbf{u} + \rho \mathbf{g}. \quad (2.51)$$

For zero viscosity, (2.51) reduces to the Euler equation (2.46) for ideal fluid.

2.11.4 Navier-Stokes in cylindrical coordinates

The incompressible form of momentum conservation for the radial, azimuthal and axial components of velocity (u, v, w) in a cylindrical polar coordinate system (r, θ, z) in differential form are:

$$\rho \left(\frac{\partial u}{\partial t} + u \frac{\partial u}{\partial r} + \frac{v}{r} \frac{\partial u}{\partial \theta} + w \frac{\partial u}{\partial z} - \frac{v^2}{r} \right) = -\frac{\partial p}{\partial r} + \rho g_r + \mu \left\{ \frac{\partial}{\partial r} \left(\frac{1}{r} \frac{\partial(ur)}{\partial r} \right) + \frac{1}{r^2} \frac{\partial^2 u}{\partial \theta^2} - \frac{2}{r^2} \frac{\partial v}{\partial \theta} + \frac{\partial^2 u}{\partial z^2} \right\} \quad (2.52a)$$

$$\rho \left(\frac{\partial v}{\partial t} + u \frac{\partial v}{\partial r} + \frac{v}{r} \frac{\partial v}{\partial \theta} + w \frac{\partial v}{\partial z} + \frac{uv}{r} \right) = -\frac{1}{r} \frac{\partial p}{\partial \theta} + \rho g_\theta + \mu \left\{ \frac{\partial}{\partial r} \left(\frac{1}{r} \frac{\partial(vr)}{\partial r} \right) + \frac{1}{r^2} \frac{\partial^2 v}{\partial \theta^2} + \frac{2}{r^2} \frac{\partial u}{\partial \theta} + \frac{\partial^2 v}{\partial z^2} \right\} \quad (2.52b)$$

$$\rho \left(\frac{\partial w}{\partial t} + u \frac{\partial w}{\partial r} + \frac{v}{r} \frac{\partial w}{\partial \theta} + w \frac{\partial w}{\partial z} \right) = -\frac{\partial p}{\partial z} + \rho g_z + \mu \left\{ \frac{1}{r} \frac{\partial}{\partial r} \left(r \frac{\partial w}{\partial r} \right) + \frac{1}{r^2} \frac{\partial^2 w}{\partial \theta^2} + \frac{\partial^2 w}{\partial z^2} \right\}, \quad (2.52c)$$

and the mass conservation equations is

$$\nabla \cdot \mathbf{u} = \frac{1}{r} \frac{\partial(ru)}{\partial r} + \frac{1}{r} \frac{\partial v}{\partial \theta} + \frac{\partial w}{\partial z} = 0. \quad (2.53)$$

Here g_r , g_θ and g_z are the r , θ and z components of gravitational acceleration.

⁴For a *compressible flow*, where σ_{ij} can depend both on e_{ij} and the identity tensor, the most general form of such a tensor is

$$\sigma_{ij} = \underbrace{2\mu \left(e_{ij} - \frac{1}{3} \delta_{ij} e_{kk} \right)}_{\text{Strain without volume change}} + \underbrace{\xi e_{kk} \delta_{ij}}_{\text{Strain due to volume change}}, \quad (2.49)$$

where μ is the viscosity ('shear viscosity' or 'first viscosity coefficient'), ξ is the "bulk viscosity" or the "second viscosity coefficient".

2.12 Boundary and initial conditions

As usual for PDEs, in order to find a unique solution one has to specify appropriate boundary conditions and initial conditions.

2.12.1 Initial conditions

The set of relevant fields must be specified at $t = 0$ at each point \mathbf{x} in the domain occupied by the fluid. For incompressible fluids, one only has to specify the initial velocity field \mathbf{u}_0

$$\mathbf{u}(\mathbf{x}, t = 0) = \mathbf{u}_0. \quad (2.54)$$

2.12.2 Boundary conditions

The number of boundary conditions required depends on the bulk equations (Euler or Navier Stokes in our case) and their form is determined by the properties of the boundaries (i.e. the physics at the boundary).

Viscous Fluids

At solid impenetrable boundaries, it has been found empirically that the fluid velocity at the boundary $\partial\Omega$ of the retaining volume Ω adjusts itself to the boundary's velocity \mathbf{U}_b : this is the famous *no-slip boundary condition*:

$$\mathbf{u}(\mathbf{x}, t) = \mathbf{U}_b(\mathbf{x}, t), \quad \mathbf{x} \in \partial\Omega. \quad (2.55)$$

Inviscid Fluids

For inviscid fluids, where one only has first derivatives of fluid velocity (no $\nabla^2 \mathbf{u}$ term), one can only enforce impenetrability of the boundary, i.e. that the normal to the boundary velocity component has to match to the one of the boundary, whereas the parallel velocity component remains arbitrary, since the fluid can slip freely along the boundary in the absence of internal friction. This is the so-called *free-slip boundary conditions* written as

$$\mathbf{u}_\perp(\mathbf{x}, t) = \mathbf{U}_{b\perp}(\mathbf{x}, t), \quad \mathbf{x} \in \partial\Omega. \quad (2.56)$$

In addition, at every point on the fluid where the fluid flows inward, the vorticity needs to be specified. This is an advanced condition, which we will not pursue in this course.

Kinematic boundary condition for moving material boundaries

For cases like the free surface, the motion of the boundary itself occurs under the influence of the fluid flow. In other words, the reason the free surface changes shape is because the fluid particles at the free surface flow. Mathematically, the free surface is a *material boundary*, i.e.,

$$\frac{D\mathbf{X}}{Dt} = \mathbf{u}(\mathbf{X}, t), \quad \text{for the Lagrangian label } \mathbf{X} \in \partial\Omega. \quad (2.57)$$

Traction condition or the dynamic boundary condition

In lieu of specifying velocity, one may also specify the traction t_i , i.e. the force per unit area on the boundary. In general, the traction condition is written as

$$T_{ij}n_j = t_i, \quad \mathbf{x} \in \partial\Omega, \quad \text{where } n_i \text{ is the unit normal.} \quad (2.58)$$

This condition is especially useful for moving free surfaces, where two conditions are needed, viz., one for specifying the rate of motion of the interface and another as a boundary condition for the fluid partial differential equations. In that case, along with the kinematic boundary condition, the traction information furnishes the second condition.

Chapter 3

One-dimensional flows

In this chapter, we will treat exact solutions of Navier-Stokes equations that result from the assumption of “one-dimensionality”. Such flows do occur in nature and are highly relevant for many common applications.

3.1 Steady flows

Several key features are common amongst the one-dimensional solutions of Navier-Stokes equations, which are summarized here.

3.1.1 One-dimensionality

The assumption of one-dimensionality underlies all the flows presented in this chapter. One-dimensionality means that in either Cartesian or cylindrical-polar coordinates, the velocity has only one non-zero component of velocity, which varies in a direction perpendicular to the flow. Here are examples, which are illustrated in Figure 3.1:

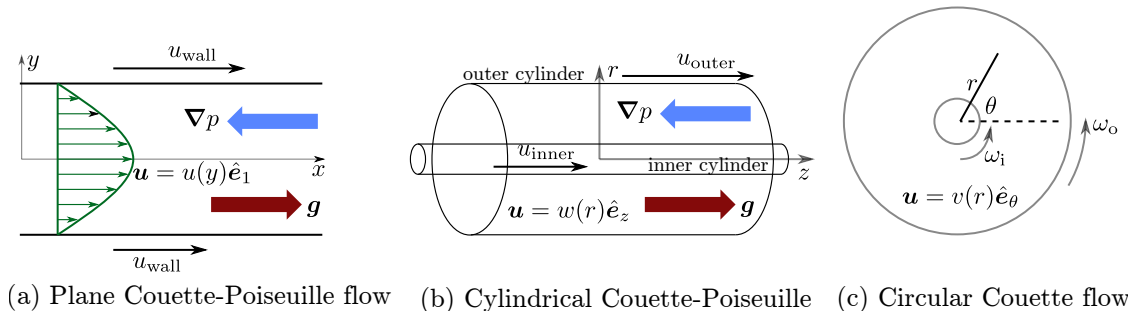


Figure 3.1: Schematic of three cases of one-dimensional flows.

1. **Plane Couette-Poiseuille flow:** This is a flow of a fluid sandwiched between two infinite planar walls, shown in Figure 3.1(a). In this case the flow is along a single direction x parallel to the wall and the flow velocity varies in the direction y perpendicular to the walls.
2. **Cylindrical Couette-Poiseuille flow**, some cases of which are also known as **Hagen-Poiseuille flow:** This is the flow in the axial (i.e., z) direction through the gap between two infinitely-long coaxial cylinders. The flow varies only with r , the radial distance from the axis.
3. **Circular Couette flow:** This is the flow of a fluid in the azimuthal (i.e., \hat{e}_θ) direction between two coaxial cylinders. The flow velocity varies only with the radial distance from the axis, i.e. r .

In practice, the walls on plane Couette-Poiseuille flow and the cylinders in the cylindrical Couette Poiseuille flow are not infinitely long. This is only meant as an approximation for the case where they are much longer than the width of the gap through which the flow occurs.

In all these cases, the component of the acceleration of the fluid in the direction of the flow is zero. In fact, the acceleration is zero for the case of plane and cylindrical Couette-Poiseuille flow. For circular Couette flow the acceleration is centripetal. Therefore, when solving for the flow using the Navier-Stokes equations, the inertial term drops out of the momentum balance in the direction of the flow.

3.1.2 The driving force

The flow could be driven by one of the following three agencies:

1. **Pressure gradient:** A gradient of pressure is said to have been set and driving the flow when an external agency, e.g., a pump, increases the pressure at the inlet of the pipe or channel, or decreases it far downstream. In this case, the flow is driven by the pressure decreasing along the length of the channel in the direction of the flow. The resulting flow is called a Poiseuille flow, after the French physicist and physiologist Jean Léonard Marie Poiseuille, who used this type of analysis to study blood flow through capillaries. The general type of question that arises for these types of flow are about the pressure gradient needed to drive a certain volumetric flow rate through the domain.
2. **Gravity:** Similar to pressure gradient, the flow could be driven by an external volumetric force, such as gravity.
3. **Motion of the walls:** An external agency could push on the walls to move along the direction of the flow, thereby dragging the fluid next to them. The general question that comes up in such cases is the shear stress needed to move the walls at prescribed speeds. This type of flow is called Couette flow, after the French physicist Maurice Marie Alfred Couette.

Note that in circular Couette flow either a pressure gradient or a constant force of gravity cannot drive the flow. This is so because of periodicity in the direction of the flow. Pressure cannot continually decrease along the flow because after an angle of 2π we return back to the original point, where we expect to find the same pressure as we started. Therefore, circular Couette flow may only be driven by motion of the walls.

All three methods of driving the flow can be used in instruments that measure the dynamic viscosity of the fluid.

3.2 Select solutions of Navier-Stokes

Here we present some examples of solutions of Navier-Stokes equations for steady one-dimensional flows.

3.2.1 Plane Poiseuille flow

This case corresponds to the pressure-driven flow in a channel. The walls of the channel are stationary in the lab frame in this case.

Given the flow profile $\mathbf{u} = u(y)\hat{\mathbf{e}}_x$, the equation of continuity is trivially satisfied and the two-dimensional Navier-Stokes equations in Cartesian coordinates simplify to

$$\frac{\partial p}{\partial x} = \mu \frac{\partial^2 u}{\partial y^2}, \quad (3.1a)$$

$$\frac{\partial p}{\partial y} = 0. \quad (3.1b)$$

According to (3.1b), the pressure does not vary with y , and hence we can assert that $p(x)$ alone. Then in (3.1a), the left-hand side depends on x alone, whereas the right-hand side on y alone, implying that both sides must be a constant. Physically, because the flow does not change with x , we do not expect the pressure gradient to vary with x either. Using the constancy of $\partial p/\partial x$, (3.1a) may be readily integrated to yield

$$u(y) = \frac{1}{2\mu} \frac{\partial p}{\partial x} y^2 + Ay + B, \quad (3.2)$$

where A and B are constants of integration. They are determined by the no-slip boundary conditions on the two walls

$$u\left(y = \pm \frac{H}{2}\right) = 0, \quad (3.3)$$

which yields

$$u(y) = -\frac{1}{2\mu} \frac{\partial p}{\partial x} \left(\frac{H^2}{4} - y^2 \right). \quad (3.4)$$

The flow rate per unit width Q/w is

$$\frac{Q}{w} = -\int_{-H/2}^{H/2} u(y) dy = -\frac{1}{2\mu} \frac{\partial p}{\partial x} \left(\frac{H^2 y}{4} - \frac{y^3}{3} \right)_{-H/2}^{H/2} = -\frac{H^3}{12\mu} \frac{\partial p}{\partial x}. \quad (3.5)$$

This is the relation between the pressure-gradient and the flow rate that is practically sought. Experimental measurements of H , $\partial p/\partial x$ and Q/w may be used to determine the dynamic viscosity μ .

Also worth noting is the result that the average fluid speed $Q/(wH)$ is $2/3$ of the maximum fluid speed $u(y=0)$.

3.2.2 Hagen-Poiseuille

This is the flow driven by a pressure gradient inside a pipe. In this case, the inside cylinder shown in Figure 3.1(b) is absent the fluid fills all the space inside the outer cylinder. Also, the outer cylinder is stationary.

Continuity is trivially satisfied by the velocity profile given by $\mathbf{u} = w(r)\hat{e}_z$. The radial and axial components of the Navier-Stokes equations, (2.52a) and (2.52c), respectively, simplify to

$$\frac{\partial p}{\partial r} = 0, \quad (3.6)$$

$$\frac{\partial p}{\partial z} = \frac{\mu}{r} \frac{\partial}{\partial r} \left(r \frac{\partial w}{\partial r} \right). \quad (3.7)$$

Similar to the case of plane Poiseuille flow, here the pressure depends on z alone and must decrease at a rate independent of z , i.e. $\partial p/\partial z$ is a constant. The z -momentum equation may then be integrated to yield

$$r \frac{\partial w}{\partial r} = \frac{r^2}{2\mu} \frac{\partial p}{\partial z} + A, \quad w(r) = \frac{r^2}{4\mu} \frac{\partial p}{\partial z} + A \ln r + B, \quad (3.8)$$

where A and B are constants of integration.

At this stage, it appears that we only have one boundary condition $w(r=R) = 0$ corresponding to no-slip on the outer wall at $r=R$. It is commonly (and in my opinion incorrectly) stated that a second condition is that the velocity cannot blow up on the axis $r=0$ and hence $A=0$. Then, one uses no-slip on $r=R$ to obtain

$$w(r) = -\frac{1}{4\mu} \frac{\partial p}{\partial z} (R^2 - r^2). \quad (3.9)$$

A much more convincing argument for setting $A=0$ is as follows. Consider the surface of an imaginary cylinder at radius r . The axial force exerted by the fluid inside of the cylinder on the fluid outside is

$$\tilde{F}_z = 2\pi r \sigma_{rz} = 2\pi r \mu \frac{\partial w}{\partial r} = 2\pi \left(\frac{r^2}{2\mu} \frac{\partial p}{\partial z} + A \right), \quad (3.10)$$

where we have used (3.8) in the final step. Now consider the limit of r approaching zero, i.e. the imaginary cylinder shrinking towards the axis. In the limit \tilde{F}_z approaches $2\pi A$. Based on this, it seems that A is related to the influence of an imaginary agency on the axis of the cylinder to exert a shear force on the fluid. Since we do not have any such agency present in the problem under consideration, \tilde{F}_z must vanish, and so must A .

The relation between pressure gradient and the volumetric flow rate through the pipe Q may also be found easily as

$$Q = \int_0^R 2\pi r w(r) dr = -\frac{2\pi}{4\mu} \frac{\partial p}{\partial z} \int_0^R r(R^2 - r^2) dr = -\frac{2\pi}{4\mu} \frac{\partial p}{\partial z} \left(\frac{R^2 r^2}{2} - \frac{r^4}{4} \right)_0^R = -\frac{\pi R^4}{8\mu} \frac{\partial p}{\partial z}. \quad (3.11)$$

Also worth noting is the result that the average fluid speed $Q/(\pi R^2)$ is $1/2$ of the maximum fluid speed $w(r=0)$.

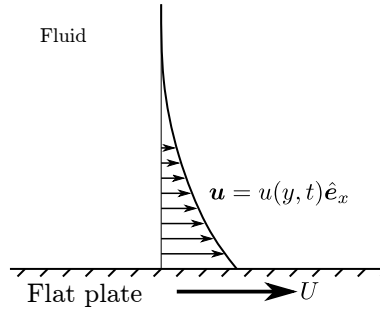


Figure 3.2: Schematic setup of the Stokes first problem.

3.3 Unsteady flows

If condition of steadiness is relaxed, then the governing equations simplify to a partial differential equation for the flow profile that depends only on one spatial coordinate and time. Here we present one such example. The same three geometrical categories and the three kinds of driving forces can be used to classify this type of flow. We will not repeat them here.

Because of the partial nature of the differential equation, the solution procedure depends on the particular problem and can be a little involved. It is illustrated for the case of Stokes first problem below.

3.3.1 Stokes first problem

An infinite flat plate borders a semi-infinite layer of fluid of density ρ and viscosity μ , see Figure 3.2. The fluid and the plate are initially stationary. At $t = 0$, the plate impulsively starts to translate parallel to itself with speed U . This drags the fluid adjacent to the plate.

In this case, the fluid velocity may be assumed to be one-dimensional as $\mathbf{u} = u(y, t)\hat{e}_x$. With this assumption, the velocity profile satisfies continuity exactly. The governing Navier-Stokes equations simplify to

$$\rho \frac{\partial u}{\partial t} = -\frac{\partial p}{\partial x} + \mu \frac{\partial^2 u}{\partial y^2}, \quad (3.12)$$

$$0 = -\frac{\partial p}{\partial y}. \quad (3.13)$$

The y -momentum balance (3.13) implies p does not vary with y . Combining this with the condition far away from the plate, where the fluid is stationary and therefore the pressure is a constant, implies that the pressure is constant everywhere. This implies that the pressure gradient in (3.12) vanishes.

The governing equations and the boundary conditions now become

$$\frac{\partial u}{\partial t} = \nu \frac{\partial^2 u}{\partial y^2}, \quad (3.14a)$$

$$u(y = 0, t) = U, \quad (3.14b)$$

$$u(y \rightarrow \infty, t) = 0, \quad (3.14c)$$

$$u(y, t = 0) = 0. \quad (3.14d)$$

This equation possesses a scaling symmetry. To see this transform

$$t = \alpha \tilde{t}, \quad y = \beta \tilde{y}, \quad u = \gamma \tilde{u}. \quad (3.15)$$

The transformed equations are

$$\frac{\partial \tilde{u}}{\partial \tilde{t}} = \nu \frac{\alpha}{\beta^2} \frac{\partial^2 \tilde{u}}{\partial \tilde{y}^2}, \quad (3.16a)$$

$$\tilde{u}(\tilde{y} = 0, \tilde{t}) = \frac{U}{\gamma}, \quad (3.16b)$$

$$\tilde{u}(\tilde{y} \rightarrow \infty, \tilde{t}) = 0, \quad (3.16c)$$

$$\tilde{u}(\tilde{y}, \tilde{t} = 0) = 0. \quad (3.16d)$$

Equations (3.16) reduce to (3.14) if $\gamma = 1$ and $\alpha = \beta^2$, which implies that the solution must satisfy the transformation rule

$$u(y, t) = \tilde{u}(\tilde{y}, \tilde{t}) = u\left(\frac{y}{\beta}, \frac{t}{\beta^2}\right), \quad (3.17)$$

where β remains a free parameter. Since we are free to choose any value for β , let us choose $\beta^2 = t$, so that the profile $u(y, t)$ at any time t is related to the profile $u\left(\frac{y}{\sqrt{t}}, 1\right)$. Loosely speaking, the scale for y increases as \sqrt{t} with time.

An apparently casual, but in fact equally rigorous, way of arriving at the same result is to perform a rough scaling balance, where, as a matter of notation, we replace partial derivatives with ratios

$$\frac{\partial u}{\partial t} \sim \frac{u}{t}, \quad \frac{\partial u}{\partial y} \sim \frac{u}{y}, \quad \frac{\partial^2 u}{\partial y^2} \sim \frac{u}{y^2}, \quad (3.18)$$

where the ‘ \sim ’ symbols stands for ‘scales as’. Equation (3.14) then becomes

$$\frac{u}{t} \sim \nu \frac{u}{y^2} \quad \text{or} \quad y \sim \sqrt{\nu t}, \quad (3.19)$$

which gives us the dependence of the scale of y with t . Using (3.14b), the scale for u is U .

This suggests the functional form for the similarity variable

$$\xi = \frac{y}{\delta(t)} \quad \text{where} \quad \delta(t) = 2\sqrt{\nu t}, \quad (3.20)$$

and the factor of 2 in δ is for future algebraic convenience. Here δ represents the scale for y . The following expressions are useful

$$\frac{d\delta}{dt} = \frac{1}{2} \frac{\delta}{t}, \quad \frac{\partial \xi}{\partial t} = -\frac{1}{2} \frac{\xi}{t}, \quad \frac{\partial \xi}{\partial y} = \frac{1}{\delta}. \quad (3.21)$$

Using these scales, we present an ansatz for the form of the velocity profile $u(y, t) = Uf(\xi)$, where U imparts the dimensions to u and the function $f(\xi)$ is dimensionless. This implies

$$\frac{\partial u}{\partial t} = Uf'(\xi) \frac{\partial \xi}{\partial t} = -\frac{U\xi}{2t} f'(\xi), \quad (3.22)$$

$$\frac{\partial^2 u}{\partial y^2} = \frac{U}{\delta^2} f''(\xi). \quad (3.23)$$

The partial differential equation (3.14) becomes

$$-\frac{U\xi}{2t} f'(\xi) = \nu \frac{U}{\delta^2} f''(\xi) \quad \implies \quad f''(\xi) + 2\xi f'(\xi) = 0. \quad (3.24)$$

In the first part of this equation, notice how the dimensional parts (U/t and $\nu U/\delta^2$) of the terms are closely related to the terms (u/t and $\nu u/y^2$) in the (3.19), and they cancel each other because of our choice of δ determined by the scaling balance. Solving the ordinary differential equation in (3.24) yields the general solution

$$f(\xi) = A + B \operatorname{erf}(\xi), \quad (3.25)$$

where erf stands for the error function, and A and B are constants of integration. The constants are determined by the boundary conditions (3.14b-3.14d), which on f become $f(0) = 1$ and $f(\infty) = 0$. The particular solution is then

$$f(\xi) = 1 - \operatorname{erf}(\xi) = \operatorname{erfc}(\xi), \quad (3.26)$$

erfc stands for the complimentary error function.

Interested students can try out the following problems of this kind:

1. the flow in the annular gap between two co-axial cylinders (see Figure 3.1c) driven by the rotation of the outer or the inner cylinder,
2. the flow driven simultaneously by pressure gradient, gravity and the motion of walls in the planar or cylindrical geometry (see Figure 3.1ab),
3. the analogue of Stokes first problem, but where the wall velocity $U = \alpha t$, i.e. the wall accelerates with a constant acceleration α ,
4. Stokes second problem, where the wall velocity oscillates sinusoidally for perpetuity.

Chapter 4

Dimensional Analysis

Dimensional analysis applies the principles of manipulating dimensions of physical quantities for reducing the complexity of a problem. It is best illustrated through examples.



Figure 4.1: Schematic of a two-dimensional flow past a cylinder.

4.1 Reducing parameters in a set of equations

A process called “non-dimensionalization” is used to reduce the number of parameters the solution of a set of equations depend on. Here, we non-dimensionalize the Navier-Stokes equations for flow past an infinitely-long cylinder.

Consider a fluid of density ρ and viscosity μ flowing with speed U along the x -axis past an infinitely long cylinder of radius R , as shown in Figure 4.1. Let us write the Navier-Stokes equations and the boundary conditions.

$$\frac{\partial u}{\partial x} + \frac{\partial v}{\partial y} = 0, \quad (4.1a)$$

$$\rho \left(\frac{\partial u}{\partial t} + u \frac{\partial u}{\partial x} + v \frac{\partial u}{\partial y} \right) = -\frac{\partial p}{\partial x} + \mu \left(\frac{\partial^2 u}{\partial x^2} + \frac{\partial^2 u}{\partial y^2} \right), \quad (4.1b)$$

$$\rho \left(\frac{\partial v}{\partial t} + u \frac{\partial v}{\partial x} + v \frac{\partial v}{\partial y} \right) = -\frac{\partial p}{\partial y} + \mu \left(\frac{\partial^2 v}{\partial x^2} + \frac{\partial^2 v}{\partial y^2} \right), \quad (4.1c)$$

$$\mathbf{u}(\mathbf{x} \rightarrow \infty, t) = U \hat{\mathbf{e}}_x, \quad (4.1d)$$

$$\mathbf{u}(|\mathbf{x}| = R, t) = \mathbf{0}. \quad (4.1e)$$

We would like to determine the drag, D , per unit length on the cylinder

$$D = \int_{\partial\Omega} \hat{\mathbf{e}}_x \cdot \mathbf{T} \cdot \hat{\mathbf{n}} \, dA, \quad \text{where} \quad T_{ij} = -p\delta_{ij} + \mu \left(\frac{\partial u_i}{\partial x_j} + \frac{\partial u_j}{\partial x_i} \right). \quad (4.2)$$

First notice the parameters of this problem: ρ , μ , U and R . We use three of these parameters (R , U and ρ) to “non-dimensionalize” all the quantities in the problem, i.e., we rescale

$$t = \frac{R}{U} \tilde{t}, \quad \mathbf{x} = R \tilde{\mathbf{x}}, \quad \mathbf{u} = U \tilde{\mathbf{u}}, \quad p = \rho U^2 \tilde{p}, \quad \text{and} \quad \mathbf{T} = \rho U^2 \tilde{\mathbf{T}}. \quad (4.3)$$

Note that \tilde{x} , $\tilde{\mathbf{u}}$, \tilde{p} and $\tilde{\mathbf{T}}$ are all dimensionless.

This transformation converts (4.1) to

$$\frac{\partial \tilde{u}}{\partial \tilde{x}} + \frac{\partial \tilde{v}}{\partial \tilde{y}} = 0, \quad (4.4a)$$

$$\left(\frac{\partial \tilde{u}}{\partial \tilde{t}} + \tilde{u} \frac{\partial \tilde{u}}{\partial \tilde{x}} + \tilde{v} \frac{\partial \tilde{u}}{\partial \tilde{y}} \right) = -\frac{\partial \tilde{p}}{\partial \tilde{x}} + \frac{1}{\text{Re}} \left(\frac{\partial^2 \tilde{u}}{\partial \tilde{x}^2} + \frac{\partial^2 \tilde{u}}{\partial \tilde{y}^2} \right), \quad (4.4b)$$

$$\left(\frac{\partial \tilde{v}}{\partial \tilde{t}} + \tilde{u} \frac{\partial \tilde{v}}{\partial \tilde{x}} + \tilde{v} \frac{\partial \tilde{v}}{\partial \tilde{y}} \right) = -\frac{\partial \tilde{p}}{\partial \tilde{y}} + \frac{1}{\text{Re}} \left(\frac{\partial^2 \tilde{v}}{\partial \tilde{x}^2} + \frac{\partial^2 \tilde{v}}{\partial \tilde{y}^2} \right), \quad (4.4c)$$

$$\tilde{\mathbf{u}}(\tilde{\mathbf{x}} \rightarrow \infty, \tilde{t}) = \hat{\mathbf{e}}_x, \quad (4.4d)$$

$$\tilde{\mathbf{u}}(|\tilde{\mathbf{x}}| = 1, \tilde{t}) = \mathbf{0}, \quad (4.4e)$$

where $\text{Re} = \frac{\rho U R}{\mu}$ is called the Reynolds number after Osborne Reynolds. The Reynolds number is the ratio of the strengths of inertial effects to viscous effects in the fluid.

The rescaled version of drag from (4.2) is

$$D = \rho U^2 R \int_{\partial \Omega} \hat{\mathbf{e}}_x \cdot \mathbf{T} \cdot \hat{\mathbf{n}} \, dA, \quad \text{where} \quad \tilde{T}_{ij} = -\tilde{p} \delta_{ij} + \frac{1}{\text{Re}} \left(\frac{\partial \tilde{u}_i}{\partial \tilde{x}_j} + \frac{\partial \tilde{u}_j}{\partial \tilde{x}_i} \right). \quad (4.5)$$

Note that the dimensionless equations (4.4) are equivalent to the dimensional one (4.1) with $\rho = 1$, $U = 1$, $R = 1$ and $\mu = \text{Re}^{-1}$. This means the flows for different sets of parameters are simply rescaled versions of each other if the Re for them is identical. Using this, the drag on these cylinders will also be related. Or, rewriting (4.5) as

$$C_D = \frac{D}{\frac{1}{2} \rho U^2 R} = 2 \int_{\partial \Omega} \hat{\mathbf{e}}_x \cdot \mathbf{T} \cdot \hat{\mathbf{n}} \, dA, \quad (4.6)$$

implies that

$$C_D = F(\text{Re}) \text{ alone.} \quad (4.7)$$

Here C_D is called the drag coefficient, and the factor of 1/2 in the denominator is for historical reasons.

4.2 Deducing dependence on parameters

Equation 4.7 may be derived without reference to partial differential equations, simply by using the arbitrariness of the system of units. Clearly, the drag on the cylinder depends on R , U , μ and ρ , i.e.,

$$D = \frac{1}{2} f(\rho, \mu, R, U), \quad (4.8)$$

where the factor of 1/2 is included to conform to convention that will be introduced later. In a different set of units, where length l , time t and mass m transforms as

$$\tilde{l} = \alpha l, \quad \tilde{t} = \beta t, \quad \tilde{m} = \gamma m, \quad (4.9)$$

where the symbols with the tilde refer to transformed units. Under this transformation, the parameters transform as

$$\tilde{\rho} = \frac{\tilde{m}}{\tilde{l}^3} = \frac{\gamma m}{\alpha^3 l^3} = \frac{\gamma}{\alpha^3} \rho, \quad (4.10)$$

$$\tilde{\mu} = \frac{\tilde{m}}{\tilde{l} \tilde{t}} = \frac{\gamma m}{\alpha \beta l t} = \frac{\gamma}{\alpha \beta} \mu, \quad (4.11)$$

$$\tilde{R} = \alpha R, \quad (4.12)$$

$$\tilde{U} = \frac{\alpha}{\beta} U, \text{ and} \quad (4.13)$$

$$\tilde{D} = \frac{\gamma}{\beta^2} D. \quad (4.14)$$

By the arbitrariness of system of units, (4.8) also holds in the transformed system, i.e.,

$$\tilde{D} = \frac{1}{2} f(\tilde{\rho}, \tilde{\mu}, \tilde{R}, \tilde{U}). \quad (4.15)$$

Transforming it back implies

$$\frac{\gamma}{\beta^2} D = \frac{1}{2} f\left(\frac{\gamma}{\alpha^3} \rho, \frac{\gamma}{\alpha\beta} \mu, \alpha R, \frac{\alpha}{\beta} U\right). \quad (4.16)$$

Because the scaling factors α , β and γ could be chosen at will, we choose

$$\alpha = 1/R, \quad \beta = \frac{U}{R}, \quad \gamma = \frac{1}{\rho R^3}. \quad (4.17)$$

Substituting in (4.15) gives

$$\frac{D}{\frac{1}{2}\rho U^2 R} = f\left(1, \frac{\mu}{\rho U R}, 1, 1\right) = F(\text{Re}), \quad (4.18)$$

where the inserted factor of $1/2$ turns the left hand side to the drag coefficient as in (4.7).

First, let us derive (4.7) using a short-cut. Notice that there are two ways to construct the dimensions of D from those of ρ , μ , R and U : (i) $\rho U^2 R$, and (ii) μU . The former neglects viscosity and the latter inertia. Since both have dimensions of D , their ratio is dimensionless; in fact

$$\frac{\rho U^2 R}{\mu U} = \text{Re}. \quad (4.19)$$

Because there are 3 basic dimensions of mass, length and time that make up the dimensions of 4 parameters, there is only $4-3=1$ dimensionless parameter that could be constructed from the 4 parameters.

We can go a little further and derive more insight into the functional form of $F(\text{Re})$. Suppose that Re is large, so inertia dominates and viscous effects are negligible. Under these circumstances, μ is eliminated as a parameter, so

$$D = f_I(\rho, U, R) = \frac{1}{2} C_D \rho U^2 R. \quad (4.20)$$

In the opposite extreme, if the fluid is extremely viscous, Re is small, the density of the fluid (which quantifies inertia) could be neglected and

$$D = f_V(\mu, R, U) = C_V \mu U, \quad (4.21)$$

where C_V is a dimensionless constant. The relation could be rearranged to determine the functional form of $F(\text{Re})$ in the limit of small or large Re .

$$F(\text{Re}) = C_D = \text{constant} \quad \dots \text{Re large}, \quad (4.22)$$

$$= \frac{C_V \mu U}{\frac{1}{2}\rho U^2 R} = \frac{2C_V}{\text{Re}} \quad \dots \text{Re small}. \quad (4.23)$$

In this way, dimensional analysis can assist in reducing the number of parameters in the physical relation between variables describing a phenomenon.

Chapter 5

Hydrostatics and Bernoulli equation

In this chapter, we will treat two closely related topics in fluid mechanics – hydrostatics and the Bernoulli equation. The reader is presumably acquainted with the concepts in hydrostatics; here we include it for completeness and to illustrate the proofs underlying some celebrated principles. The Bernoulli equation is one of the most important results in fluid dynamics because, unlike the Navier-Stokes equations, it yields answers to questions inspired by applications.

5.1 Hydrostatics

Hydrostatics is the study of the mechanics of static fluids. In this case $\mathbf{u} = 0$ and the Navier-Stokes equations reduce to

$$\nabla p = \rho \mathbf{g}, \quad (5.1)$$

which may be readily integrated to yield

$$p = p_0 + \rho \mathbf{g} \cdot (\mathbf{x} - \mathbf{x}_0), \quad (5.2)$$

where p_0 is the pressure at a reference point \mathbf{x}_0 . The general result is that pressure increases with depth at a rate that balances the increase of weight of the fluid per unit area.

5.1.1 Archimedes principle

A cornerstone of hydrostatics is force exerted by a static fluid on immersed (or floating) bodies given by the Archimedes principle. We can now derive this principle for a body occupying a volume Ω as follows. The net hydrostatic force on the body, \mathbf{F}_h , is due to hydrostatic pressure

$$\mathbf{F}_h = \int_{\partial\Omega} -p \hat{\mathbf{n}} \, dA = \int_{\partial\Omega} (p_0 + \rho \mathbf{g} \cdot (\mathbf{x} - \mathbf{x}_0)) \hat{\mathbf{n}} \, dA, \quad (5.3)$$

where $\hat{\mathbf{n}}$ is the unit normal pointing out of the body. This expression can be simplified using the divergence theorem as

$$\mathbf{F}_h = \int_{\Omega} \rho \mathbf{g} \, d\Omega. \quad (5.4)$$

In other words, the net force on the immersed body is equal to the net volumetric force acting on the fluid displaced by the body. This is the statement of Archimedes principle.

5.2 Bernoulli equation

The Bernoulli equation is a celebrated result in fluid dynamics, which could be considered as a generalization of hydrostatics. There are two different conditions for incompressible flow under which two different versions

of Bernoulli equation apply. Here we present those two. Analogues of these equations for compressible flow are also possible, which we do not treat.

Underlying both of these versions is an expression of incompressible momentum balance in differential form that uses the identity

$$\mathbf{u} \times \boldsymbol{\omega} = \mathbf{u} \times (\nabla \times \mathbf{u}) = \nabla \left(\frac{1}{2} |\mathbf{u}|^2 \right) - \mathbf{u} \cdot \nabla \mathbf{u}. \quad (5.5)$$

Using (5.5) to re-write the $\mathbf{u} \cdot \nabla \mathbf{u}$ term in the momentum balance yields

$$\left(\rho \frac{\partial \mathbf{u}}{\partial t} + \nabla \left(\frac{1}{2} \rho |\mathbf{u}|^2 + p - \rho \mathbf{g} \cdot \mathbf{x} \right) \right) = \mu \nabla^2 \mathbf{u} + \rho \mathbf{u} \times \boldsymbol{\omega}. \quad (5.6)$$

5.2.1 Steady incompressible inviscid flow

For a steady inviscid flow, (5.6) simplifies to

$$\nabla \tilde{B} = \rho \mathbf{u} \times \boldsymbol{\omega}, \quad \text{where} \quad \tilde{B} = \frac{1}{2} \rho |\mathbf{u}|^2 + p - \rho \mathbf{g} \cdot \mathbf{x} \quad (5.7)$$

The derivative of \tilde{B} in the direction of either \mathbf{u} or $\boldsymbol{\omega}$ is zero, i.e.,

$$\mathbf{u} \cdot \nabla \tilde{B} = \rho \mathbf{u} \cdot (\mathbf{u} \times \boldsymbol{\omega}) = 0 \quad \text{and} \quad \boldsymbol{\omega} \cdot \nabla \tilde{B} = \rho \boldsymbol{\omega} \cdot (\mathbf{u} \times \boldsymbol{\omega}) = 0. \quad (5.8)$$

Therefore, \tilde{B} is constant along a curve that is everywhere tangent to the velocity (i.e. along a streamline) or to the vorticity (i.e. along a curve known as the vortex line).

5.2.2 Unsteady incompressible potential flow

Potential flow implies that the velocity is the gradient of a scalar function, $\phi(\mathbf{x}, t)$, called the vector potential, i.e., $\mathbf{u} = \nabla \phi$, everywhere in the domain of interest. Due to incompressibility, the velocity potential satisfies the Laplace equation

$$\nabla \cdot \mathbf{u} = 0 \quad \implies \quad \nabla \cdot (\nabla \phi) = \nabla^2 \phi = 0. \quad (5.9)$$

Furthermore, owing to the identity that the curl of a gradient vanishes,

$$\boldsymbol{\omega} = \nabla \times \mathbf{u} = \nabla \times \nabla \phi = 0. \quad (5.10)$$

The two terms on the right-hand side of (5.6) vanish because $\nabla^2 \mathbf{u} = \nabla^2 (\nabla \phi) = \nabla (\nabla^2 \phi) = \mathbf{0}$, and $\boldsymbol{\omega} = \mathbf{0}$. The unsteady term on the left hand side can also be included inside the gradient to yield

$$\nabla \hat{B} = \mathbf{0}, \quad \text{where} \quad \hat{B} = \rho \frac{\partial \phi}{\partial t} + \frac{1}{2} \rho |\mathbf{u}|^2 + p - \rho \mathbf{g} \cdot \mathbf{x}. \quad (5.11)$$

Because the gradient of \hat{B} vanishes everywhere, \hat{B} does not vary with the spatial coordinates, but may depend on time. Note that there is no condition on the viscosity of the fluid in this case.

5.3 Applications and examples

The main use of Bernoulli equation is to determine pressure once the form of velocity is known. In the discussion surrounding the Navier-Stokes equations (see §2.11.2), the difficulty of determining pressure for an incompressible flow was identified. In general, for incompressible fluids, pressure is a variable that is determined implicitly through the condition that the fluid density is not altered by the flow. This difficulty is overcome by the Bernoulli equation when one of the conditions for its validity applies. Also note that the two forms of Bernoulli equation reduce to hydrostatics for the case $\mathbf{u} \equiv \mathbf{0}$. Here we will present examples of the application of Bernoulli equation.

In many cases, the application of Bernoulli in the steady inviscid case does not require an explicit specification of the complete velocity profile. Instead, the velocity is known at some specific location, and use is made of it to derive relations of practical use.

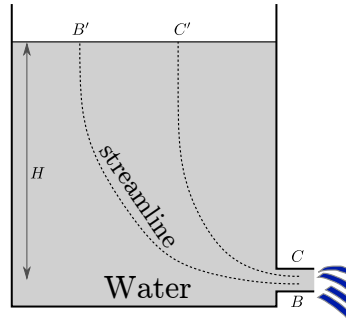


Figure 5.1: Schematic setup for flow out of an opening in a tank.

5.3.1 Flow through an opening in a tank

Consider water flowing out of a tank through a opening of area A , which is small relative to the area of the tank viewed from above, as shown in Figure 5.1, thereby draining the tank. The question is to determine the rate at which the tank empties. We will see that the rate of emptying will depend on the level of water, H , above the level of the opening.

Here note that the flow is not steady. This is because as the water-level falls, the driving force H decreases, thereby reducing the flow with time. But if the water-level doesn't fall too fast, for example, the opening being too small to drain the water, then a steady approximation might be worthwhile to make. Nor is water inviscid, but we imagine considering the limit of the fluid being inviscid to examine what the consequence of that assumption would be. If the consequence of these approximations agrees with observations, then we will deduce that the assumptions are useful. So let's get on with it.

We are not given any details of the velocity field. So we will assume the velocity to be uniform, with a value U , across the area of the opening. Now let's trace back a streamline from some point near the opening to another point where we might be able to approximate the velocity and pressure. Note that, by the definition of a streamline, it depicts the instantaneous chain of displacement of fluid particles. Since the fluid exiting the opening is ultimately being displaced by the falling water-level, every streamline that starts in the opening must terminate at the free surface. Thus we consider a streamline BB' or CC' for our consideration.

On such a streamline, Bernoulli equation for steady inviscid flow states

$$\tilde{B} = \frac{1}{2}\rho|\mathbf{u}|^2 + p - \rho\mathbf{g} \cdot \mathbf{x} = \text{constant}, \quad (5.12)$$

and, therefore,

$$p_B + \frac{1}{2}\rho U^2 - \rho\mathbf{g} \cdot \mathbf{x}_B = p_{B'} + \frac{1}{2}\rho U_{B'}^2 - \rho\mathbf{g} \cdot \mathbf{x}_{B'}. \quad (5.13)$$

Here we use our approximation $U_{B'} \ll U$, so the term $\rho U_{B'}^2/2$ on the right-hand side is negligible. We also use that both p_B and $p_{B'}$ are close to atmospheric values (because both the free surface and the opening are exposed to open air), so they cancel each other from the two sides of this equation. Then using $\mathbf{g} \cdot (\mathbf{x}_B - \mathbf{x}_{B'}) = gH$ and solving for U yields

$$U = \sqrt{2gH}. \quad (5.14)$$

Water exits the opening at the same speed as an object freely falling under gravitational acceleration g from a height H !

5.3.2 A wind turbine

A wind turbine is a device that extracts the kinetic energy from an otherwise uniform flow of a fluid, in this case air. Due to the law of conservation of energy, the fluid in the wake of the turbine must lack in kinetic energy flux. The turbine must necessarily exert a drag on the flow to slow it down. Without this drag, the flow in the wake of the turbine could not be retarded to generate a deficit in the kinetic energy flux. A simple calculation reveals that there exists an optimum amount of drag for a turbine to extract the most power from the flow.

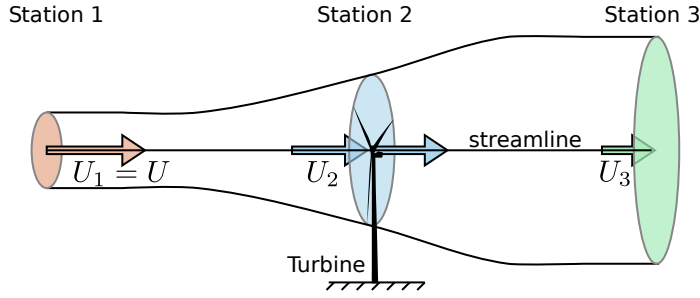


Figure 5.2: Depiction of the actuator disc idealization of a wind turbine. The blue shaded region at “Station 2” swept by the blades of the model turbine is the actuator disc. The stream tube flowing through the actuator disc is also shown bounded by the black curves. The brown shaded region shows the stream tube at “Station 1”, which is far upstream of the turbine, and the green shaded region at “Station 3” far downstream. The fluid speed at “Station i ” is U_i .

This calculation is based on the abstraction of the wind turbine as the so-called “linear momentum actuator disc”, or simply an “actuator disc”. An actuator disc is a thin disc-shaped region of space where a concentrated force acts. An example of an actuator disc, in the context of analyzing the response of a wind turbine, is shown in Figure 5.2. The region swept by the blades of the turbine is the actuator disc; the region is called a disc because it is thin along the streamwise direction. As an idealization, the influence of the turbine on the flow is replaced by a concentrated body force opposing the flow exerted on the fluid occupying this disc. While the force exerted by the blades of a real turbine on the fluid is unsteady (because of the rotation of the blades), the unsteadiness is ignored in the idealization and replaced by a steady force uniformly distributed throughout the disc. In practice, as the turbine spins faster, the greater the average force it exerts on the fluid. (This is similar to the operation of a fan – the faster the blades of the fan spin the greater the force it exerts on the surrounding fluid and faster the resulting flow.)

Now we ask, how much force should the turbine exert on the flow. If the exerted force is too weak then the kinetic energy deficit in the wake, and thereby the power extracted, is also small. But if the exerted force is too strong then the turbine acts as a fan and blows the fluid backwards thus pumping power back into the flow, instead of extracting it from the flow. Hence, there must be an optimal amount of force to exert on the fluid to maximize power extraction. This principle can be understood quantitatively using the actuator disc idealization for the turbine which exerts a steady force on the fluid.

The problem is stated as follows. A turbine of radius R operates in an incompressible fluid of density ρ flowing uniformly at speed U . What is the maximum power, P , it can extract from the flow? We do not anticipate the fluid viscosity to be a dominant effect. It then follows from dimensional analysis that

$$P = \eta \times \frac{1}{2} \rho U^3 \pi R^2, \quad (5.15)$$

where η is a dimensionless number called the efficiency of the turbine. The efficiency is interpreted to be the fraction of the kinetic energy flux $\frac{1}{2} \rho U^3 \pi R^2$ incident on the swept area of the turbine blades that the turbine can convert to power. Similarly, the drag is

$$D = C_D \times \frac{1}{2} \rho U^2 \pi R^2, \quad (5.16)$$

where C_D is the coefficient of drag. According to the argument in the previous paragraph, the efficiency is expected to be maximum for a particular drag coefficient.

Let us now construct estimates of the efficiency and the drag coefficient, which happens to be convenient to do in terms of the wake deficit. Consider three stations on the stream tube incident on the turbine, shown in Figure 5.2 – Station 1 far upstream of the turbine, Station 2 at the turbine, and Station 3 far downstream. The fluid velocity at Station 1 is expected to be uniform, with a magnitude equal to the given freestream U , so $U_1 = U$. Similarly, the fluid velocity at Station 3 is also expected to be uniform in the stream tube – we will take the speed to be U_3 . (Outside the streamtube, far downstream, the fluid speed is U .) If the turbine extracts power from the flow, we expect $U_3 < U$. The cross-section area of the stream tube at Stations 1, 2 and 3, is taken to be A_1 , A_2 and A_3 , respectively, with $A_2 = \pi R^2$ given. The fluid pressure at Stations 1 and 3 are equal to the atmospheric value p_∞ .

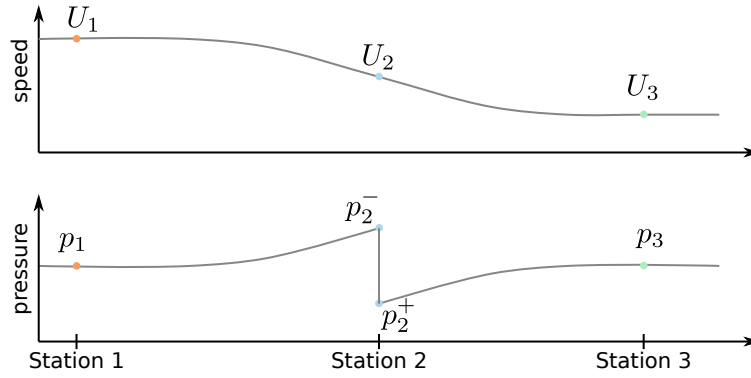


Figure 5.3: Schematic of profiles of speed and pressure along the streamline shown in Figure 5.2.

Now we apply laws of conservation of mass and momentum in integral form to the volume Ω occupied by the stream tube. According to the law of conservation of mass

$$U_1 A_1 = U_2 A_2 = U_3 A_3. \quad (5.17)$$

Momentum conservation between Stations 1 and 3 implies

$$\rho U_1^2 A_1 - \rho U_3^2 A_3 + \int_{\partial\Omega} (p - p_\infty) \hat{\mathbf{n}} \, dA - D = 0. \quad (5.18)$$

It is left as an exercise for the reader by considering mass and momentum balance on the fluid outside Ω to show that the pressure integral $\int_{\partial\Omega} (p - p_\infty) \hat{\mathbf{n}} \, dA = 0$, thereby

$$D = \rho U_1^2 A_1 - \rho U_3^2 A_3 = \rho U_2 A_2 (U_1 - U_3). \quad (5.19)$$

Similarly, mechanical energy conservation implies

$$P = \frac{1}{2} \rho U_1^3 A_1 - \frac{1}{2} \rho U_3^3 A_3 = \frac{1}{2} \rho U_2 A_2 (U_1^2 - U_3^2). \quad (5.20)$$

Note that no characteristics of the turbine are used to derive these relations.

It is now time to relate these results from the integral form of the conservation laws to the size of the turbine itself. To facilitate the subsequent analysis, consider the profiles of velocity and pressure along the centerline of the stream tube, which also happens to be a streamline due to axisymmetry. These profiles are shown schematically in Figure 5.3. The fluid speed far upstream of the turbine is $U_1 = U$, but under the influence of the drag exerted by the actuator disc, it decreases monotonically along the streamline to U_2 at the turbine and to U_3 far downstream. On the streamlines upstream of the turbine and downstream of the turbine, the fluid pressure profile obeys the Bernoulli equation. Therefore, upstream of the turbine, the pressure grows monotonically, starting with $p_1 = p_\infty$ far upstream. At the turbine itself, because of the drag on the actuator disc, the pressure profile suffers a jump. Downstream of the turbine, the pressure again grows monotonically to $p_3 = p_\infty$ far downstream.

The jump in the pressure across the actuator disc may be determined by applying the Bernoulli equation along the streamline between Stations 1 and 2, and 2 and 3, respectively, which reads

$$p_1 + \frac{1}{2} \rho U_1^2 = p_2^- + \frac{1}{2} \rho |U_2|^2, \quad (5.21)$$

$$p_3 + \frac{1}{2} \rho U_3^2 = p_2^+ + \frac{1}{2} \rho |U_2|^2. \quad (5.22)$$

Here we have tacitly assumed that the component of fluid velocity tangential to the actuator disc does not suffer a jump at Station 2. (Note that the normal component must be continuous owing to mass conservation.) The difference between the two yields

$$p_2^- - p_2^+ = \frac{1}{2} \rho (U_1^2 - U_3^2). \quad (5.23)$$

Note that the magnitude of the pressure jump across the actuator disc depends only on the far upstream and far downstream speed on the streamline passing through any point on the actuator disc, and is therefore

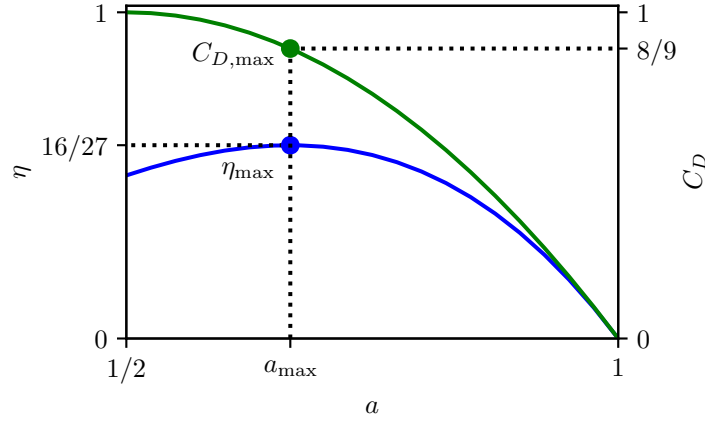


Figure 5.4: Efficiency η and drag coefficient C_D as a function of the turbine induction factor a .

independent of the location on the actuator disc. Applying conservation of momentum across the actuator disc then yields the drag on it to be

$$D = (p_2^- - p_2^+)A_2 = \frac{1}{2}\rho A_2 (U_1^2 - U_3^2). \quad (5.24)$$

Equating the expressions for drag from (5.19) and (5.24) yields a celebrated equation on this topic

$$U_2 = \frac{U_1 + U_3}{2}. \quad (5.25)$$

This equation states that at the actuator disc, the fluid speed is equal to the average of the far upstream and downstream values.

Now we are prepared to write the power extracted and the drag exerted by the actuator disc in terms of the wake deficit, which we parametrize by U_2 . For convenience, we non-dimensionalize $U_2 = aU$ and $U_3 = bU$ so that (5.25) becomes

$$a = \frac{1+b}{2} \quad \text{or} \quad b = 2a - 1. \quad (5.26)$$

The parameters a and b are called the turbine induction factor and the wake induction factor, respectively. Based on this result, and that the minimum value of b is zero, the minimum value of a is $1/2$. In other words, the greatest deficit in the wake we consider is when the fluid in the wake comes to a complete stop, in which case the fluid speed at the turbine is half that of the freestream.

Substituting (5.26) in (5.19) and (5.20) yields

$$D = \rho U^2 \pi R^2 a(1-b) = \frac{1}{2}\rho U^2 \pi R^2 \times 4a(1-a), \quad (5.27)$$

$$P = \frac{1}{2}\rho U^3 \pi R^2 a(1-b^2) = \frac{1}{2}\rho U^3 \pi R^2 \times 4a^2(1-a), \quad (5.28)$$

where by comparison with (5.16) and (5.15), the drag coefficient and efficiency are

$$C_D = 4a(1-a), \quad \text{and} \quad \eta = 4a^2(1-a). \quad (5.29)$$

The dependence of η and C_D on a is shown in Figure 5.4. Both these variables are zero when $a = 1$, because there is no wake-deficit in this case. As a decreases below unity, the wake deficit builds up, the turbine experiences drag and can extract some power. The extracted power reaches a maximum at $a = a_{\max}$, which may be found by setting

$$\frac{d\eta}{da} = 4(2a - 3a^2) = 0 \quad \implies \quad a_{\max} = \frac{2}{3} \quad \text{and} \quad \eta_{\max} = \frac{16}{27} \approx 0.59. \quad (5.30)$$

Decreasing a below a_{\max} reduces the extracted power more. The drag coefficient that leads to maximum power extraction is $C_{D,\max} = 8/9$.

This calculation introduces one of the most basic concepts to evaluate the performance of a wind turbine – its efficiency. Furthermore, no turbines have been invented with efficiency greater than $16/27$. This limit on the maximum efficiency of a linear momentum actuator disc is known as the 'Betz limit' or the 'Betz-Joukowski limit' commemorating the contributions of the German physicist Albert Betz and the Russian scientist and mathematician Nikolay Joukowski, for providing a detailed rationale behind its validity.

5.3.3 A water wave

The Cartesian components of velocity (u, v, w) in a semi-infinite layer of fluid ($y \leq 0$) of density ρ are given by

$$u = k \sin(\omega t) \cos(kx) e^{-|k|y}, \quad v = -|k| \sin(\omega t) \sin(kx) e^{-|k|y}, \quad w = 0,$$

where ω and k are constants and t is time. Gravity or any other volumetric force is absent. This velocity field closely approximates the flow under a sinusoidal train of water waves. The question is to deduce the pressure on the surface $y = 0$.

This is unsteady flow. It will be extremely useful if we could apply the unsteady version of Bernoulli equation here. Let us first examine if the conditions for it are satisfied.

1. Is the flow incompressible?

$$\nabla \cdot \mathbf{u} = \frac{\partial u}{\partial x} + \frac{\partial v}{\partial y} + \frac{\partial w}{\partial z} = \sin(\omega t) e^{-|k|y} (-k^2 \sin(kx) + |k|^2 \sin(kx) + 0) = 0. \quad (5.31)$$

Yes!

2. Is the flow irrotational? The velocity is two-dimensional, so we only need to verify the z -component of vorticity

$$\omega_z = \frac{\partial v}{\partial x} - \frac{\partial u}{\partial y} = \sin(\omega t) e^{-|k|y} (-k|k| \cos(kx) - (-k|k|) \cos(kx)). \quad (5.32)$$

Yes! So the velocity may be written as the gradient of a potential ϕ .

$$\frac{\partial \phi}{\partial x} = u = k \sin(\omega t) \cos(kx) e^{-|k|y}, \quad \frac{\partial \phi}{\partial y} = v = -|k| \sin(\omega t) \sin(kx) e^{-|k|y}, \quad (5.33)$$

which yields

$$\phi = \sin(\omega t) \sin(kx) e^{-|k|y}. \quad (5.34)$$

According to Bernoulli (in the absence of gravity),

$$p = -\rho \frac{\partial \phi}{\partial t} - \frac{1}{2} \rho |\mathbf{u}|^2 = -\rho \omega \cos(\omega t) \sin(kx) e^{-|k|y} - \frac{1}{2} \rho k^2 \sin^2(\omega t) e^{-2|k|y}. \quad (5.35)$$

On $y = 0$, the pressure is

$$p|_{y=0} = -\rho \omega \cos(\omega t) \sin(kx) - \frac{1}{2} \rho k^2 \sin^2(\omega t). \quad (5.36)$$

A useful homework is to deduce the pressure using the Navier-Stokes equations and verify that it agrees with the one obtained using Bernoulli.

Chapter 6

Potential flow

The case where the fluid velocity is given by

$$\mathbf{u} = \nabla\phi, \quad \nabla^2\phi = 0, \quad (6.1)$$

is called potential flow. Velocity profiles of this type arise in a number of situations in practice, but most importantly this theory allows fluid dynamicists to construct flow profiles that automatically satisfy conservation of mass and momentum. Here we treat this subject.

6.1 Conditions for and implications of potential flow

The conditions under which potential flow is realized are those of incompressibility and irrotationality, i.e.,

$$\nabla \cdot \mathbf{u} = 0 \quad \text{and} \quad \nabla \times \mathbf{u} = \mathbf{0}, \quad \text{respectively.} \quad (6.2)$$

A necessary and sufficient condition for irrotationality is

$$\nabla \times \mathbf{u} = \mathbf{0} \quad \iff \quad \mathbf{u} = \nabla\phi, \quad (6.3)$$

where ϕ is a scalar field known as the velocity potential. Substituting this form of \mathbf{u} into the incompressibility conditions yields Laplace equation $\nabla^2\phi = 0$ for ϕ . In this way, mass is conserved.

We have seen in (5.11), that momentum is conserved if the pressure satisfies the Bernoulli equation, i.e.,

$$\rho \frac{\partial\phi}{\partial t} + \frac{1}{2}\rho|\mathbf{u}|^2 + p - \rho\mathbf{g} \cdot \mathbf{x} = \text{constant in } \mathbf{x}. \quad (6.4)$$

In this manner, potential flow satisfies mass and momentum conservation for a viscous fluid.

To construct a potential flow, one solves the Laplace equation (6.1) for ϕ subject to appropriate boundary conditions. Given the nature of Laplace equation, on the boundaries only one of the two components of velocity may be imposed, but not both. On the boundary between the fluid and a solid object, a condition of no-normal flow is imposed, i.e.,

$$\nabla\phi \cdot \hat{\mathbf{n}} = 0, \quad \text{on solid walls.} \quad (6.5)$$

Therefore, in general, the no-slip condition cannot be satisfied by potential flow past solid objects and potential flow generally slips past the walls. Regardless, potential flow is incredibly successful in providing insight into situations where solid bodies are either not present or could be abstracted away.

6.2 Incompressible and irrotational flow in two-dimensions

While the general concept of potential flow applies in three dimensions, the application of complex variables makes potential flow much more powerful in two dimensions. Essentially, the use of complex variables trivializes

the solution of Laplace equation. The only remaining complexity that remains is the satisfaction of the boundary conditions. In the rest of this chapter, we will focus on two-dimensional incompressible irrotational flow.

Irrotationality in two dimension implies for the components of velocity $\mathbf{u} = (u, v)$

$$\nabla \times \mathbf{u} = \left(\frac{\partial v}{\partial x} - \frac{\partial u}{\partial y} \right) \hat{e}_z = \mathbf{0} \quad \iff \quad u = \frac{\partial \phi}{\partial x}, \quad v = \frac{\partial \phi}{\partial y}. \quad (6.6)$$

Similarly, incompressibility implies

$$\nabla \cdot \mathbf{u} = \frac{\partial u}{\partial x} + \frac{\partial v}{\partial y} = 0 \quad \iff \quad u = \frac{\partial \psi}{\partial y}, \quad v = -\frac{\partial \psi}{\partial x}, \quad (6.7)$$

where ψ is a field called stream function.

This type of reciprocal relation between the derivatives of two scalar functions, in our case ϕ and ψ , are called the Cauchy-Reimann conditions:

$$\frac{\partial \phi}{\partial x} = \frac{\partial \psi}{\partial y}, \quad \frac{\partial \phi}{\partial y} = -\frac{\partial \psi}{\partial x}. \quad (6.8)$$

Owing to this relation, both ϕ and ψ satisfy Laplace equation, i.e., $\nabla^2 \phi = \nabla^2 \psi = 0$. Furthermore, ϕ and ψ are the real and imaginary part of a holomorphic function w of the complex variable z , i.e.

$$w(z) = \phi(x, y) + i\psi(x, y), \quad \text{where} \quad z = x + iy. \quad (6.9)$$

Thus, the strategy for generating potential flows is to construct holomorphic functions $w(z)$ called complex potentials that satisfy the necessary boundary condition. The fluid velocity is given by the relation

$$u - iv = \frac{dw}{dz}. \quad (6.10)$$

Here are some geometric relations between ϕ , ψ and streamlines.

6.2.1 Stream function and streamlines

Contours of constant stream function are streamlines of the flow. To see this, consider the directional derivative of the stream function in the direction of the streamline, i.e. in the direction of velocity

$$\nabla \psi \cdot \mathbf{u} = \frac{\partial \psi}{\partial x} u + \frac{\partial \psi}{\partial y} v = -vu + uv = 0. \quad (6.11)$$

Thus, irrespective of location in the flow, ψ does not vary in the direction of streamlines. Therefore, ψ is a constant along a streamline. In other words, streamlines are contours of constant stream function.

6.2.2 Stream function and velocity potential

Contours of constant stream function and those of constant velocity potential meet orthogonally. To see this, consider the dot product of $\nabla \phi$ and $\nabla \psi$, the normals of the contours at a given point:

$$\nabla \phi \cdot \nabla \psi = \frac{\partial \psi}{\partial x} \frac{\partial \phi}{\partial x} + \frac{\partial \psi}{\partial y} \frac{\partial \phi}{\partial y} = 0. \quad (6.12)$$

Since the normals are orthogonal, the tangents must be too, and therefore the curves must be too.

6.3 Elementary complex potentials

Some basic elements that are used to construct the complex potentials.

6.3.1 Uniform flow

Consider the complex potential

$$w(z) = Ue^{-i\alpha}z \quad \implies \quad \phi = U(x \cos \alpha + y \sin \alpha), \quad \psi = U(y \cos \alpha - x \sin \alpha). \quad (6.13)$$

The flow velocity corresponding to this potential is

$$u = U \cos \alpha, \quad v = U \sin \alpha, \quad (6.14)$$

i.e., a uniform flow at an angle α to the x -axis. An example of this flow is shown in Figure 6.1(a).

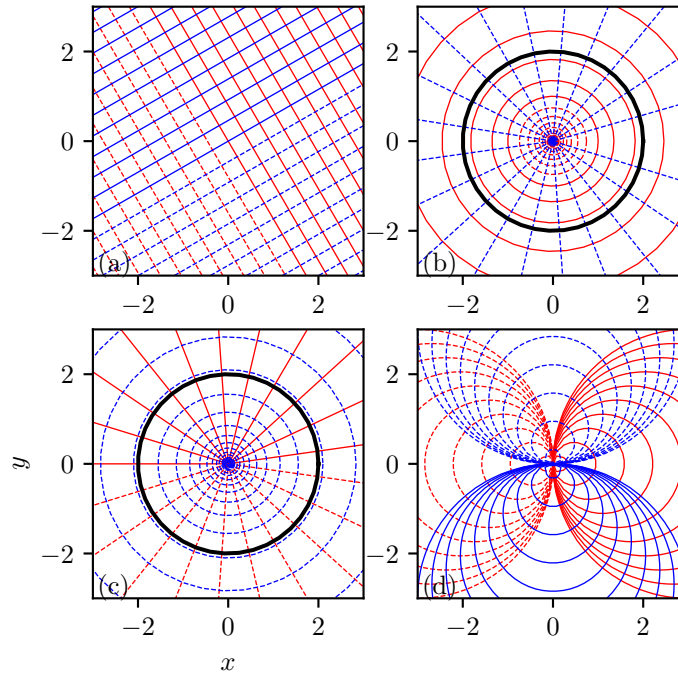


Figure 6.1: Visualization of Elementary flows. Streamlines are in blue and equipotential lines are in red. (a) Uniform flow at an angle of 30° to the x -axis. Potential $w(z) = ze^{i\pi/6}$. (b) Flow due to a point source. Potential $w(z) = \log z$. (c) Flow due to a point vortex. Potential $w(z) = i \log z$. (d) Flow due to a point dipole. Potential $w(z) = 1/z$. The black circle in panels (b) and (c) depicts the contour used for illustrating the concentrated nature of the point source and vortex.

6.3.2 Point source

Consider the complex potential

$$w(z) = \frac{Q}{2\pi} \log z \quad \implies \quad \phi = \frac{Q}{2\pi} \log r, \quad \psi = \frac{Q\theta}{2\pi}, \quad (6.15)$$

where $z = r^{i\theta}$ is the polar representation of the complex variable z . The flow velocity corresponding to this potential is

$$\mathbf{u} = \frac{Q}{2\pi r} \hat{\mathbf{e}}_r, \quad (6.16)$$

i.e., a radially outward flow decaying inversely proportional with distance. An example of this flow is shown in Figure 6.1(b). For what follows, let $\mathbf{u} \cdot \hat{\mathbf{e}}_r = u_r$ and $\mathbf{u} \cdot \hat{\mathbf{e}}_\theta = u_\theta$.

To understand why the flow corresponding to this potential is termed as the point source, consider the divergence and curl of the velocity field:

$$\nabla \cdot \mathbf{u} = \frac{1}{r} \left(\frac{\partial(ru_r)}{\partial r} + \frac{\partial u_\theta}{\partial \theta} \right) = 0, \quad (6.17)$$

$$\nabla \times \mathbf{u} = \frac{1}{r} \left(\frac{\partial(ru_\theta)}{\partial r} - \frac{\partial u_r}{\partial \theta} \right) \hat{\mathbf{e}}_z = \mathbf{0} \quad (6.18)$$

for $r > 0$, but this calculation says nothing about $r = 0$. To deduce that, consider the line integrals along the circle of radius r

$$\int_C \mathbf{u} \cdot \hat{\mathbf{n}} \, ds = \int_0^{2\pi} \frac{Q}{2\pi r} \hat{\mathbf{e}}_r \cdot \hat{\mathbf{e}}_r \, r d\theta = Q, \quad (6.19)$$

$$\int_C \mathbf{u} \cdot \hat{\mathbf{t}} \, ds = \int_0^{2\pi} \frac{Q}{2\pi r} \hat{\mathbf{e}}_r \cdot \hat{\mathbf{e}}_\theta \, r d\theta = 0, \quad (6.20)$$

where $\hat{\mathbf{n}}$ and $\hat{\mathbf{t}}$ are the unit normal and tangential vectors to the curve C . Given that, due to the divergence and Stokes theorems, respectively,

$$\int_C \mathbf{u} \cdot \hat{\mathbf{n}} \, ds = \int_A \nabla \cdot \mathbf{u} \, dA, \quad \text{and} \quad (6.21)$$

$$\int_C \mathbf{u} \cdot \hat{\mathbf{t}} \, ds = \int_A (\nabla \times \mathbf{u}) \cdot \hat{\mathbf{e}}_z \, dA, \quad (6.22)$$

the inescapable conclusion is that for this flow $\nabla \cdot \mathbf{u} = Q\delta(\mathbf{x})$, where δ is the Dirac-delta function and $\nabla \times \mathbf{u} = \mathbf{0}$. Thus, this flow is irrotational everywhere, but incompressible only for $r > 0$. Volume is not conserved at $r = 0$, but instead is generated there. Hence the terminology to describe this flow as a “point source”.

6.3.3 Point vortex

Consider the complex potential

$$w(z) = -\frac{i\Gamma}{2\pi} \log z \quad \implies \quad \phi = \frac{\Gamma\theta}{2\pi}, \quad \psi = -\frac{\Gamma}{2\pi} \log r. \quad (6.23)$$

The flow velocity corresponding to this potential is

$$\mathbf{u} = \frac{Q}{2\pi r} \hat{\mathbf{e}}_\theta, \quad (6.24)$$

i.e., an azimuthal flow decaying inversely proportional with distance. An example of this flow is shown in Figure 6.1(c).

We again examine $\nabla \cdot \mathbf{u}$ and $\nabla \times \mathbf{u}$ to understand the terminology associated with this flow. Just as for the point source,

$$\nabla \cdot \mathbf{u} = \frac{1}{r} \left(\frac{\partial(ru_r)}{\partial r} + \frac{\partial u_\theta}{\partial \theta} \right) = 0, \quad (6.25)$$

$$\nabla \times \mathbf{u} = \frac{1}{r} \left(\frac{\partial(ru_\theta)}{\partial r} - \frac{\partial u_r}{\partial \theta} \right) \hat{\mathbf{e}}_z = \mathbf{0} \quad (6.26)$$

for $r > 0$, but which says nothing about $r = 0$. The line integrals along the circle of radius r

$$\int_C \mathbf{u} \cdot \hat{\mathbf{n}} \, ds = \int_0^{2\pi} \frac{\Gamma}{2\pi r} \hat{\mathbf{e}}_\theta \cdot \hat{\mathbf{e}}_r \, r d\theta = 0, \quad (6.27)$$

$$\int_C \mathbf{u} \cdot \hat{\mathbf{t}} \, ds = \int_0^{2\pi} \frac{\Gamma}{2\pi r} \hat{\mathbf{e}}_\theta \cdot \hat{\mathbf{e}}_\theta \, r d\theta = \Gamma, \quad (6.28)$$

which, in view of (6.21-6.22) lead to the inescapable conclusion that the flow is incompressible everywhere but irrotational only for $r > 0$. The vorticity is, in fact, $\nabla \times \mathbf{u} = \Gamma\delta(\mathbf{x})\hat{\mathbf{e}}_z$. Hence the flow due to this potential is termed as the “point vortex”.

6.3.4 Point dipole

The flow constructed by the linear superposition of a point source and an equal point sink (i.e., a source with negative strength) located vanishingly small distances apart constitutes a point dipole. The complex potential is constructed as

$$w(z) = \lim_{\epsilon \rightarrow 0} \frac{Q}{2\pi} (\log(z + \epsilon) - \log(z - \epsilon)). \quad (6.29)$$

Of course, in the limit $\epsilon \rightarrow 0$, the potential would vanish, unless the source-sink pair also strengthened in the process. In particular, let $Q = D/(2\epsilon)$, so that the source-sink pair strength is inversely proportional to the distance between them. Here D is the strength of the point dipole. With this assumption,

$$w(z) = \lim_{\epsilon \rightarrow 0} \frac{D}{2\pi} \left(\frac{\log(z + \epsilon) - \log(z - \epsilon)}{2\epsilon} \right) = \frac{D}{2\pi z}. \quad (6.30)$$

The flow due to the point dipole is depicted in Figure 6.1(d). The streamlines and equipotential lines are both sets of circles that are tangential to the x and y axes, respectively, at the origin.

6.3.5 Higher multipoles

Note that, due to its construction, the potential due to a point dipole is the derivative of the potential due to a point source. This can be extended to higher orders called “multipoles”. For example, a point quadrupole is a point dipole of point dipoles with a complex potential proportional to $1/z^2$. And octupole is a point dipole of quadrupoles with potential $1/z^3$. And so on.

In this manner, the general complex potential with the farfield approaching uniform flow may be written as

$$w(z) = Uz + \frac{Q - i\Gamma}{2\pi} \log z + \frac{a_1}{z} + \frac{a_2}{z^2} + \frac{a_3}{z^3} + \dots \quad (6.31)$$

Here, the coefficients U , Q , Γ , a_1 , a_2 , etc, may be functions of time.

6.4 Potential flow past immersed bodies

The coefficients Q , Γ , a_1 , a_2 , \dots , may be chosen to construct the complex potential for flow past bodies. Here are some examples.

6.4.1 Rankine half-body

The linear superposition of a uniform flow and a point source may be used to represent flow past a semi-infinite body, called the Rankine half-body. The complex potential is

$$w(z) = Uz + \frac{Q}{2\pi} \log z. \quad (6.32)$$

The flow streamlines and equipotential lines are shown in Figure 6.2(a). Any region of the plane on one side of a streamline may be replaced by a solid body and the complex potential in the remaining region describes potential flow past this solid body. For example, consider the streamline given by $\psi = Q/2$, where

$$\psi = \text{Im}(w) = Ur \sin \theta + \frac{Q\theta}{2\pi} \quad \text{so the streamline is} \quad r = \frac{Q(\pi - \theta)}{2\pi U \sin \theta}. \quad (6.33)$$

The streamline is shown in Figure 6.2(b) and the area inside the streamline, shaded blue in the figure, is the Rankine half-body. The complex potential $w(z)$ in (6.32) describes the flow past this Rankine half-body.

6.4.2 Rankine oval

The linear superposition of a uniform flow, a point source and a point sink may be used to represent flow past a finite body, called the Rankine oval. The complex potential is

$$w(z) = Uz + \frac{Q}{2\pi} (\log(z - 1) - \log(z + 1)). \quad (6.34)$$

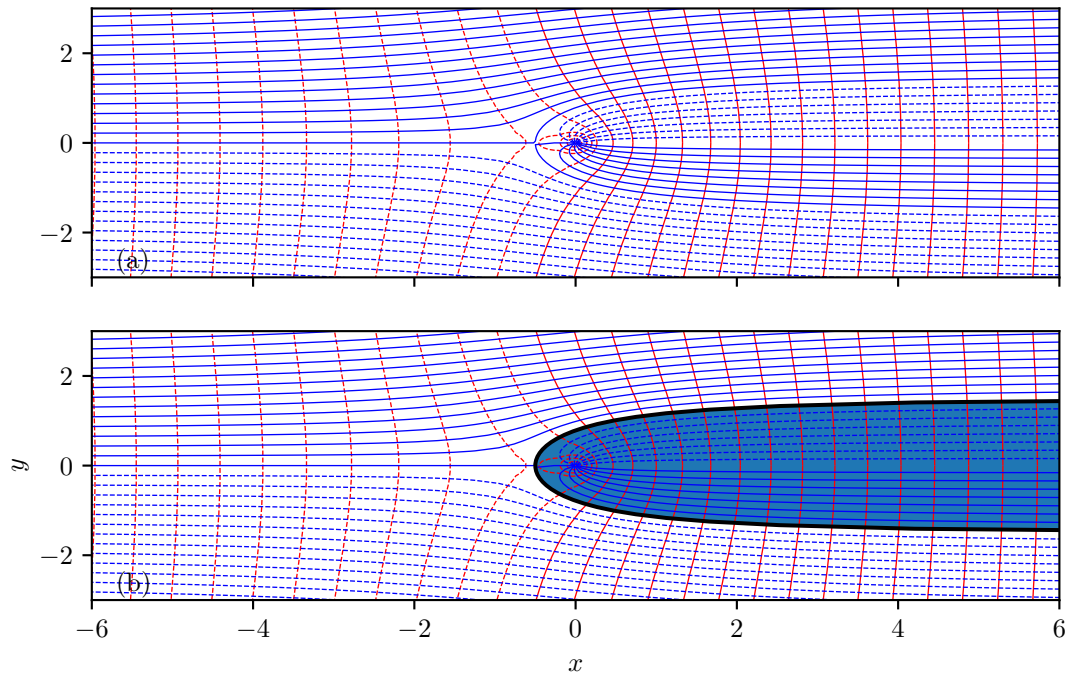


Figure 6.2: Flow around a Rankine half-body. (a) The flow streamlines (blue) and equipotential lines (red) for the potential given by (6.32) for $U = 1$ and $Q = \pi$. (b) Same as (a) but with the streamline $\psi = Q/2$ drawn in solid black and the area inside this streamline shaded in blue. The shaded region is the Rankine half-body.

The flow streamlines and equipotential lines are shown in Figure 6.3(a). Consider the streamline given by $\psi = 0$, where

$$\psi = \text{Im}(w) = Ur \sin \theta + \frac{Q(\theta_1 - \theta_2)}{2\pi} \quad \text{so the streamline is given by} \quad Ur \sin \theta + \frac{Q(\theta_1 - \theta_2)}{2\pi} = 0, \quad (6.35)$$

where $\tan \theta_1 = r \sin \theta / (r \cos \theta + 1)$ and $\tan \theta_2 = r \sin \theta / (r \cos \theta - 1)$. The streamline is shown in Figure 6.3(b) and the area inside the streamline, shaded blue in the figure, is the Rankine oval. The complex potential $w(z)$ in (6.34) describes the flow past this Rankine oval.

6.4.3 Circle

The Rankine oval approaches a circle as the source and the sink approach each other to form a dipole. The complex potential in this case is

$$w(z) = U \left(z + \frac{a^2}{z} \right). \quad (6.36)$$

The flow streamlines and equipotential lines are shown in Figure 6.4(a). Consider the streamline given by $\psi = 0$, where

$$\psi = \text{Im}(w) = U \sin \theta \left(r - \frac{a^2}{r} \right), \quad \text{so that } \psi = 0 \text{ on } r = a. \quad (6.37)$$

The streamline is shown in Figure 6.4(b) and the area inside the streamline, shaded blue in the figure, is a circle of radius a . The complex potential $w(z)$ in (6.36) describes the flow past this circle.

An arbitrary point vortex centered at the center of the circle may be added to the mix without violating the boundary condition on the circle. The most general potential flow around a circle is given by

$$w(z) = U \left(z + \frac{a^2}{z} \right) - \frac{i\Gamma}{2\pi} \log z. \quad (6.38)$$

Here Γ is the circulation around the circle, perhaps due to the spinning of the circle. The flow due to this potential is shown in Figure 6.4(c).

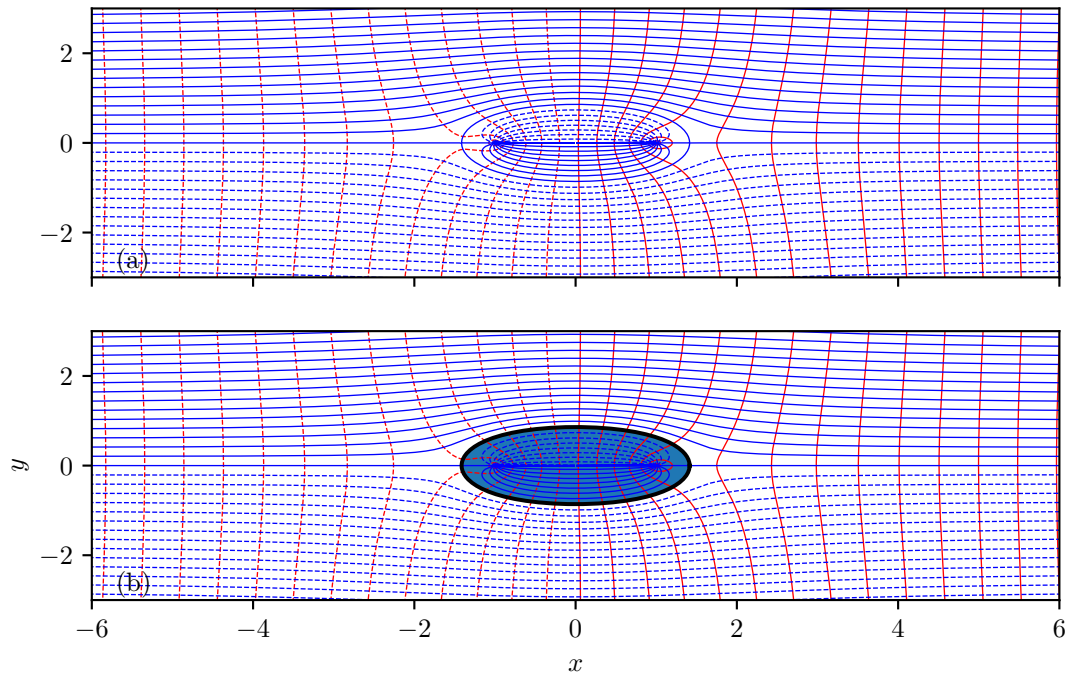


Figure 6.3: Flow around a Rankine oval. (a) The flow streamlines (blue) and equipotential lines (red) for the potential given by (6.34) for $U = 1$ and $Q = \pi$. (b) Same as (a) but with the streamline $\psi = 0$ drawn in solid black and the area inside this streamline shaded in blue. The shaded region is the Rankine half-body.

6.5 Force on a immersed body

The force on the body due to the potential flow (6.31) may be calculated by integrating the force due to the fluid pressure. The force on the body per unit length out of the plane of the paper is

$$\mathbf{F} = \int_C -p\hat{\mathbf{n}} ds, \quad (6.39)$$

where C is the bounding closed streamline defining the body. The fluid pressure is determined by Bernoulli equations as

$$p = -\rho \left(\frac{\partial \phi}{\partial t} + \frac{1}{2} |\mathbf{u}|^2 \right) + \rho \mathbf{g} \cdot \mathbf{x}, \quad (6.40)$$

The contribution to the force due to gravity is the force of buoyancy from Archimedes principle. Here we calculate the contribution from the remaining two terms.

6.5.1 Force in a steady potential flow

In steady potential flow, only the term $\rho |\mathbf{u}|^2/2$ contributes to the net unbalanced force beyond buoyancy. In complex variables, let the components of the force $\mathbf{F} = F_x \hat{\mathbf{e}}_x + F_y \hat{\mathbf{e}}_y$ be written as $F_x + iF_y$. If the tangent to C makes an angle θ to the x -axis, then $\mathbf{u} = |\mathbf{u}|e^{i\theta}$ because the flow is tangential to the streamline. Also, because the components of velocity are $w'(z) = u - iv = |\mathbf{u}|e^{-i\theta}$, $|\mathbf{u}|^2 = w'(z)^2 e^{2i\theta}$. The product of the unit normal and the infinitesimal line element is $-ie^{i\theta} ds$. The complex conjugate of the force is

$$F_x - iF_y = \int_C \frac{1}{2} \rho w'(z)^2 e^{2i\theta} (ie^{-i\theta} ds) = \frac{i\rho}{2} \int_C w'(z)^2 dz, \quad (6.41)$$

where the complex integration infinitesimal $dz = e^{i\theta} ds$.

Using this expression for force, and substituting (6.31) in (6.41) yields

$$F_x - iF_y = -\rho U(Q - i\Gamma), \quad (6.42)$$

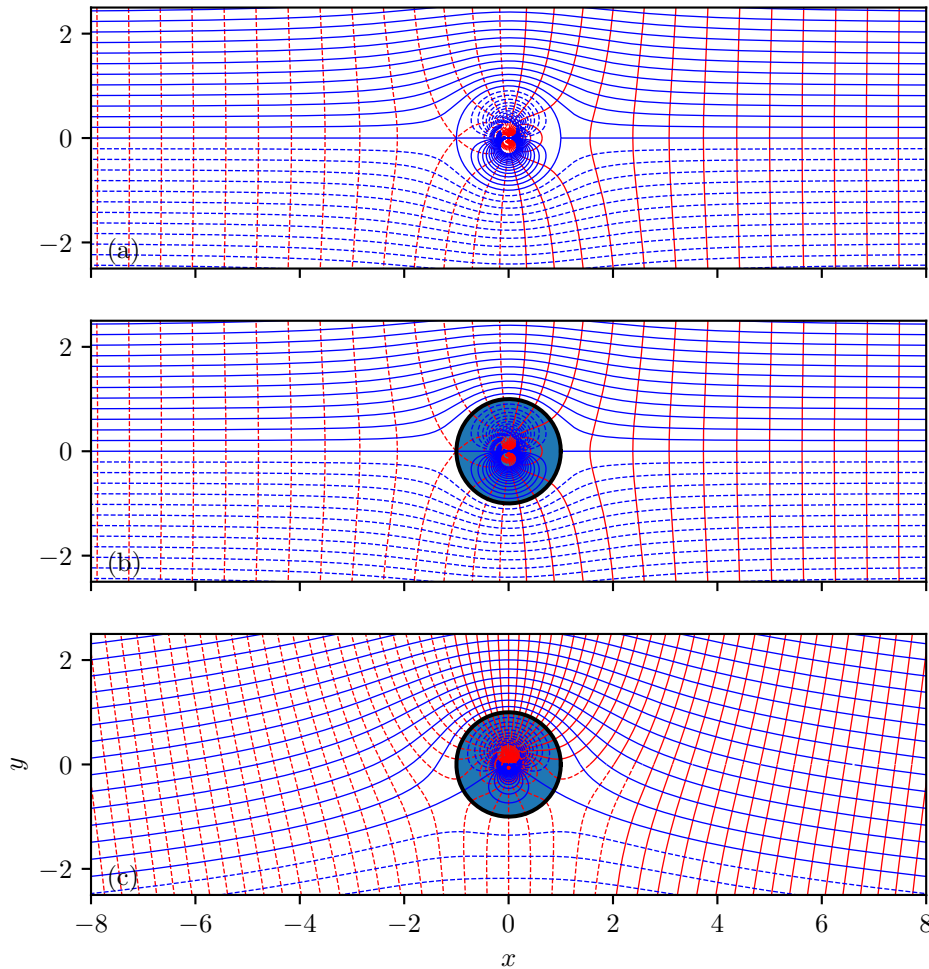


Figure 6.4: Flow around a Rankine oval. (a) The flow streamlines (blue) and equipotential lines (red) for the potential given by (6.36) for $U = 1$ and $a = 1$. (b) Same as (a) but with the streamline $\psi = 0$ drawn in solid black and the area inside this streamline shaded in blue. The shaded region is a circle. (c) The flow around a spinning circle corresponding to the complex potential given by (6.38) for $U = 1$, $a = 1$, $\Gamma = 2\pi$.

where Cauchy's residue theorem is employed for calculating the contour integral. Law of conservation of mass demands that for a body immersed in the flow $Q = 0$, and therefore,

$$F_x = 0 \quad \text{and} \quad F_y = -\rho U \Gamma. \quad (6.43)$$

The drag on an object is the force it experiences in the direction of the flow, while the lift is the force perpendicular to the flow. According to (6.43), the lift on an immersed body due to the potential flow is $\rho U \Gamma$, which is the statement of the Kutta-Joukowski (also spelled Joukowski, Zhukowski or Zhukovsky) theorem in aerodynamics. The lift on the spinning circle, due to this theorem, is $\rho U \Gamma$.

The fact that a body immersed in a potential flow does not experience any drag is the subject of the D'Alembert paradox. Neither the Rankine oval, nor the circle, nor body of any other shape experiences any drag in potential flow. D'Alembert paradox exist because potential flow does not satisfy the no-slip condition. The friction of a viscous fluid with the solid boundary generates vorticity, which is transported by the fluid to regions away from the immersed body. In this manner, application of the no-slip boundary condition on viscous fluids invalidates the assumptions underlying potential flow, especially that the flow be irrotational. In fact, the shedding of vorticity into the flow is the origin of fluid dynamical drag (this we state without proof at this point).

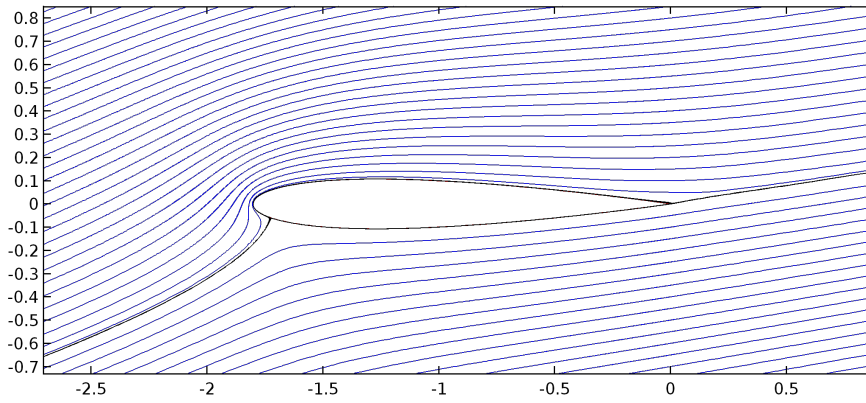


Figure 6.5: Flow around an airfoil at an angle of attack computed using the commercial software COMSOL. The streamlines are shown in blue, and the black curve is the stagnation streamline, part of which makes the airfoil shape. The angle of attack for this case is 14° .

6.5.2 Added mass from the unsteady term

Consider the contribution of the term $\rho \frac{\partial \phi}{\partial t}$. The resulting force is

$$\int_C \rho \frac{\partial \phi}{\partial t} \hat{\mathbf{n}} \, ds. \quad (6.44)$$

Let us examine this expression for the case of flow around a circle, so that $w(z)$ is given by (6.36). This corresponds to

$$\phi = \operatorname{Re}(w) = U \cos \theta \left(r + \frac{a^2}{r} \right), \quad \text{which on } r = a \text{ is } \phi = 2Ua \cos \theta. \quad (6.45)$$

The integral for force yields

$$\mathbf{F} = \int_0^{2\pi} 2\rho \frac{dU}{dt} a \cos \theta (\cos \theta \hat{\mathbf{e}}_x + \sin \theta \hat{\mathbf{e}}_y) a \, d\theta = \rho \pi a^2 \frac{dU}{dt} \hat{\mathbf{e}}_x. \quad (6.46)$$

This result may be interpreted in the following way. Any acceleration of the circle implies an acceleration of the fluid around it. This acceleration needs an additional force proportional to the acceleration. The coefficient of proportionality between this additional force and the acceleration is the “added mass” the fluid presents to the motion of the circle. In this case, the added mass is $\rho \pi a^2$.

6.6 Flow around an airfoil

The lift generated by an airfoil is a central result in aerodynamics, which makes use of potential flow. Some salient features of this flow are visualized in Figure 6.5. The stagnation streamline is incident on the lower surface of the airfoil, which develops the stagnation pressure under the airfoil. The streamlines curve around the leading edge of the airfoil, generating a low-pressure area above the airfoil. Finally and crucially, note that the stagnation streamline separates from the plate at the trailing edge. These are the features that will guide us in constructing the appropriate potential flow.

Here we will present one calculation, that of the lift on the prototypical airfoil – a flat plate, which highlights this central result. The underlying potential flow is constructed in this case using a technique known as conformal mapping (the same technique can be used to construct flow around airfoils of other shapes).

A conformal map is a map between two complex variables, which we take to be z and ζ . Here $z = x + iy$ corresponds to the physical spatial variable, in which the flat plate exists, and ζ is the mapped variable, in which the flat plate is mapped to a circle. The particular map we use is called the Joukowski map:

$$z = f(\zeta) = (1 + \epsilon)\zeta + (1 - \epsilon)\frac{a^2}{\zeta}. \quad (6.47)$$

A circle in ζ -plane, $\zeta = ae^{i\theta}$ is mapped to

$$z = a(1 + \epsilon)e^{i\theta} + a(1 - \epsilon)e^{-i\theta} = 2a \cos \theta + 2ia\epsilon \sin \theta, \quad (6.48)$$

which is an ellipse of major axis $2a$ along the x -axis and minor axis $2a\epsilon$ along the y -axis. In the limit $\epsilon \rightarrow 0$, the ellipse approaches a flat plate $-2a \leq x \leq 2a$. The point $\zeta = a$ is mapped to the trailing edge of the plate $z = 2a$. The chord of the flat plate is $c = 4a$.

While it is possible to solve for the inverse map $\zeta = f^{-1}(z)$ in closed form, the idea is to not need the explicit expression for the inverse. However, we do need the inverse map to be analytic so that the complex potential

$$W(z) = w(f^{-1}(z)) \quad (6.49)$$

automatically deforms the streamlines and converts the circular streamline in the ζ coordinates to be a flat plate in the z coordinates, whilst preserving the analyticity of the complex potential.

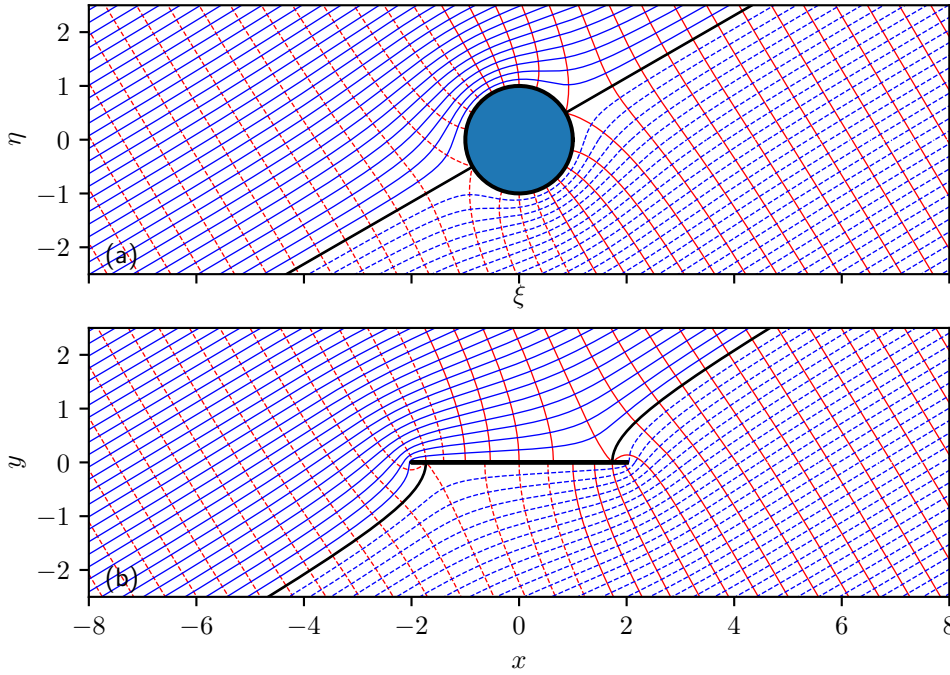


Figure 6.6: Flow around a flat plate at an angle of 30° to the flow and $\Gamma = 0$. (a) The flow in the $\zeta = \xi + i\eta$ coordinates. Streamlines are in blue and equipotential lines in red. Black curve shows the stagnation streamline. (b) The same flow in the $z = x + iy$ coordinates.

We start with the complex potential (6.38) for flow around a circle, but now expressed in ζ and with an angle of attack α , i.e.,

$$w(\zeta) = U \left(\zeta e^{-i\alpha} + \frac{a^2}{\zeta e^{-i\alpha}} \right) - \frac{i\Gamma}{2\pi} \log \zeta. \quad (6.50)$$

As $\zeta \rightarrow \infty$, the largest term in $w(\zeta)$ is $U\zeta e^{-i\alpha}$, corresponding with uniform flow at an angle α to the flat plate. The complex velocity in the ζ plane is

$$w'(\zeta) = U \left(e^{-i\alpha} - \frac{a^2}{\zeta^2} e^{i\alpha} \right) - \frac{i\Gamma}{2\pi\zeta}. \quad (6.51)$$

The velocity in the z -coordinates is

$$\frac{dW}{dz} = \frac{w'(\zeta)}{z'(\zeta)} = \frac{U \left(e^{-i\alpha} - \frac{a^2}{\zeta^2} e^{i\alpha} \right) - \frac{i\Gamma}{2\pi\zeta}}{1 - \frac{a^2}{\zeta^2}}. \quad (6.52)$$

As $\zeta \rightarrow \infty$, dW/dz approaches U .

Consider the case $\Gamma = 0$. An example of the flow corresponding to this case is shown in Figure 6.6. Note that the stagnation point in the ζ -plane is at $\zeta = \pm ae^{i\alpha}$. This point maps in the z -plane to $z = -2a \cos \alpha$ below the flat plate, and $z = 2a \cos \alpha$ above it. Note that in this flow, the stagnation streamline does not separate from the trailing edge $z = 2a$.

The stagnation point may be moved by judiciously choosing the value of Γ . The condition that the trailing edge be the rear stagnation point is called the *Kutta condition*. We impose the Kutta condition by ensuring that the stagnation point in the ζ -coordinates is at $\zeta = a$. Substituting the velocity $w'(\zeta) = 0$ at $\zeta = a$ yields

$$\Gamma = -4\pi U a \sin \alpha \quad (6.53)$$

The streamlines and equipotential lines corresponding to the value of Γ that enforces the Kutta condition, shown in Figure 6.7, illustrate this condition.

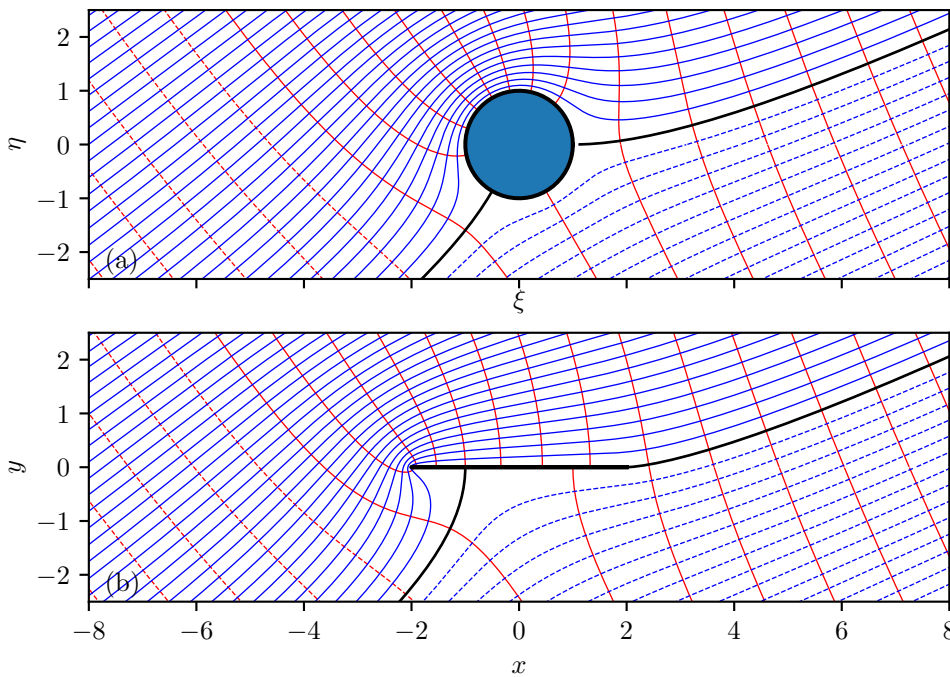


Figure 6.7: Flow around a flat plate at an angle of 30° to the flow and Γ given by (6.53). (a) The flow in the $\zeta = \xi + i\eta$ coordinates. Streamlines are in blue and equipotential lines in red. Black curve shows the stagnation streamline. (b) The same flow in the $z = x + iy$ coordinates.

The lift F_y on the flat-plate is given by

$$F_y = -\rho U \Gamma = 4\pi \rho U^2 a \sin \alpha. \quad (6.54)$$

This result can be converted to a dimensionless form in terms of the coefficient of lift, C_L , defined as

$$C_L = \frac{F_y}{\frac{1}{2} \rho U^2 c}. \quad (6.55)$$

Using the result (6.54), the lift coefficient depends on the angle of attack as

$$C_L = \frac{4\pi \rho U^2 a \sin \alpha}{\frac{1}{2} \rho U^2 (4a)} = 2\pi \sin \alpha. \quad (6.56)$$

Figure 6.8 shows that the results of (6.56) compare well with the lift coefficient computed using the commercial software COMSOL for small α . The agreement worsens around $\alpha \approx 10^\circ$ due to a phenomenon called stall, in which the stagnation streamline also separates from the leading edge. A careful treatment of the influence of viscosity is needed to gain a deeper understanding of stall.

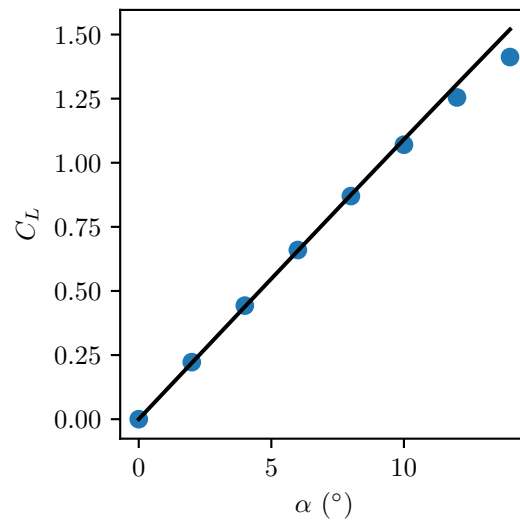


Figure 6.8: Lift coefficient C_L as a function of angle of attack α . Blue circles show the lift calculated from computations in COMSOL. Black line shows results of (6.56).

Chapter 7

Boundary layers

Boundary layers are regions of space adjacent to boundaries of fluid domains where effects of viscosity may not be ignored no matter how small the coefficient of viscosity may be. The characteristics of and the dynamics within boundary layers are of interest especially when the coefficient of viscosity is vanishingly small. The example of the boundary layer next to a flat plate aligned with the flow, the topic of this chapter, illustrates the essential features.

7.1 Flow next to a flat plate

Consider a uniform flow of speed U along the x -axis being incident on a flat plate of infinitesimal thickness and length L aligned with the flow, as schematically shown in Figure 7.1. The plate is oriented perpendicular to the plane of paper. The fluid has viscosity μ and density ρ . We ignore gravity in this example. The potential flow $\mathbf{u} = U\hat{\mathbf{e}}_x$ with a uniform pressure satisfies mass and momentum conservation, and the no-penetration condition on the flat plate, but not the no-slip condition. For an inviscid fluid, this is a perfectly valid flow, but not for a viscous fluid, no matter how small the viscosity coefficient. In this manner, this example offers the opportunity to study how the imposition of the no-slip condition modifies the simplest of potential flows in the presence of the slightest of viscosity. Hence, we choose a vanishingly small coefficient of viscosity μ .

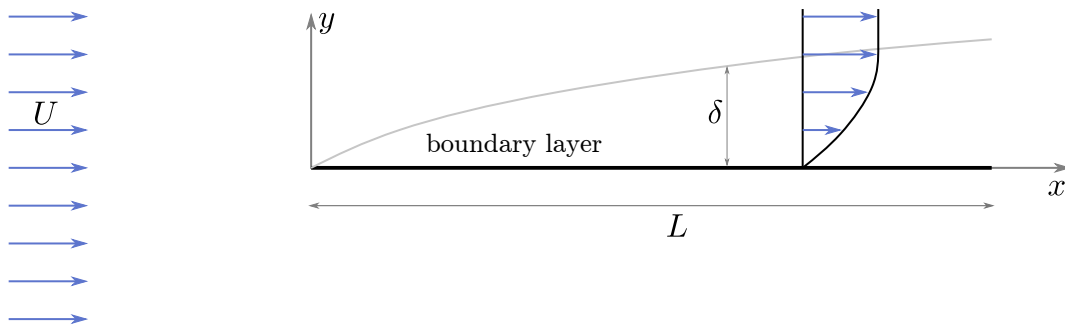


Figure 7.1: Schematic of a flow past a flat plate aligned with the flow. Here the thickness of the boundary layer is denoted as δ .

7.1.1 Qualitative description of the flow

Let us first develop a picture of the dynamics of this flow in our minds. The approach we take is to make various assumptions about the flow now and verify them later. This flow is driven by the inertia of the fluid in the freestream. The fluid particles away from the plate start out with speed U and will continue to do so unless an unbalanced force makes them decelerate. The action of the no-slip boundary condition and the shear stress that develops in the fluid is expected to slow down the fluid in the vicinity of the flat plate. A typical profile u versus y is shown in Figure 7.1. The boundary layer, the region where the flow speed appreciably falls

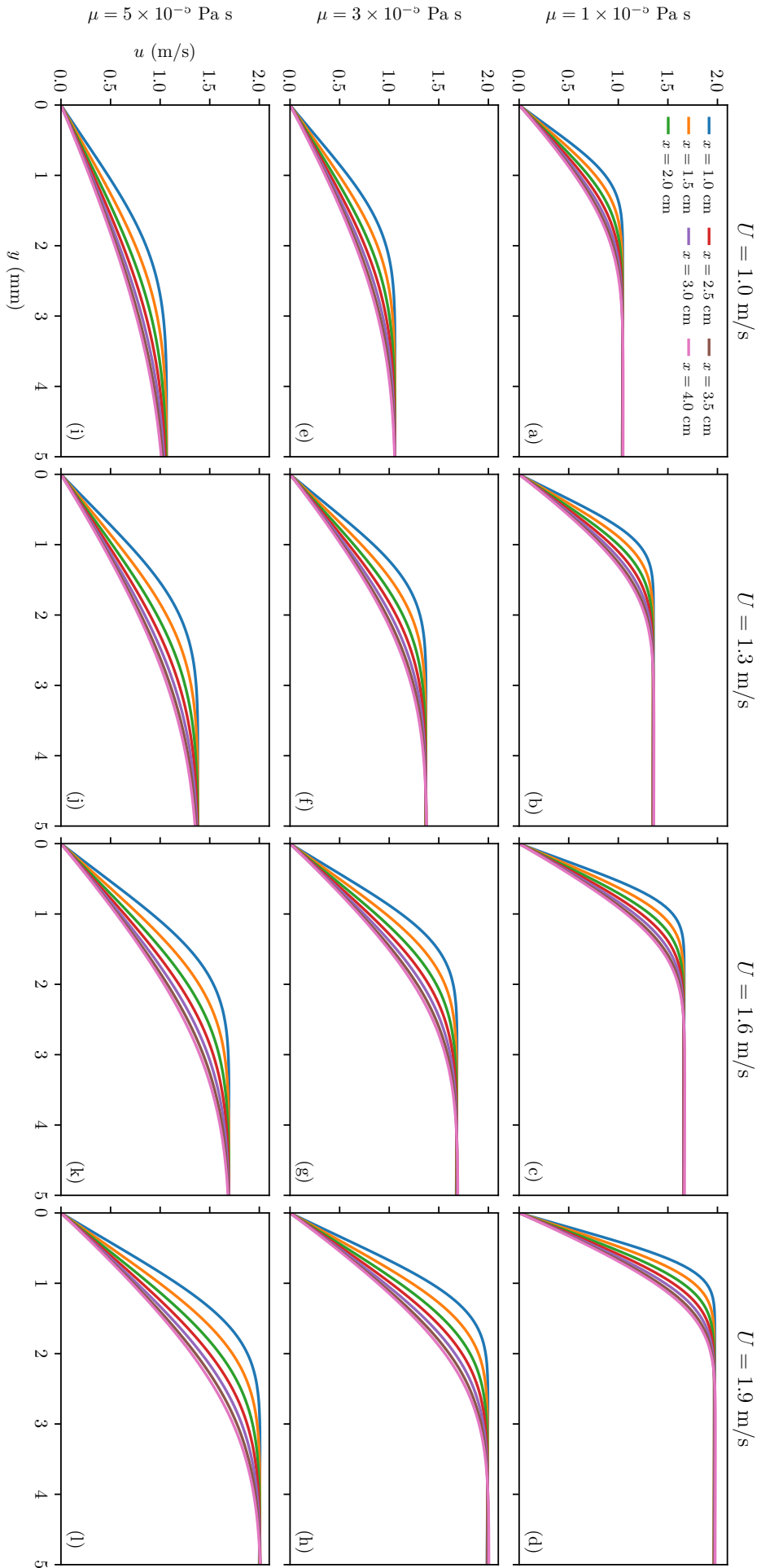


Figure 7.2: Profiles of u versus y taken at 7 distances from the leading edge of the plate. (a-l) Columns correspond to constant U listed at the top of each column and rows to constant μ listed to the left.

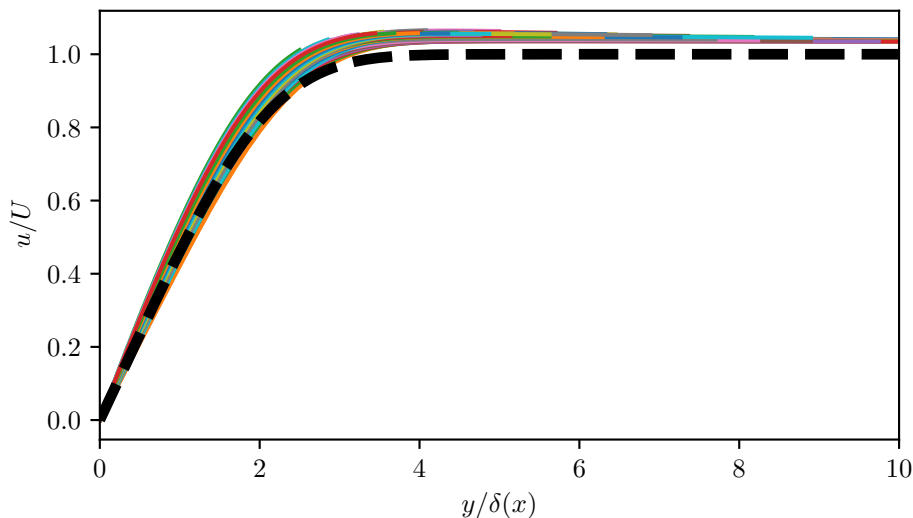


Figure 7.3: Collapse of the profiles of u versus y when rescaled. Each of the curves in Figure 7.2 is plotted as the coloured curves in this figure. Here δ is from (7.18). The dashed black curve corresponds to the solution of (7.24-7.25).

blow the freestream value U , is expected to be of thickness δ that is also vanishingly small with the coefficient of viscosity. Outside this layer, we expect the flow to be approximately uniform, and certainly described by potential flow. A natural consequence of the slowing down of the flow in the boundary layer is that the fluid upstream that is incident just above the plate now needs to be deflected away from the plate. Therefore, a y components of velocity also naturally appears in the flow. However, because of the thinness of the boundary layer, the amount of deflection is weak and the y component is expected to be smaller in magnitude than the x component.

A computational solution of Navier-Stokes equations is used to assist with the qualitative description of the flow. The commercial finite elements software COMSOL is used to obtain the solution. The particular case considered is for $L = 5$ cm, $\rho = 1$ kg/m³ and several values for μ and U (listed in Figure 7.2. The plate in this case has a finite thickness equal to $1/64$ the length. The computational box is chosen to be 10 cm \times 10 cm. (See the LectureCapture video from March 6, 2020, for more details.)

To obtain some insight into the thickness of the boundary layer, Figure 7.2 shows the computed profiles of velocity for different values of U and ν . It is evident that increasing U decreases δ , while increasing μ increases it. The growth of the boundary layer with x , the distance from the leading edge, is also evident. These are the features we seek to explain in the subsequent analysis.

A scaling estimate for δ may be made in the following way. A fluid particle starting from the leading edge of the plate traveling with speed U takes time $t = x/U$ to traverse the distance x . Perpendicular to the direction of travel, viscosity influences a distance $\delta = \sqrt{\nu t}$ in time t , where $\nu = \mu/\rho$ is the kinematic viscosity. In this case, this implies $\delta = \sqrt{\nu x/U}$. Miraculously, replotting a rescaled version of the data shown in Figure 7.2 collapses each one of those profiles of u versus y very close to a universal curves. Figure 7.3 demonstrates this collapse where y is rescaled using $\delta(x)$ and u with U . To explain this miraculous collapse, to determine the universal shape the velocity collapses to, and to better understand the underlying fluid dynamics, we proceed with certain simplifying assumptions about the flow.

It can be seen from this estimate that the boundary layer becomes vanishingly thin as ν approaches zero. The slope of the growing boundary layer thickness is proportional to δ/x , and therefore, we expect the y component of velocity to be of the magnitude $U\delta/x$. Subsequent analysis proceeds under the assumption that δ is much smaller than L in the following analysis to derive the so-called Prandtl boundary-layer equations.

7.1.2 Derivation of the Prandtl boundary layer equations

In the limit of small viscosity, and especially due to the boundary layer being thinner than the length of the plate, the governing Navier-Stokes equations simplify to the simpler Prandtl boundary layer equations. To

Equation	Terms and their magnitudes				
Mass conservation (7.1a)	$\frac{\partial u}{\partial x} \sim \frac{U}{L}$	$\frac{\partial v}{\partial y} \sim \frac{V}{\delta}$			
x -momentum conservation (7.1b)	$\rho u \frac{\partial u}{\partial x} \sim \frac{\rho U^2}{L}$	$\rho v \frac{\partial u}{\partial y} \sim \frac{\rho UV}{\delta}$	$\frac{\partial p}{\partial x} \sim \frac{P}{L}$	$\mu \frac{\partial^2 u}{\partial x^2} \sim \frac{\mu U}{L^2}$	$\mu \frac{\partial^2 u}{\partial y^2} \sim \frac{\mu U}{\delta^2}$
y -momentum conservation (7.1c)	$\rho u \frac{\partial v}{\partial x} \sim \frac{\rho UV}{L}$	$\rho v \frac{\partial v}{\partial y} \sim \frac{\rho V^2}{\delta}$	$\frac{\partial p}{\partial y} \sim \frac{P}{\delta}$	$\mu \frac{\partial^2 v}{\partial x^2} \sim \frac{\mu V}{L^2}$	$\mu \frac{\partial^2 v}{\partial y^2} \sim \frac{\mu V}{\delta^2}$
(magnitudes of (7.1c) simplified)	$\frac{\rho U^2}{L} \frac{1}{\sqrt{\text{Re}}}$	$\frac{\rho U^2}{L} \frac{1}{\sqrt{\text{Re}}}$	$\frac{\rho U^2}{L} \sqrt{\text{Re}}$	$\frac{\rho U^2}{L} \frac{1}{\sqrt{\text{Re}}^3}$	$\frac{\rho U^2}{L} \frac{1}{\sqrt{\text{Re}}}$

Table 7.1: Scaling estimate of the magnitude of terms in (7.1).

derive them, let us start with the steady two-dimensional Navier-Stokes equations

$$\frac{\partial u}{\partial x} + \frac{\partial v}{\partial y} = 0, \quad (7.1a)$$

$$\rho \left(u \frac{\partial u}{\partial x} + v \frac{\partial u}{\partial y} \right) = -\frac{\partial p}{\partial x} + \mu \left(\frac{\partial^2 u}{\partial x^2} + \frac{\partial^2 u}{\partial y^2} \right), \quad (7.1b)$$

$$\rho \left(u \frac{\partial v}{\partial x} + v \frac{\partial v}{\partial y} \right) = -\frac{\partial p}{\partial y} + \mu \left(\frac{\partial^2 v}{\partial x^2} + \frac{\partial^2 v}{\partial y^2} \right). \quad (7.1c)$$

Noting the reflection symmetry of the flow around $y = 0$, we only solve for u , v and p for $y \geq 0$. These equations are to be solved with the boundary conditions

$$u(x \geq 0, y = 0) = 0, \quad (7.2a)$$

$$v(x \geq 0, y = 0) = 0, \quad (7.2b)$$

$$u(x, y \rightarrow \infty) = U. \quad (7.2c)$$

Scaling estimate of the size of terms in Navier-Stokes equations

The first step is to develop a scaling estimate for each of the terms in these equations. Here our objective is to identify how each term in (7.1) scales with the parameters of the problem, viz., ρ , μ , U and L , and then balance the magnitudes of the dominant terms.

Each dependent and independent variable is assigned a constant magnitude in terms of the parameters governing the problem. For example, the magnitude of u is taken to be U , expressed as $u \sim U$. Similarly, the scale for x is taken to be L , i.e. $x \sim L$. We do not yet know the magnitudes for v , y and p , so we define symbols V , δ and P , respectively, to represent them. The magnitudes of partial derivatives are estimated using ratios of the variables in the derivative, e.g., $\frac{\partial u}{\partial x} \sim \frac{U}{L}$. Our task is to express these undefined symbols in terms of the known parameters using dominant balances.

As an illustration, consider the mass conservation equation (7.1a). The magnitude of the two terms in this equation are presented in the second row of Table 7.1. Balancing the magnitudes of the two terms yields the magnitude for v as

$$\frac{U}{L} = \frac{V}{\delta} \quad \implies \quad V = \frac{U\delta}{L}. \quad (7.3)$$

Note that this is consistent with our estimates in the simple picture in §7.1.1.

Table 7.1 also shows the magnitude estimates for the momentum conservation equations in (7.1). Using (7.3), it is evident that in (7.1b)

$$\frac{\rho U^2}{L} = \frac{\rho UV}{\delta}, \quad (7.4)$$

implying that both the terms $\rho u \frac{\partial u}{\partial x}$ and $\rho v \frac{\partial u}{\partial y}$ are of equal magnitude. Furthermore, given that the pressure field is established to enforce incompressibility, its magnitude is set up to balance the strongest term in the equations. This implies that the $\rho u \frac{\partial u}{\partial x}$ is of a magnitude comparable to $\frac{\partial p}{\partial x}$, or

$$\frac{P}{L} = \frac{\rho U^2}{L} \quad \implies \quad P = \rho U^2. \quad (7.5)$$

Between the two viscous terms, $\mu \frac{\partial^2 u}{\partial x^2}$ and $\mu \frac{\partial^2 u}{\partial y^2}$, which scale as $\mu U/L^2$ and $\mu U/\delta^2$, respectively, because $\delta \ll L$ it is evident that, $\mu \frac{\partial^2 u}{\partial x^2} \ll \mu \frac{\partial^2 u}{\partial y^2}$. Thus, the term $\mu \frac{\partial^2 u}{\partial x^2}$ is perhaps negligible compared to at least one other term in (7.1b). Neglecting the $\mu \frac{\partial^2 u}{\partial x^2}$ also will render the dominant balance equivalent to that of an inviscid fluid, which is contrary to our original intention of studying the influence of viscosity. Therefore, balancing the dominant of the two viscous terms $\mu \frac{\partial^2 u}{\partial y^2}$ with the inertial terms yields

$$\frac{\rho U^2}{L} = \frac{\mu U}{\delta^2} \quad \implies \quad \delta = \sqrt{\frac{\nu L}{U}}. \quad (7.6)$$

This expression is eerily similar to one derived in §7.1.1, except that x is replaced by L . We can now verify our assumption

$$\frac{\delta}{L} \ll 1 \quad \iff \quad \sqrt{\frac{\nu}{UL}} = \text{Re}^{-1/2} \ll 1 \quad \iff \quad \text{Re} \gg 1, \quad (7.7)$$

where we define the Reynolds number $\text{Re} = UL/\nu$.

We now turn our attention to (7.1c). Substituting V from (7.3) and P from (7.5) into (7.1c) yields the magnitude of every term in (7.1c). In light of the assumption $\delta \ll L$ yields the most dominant term in that equation to be $\frac{\partial p}{\partial y}$, which scales as $\frac{\rho U^2}{L} \times \sqrt{\text{Re}}$, while all the other terms are negligible in comparison. See Table 7.1 for details.

With these estimates, (7.1) simplify to

$$\frac{\partial u}{\partial x} + \frac{\partial v}{\partial y} = 0, \quad (7.8a)$$

$$\rho \left(u \frac{\partial u}{\partial x} + v \frac{\partial u}{\partial y} \right) = -\frac{\partial p}{\partial x} + \mu \frac{\partial^2 u}{\partial y^2}, \quad (7.8b)$$

$$0 = -\frac{\partial p}{\partial y}, \quad (7.8c)$$

which are subject to boundary conditions given by (7.2). The set of equations (7.8) are known as the Prandtl boundary-layer equations after Ludwig Prandtl, who first identified the presence of boundary layers in high Reynolds number flow of viscous fluids, and the approximation leading to them is called the Prandtl boundary-layer approximation.

For flow past a flat plate, the flow is uniform outside the boundary layer, and consequently the pressure is uniform there. Combined with (7.8c), this implies that the pressure is uniform everywhere and $\frac{\partial p}{\partial x} = 0$. Thus, for the case of flow past a flat plate, (7.8) simplify further to

$$\frac{\partial u}{\partial x} + \frac{\partial v}{\partial y} = 0, \quad (7.9a)$$

$$u \frac{\partial u}{\partial x} + v \frac{\partial u}{\partial y} = \nu \frac{\partial^2 u}{\partial y^2}. \quad (7.9b)$$

7.1.3 Self-similar flow past a semi-infinite flat plate

In a region closer to the leading edge of the plate, say a distance x , which is much larger than ν/U but much smaller than the plate length, L , a self-similar structure emerges for the flow. We expose this structure in this section.

Scale invariance

The scale invariance of the geometry of the flow past a long plate, approximated as semi-infinite, is evident. Upon zooming out, the plate appears semi-infinite and the uniform flow remains uniform. The governing dynamics in the boundary layer are also scale invariant. To see this, rescale the variables in (7.9) and (7.2) as

$$u = \alpha \tilde{u}, \quad v = \beta \tilde{v}, \quad x = \gamma \tilde{x} \quad \text{and} \quad y = \delta \tilde{y}, \quad (7.10)$$

where α , β , γ and δ are positive transformation factors. The rescaled equations (7.9) and (7.2) are

$$\frac{\alpha}{\gamma} \frac{\partial \tilde{u}}{\partial \tilde{x}} + \frac{\beta}{\delta} \frac{\partial \tilde{v}}{\partial \tilde{y}} = 0, \quad (7.11a)$$

$$\frac{\alpha^2}{\gamma} \tilde{u} \frac{\partial \tilde{u}}{\partial \tilde{x}} + \frac{\alpha\beta}{\delta} \tilde{v} \frac{\partial \tilde{u}}{\partial \tilde{y}} = \frac{\alpha}{\delta^2} \nu \frac{\partial^2 \tilde{u}}{\partial \tilde{y}^2}, \quad (7.11b)$$

and

$$\alpha \tilde{u}(\alpha \tilde{x} \geq 0, \delta \tilde{y} = 0) = 0, \quad \implies \quad \tilde{u}(\tilde{x} \geq 0, \tilde{y} = 0) = 0 \quad (7.12a)$$

$$\beta \tilde{v}(\alpha \tilde{x} \geq 0, \delta \tilde{y} = 0) = 0, \quad \implies \quad \tilde{v}(\tilde{x} \geq 0, \tilde{y} = 0) = 0 \quad (7.12b)$$

$$\alpha \tilde{u}(\alpha \tilde{x}, \delta \tilde{y} \rightarrow \infty) = U. \quad \implies \quad \tilde{u}(\tilde{x}, \tilde{y} \rightarrow \infty) = \frac{U}{\alpha} \quad (7.12c)$$

Equation (7.11) and (7.12) are identical to (7.9) and (7.2) if

$$\frac{\beta}{\delta} = \frac{\alpha}{\gamma}, \quad \frac{\alpha^2}{\gamma} = \frac{\alpha}{\delta^2}, \quad \text{and} \quad \alpha = 1. \quad (7.13)$$

These relations between the scaling factors are satisfied if $\alpha = 1$, $\delta = \sqrt{\gamma}$ and $\beta = 1/\sqrt{\gamma}$, irrespective of the value of γ . This demonstrates the invariance of the governing equations, and thereby the flow, to the (anisotropic) scaling of the independent and dependent variables.

The scale invariance implies that the flow velocity at points related by the transformation is also related. In particular, if the functional form of $u(x, y)$ is given by $u(x, y) = F(x, y)$, then an identical form describes the velocity in the transformed coordinates, i.e., $\tilde{u}(\tilde{x}, \tilde{y}) = F(\tilde{x}, \tilde{y})$. Given the relation between u and \tilde{u} from (7.10),

$$F(x, y) = \alpha F(\tilde{x}, \tilde{y}) = \alpha F\left(\frac{x}{\gamma}, \frac{y}{\delta}\right). \quad (7.14)$$

Expressing α and δ in terms of γ and F in terms of u yields

$$u(x, y) = u\left(\frac{x}{\gamma}, \frac{y}{\sqrt{\gamma}}\right). \quad (7.15)$$

Choosing $\gamma = x$ reduces this relation to a form useful for our interpretation as

$$u(x, y) = u\left(1, \frac{y}{\sqrt{x}}\right). \quad (7.16)$$

This equation states that the profile of u versus y at any location x is related to that at $x = 1$ (arbitrary units) by a simple rescaling of y by \sqrt{x} . Similarly,

$$v(x, y) = \frac{1}{\sqrt{x}} v\left(1, \frac{y}{\sqrt{x}}\right). \quad (7.17)$$

In this way, we expect the velocity profile to not be independently dependent on x and y , but merely on the combination y/\sqrt{x} alone.

Determination of the Blasius self-similar profile

Once the possibility of self-similarity is established, the following approach can be used to simplify the governing equations. First, a precursory method incorporates the dependence of the dimensional parameters into the scaling invariance. At this stage, we simply replace derivatives in (7.9) with ratios, and replace the dependent and independent variables with the scaling estimates in terms of known problem parameters, very similar to scaling estimates in §7.1.2. In this analysis, armed by the knowledge of scale invariance, we recognize that x

itself represents the scale for the independent variable x , and $\delta(x)$ for y . The scales for u and v are U and $U\delta(x)/x$, respectively, in view of (7.9a). The dominant balance between terms in (7.9b) is

$$\frac{U^2}{x} = 2\nu \frac{U}{\delta(x)^2} \quad \Longrightarrow \quad \delta(x) = \sqrt{\frac{2\nu x}{U}}, \quad (7.18)$$

in agreement with the intuition presented in §7.1.1, except for the factor of 2. (The explanation for this factor being an algebraic convenience will appear soon.) This approach also explains the appearance of L in the expression for δ in (7.6) instead of x as in (7.18). Because of the scale-invariance, the plate length L is not the appropriate scale for x , but x itself is. Apart from this difference, the balance of terms that led to (7.18) and (7.6) are identical. Equation (7.18) now incorporates the dimensional dependence on the parameters ν and U .

We proceed to determine the self-similar flow profile by incorporating the results (7.18) and (7.16) by asserting that

$$u = Uf'(\xi), \quad \text{where} \quad \xi = \frac{y}{\delta(x)}. \quad (7.19)$$

Here the variables ξ and $f(\xi)$ are dimensionless and $'$ denotes differentiation with respect to the argument. There exist multiple equivalent formulations, which represent the same flow, from which we choose one. To facilitate the subsequent analysis, note that

$$\frac{d\delta}{dx} = \sqrt{\frac{\nu}{2Ux}} = \frac{\delta}{2x} \quad \text{so} \quad \frac{\partial \xi}{\partial x} = -\frac{y}{\delta^2} \delta'(x) = -\frac{\xi}{2x} \quad \text{and} \quad \frac{\partial \xi}{\partial y} = \frac{1}{\delta}. \quad (7.20)$$

Using (7.20),

$$\frac{\partial u}{\partial x} = Uf''(\xi) \frac{\partial \xi}{\partial x} = -\frac{U}{2x} \xi f''(\xi), \quad (7.21a)$$

$$\frac{\partial u}{\partial y} = Uf''(\xi) \frac{\partial \xi}{\partial y} = \frac{U}{\delta} f''(\xi), \quad (7.21b)$$

$$\frac{\partial^2 u}{\partial y^2} = \frac{U}{\delta^2} f'''(\xi), \quad (7.21c)$$

$$\frac{\partial v}{\partial y} = \frac{1}{\delta} \frac{\partial v}{\partial \xi}. \quad (7.21d)$$

Substitution into (7.9a) yields

$$\frac{\partial v}{\partial \xi} = U \frac{\delta}{2x} \xi f''(\xi), \quad \Longrightarrow \quad v = U \frac{\delta}{2x} (\xi f'(\xi) - f(\xi)). \quad (7.22)$$

Substituting (7.19) and (7.22) in (7.9b) yields

$$\frac{U^2}{2x} (-\xi f'(\xi) f''(\xi) + (\xi f'(\xi) - f(\xi)) f''(\xi)) = \nu \frac{U}{\delta^2} f'''(\xi). \quad (7.23)$$

This equation reveals the utility of the dominant balance using scaling. Note that in (7.18) we balanced the terms U^2/x and $\nu U/\delta^2$, which are also the dimensional pre-factors of the terms in (7.23). The additional factor of 2 in (7.18) is simply to account for the factor of 2 that arises in (7.23) – this factor is not necessary for deriving the self-similar flow profile. The essential reason underlying the utility of the method to derive (7.18) is that, according to the chain rule applied in (7.20) and (7.21), differentiation with respect to x yields a dimensional factor of $1/x$, and with respect to y yields $1/\delta$. These were precisely the rules we used to derive (7.18).

In view of (7.18), equation (7.23) simplifies to

$$f'''(\xi) + f(\xi) f''(\xi) = 0. \quad (7.24)$$

The boundary conditions (7.2) simplify to

$$f'(\xi = 0) = 0, \quad (7.25a)$$

$$f(\xi = 0) = 0, \quad (7.25b)$$

$$f'(\xi \rightarrow \infty) = 1. \quad (7.25c)$$

Equations (7.24-7.25) are called the Blasius equations for the self-similar profile. They constitute an ordinary differential boundary value problem, which cannot be solved in closed form analytically but can be easily solved numerically. The solution is shown in Figure 7.3 as the dashed curve, which agrees very well with the numerically computed profiles.

μ (Pa s) / U (m/s)	$\mu = 10^{-5}$	3×10^{-5}	5×10^{-5}	μ (Pa s) / U (m/s)	$\mu = 10^{-5}$	3×10^{-5}	5×10^{-5}
$U = 1.0$	4.13	7.85	10.6	$U = 1.0$	4.70	8.13	10.5
$U = 1.3$	5.99	11.4	15.4	$U = 1.3$	6.96	12.1	15.6
$U = 1.6$	8.04	15.3	20.6	$U = 1.6$	9.50	16.5	21.2
$U = 1.9$	10.3	19.5	26.3	$U = 1.9$	12.3	21.3	27.5

Table 7.2: Drag on the plate computed using COMSOL (left) compared with the result of the boundary layer approximation (7.29) (right).

7.1.4 Drag on the plate

With the complete flow field described analytically, we now return to our original motivation of estimating the drag on the plate because of viscous shear stress. The uniform potential flow violates the no-slip boundary condition and, in the process, also fails to account for the drag on the plate. The boundary layer approximation retains the no-slip condition, and thus might be able to explain the drag on the plate.

The drag on the upper surface of the plate is calculated by integrating the tangential component of the shear stress. The components of the total (i.e., Cauchy) stress tensor are

$$\mathbf{T} = -p \begin{bmatrix} 1 & 0 \\ 0 & 1 \end{bmatrix} + \mu \begin{bmatrix} 2\frac{\partial u}{\partial x} & \frac{\partial u}{\partial y} + \frac{\partial v}{\partial x} \\ \frac{\partial u}{\partial y} + \frac{\partial v}{\partial x} & 2\frac{\partial v}{\partial y} \end{bmatrix}. \quad (7.26)$$

The tangential component of the traction on the plate is

$$\hat{\mathbf{e}}_x \cdot \mathbf{T} \cdot \hat{\mathbf{e}}_y = \mu \left(\frac{\partial u}{\partial y} + \frac{\partial v}{\partial x} \right) \approx \mu \frac{\partial u}{\partial y}. \quad (7.27)$$

Note that the component of stress due to pressure does not exert a tangential force on the plate. And using scaling estimates developed in §7.1.2, amongst the terms in (7.27), $\frac{\partial u}{\partial y}$ scales as U/δ and dominates over $\frac{\partial v}{\partial x}$, which scales as $V/L = U\delta/L^2$. Therefore, to the level of approximation we have retained, the term $\frac{\partial v}{\partial x}$ may be neglected.

The total force, D , per unit length out of the plane of the paper now may be estimated using (7.21b) as

$$D = \int_0^L \mu \frac{\partial u}{\partial y} \Big|_{y=0} dx = \int_0^L \frac{\mu U}{\delta(x)} f''(\xi = 0) dx = \sqrt{\frac{\mu^2 U^3}{2\nu}} f''(\xi) \int_0^L \frac{dx}{\sqrt{x}} = \sqrt{2\mu\rho U^3 L} f''(0). \quad (7.28)$$

The value of $f''(0)$ from the solution of (7.24-7.25) is 0.4696. Substituting this value yields an expression for the drag on a flat plate align with a flow at high Reynolds number as

$$D = 0.664 \sqrt{\rho \mu U^3 L}. \quad (7.29)$$

A comparison of the results of (7.29) with that of the complete solution computed using COMSOL is shown in Table 7.2. The simple expression in (7.29) agrees well with the results of the full computational solution. Reasons for the remaining slight disagreement are the finite thickness of the plate in the COMSOL simulation and the approximations made in the boundary layer theory.

According to (7.29), longer plates experience greater drag but drag does not grow proportional to the plate length. It is so because the boundary layer is thinner near the leading edge of the plate, where the plate experiences most drag. The drag is super-linear in the freestream fluid speed, growing as $U^{3/2}$, which is because the boundary layer thickness itself decreases with U thereby enhancing the shear stress on the plate. Also, in the limit of vanishing viscosity, the drag decreases to zero proportional to $\sqrt{\mu}$. The physical explanation for why the drag might vanish with vanishing fluid density is left for the astute student to discover.

Chapter 8

Acoustics and Incompressibility

We have extensively employed the incompressible approximation despite being acutely aware of the fact that no physical material is exactly incompressible. In this chapter, we examine the justification underlying this assumption using dimensional analysis. The theory underlying the acoustic limit of Navier-Stokes equations is needed to support our analysis. Let us derive this theory.

8.1 Acoustic limit of Navier-Stokes equations

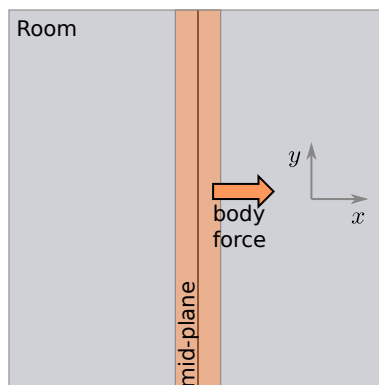


Figure 8.1: Schematic of the thought experiment to develop the acoustic approximation. A body force is applied to a thin slice of the fluid near the mid-plane for a short duration of time.

Consider the following thought experiment in a rectangular room filled with air. Imagine a fictitious agency exerting a body force concentrated on a thin slice around the mid-plane of the room for a short duration. Let us imagine the slice to be much thinner than the room length and the duration to be short. This setup is schematically shown in Figure 8.1.

If the fluid were incompressible, the response of the fluid would simply be to be compressed in the right half of the room and be de-compressed in the left half for the duration of the pulse. However, for a fluid with properties similar to air, a computational solution obtained using COMSOL illustrates a different outcome. For this simulation, the ambient pressure was taken to be $p_0 = 1$ Pa and the ambient density to be $\rho_0 = 1$ kg/m³. The equation of state is

$$p = p_0 \left(\frac{\rho}{\rho_0} \right)^\gamma, \quad (8.1)$$

where γ is the adiabatic gas index, which is equal to the ratio of specific heats of the gas under constant pressure and under constant volume. For air, $\gamma = 1.4$ approximately. A body force impulse was applied to a slice of about 0.5 m around the mid-plane of a 20 m \times 20 m room for about 10 ms. Figure 8.2 shows the snapshots of the fluid pressure that develop in the room every 2 seconds. Clearly, the fluid in the room does not behave according to our expectations for an incompressible fluid. Two pulses of pressure originate near the mid-plane. The high-pressure pulse propagates to the right and the low-pressure pulse to the left. When they encounter the

walls of the room, they get reflected and the reflected pulses meet near the mid-plane. Clearly, this behaviour is similar to that of a wave, in this case a sound wave.

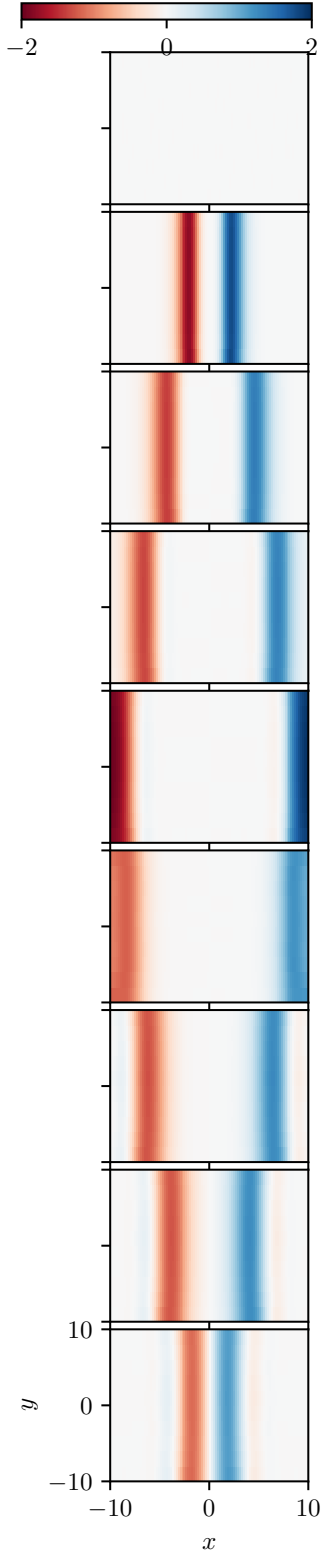


Figure 8.2: Snapshots of pressure perturbation in millibars at 2 s intervals from $t = 0$ (top) to $t = 16$ s (bottom).

An acoustic limit of the Navier-Stokes equations explains the origins of sound propagation in compressible media and many features of the observations from the COMSOL simulation, such as the speed of propagation of the pulses.

8.1.1 The Acoustic limit

To derive the acoustic limit of Navier-Stokes equations, we linearly perturb the inviscid compressible version of the equations to small amplitude motion. The inviscid compressible governing equations are

$$\frac{\partial \rho}{\partial t} + \nabla \cdot (\rho \mathbf{u}) = 0, \quad (8.2)$$

$$\rho \left(\frac{\partial \mathbf{u}}{\partial t} + \mathbf{u} \cdot \nabla \mathbf{u} \right) = -\nabla p. \quad (8.3)$$

To perform the linearization, we note that the static fluid at the ambient pressure and density satisfies the governing equations (8.1-8.3). This trivial solution, called the base state or the unperturbed state, is given by

$$p = p_0, \quad \rho = \rho_0, \quad \mathbf{u} = \mathbf{0}. \quad (8.4)$$

We now perturb this state infinitesimally as

$$p = p_0 + \epsilon p', \quad \rho = \rho_0 + \epsilon \rho', \quad \mathbf{u} = \mathbf{0} + \epsilon \mathbf{u}', \quad (8.5)$$

where we consider the limit of the scalar parameter $\epsilon \rightarrow 0$ to impose the infinitesimal size of the perturbation. Substituting these perturbed quantities in (8.1-8.3) yields

$$\epsilon p' = p_0 \left[\left(1 + \epsilon \frac{\rho'}{\rho_0} \right)^\gamma - 1 \right], \quad (8.6)$$

$$\frac{\partial \rho_0}{\partial t} + \epsilon \frac{\partial \rho'}{\partial t} + \epsilon \nabla \cdot ((\rho_0 + \epsilon \rho') \mathbf{u}) = 0, \quad (8.7)$$

$$(\rho_0 + \epsilon \rho') \left(\epsilon \frac{\partial \mathbf{u}'}{\partial t} + \epsilon^2 \mathbf{u}' \cdot \nabla \mathbf{u}' \right) = -\nabla p_0 - \epsilon \nabla p' \quad (8.8)$$

Note that $\frac{\partial \rho_0}{\partial t}$ and ∇p_0 vanish. We now expand these equations in a series in ϵ .

$$\epsilon p' = p_0 \left[\epsilon \gamma \frac{\rho'}{\rho_0} + \epsilon^2 \frac{\gamma(\gamma-1)}{2} \left(\frac{\rho'}{\rho_0} \right)^2 + \dots \right], \quad (8.9)$$

$$\epsilon \left(\frac{\partial \rho'}{\partial t} + \rho_0 \nabla \cdot \mathbf{u}' \right) + \epsilon^2 \nabla \cdot (\rho' \mathbf{u}') = 0, \quad (8.10)$$

$$\epsilon \rho_0 \frac{\partial \mathbf{u}'}{\partial t} + \epsilon^2 \left(\rho' \frac{\partial \mathbf{u}'}{\partial t} + \rho_0 \mathbf{u}' \cdot \nabla \mathbf{u}' \right) + \epsilon^2 \rho' \mathbf{u}' \cdot \nabla \mathbf{u}' = -\epsilon \nabla p'. \quad (8.11)$$

Note that in the limit $\epsilon \rightarrow 0$, each of the terms in these equations vanish, thus ascertaining the validity of the base state as a valid solution of the governing equations. To derive the equations governing the perturbations, it is necessary to divide each term by a factor of ϵ , and then take the limit as $\epsilon \rightarrow 0$. This yields

$$p' = \frac{\gamma p_0}{\rho_0} \rho', \quad (8.12)$$

$$\frac{\partial \rho'}{\partial t} + \rho_0 \nabla \cdot \mathbf{u}' = 0, \quad (8.13)$$

$$\rho_0 \frac{\partial \mathbf{u}'}{\partial t} = -\nabla p'. \quad (8.14)$$

Eliminating ρ' and \mathbf{u}' to derive a single equation for pressure as

$$\frac{\partial^2 p'}{\partial t^2} = c^2 \nabla^2 p' \quad \text{where} \quad c^2 = \frac{\gamma p_0}{\rho_0}. \quad (8.15)$$

This is the wave equation for the perturbation to the pressure and c is the speed of the wave, in this case the sound wave. In other words, small perturbations in pressure propagate as sound waves at a speed given by c .

8.2 Incompressible approximation

The incompressibility condition neglects the variations of density of the fluid. We are now in a position to derive conditions based on dimensional analysis for the assuming the fluid to be incompressible. These conditions are of two kinds. The first ensures that the pressure variations in the fluid are not so large as to induce appreciable changes in the density. And the second ensures that the temporal dynamics associated with propagation of pressure impulses may be considered essentially instantaneous. In what follows, we will take a flow with characteristic length, time, and speed to be L , T and U , respectively. We will take the ambient density and pressure to be ρ_0 and p_0 , respectively.

8.2.1 Variations in density due to pressure

In an incompressible flow, the pressure field establishes itself to ascertain that the density of the fluid does not change due to the flow of material. Therefore, the magnitude of pressure variations is set by the strongest forces in the flow. For flows with large Reynolds numbers, this force is the fluid inertia, whereas at small Reynolds numbers, it is the fluid viscosity. Therefore, we need two different cases.

Inertially-dominated flows

When the fluid inertia is the dominant force in the fluid, the variations in pressure generally (but not always¹) scale as ρU^2 . The scaling estimate for the corresponding change in density is

$$\rho' = \frac{\rho_0 U^2}{\left(\frac{\partial p}{\partial \rho}\right)}. \quad (8.16)$$

Noting that $\frac{\partial p}{\partial \rho}$ scales with c^2 , where c is the speed of sound in the medium, we arrive at

$$\frac{\rho'}{\rho_0} = \frac{U^2}{c^2} = \text{Ma}^2, \quad \text{where} \quad \text{Ma} = \frac{U}{c}. \quad (8.17)$$

Here Ma is the Mach number. The flow may be approximated to be incompressible if $\text{Ma} \ll 1$. For aerospace applications, when $\text{Ma} \lesssim 0.3$, the flow is found to be approximated well by the incompressible assumption. For other applications, the mileage of this condition may vary.

Viscously-dominated flows

The scale for pressure variations in a viscously-dominated flow is $\mu U/L$. The corresponding variations in density are

$$\frac{\rho'}{\rho_0} = \frac{\mu U/L}{\rho_0 \left(\frac{\partial p}{\partial \rho}\right)} = \frac{\text{Ma}^2}{\text{Re}}. \quad (8.18)$$

Thus, when Re is small, the condition for violating incompressibility is that Ma^2 be much larger than Re. For practical materials, this condition is difficult to violate.

¹For example, the pressure is uniform in Stokes first problem, despite inertia being a dominant force and the scale of fluid velocity variations being $U \neq 0$.

8.2.2 The finite propagation-speed of sound

The second criteria for incompressibility is that sound propagation be considered instantaneous. Given the finite speed of propagation of sound, pressure pulses travel a distance cT in time T . If the transient dynamics on time-scale T are of interest to the analysis (e.g., the flow may be driven on a rapid time scale), and the system size of interest is much larger than cT , then the propagation of sound waves may not be ignored. This condition may be stated as

$$\frac{L}{cT} \ll 1, \tag{8.19}$$

for incompressibility to be a valid approximation to the resulting flow.

Chapter 9

Stokes Flow

In this chapter, we will be considering situations where inertial forces are negligible such that the flows have small Reynolds numbers. Such flows are named Stokes flows after George G. Stokes who first calculated the drag on a sphere moving through a viscous fluid. The applications of Stokes flows are wide ranging, from biological applications at the small scale (e.g. the swimming of microorganisms) to geological applications at the large scale (e.g. the flow of lava).

9.1 Recap: Governing Equations

9.1.1 Navier-Stokes Equations

For an incompressible fluid, the equations for mass and momentum balance are (see §2.8 and §2.9):

$$\nabla \cdot \mathbf{u} = 0 \quad \text{and} \quad \rho \frac{D\mathbf{u}}{Dt} = \mathbf{f} + \nabla \cdot \mathbf{T}, \quad (9.1)$$

where \mathbf{u} is the velocity, ρ is the constant density, t is time, \mathbf{T} is the stress tensor and \mathbf{f} is a body force (i.e. $\mathbf{f} = \rho\mathbf{g}$).

Internal viscous stresses are produced by deformation. The fluid is Newtonian if the relationship between the rate of deformation ($\gamma_{ij} = \partial u_i / \partial x_j$) and the stress \mathbf{T} is local, linear, instantaneous and isotropic. If the fluid is also incompressible, the Newtonian constitutive law is

$$\mathbf{T} = -p\mathbf{I} + \mu(\nabla\mathbf{u} + \nabla\mathbf{u}^T). \quad (9.2)$$

Substituting this into the momentum balance (9.1) gives the *incompressible Navier-Stokes equations*:

$$\rho \frac{D\mathbf{u}}{Dt} = -\nabla p + \mu \nabla^2 \mathbf{u} + \mathbf{f} \quad (9.3)$$

9.1.2 Reynolds number

To non-dimensionalise the problem we write

$$\mathbf{u} = U\tilde{\mathbf{u}}, \quad \mathbf{x} = L\tilde{\mathbf{x}}, \quad t = \frac{L}{U}\tilde{t}, \quad p = P\tilde{p}, \quad (9.4)$$

where U is a characteristic velocity scale, L is a characteristic lengthscale, and P is a characteristic pressure scale. Substituting these into equation (9.3) when $\mathbf{f} = \mathbf{0}$ and rearranging we arrive at

$$\frac{\rho UL}{\mu} \left(\frac{\partial \tilde{\mathbf{u}}}{\partial \tilde{t}} + \tilde{\mathbf{u}} \cdot \tilde{\nabla} \tilde{\mathbf{u}} \right) = -\frac{PL}{\mu U} \tilde{\nabla} \tilde{p} + \tilde{\nabla}^2 \tilde{\mathbf{u}}, \quad (9.5)$$

where $\tilde{\nabla} \equiv \partial / \partial \tilde{x}_i$. We choose the viscous scaling for the pressure $P = \mu U / L$ (we could have chosen the alternative inertial scaling $P = \rho U^2$). This leaves one non-dimensional group called the Reynolds number:

$$\text{Re} = \frac{\rho UL}{\mu} = \frac{UL}{\nu} \equiv \frac{\text{inertia}}{\text{viscous stresses}}, \quad (9.6)$$

where $\nu = \mu/\rho$ is the kinematic viscosity (μ is denoted the dynamic viscosity). In this section we will be focusing on the limit where $\text{Re} \ll 1$ such that inertia is negligible and we can ignore the left-hand side of (9.5). The mass and momentum balance, known as *Stokes Equations*, are then given by

$$\nabla \cdot \mathbf{u} = 0 \quad \text{and} \quad \mathbf{0} = -\nabla p + \mu \nabla^2 \mathbf{u} + \mathbf{f}. \quad (9.7)$$

9.1.3 Energy and Dissipation

Taking the dot product of the full momentum equation (9.1) with the velocity \mathbf{u} and integrating over a volume Ω gives

$$\int_{\Omega} \rho \mathbf{u} \cdot \frac{\partial \mathbf{u}}{\partial t} d\Omega + \int_{\Omega} \rho \mathbf{u} \cdot (\mathbf{u} \cdot \nabla \mathbf{u}) d\Omega = \int_{\Omega} \mathbf{u} \cdot \mathbf{f} d\Omega + \int_{\Omega} \mathbf{u} \cdot (\nabla \cdot \mathbf{T}) d\Omega. \quad (9.8)$$

This can also be written in summation convention

$$\int_{\Omega} \rho u_i \frac{\partial u_i}{\partial t} d\Omega + \int_{\Omega} \rho u_i u_j \frac{\partial u_i}{\partial x_j} d\Omega = \int_{\Omega} u_i f_i d\Omega + \int_{\Omega} u_i \frac{\partial T_{ij}}{\partial x_j} d\Omega. \quad (9.9)$$

Rearranging, applying the divergence theorem and mass conservation, the left-hand side becomes

$$\begin{aligned} \text{LHS} &= \int_{\Omega} \frac{1}{2} \frac{\partial}{\partial t} (\rho u_i u_i) - \frac{1}{2} u_i u_i \frac{\partial \rho}{\partial t} d\Omega + \int_{\Omega} \frac{1}{2} \frac{\partial}{\partial x_j} (\rho u_i u_i u_j) - \frac{1}{2} u_i u_i \frac{\partial}{\partial x_j} (\rho u_j) d\Omega \\ &= \frac{d}{dt} \int_{\Omega} \frac{1}{2} \rho u_i u_i d\Omega + \int_{\partial\Omega} \frac{1}{2} \rho u_i u_i u_j n_j dA - \underbrace{\int_{\Omega} \frac{1}{2} u_i u_i \left(\frac{\partial \rho}{\partial t} + \frac{\partial}{\partial x_j} (\rho u_j) \right) d\Omega}_{=0}. \end{aligned}$$

Similarly, the right-hand side becomes

$$\begin{aligned} \text{RHS} &= \int_{\Omega} u_i f_i d\Omega + \int_{\Omega} \frac{\partial}{\partial x_j} (u_i T_{ij}) - T_{ij} \frac{\partial u_i}{\partial x_j} d\Omega \\ &= \int_{\Omega} u_i f_i d\Omega + \int_{\partial\Omega} u_i T_{ij} n_j dA - \int_{\Omega} T_{ij} \frac{\partial u_i}{\partial x_j} d\Omega. \end{aligned}$$

The *mechanical energy equation* is then written as

$$\underbrace{\frac{d}{dt} \int_{\Omega} \frac{1}{2} \rho u^2 d\Omega}_{(1)} + \underbrace{\int_{\partial\Omega} \frac{1}{2} \rho u^2 \mathbf{u} \cdot \mathbf{n} dA}_{(2)} = \underbrace{\int_{\Omega} \mathbf{u} \cdot \mathbf{f} d\Omega}_{(3)} + \underbrace{\int_{\partial\Omega} u_i T_{ij} n_j dA}_{(4)} - \underbrace{\int_{\Omega} T_{ij} \frac{\partial u_i}{\partial x_j} d\Omega}_{(5)}, \quad (9.10)$$

where

1. the rate of change of **kinetic energy** in volume Ω is due to:
2. the flux of **kinetic energy** over the boundary A ,
3. the rate of working by body forces \mathbf{f} in volume Ω ,
4. the rate of working of surface forces in A ,
5. and the stress working in volume Ω .

The mechanical energy equation above is for a general continuum. We can now look more specifically for a Newtonian viscous fluid with constitutive law,

$$T_{ij} = -p\delta_{ij} + 2\mu e_{ij} \quad \text{where} \quad e_{ij} = \frac{1}{2} \left(\frac{\partial u_i}{\partial x_j} + \frac{\partial u_j}{\partial x_i} \right). \quad (9.11)$$

The stress working per unit volume then becomes

$$T_{ij} \frac{\partial u_i}{\partial x_j} = -p\delta_{ij} \frac{\partial u_i}{\partial x_j} + 2\mu e_{ij} \frac{\partial u_i}{\partial x_j}. \quad (9.12)$$

Remembering some properties of the rate of strain and rotation tensors, we know that

$$\delta_{ij} \frac{\partial u_i}{\partial x_j} = \frac{\partial u_i}{\partial x_i} = \nabla \cdot \mathbf{u} = 0, \quad e_{ij} + r_{ij} = \frac{1}{2} \left(\frac{\partial u_i}{\partial x_j} + \frac{\partial u_j}{\partial x_i} \right) + \frac{1}{2} \left(\frac{\partial u_i}{\partial x_j} - \frac{\partial u_j}{\partial x_i} \right) = \frac{\partial u_i}{\partial x_j}, \quad (9.13)$$

$$e_{ij} r_{ij} = \frac{1}{4} \left(\frac{\partial u_i}{\partial x_j} + \frac{\partial u_j}{\partial x_i} \right) \left(\frac{\partial u_i}{\partial x_j} - \frac{\partial u_j}{\partial x_i} \right) = 0. \quad (9.14)$$

Hence, the stress working, also known as the *viscous dissipation* Φ , per unit volume is given by

$$\Phi = T_{ij} \frac{\partial u_i}{\partial x_j} = 2\mu e_{ij} e_{ij}. \quad (9.15)$$

The viscous dissipation Φ describes the rate of loss of mechanical energy due to friction in the volume Ω .

9.1.4 Additional comments

The approximation of Stokes Flow is good if the velocity or length scales U, L are small (e.g. swimming microorganisms), or the dynamic viscosity μ is large (e.g. in geophysics, flow in porous media, or the flow of lava or ice). Some examples are:

	L	U	ρ	μ	ν	Re
Sperm in water:	$50 \mu\text{m}$	$200 \mu\text{m/s}$	10^3 kg/m^3	10^{-3} Pas	$10^6 \text{ m}^2/\text{s}$	10^{-2}
Mantle:	$3 \times 10^3 \text{ km}$	1 cm/yr	3300 kg/m^3	10^{21} Pas	$3 \times 10^{17} \text{ m}^2/\text{s}$	3×10^{-21}

(See E. M. Purcell (1977) Life at Low Reynolds Number, American Journal of Physics).



Figure 9.1: (a) Swimming sperm. (b) Flow of lava.

When approximating the Reynolds number, there are some caveats. Firstly there may be more than one relevant lengthscale, e.g. in Lubrication theory later in the course the vertical lengthscale H is much smaller than the horizontal lengthscale L . These lengthscales may also vary with position e.g. flow past a body where in the far field $\text{Re} \sim Ur/\nu$ where r is the radial distance away from the body. Finally, the time scale may not be L/U but instead may be specified by an external driving force e.g. an oscillating boundary condition with timescale $T \sim \omega^{-1}$.

9.2 Properties of Stokes Flows

1. **Instantaneity** Instantaneity of the flow means there are no time derivatives $\partial \mathbf{u}/\partial t$, so no inertia. The flow has no memory and only knows about the current boundary conditions and applied forcing, responding immediately to any changes. The flow is said to be “quasi-steady” as \mathbf{u} can vary in time if the boundary conditions and applied forcing $\mathbf{f}(t)$ varies in time.

E.g. for a translating body with speed $\mathbf{U}(t)$, the fluid force on the body is proportional to its velocity $\mathbf{f}(t) \propto \mathbf{U}(t)$ and not to its acceleration $d\mathbf{U}(t)/dt$.

2. **Linearity:** Linearity means that the flow is linearly forced whether it is by a boundary motion or body force. In Stokes Equations there is no $\mathbf{u} \cdot \nabla \mathbf{u}$, so $\mathbf{u}(\mathbf{x}, t)$ and p are linear in \mathbf{f} and the boundary conditions.

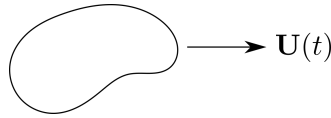


Figure 9.2: A translating body.

3. **Reversibility:** *Reversible in time:* if you apply a force $\mathbf{f}(t)$ in $0 \leq t < T$ and then reverse the force and its history $\mathbf{f}(t) = \mathbf{f}(2T - t)$ in $T \leq t < 2T$ then the flow reverses and the fluid particles return to their starting position.

Reversible in space: reversibility in time and the symmetry of geometry can often be used to rule out some components of velocity \mathbf{u} .

E.g. does a sphere sedimenting next to a vertical wall migrate towards the wall?

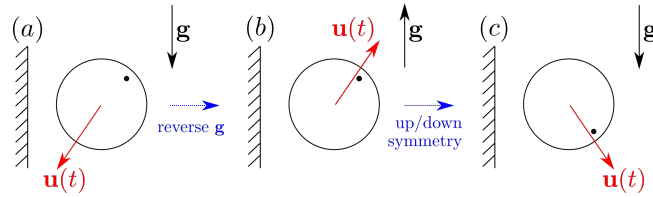


Figure 9.3: Sedimenting sphere. Reversing the forcing \mathbf{g} must reverse the velocity \mathbf{u} by reversibility in time. Because of the symmetry of the sedimenting sphere we can reverse the system in z . In order for (a) to be the same as (c) we require the sphere to fall vertically with no horizontal component.

4. Forces Balance:

Since there is no inertia the forces in the system must balance:

$$\nabla \cdot \mathbf{T} = -\mathbf{f} \quad \Rightarrow \quad \int_{\Omega} \nabla \cdot \mathbf{T} \, d\Omega = \int_{\Omega} -\mathbf{f} \, d\Omega. \quad (9.16)$$

Applying the divergence theorem then gives

$$\int_{\partial\Omega} \mathbf{T} \cdot \mathbf{n} \, dA + \int_{\Omega} \mathbf{f} \, d\Omega = 0. \quad (9.17)$$

This checks the consistency of the stress boundary conditions. In a similar way, we can check the consistency of the velocity boundary conditions by integrating the mass balance equation:

$$\nabla \cdot \mathbf{u} = 0 \quad \Rightarrow \quad \int_{\Omega} \nabla \cdot \mathbf{u} \, d\Omega = \int_{\partial\Omega} \mathbf{u} \cdot \mathbf{n} \, dA = 0. \quad (9.18)$$

5. **Work Balances Dissipation:** Since there is no kinetic energy in the mechanical energy balance, from (9.10) we know that the work done by body and surface forces must balance the viscous dissipation in a given volume:

$$\int_{\Omega} \Phi \, d\Omega = \int_{\Omega} T_{ij} \frac{\partial u_i}{\partial x_j} \, d\Omega = \int_{\Omega} \mathbf{u} \cdot \mathbf{f} \, d\Omega + \int_{\partial\Omega} u_i T_{ij} n_j \, dA. \quad (9.19)$$

Useful Lemma: Let \mathbf{u}^i be an incompressible flow and \mathbf{u}^s be a Stokes flow with body force \mathbf{f}^s such that

$$\nabla \cdot \mathbf{u}^i = 0 \quad \text{and} \quad \nabla \cdot \mathbf{u}^s = 0, \quad \nabla \cdot \mathbf{T}^s = -\mathbf{f}^s. \quad (9.20)$$

Then,

$$2\mu \int_{\Omega} e_{ij}^s e_{ij}^i \, d\Omega = \int_{\partial\Omega} u_i^s T_{ij}^s n_j \, dA + \int_{\Omega} u_i^i f_i^s \, d\Omega. \quad (9.21)$$

Proof: We know that for a Stokes flow $2\mu e_{ij}^s = T_{ij}^s + p^s \delta_{ij}$. Hence,

$$2\mu e_{ij}^s e_{ij}^i = T_{ij}^s e_{ij}^i + \underbrace{p^s \delta_{ij} e_{ij}^i}_{=0} \quad (9.22)$$

due to incompressibility. Also, using the fact that T_{ij} is symmetric and that $\partial u_i / \partial x_j = e_{ij} + r_{ij}$ where r_{ij} is antisymmetric, we find

$$2\mu e_{ij}^s e_{ij}^i = T_{ij}^s \left(\frac{\partial u_i^i}{\partial x_j} - r_{ij}^i \right) = T_{ij}^s \frac{\partial u_i^i}{\partial x_j} - \underbrace{T_{ij}^s r_{ij}^i}_{=0}, \quad (9.23)$$

$$= \frac{\partial}{\partial x_j} (T_{ij}^s u_i^i) - u_i^i \frac{\partial T_{ij}^s}{\partial x_j}. \quad (9.24)$$

Integrating over a volume Ω and applying the divergence theorem then gives the result:

$$2\mu \int_{\Omega} e_{ij}^s e_{ij}^i d\Omega = \int_{\Omega} \frac{\partial}{\partial x_j} (T_{ij}^s u_i^i) d\Omega - \int_{\Omega} u_i^i \frac{\partial T_{ij}^s}{\partial x_j} d\Omega = \int_{\partial\Omega} u_i^i T_{ij}^s n_j dA + \int_{\Omega} u_i^i f_i^s d\Omega. \quad (9.25)$$

6. **Uniqueness:** Uniqueness means that each Stokes flow is unique but can be represented in many ways. Let \mathbf{u}^1 and \mathbf{u}^2 be Stokes flows with the same body forcing and boundary conditions, i.e. $\mathbf{f}^1 = \mathbf{f}^2$ in Ω and either $\mathbf{u}^1 = \mathbf{u}^2$ or $\mathbf{T}^1 \cdot \mathbf{n} = \mathbf{T}^2 \cdot \mathbf{n}$ on $\partial\Omega$. Then $\mathbf{u}^1 = \mathbf{u}^2$.

To show this we consider the flow $\mathbf{u}^* = \mathbf{u}^1 - \mathbf{u}^2$. From the property of linearity we know that \mathbf{u}^* must also be a Stokes flow with $\mathbf{f}^* = \mathbf{0}$ and either $\mathbf{u}^* = \mathbf{0}$ or $\mathbf{T}^* \cdot \mathbf{n} = \mathbf{0}$ on $\partial\Omega$. From the above *lemma*, we can show that

$$2\mu \int_{\Omega} e_{ij}^* e_{ij}^* d\Omega = 0. \quad (9.26)$$

The integrand is positive so must vanish, hence $e_{ij}^* = 0$. The flow is strain less so must be in solid body motion $\mathbf{U} + \boldsymbol{\Omega} \times \mathbf{x}$. Velocity boundary conditions of $\mathbf{u}^1 = \mathbf{u}^2$ on $\partial\Omega$ imply that $\mathbf{u}^1 = \mathbf{u}^2$ everywhere. [N.B. Stress conditions can lead to solid body motion].

7. **Minimum Dissipation:** Among all incompressible flows with the same velocity boundary conditions, the dissipation is minimised by the Stokes flow with no body force.

Let \mathbf{u}^i be an incompressible flow and \mathbf{u}^s be a Stokes flow with $\mathbf{f}^s = \mathbf{0}$ and $\mathbf{u}^i = \mathbf{u}^s = \mathbf{U}$. We know that

$$2\mu \int_{\Omega} (e_{ij}^i - e_{ij}^s)(e_{ij}^i - e_{ij}^s) d\Omega \geq 0 \quad (\text{positive integrand}) \quad (9.27)$$

$$= 2\mu \int_{\Omega} (e_{ij}^i e_{ij}^i - e_{ij}^s e_{ij}^s) d\Omega + \underbrace{4\mu \int_{\Omega} (e_{ij}^s - e_{ij}^i) e_{ij}^s d\Omega}_{=0}, \quad (9.28)$$

from the *lemma* above. Therefore the dissipation is minimised for a Stokes flow

$$2\mu \int_{\Omega} e_{ij}^i e_{ij}^i d\Omega \geq 2\mu \int_{\Omega} e_{ij}^s e_{ij}^s d\Omega. \quad (9.29)$$

8. **Geometric bounding:** The minimum dissipation theorem can be used to calculate bounds for the flow around more complicated geometries. Consider a cube of side length $2L$ moving at a velocity \mathbf{U} in a fluid, with drag force \mathbf{F}^C , and Stokes flow $\mathbf{u}^s(\mathbf{x})$ outside the cube. We can write down the dissipation (using

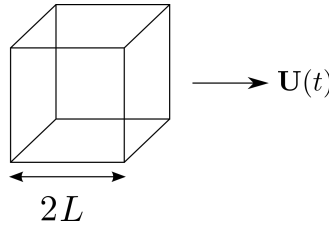


Figure 9.4: Stokes flow around a translating cube

the Stokes flow property that work balances dissipation) as

$$\int_{vol. \text{ outside cube}} 2\mu e_{ij}^s e_{ij}^s d\Omega = \int_{cube} U_i T_{ij} n_j dA = \mathbf{U} \cdot \int_{cube} \mathbf{T} \cdot \mathbf{n} dA = -\mathbf{U} \cdot \mathbf{F}^C. \quad (9.30)$$

We are considering the dissipation in the volume outside of the cube so the normal to the surface points inwards. This is the opposite to calculating drag on the sphere and hence a minus sign is introduced. Now consider a sphere that just contains the cube so have side length $\sqrt{3}L$. We can define an incompressible flow $\mathbf{u}(\mathbf{x})^i$ outside the cube made up of a Stokes flow outside the sphere and a flow with constant flow velocity \mathbf{U} between the sphere and the cube:

$$\mathbf{u}^i(\mathbf{x}) = \begin{cases} \mathbf{u}(\mathbf{x}) & \text{(Stokes flow past sphere)} \\ \mathbf{U} & \text{between sphere and cube} \end{cases} \quad \mathbf{x} \text{ outside sphere} \quad (9.31)$$

The dissipation for this flow is given by

$$\int_{\text{vol. outside cube}} 2\mu e_{ij}^i e_{ij}^i d\Omega = \int_{\text{vol. outside sphere}} 2\mu e_{ij}^i e_{ij}^i d\Omega = -\mathbf{U} \cdot \mathbf{F}^{\text{sphere}} = 6\pi\mu\sqrt{3}LU \cdot \mathbf{U}, \quad (9.32)$$

where we have used the fact that the strain rate for a flow with constant velocity is zero ($\partial U_i / \partial x_j = 0$) and the drag on a sphere of radius $a = \sqrt{3}L$ is $\mathbf{F} = -6\pi\mu a \mathbf{U}$. Finally, we know that the dissipation is minimised for a Stokes flow, and hence

$$6\pi\mu\sqrt{3}LU \cdot \mathbf{U} \geq -\mathbf{U} \cdot \mathbf{F}^C. \quad (9.33)$$

This gives an upper bound on the drag force on the cube. We can go through a similar argument to find a lower bound by considering the flow outside of a sphere that just fits inside the cube, with radius $a = L$. We won't repeat the analysis here but the result should give

$$6\pi\mu\sqrt{3}LU \cdot \mathbf{U} \geq -\mathbf{U} \cdot \mathbf{F}^C \geq 6\pi\mu LU \cdot \mathbf{U}. \quad (9.34)$$

9. **Reciprocal theorem:** Consider Stokes flows $\mathbf{u}^1(\mathbf{x})$ and $\mathbf{u}^2(\mathbf{x})$ in a given volume with different boundary conditions and no body forces. Taking the first flow to be the Stokes flow $\mathbf{u}^s = \mathbf{u}^1(\mathbf{x})$, the second flow to be the incompressible flow $\mathbf{u}^i = \mathbf{u}^2(\mathbf{x})$ and using the above *lemma* we have

$$2\mu \int_{\Omega} e_{ij}^1 e_{ij}^2 d\Omega = \int_{\partial\Omega} u_i^2 T_{ij}^1 n_j dA. \quad (9.35)$$

If we instead take the second flow to be the Stokes flow $\mathbf{u}^s = \mathbf{u}^2(\mathbf{x})$, in a similar manner we have

$$2\mu \int_{\Omega} e_{ij}^2 e_{ij}^1 d\Omega = \int_{\partial\Omega} u_i^1 T_{ij}^2 n_j dA. \quad (9.36)$$

Equating the two we find that the rate of working of surface forces of flow 1 against flow 2 equals the rate of working of surface forces of flow 2 against flow 1 (reciprocal theorem):

$$\int_{\partial\Omega} u_i^2 T_{ij}^1 n_j dA = \int_{\partial\Omega} u_i^1 T_{ij}^2 n_j dA. \quad (9.37)$$

If the boundary conditions are a uniform translation velocity $\mathbf{U}^{1,2}$, the reciprocal theorem reduces to

$$\mathbf{U}^1 \cdot \mathbf{F}^2 = \mathbf{U}^2 \cdot \mathbf{F}^1, \quad (9.38)$$

where $\mathbf{F}^{1,2}$ are the corresponding surface forces.

9.3 Stokes Flow Solutions

9.3.1 Representation as Harmonic Functions

Consider Stokes equations with body force $\mathbf{f} = \mathbf{0}$:

$$-\nabla p + \mu \nabla^2 \mathbf{u} = \mathbf{0}, \quad \nabla \cdot \mathbf{u} = 0. \quad (9.39)$$

$$1. \quad \nabla \cdot (-\nabla p + \mu \nabla^2 \mathbf{u}) = 0 \quad \Rightarrow \quad \nabla^2 p = 0 \quad (9.40)$$

$$2. \quad \nabla \times (-\nabla p + \mu \nabla^2 \mathbf{u}) = \mathbf{0} \quad \Rightarrow \quad \nabla^2 \boldsymbol{\omega} = \mathbf{0} \quad \text{where} \quad \boldsymbol{\omega} = \nabla \times \mathbf{u} \quad (9.41)$$

$$3. \quad \nabla^2 (-\nabla p + \mu \nabla^2 \mathbf{u}) = \mathbf{0} \quad \Rightarrow \quad \nabla^4 \mathbf{u} = \mathbf{0}. \quad (9.42)$$

Hence, p and $\boldsymbol{\omega}$ are harmonic and \mathbf{u} is biharmonic.

9.3.2 Papkovitch-Neuber Solutions

A method for finding the solution of Stokes flows comes from the *Papkovitch-Neuber* representation. Suppose we can write the pressure $p = \nabla^2 \Pi$. Then

$$\nabla^2(-\nabla \Pi + \mu \mathbf{u}) = \mathbf{0} \quad \Rightarrow \quad \mu \mathbf{u} = \nabla \Pi - \Phi \quad \text{where} \quad \nabla^2 \Phi = \mathbf{0}. \quad (9.43)$$

Using the incompressibility condition, we have

$$\mu \nabla \cdot \mathbf{u} = \nabla \cdot (\nabla \Pi - \Phi) = 0 \quad \Rightarrow \quad \nabla^2 \Pi = \nabla \cdot \Phi \quad \Rightarrow \quad \Pi = \frac{1}{2}(\mathbf{x} \cdot \Phi + \chi) \quad \text{where} \quad \nabla^2 \chi = 0. \quad (9.44)$$

We can check this last relation:

$$\frac{\partial^2 \Pi}{\partial x_i \partial x_i} = \frac{\partial^2}{\partial x_i \partial x_i} \left(\frac{1}{2} x_j \Phi_j + \frac{1}{2} \chi \right) = \frac{1}{2} \frac{\partial}{\partial x_i} \left(\frac{\partial x_j}{\partial x_i} \Phi_j + x_j \frac{\partial \Phi_j}{\partial x_i} \right) + \frac{1}{2} \underbrace{\frac{\partial^2 \chi}{\partial x_i \partial x_i}}_{=0} \quad (9.45)$$

$$= \frac{1}{2} \frac{\partial}{\partial x_i} \left(\delta_{ij} \Phi_j + x_j \frac{\partial \Phi_j}{\partial x_i} \right) = \frac{1}{2} \left(\frac{\partial \Phi_i}{\partial x_i} + \delta_{ij} \frac{\partial \Phi_j}{\partial x_i} + x_j \underbrace{\frac{\partial^2 \Phi_j}{\partial x_i \partial x_i}}_{=0} \right) = \frac{\partial \Phi_i}{\partial x_i}. \quad (9.46)$$

Any Stokes flow with $\mathbf{f} = \mathbf{0}$ can be written in terms of a harmonic vector Φ and a harmonic scalar χ :

$$2\mu \mathbf{u} = \nabla(\mathbf{x} \cdot \Phi + \chi) - 2\Phi \quad \text{and} \quad p = \nabla \cdot \Phi. \quad (9.47)$$

9.3.3 Spherical Harmonic Solutions

Spherical harmonic functions are used for solutions involving points, spheres and cylinders that have no preferred direction or orientation. Let the radial coordinate $r = |\mathbf{x}| \equiv (\mathbf{x} \cdot \mathbf{x})^{1/2}$. We can show that $\nabla^2 \frac{1}{r} = 0$, except when $r = 0$:

$$\frac{\partial^2}{\partial x_j \partial x_j} \left((x_i x_i)^{-1/2} \right) = -\frac{\partial}{\partial x_j} \left((x_k x_k)^{-3/2} x_i \delta_{ij} \right) = -\frac{\partial}{\partial x_j} \left((x_k x_k)^{-3/2} x_j \right) \quad (9.48)$$

$$= -3(x_k x_k)^{-3/2} + 3(x_m x_m)^{-5/2} x_k x_j \delta_{kj} = 0. \quad (9.49)$$

All other harmonic functions ϕ with $\phi \rightarrow 0$ and $r \rightarrow \infty$ are made up of

$$\frac{1}{r}, \quad \nabla \frac{1}{r}, \quad \nabla \nabla \frac{1}{r}, \quad \nabla \nabla \nabla \frac{1}{r}, \quad \dots \quad (9.50)$$

Harmonic functions that are bounded at $r = 0$ are made up of

$$r \frac{1}{r}, \quad r^3 \nabla \frac{1}{r}, \quad r^5 \nabla \nabla \frac{1}{r}, \quad \dots \quad r^{2n+1} \nabla^n \frac{1}{r}, \quad \dots \quad (9.51)$$

These solutions only depend on r and \mathbf{x} and have no preferred orientation. Some useful derivatives to remember are:

$$1. (\nabla \mathbf{x})_{ij} = \frac{\partial x_i}{\partial x_j} = \delta_{ij} \quad (\text{identity}) \quad (9.52)$$

$$2. (\nabla r)_i = \frac{x_i}{r} \quad (9.53)$$

$$3. \left(\nabla \frac{1}{r} \right)_i = -\frac{x_i}{r^3} \quad (9.54)$$

$$4. (\nabla f(r))_i = f'(r) (\nabla r)_i = f'(r) \frac{x_i}{r} \quad (9.55)$$

Since we know that Stokes flows are linear in boundary conditions and forcing, we can form Papkovitch-Neuber solutions by multiplying them by constant scalars, vectors, tensors, and forming dot-products, for example

$$\mathbf{A} \frac{1}{r}, \quad B \nabla \frac{1}{r}, \quad \mathbf{C} \cdot \nabla \frac{1}{r}, \quad \dots \quad (9.56)$$

9.3.4 Tensors and Pseudotensors

When building these solutions there are some properties it is useful to recall about tensors. An n th-rank tensor is a set of objects that transform like a product of n vectors. For example, if $T_{i_1 i_2 \dots i_n}$ is an n th-rank tensor, then

$$T'_{j_1 j_2 \dots j_n} = O_{j_1 i_1} O_{j_2 i_2} \dots O_{j_n i_n} T_{i_1 i_2 \dots i_n}, \quad (9.57)$$

where O_{ij} is a transformation matrix. Symmetry properties are tensor invariant, so if $T_{i_1 i_2 \dots i_n}$ is symmetric (antisymmetric) under an exchange of i_1 and i_2 then $T'_{j_1 j_2 \dots j_n}$ is also symmetric (antisymmetric) under an exchange of j_1 and j_2 . Examples of tensors in our problems would be

$$\text{velocity } \mathbf{u}, \quad \text{force } \mathbf{F} = \int \mathbf{T} \cdot \mathbf{n} \, dA, \quad \text{position } \mathbf{x}, \quad \text{grad } \nabla, \quad \text{identity } \mathbf{I}. \quad (9.58)$$

In contrast, pseudotensors, such as the Levi-Civita ϵ_{ijk} , change sign under transformation by reflections. Examples of pseudotensors we will come across are

$$\text{angular velocity } \boldsymbol{\Omega}, \quad \text{couple } \mathbf{G} = \int \mathbf{x} \times (\mathbf{T} \cdot \mathbf{n}) \, dA, \quad \text{cross product } \mathbf{u} \times \mathbf{x}, \quad \text{vorticity } \boldsymbol{\omega} = \nabla \times \mathbf{u}. \quad (9.59)$$

If we want to find the velocity \mathbf{u} using the Papkovitch-Neuber representation, then we want Φ and χ to be tensors.

9.3.5 Point Force and Source Flow

Point force (Stokeslet): We want to find the velocity field for a point force. Consider the following:

$$\nabla \cdot \mathbf{T} = \mu \nabla^2 \mathbf{u} - \nabla p = -\mathbf{F} \delta(\mathbf{x}) \quad (9.60)$$

$$\nabla \cdot \mathbf{u} = 0, \quad \mathbf{u} \rightarrow \mathbf{0} \quad \text{as} \quad |\mathbf{x}| \rightarrow \infty. \quad (9.61)$$

We know that

- by linearity, the velocity field must be linear in the forcing \mathbf{F}
- solution must decay in the far field
- there is no preferred direction in the problem, can use spherical harmonics
- the velocity field \mathbf{u} must be made up of tensors

Using this information, we can now try to build harmonic functions Φ and χ using the solutions in (9.50)-(9.51). Let's try the following ansatzes:

$$\Phi = \frac{\alpha \mathbf{F}}{r} \quad \checkmark \quad (9.62)$$

$$\Phi = \alpha \mathbf{F} \cdot \nabla \nabla \frac{1}{r} \quad \left(\text{equivalently } \chi = \beta \mathbf{F} \cdot \nabla \frac{1}{r} \right) \quad \rightarrow \quad \text{too singular at } r = 0 \quad \times \quad (9.63)$$

$$\Phi = \alpha \mathbf{F} \times \nabla \frac{1}{r} \quad \rightarrow \quad \text{pseudotensor} \quad \times \quad (9.64)$$

The first ansatz is the only one that decays in the far field and will not blow up at the origin. We proceed by substituting Φ into the solution (9.47):

$$2\mu \mathbf{u} = \nabla \left(\alpha \frac{\mathbf{F} \cdot \mathbf{x}}{r} \right) - \frac{2\alpha \mathbf{F}}{r} = -\alpha \left(\frac{\mathbf{F}}{r} + \frac{(\mathbf{F} \cdot \mathbf{x}) \mathbf{x}}{r^3} \right). \quad (9.65)$$

To fully specify the solution we need to find α . Going back to the problem statement, we want the solution to satisfy

$$\nabla \cdot \mathbf{u} = 0 \quad \Rightarrow \quad \int_{r=R} \mathbf{u} \cdot \mathbf{n} \, dA = 0, \quad (9.66)$$

(this is built into the Papkovitch-Neuber representation), and

$$-\mathbf{F}\delta(\mathbf{x}) = \nabla \cdot \mathbf{T} \quad \Rightarrow \quad -\mathbf{F} = \int_{r=R} \mathbf{T} \cdot \mathbf{n} \, dA. \quad (9.67)$$

On a sphere $r = R$, $\mathbf{x} = R\mathbf{n}$, the normal velocity can be calculated

$$\mathbf{u} \cdot \mathbf{n}|_{r=R} = -\frac{\alpha}{2\mu} \left(\frac{\mathbf{F}}{R} + \frac{(\mathbf{F} \cdot R\mathbf{n})R\mathbf{n}}{R^3} \right) \cdot \mathbf{n} = -\frac{\alpha(\mathbf{F} \cdot \mathbf{n})}{\mu R} \quad (9.68)$$

$$\Rightarrow \int_{r=R} \mathbf{u} \cdot \mathbf{n} \, dA = -\frac{\alpha \mathbf{F}}{\mu R} \cdot \underbrace{\int_{r=R} \mathbf{n} \, dA}_{=0, \text{ isotropic}} = 0. \quad (9.69)$$

The normal stress can also be calculated, but requires a bit more algebra:

$$\mathbf{T} \cdot \mathbf{n}|_{r=R} = (-p\mathbf{I} + \mu(\nabla \mathbf{u} + \nabla \mathbf{u}^T)) \cdot \mathbf{n}|_{r=R} \quad (9.70)$$

with

$$p = \nabla \cdot \left(\frac{\alpha \mathbf{F}}{r} \right) = -\frac{\alpha \mathbf{F} \cdot \mathbf{x}}{r^3}, \quad \nabla \mathbf{u} = -\frac{\alpha}{2\mu} \left(\frac{(\mathbf{F} \cdot \mathbf{x})\mathbf{I}}{r^3} - 3\frac{(\mathbf{F} \cdot \mathbf{x})\mathbf{x}\mathbf{x}}{r^5} \right), \quad (9.71)$$

$$\mathbf{T} \cdot \mathbf{n}|_{r=R} = \frac{3\alpha(\mathbf{F} \cdot \mathbf{n})\mathbf{n}}{R^2} \quad \Rightarrow \quad \int_{r=R} \mathbf{T} \cdot \mathbf{n}|_{r=R} \, dA = \frac{3\alpha \mathbf{F}}{R^2} \cdot \underbrace{\int_{r=R} \mathbf{n} \mathbf{n} \, dA}_{\mathbf{A}} = \frac{3\alpha \mathbf{F}}{R^2} \cdot \frac{4\pi R^2 \mathbf{I}}{3} \quad (9.72)$$

Here, we have noticed that the integral marked \mathbf{A} is an isotropic second rank tensor so must be $\propto \delta_{ij}$. We can determine the constant of proportionality by calculating the trace, $A_{ii} = 4\pi R^2$. Hence, $\alpha = -1/4\pi$. Notice that α is independent of R . If we had chosen one of the other harmonic solutions with higher powers of $1/r$, they would be too singular to satisfy the force condition.

Source Flow (Point mass source): We want to find the velocity field for a point source in three-dimensions. Consider the following:

$$\nabla \cdot \mathbf{T} = \mu \nabla^2 \mathbf{u} - \nabla p = \mathbf{0} \quad (9.73)$$

$$\nabla \cdot \mathbf{u} = Q\delta(\mathbf{x}), \quad \mathbf{u} \rightarrow \mathbf{0} \quad \text{as} \quad |\mathbf{x}| \rightarrow \infty. \quad (9.74)$$

Strictly speaking this flow is only incompressible for $r > 0$ as volume is not conserved at $r = 0$ but generated there instead.

We know that

- by linearity, the velocity field must be linear in the source flux Q
- solution must decay in the far field
- there is no preferred direction in the problem, can use spherical harmonics
- the velocity field \mathbf{u} must be made up of tensors

Let's try harmonic function

$$\chi = \frac{\beta Q}{r} \quad \left(\text{equivalently} \quad \Phi = \hat{\beta} Q \nabla \frac{1}{r} \right). \quad (9.75)$$

In a similar manner to the point force, the other harmonic solutions with higher powers of $1/r$ would be too singular to satisfy the source condition. Substituting into the solution (9.47) we find:

$$2\mu \mathbf{u} = \nabla \left(\frac{\beta Q}{r} \right) \quad \Rightarrow \quad \mathbf{u} = -\frac{\beta Q \mathbf{x}}{2\mu r^3}. \quad (9.76)$$

To find β , we use the source condition at $r = 0$:

$$\nabla \cdot \mathbf{u} = Q\delta(\mathbf{x}) \quad \Rightarrow \quad Q = \int_{r=R} \mathbf{u} \cdot \mathbf{n} \, dA = -\frac{\beta Q}{2\mu R^2} \int_{r=R} \mathbf{n} \cdot \mathbf{n} \, dA = -\frac{\beta Q}{2\mu R^2} 4\pi R^2. \quad (9.77)$$

Hence, $\beta = -\mu/2\pi$. The velocity field then becomes $\mathbf{u} = Q\mathbf{x}/4\pi r^3$ which is independent of viscosity μ . This is the three-dimensional extension of the potential flow for a point source studied in §6.

9.3.6 Motion of a rigid particle

A sphere of radius $r = a$ translating with velocity \mathbf{U} and rotating with angular velocity $\boldsymbol{\Omega}$ moves with velocity

$$\mathbf{u}|_{r=a} = \mathbf{U} + \boldsymbol{\Omega} \times \mathbf{x} \quad (9.78)$$

and exerts a force \mathbf{F} and couple \mathbf{G} on the fluid. The dissipation in the fluid due to the particle is (using work balances dissipation)

$$\int_{\Omega} \Phi \, d\Omega = \int_{\partial\Omega} \mathbf{u} \cdot \mathbf{T} \cdot \mathbf{n} \, dA = \int_{particle} (\mathbf{U} + \boldsymbol{\Omega} \times \mathbf{x}) \cdot \mathbf{T} \cdot \mathbf{n} \, dA \quad (9.79)$$

$$= \mathbf{U} \cdot \int_{particle} \mathbf{T} \cdot \mathbf{n} \, dA + \boldsymbol{\Omega} \cdot \int_{particle} \mathbf{x} \times (\mathbf{T} \cdot \mathbf{n}) \, dA \quad (9.80)$$

$$= \mathbf{U} \cdot \mathbf{F} + \boldsymbol{\Omega} \cdot \mathbf{G}, \quad (9.81)$$

where the normal points out of the fluid into the body, with

$$\text{force } \mathbf{F} = \int_{particle} \mathbf{T} \cdot \mathbf{n} \, dA \quad \text{and} \quad \text{couple } \mathbf{G} = \int_{particle} \mathbf{x} \times (\mathbf{T} \cdot \mathbf{n}) \, dA \quad (9.82)$$

exerted on the fluid by the sphere.

9.3.7 Translating Rigid Sphere

Velocity Field: We would like to calculate the velocity field for a rigid sphere of radius $r = a$ translating with velocity $\mathbf{u} = \mathbf{U}$. Consider the following:

$$\boldsymbol{\nabla} \cdot \mathbf{T} = \mu \nabla^2 \mathbf{u} - \nabla p = \mathbf{0}, \quad \boldsymbol{\nabla} \cdot \mathbf{u} = 0, \quad (9.83)$$

$$\mathbf{u} = \mathbf{U} \quad \text{at} \quad r = a, \quad \mathbf{u} \rightarrow \mathbf{0} \quad \text{as} \quad |\mathbf{x}| \rightarrow \infty. \quad (9.84)$$

We know that

- by linearity, the velocity field must be linear in the forcing \mathbf{U}
- solution must decay in the far field
- there is no preferred direction in the problem, can use spherical harmonics
- the velocity field \mathbf{u} must be made up of tensors

Let's try

$$\frac{\Phi}{2\mu} = \frac{\alpha \mathbf{U}}{r} \quad \text{and} \quad \frac{\chi}{2\mu} = \beta \mathbf{U} \cdot \boldsymbol{\nabla} \frac{1}{r}. \quad (9.85)$$

This then gives velocity field

$$\mathbf{u} = \boldsymbol{\nabla} \left(\frac{\alpha \mathbf{U} \cdot \mathbf{x}}{r} - \frac{\beta \mathbf{U} \cdot \mathbf{x}}{r^3} \right) - \frac{2\alpha \mathbf{U}}{r} = \alpha \left[-\frac{\mathbf{U}}{r} - \frac{(\mathbf{U} \cdot \mathbf{x})\mathbf{x}}{r^3} \right] + \beta \left[-\frac{\mathbf{U}}{r^3} + \frac{3(\mathbf{U} \cdot \mathbf{x})\mathbf{x}}{r^5} \right]. \quad (9.86)$$

Applying the boundary condition $\mathbf{u} = \mathbf{U}$ at $r = a$ gives

$$1 = -\frac{\alpha}{a} - \frac{\beta}{a^3}, \quad 0 = -\frac{\alpha}{a} + \frac{3\beta}{a^3} \quad \Rightarrow \quad \alpha = -\frac{3a}{4}, \quad \beta = -\frac{a^3}{4}, \quad (9.87)$$

and

$$\mathbf{u} = \frac{3\mathbf{U}}{4} \left(\frac{a}{r} + \frac{a^3}{3r^3} \right) + \frac{3(\mathbf{U} \cdot \mathbf{x})\mathbf{x}}{4} \left(\frac{a}{r^3} - \frac{a^3}{r^5} \right). \quad (9.88)$$

The pressure field can also be calculated

$$p = -\frac{3\mu a \mathbf{U}}{2} \cdot \boldsymbol{\nabla} \frac{1}{r} = \frac{3\mu a (\mathbf{U} \cdot \mathbf{x})}{2r^3}. \quad (9.89)$$

When finding the velocity field for the point force and point source, we were restricted with the possible harmonic functions to choose from because of the behaviour at $r = 0$. For the translating sphere this is no longer the case. You will notice that if we set either α or β to zero we can no longer satisfy the boundary condition on $r = a$.

Force and stress on the sphere: We start by calculating the stress \mathbf{T} from the velocity and pressure fields,

$$\mathbf{T} = -p\mathbf{I} + \mu(\nabla\mathbf{u} + \nabla\mathbf{u}^T) \tag{9.90}$$

$$= -\frac{3\mu a(\mathbf{U} \cdot \mathbf{x})\mathbf{I}}{2r^3} + \mu \left\{ \frac{3}{4} \left(-\frac{a}{r^3} - \frac{a^3}{r^5} \right) (\mathbf{U}\mathbf{x} + \mathbf{x}\mathbf{U}) + \frac{3}{2} \left(\frac{-3a}{r^5} + \frac{5a^3}{r^7} \right) (\mathbf{U} \cdot \mathbf{x})\mathbf{x}\mathbf{x} \right. \tag{9.91}$$

$$\left. + \frac{3}{4} \left(\frac{a}{r^3} - \frac{a^3}{r^5} \right) [2(\mathbf{U} \cdot \mathbf{x})\mathbf{I} + \mathbf{U}\mathbf{x} + \mathbf{x}\mathbf{U}] \right\} \tag{9.92}$$

On $r = a$, $\mathbf{x} = a\mathbf{n}$, the stress is

$$\mathbf{T} \cdot \mathbf{n}|_{r=a} = -\frac{3\mu\mathbf{U}}{2a}. \tag{9.93}$$

The stress on the sphere is constant. Calculating the force, or drag, on the sphere is then relatively straightforward

$$\text{drag} = \mathbf{F} = \int_{r=a} -\frac{3\mu\mathbf{U}}{2a} dA = -6\pi\mu a\mathbf{U}. \tag{9.94}$$

Gravitational settling: Now that we have the drag on a sphere translating at a given velocity, we can reverse the problem and ask what is the settling speed of a sphere falling under gravity. Balancing the forces on a

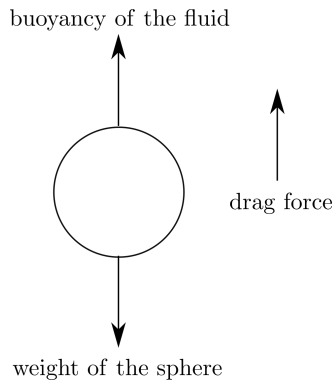


Figure 9.5: Sketch of settling sphere with forces.

steady fall we have

$$\underbrace{\mathbf{0}}_{(1)} = \underbrace{\frac{4\pi a^3 \rho_f \mathbf{g}}{3}}_{(2)} - \underbrace{\frac{4\pi a^3 \rho \mathbf{g}}{3}}_{(3)} - \underbrace{6\pi\mu a\mathbf{U}}_{(4)} \Rightarrow \mathbf{U} = \frac{2\Delta\rho a^2 \mathbf{g}}{9\mu}. \tag{9.95}$$

where

1. no inertia (steady fall, no acceleration)
2. weight of the sphere, density ρ
3. buoyancy (weight of displaced fluid, density ρ_f)
4. Stokes drag

E.g. For a ball bearing with density $\rho = 8g/cm^3$ we can calculate the sedimenting speed for different fluids:

	a	ρ_f	$\Delta\rho$	μ	U	Re
Water:	$1\ \mu m$	$1\ g/cm^3$	$7\ g/cm^3$	$10^{-3}\ Pas$	$15\ \mu m/s$	$10^{-4} \ll 1$
Golden syrup:	$1\ mm$	$1.4\ g/cm^3$	$6.6\ g/cm^3$	$60\ Pas$	$0.24\ mm/s$	$3 \times 10^{-5} \ll 1$

This experiment can be used to calculate the viscosity of different fluids.

Far-field approximation: Far away from the sphere, we can show that the disturbance looks like a point force. The velocity field when $r \rightarrow \infty$ is

$$\mathbf{u} = \frac{3a\mathbf{U}}{4r} + \frac{3a(\mathbf{U} \cdot \mathbf{x})\mathbf{x}}{4r^3}. \quad (9.96)$$

The force exerted across ' $r = \infty$ ' must balance the force exerted across $r = a$ so the strength of the point force $\mathbf{F}' = 6\pi\mu a\mathbf{U}$. Substituting this into the velocity field gives

$$\mathbf{u} = \frac{1}{8\pi\mu} \left(\frac{\mathbf{F}'}{r} + \frac{(\mathbf{F}' \cdot \mathbf{x})\mathbf{x}}{r^3} \right). \quad (9.97)$$

This disturbance flow only knows the total force exerted and is independent of particle radius a .

Chapter 10

Lubrication Theory

Lubrication theory is used to describe fluid flows in a geometry where the characteristic lengthscale in one dimension is significantly smaller than the others. Lubrication theory is important for understanding lubrication of components in machinery such as a fluid bearing, and in biological fluid dynamics such as understanding the flow of red blood cells in narrow capillaries.

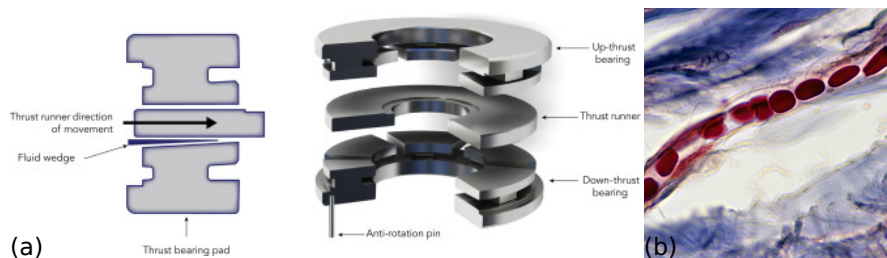


Figure 10.1: (a) Thrust bearing. (b) Red blood cells flowing in a capillary.

10.1 Lubrication approximation for flow in a thin layer

Let H be a characteristic vertical lengthscale and L be a characteristic horizontal lengthscale in the direction of fluid flow. In the lubrication approximation we assume the layer is shallow such that

$$\epsilon = H/L \ll 1. \tag{10.1}$$

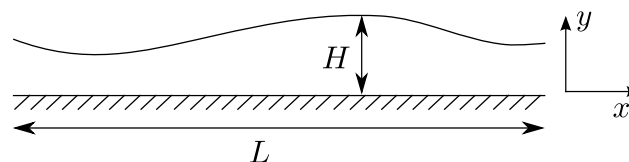


Figure 10.2: Sketch of flow in a thin layer.

In addition, let U be the scale of the horizontal velocity u (in the direction of fluid flow). From incompressibility ($\nabla \cdot \mathbf{u} = 0$) we know that the vertical velocity v must scale as UH/L . Note, here we are assuming that the flow is two-dimensional with no dependence on the coordinate z out of the page ($w = 0$). We will now non-dimensionalise the Navier-Stokes equations using these scales. As a recap here, refer back to chapter §4 on Dimensional Analysis.

We now introduce dimensionless variables (denoted by the tilde)

$$t = T\tilde{t}, \quad x = L\tilde{x}, \quad y = H\tilde{y}, \quad u = U\tilde{u}, \quad v = \frac{UH}{L}\tilde{v}, \quad p = P\tilde{p}. \tag{10.2}$$

For a Newtonian fluid, the equation for mass balance (see §2.8) becomes

$$\frac{\partial \tilde{u}}{\partial \tilde{x}} + \frac{\partial \tilde{v}}{\partial \tilde{y}} = 0, \quad (10.3)$$

owing to the choice of scalings for the the vertical velocity. The horizontal momentum equation (see §2.9) is

$$\frac{\rho U}{T} \frac{\partial \tilde{u}}{\partial \tilde{t}} + \frac{\rho U^2}{L} \left(\tilde{u} \frac{\partial \tilde{u}}{\partial \tilde{x}} + \tilde{v} \frac{\partial \tilde{u}}{\partial \tilde{y}} \right) = -\frac{P}{L} \frac{\partial \tilde{p}}{\partial \tilde{x}} + \frac{\mu U}{L^2} \frac{\partial^2 \tilde{u}}{\partial \tilde{x}^2} + \frac{\mu U}{H^2} \frac{\partial^2 \tilde{u}}{\partial \tilde{y}^2}. \quad (10.4)$$

Dividing by $\mu U/H^2$, the equation becomes

$$\frac{H^2}{\nu T} \frac{\partial \tilde{u}}{\partial \tilde{t}} + \frac{UH^2}{\nu L} \left(\tilde{u} \frac{\partial \tilde{u}}{\partial \tilde{x}} + \tilde{v} \frac{\partial \tilde{u}}{\partial \tilde{y}} \right) = -\frac{PH^2}{\mu UL} \frac{\partial \tilde{p}}{\partial \tilde{x}} + \frac{H^2}{L^2} \frac{\partial^2 \tilde{u}}{\partial \tilde{x}^2} + \frac{\partial^2 \tilde{u}}{\partial \tilde{y}^2}. \quad (10.5)$$

From this non-dimensional version of the equation we can see that inertia can be neglected if the modified Reynolds number based on H and L satisfies

$$\text{Re} \frac{H^2}{L^2} = \frac{UL}{\nu} \frac{H^2}{L^2} \ll 1, \quad (10.6)$$

with timescale $T = L/U$. Choosing pressure scale $P = \mu UL/H^2$, the horizontal momentum equation can finally be approximated as

$$0 = -\frac{\partial \tilde{p}}{\partial \tilde{x}} + \frac{\partial^2 \tilde{u}}{\partial \tilde{y}^2}. \quad (10.7)$$

Using these scales for the pressure and time we can repeat the non-dimensionalisation for the vertical momentum equation:

$$\frac{UH}{\nu} \frac{H^3}{L^3} \left(\frac{\partial \tilde{v}}{\partial \tilde{t}} + \tilde{u} \frac{\partial \tilde{v}}{\partial \tilde{x}} + \tilde{v} \frac{\partial \tilde{v}}{\partial \tilde{y}} \right) = -\frac{\partial \tilde{p}}{\partial \tilde{y}} + \frac{H^4}{L^4} \frac{\partial^2 \tilde{v}}{\partial \tilde{x}^2} + \frac{H^2}{L^2} \frac{\partial^2 \tilde{v}}{\partial \tilde{y}^2}. \quad (10.8)$$

We find that to leading order (setting $\epsilon = H/L = 0$) inertia can be neglected and the pressure is independent of vertical coordinate \tilde{y} i.e. $\tilde{p} = \tilde{p}(\tilde{x}, \tilde{t})$. Here, we have ignored any body forces such as gravity. If we were to include gravity we'd find the scaling of the vertical momentum equation implies that the pressure is hydrostatic (with $P = \rho gH$ and $U = gH^3/\nu L$). We will come across this in some of the examples we cover later.

10.2 Squeeze flow

10.2.1 Thrust bearing

Let's first consider the squeeze flow in a thrust bearing. Figure 10.3 shows the geometry and coordinate system where the bearing remains stationary and the plane underneath the fluid moves with horizontal velocity $-U$. The fluid film wedge generates a hydrodynamic pressure that supports an applied load on the bearing with a small tangential force for good lubrication. We would like to calculate the pressure in the fluid and hence the forces exerted on the bearing by the fluid. To solve the lubrication problem we: describe the *geometry*, solve for (almost) *unidirectional flow*, apply *mass conservation* to close the system, and calculate *quantities of interest* in this case the forces on the bearing.

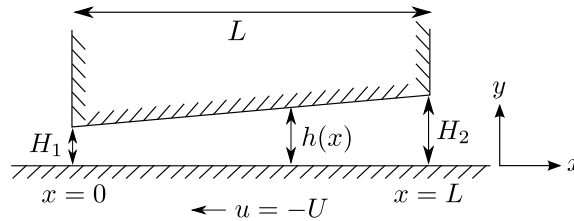


Figure 10.3: Thrust bearing geometry

Geometry The fluid film thickness is given by the geometry of the bearing

$$h(x) = H_1 + \alpha x \quad \text{where} \quad \alpha = \frac{H_2 - H_1}{L}. \quad (10.9)$$

For the thin film approximation we require $h \ll L$. This means that the gradient of the bearing is also small, $|h'| = \alpha \ll 1$, and flow is predominantly in the x direction.

Unidirectional flow Given that the flow is approximately in the x direction we can write the velocity as $\mathbf{u} = (u, 0, 0)$. The momentum equations are then

$$0 = -\frac{\partial p}{\partial x} + \mu \frac{\partial^2 u}{\partial y^2} \quad \text{and} \quad 0 = -\frac{\partial p}{\partial y}. \quad (10.10)$$

The y -momentum balance tells us that the pressure is independent of y . If p is independent of y then $\partial p/\partial x$ must also be independent of y . Hence, we can integrate the x -momentum balance twice:

$$u = \frac{1}{2\mu} \frac{dp}{dx} y^2 + Ay + B \quad \Rightarrow \quad u = -\frac{1}{2\mu} \frac{dp}{dx} y(h-y) - \frac{U(h-y)}{h}, \quad (10.11)$$

using the boundary conditions $u|_{y=0} = -U$ and $u|_{y=h} = 0$ since the underlying plane is moving and the bearing is stationary (and we have assumed no-slip on both surfaces). The final quantity to determine is the pressure gradient dp/dx .

Mass conservation In order to calculate the pressure (and pressure gradient) we can use global mass conservation and boundary conditions on the pressure. By global mass conservation we know that the volume flux (per unit z -width) must be constant. We also assume that away from the bearing the pressure must be atmospheric, $p = p_0$ at $x = 0, L$. In more detail:

$$Q = \int_0^h u \, dy = -\frac{h^3}{12\mu} \frac{dp}{dx} - \frac{Uh}{2} = \text{const} \quad \Rightarrow \quad \frac{dp}{dx} = -\frac{12\mu Q}{h^3} - \frac{6\mu U}{h^2}. \quad (10.12)$$

Integrating the pressure and applying the boundary conditions at $x = 0$ gives

$$p = p_0 + \frac{6\mu Q}{\alpha} \left(\frac{1}{h^2} - \frac{1}{H_1^2} \right) + \frac{6\mu U}{\alpha} \left(\frac{1}{h} - \frac{1}{H_1} \right). \quad (10.13)$$

Applying the boundary condition at $x = L$ allows us to determine the constant volume flux Q :

$$p_0 = p_0 + \frac{6\mu Q}{\alpha} \left(\frac{1}{H_2^2} - \frac{1}{H_1^2} \right) + \frac{6\mu U}{\alpha} \left(\frac{1}{H_2} - \frac{1}{H_1} \right) \quad \Rightarrow \quad Q = -\frac{UH_1H_2}{H_1 + H_2}. \quad (10.14)$$

The volume flux Q and the pressure p could then be substituted back into the expression for the horizontal velocity u . The pressure gradient generated by the lubrication flow ensures that the mass flow is constant through the narrow gap. From $x = 0$ the pressure increases up to a maximum when dp/dx is zero. The pressure then decreases again to match the atmospheric pressure at $x = L$.

$$\frac{dp}{dx} = 0 \quad \Rightarrow \quad U = -\frac{2Q}{h} \quad \text{and} \quad h = \frac{2H_1H_2}{H_1 + H_2}. \quad (10.15)$$

The pressure field is plotted for different angle bearings in figure 10.4. In a similar manner, we could look at what the tangential stress on the boundaries is by calculating $\mu \partial u/\partial y$ at $y = 0, h$.

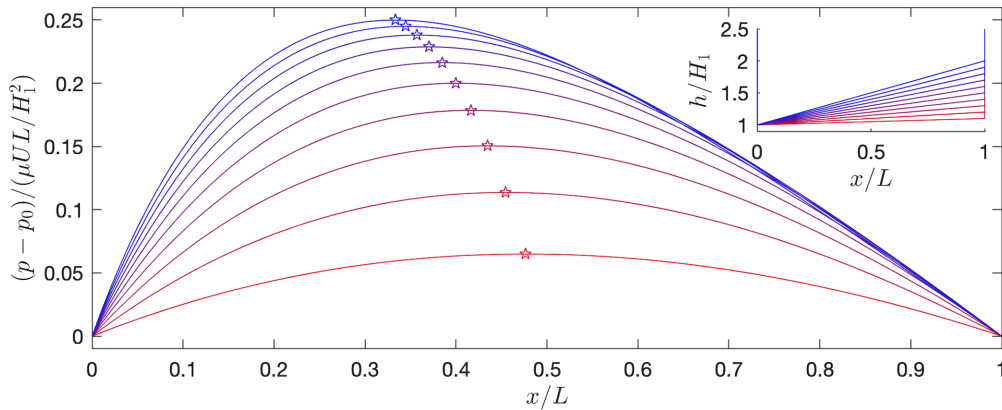


Figure 10.4: Plot of the non-dimensional pressure for $\frac{H_2}{H_1} = 0.1, 0.2, \dots, 1$ (red to blue). The stars indicate the maximum pressure in the fluid layer. Inset shows the corresponding non-dimensional geometry of the bearing.

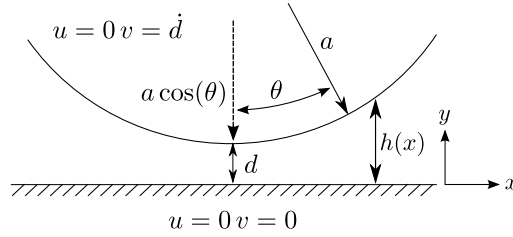


Figure 10.5: Cylinder geometry

Forces A thrust bearing is supposed to support high applied loads with reduced friction. To see when this is the case we can calculate the force on the boundaries per unit z -width:

$$\int_0^L \mathbf{T} \cdot \mathbf{n} \, dx, \quad (10.16)$$

where

$$\mathbf{T} = -p\mathbf{I} + \mu(\nabla\mathbf{u} + \nabla\mathbf{u}^T) \simeq \begin{pmatrix} -p & \mu\frac{\partial u}{\partial y} & 0 \\ \mu\frac{\partial u}{\partial y} & -p & 0 \\ 0 & 0 & -p \end{pmatrix}, \quad (10.17)$$

where we have kept only the leading order terms [$\partial u/\partial x \sim \partial v/\partial y \sim \epsilon\partial u/\partial y$]. The normal vector is

$$\mathbf{n} = \begin{cases} (0, -1, 0) & y = 0 \\ (-h', 1, 0)/(1 + h'^2)^{1/2} & y = h. \end{cases} \quad (10.18)$$

Remember, a normal vector to a plane specified $f = ax + by + cz + d = 0$ is given by ∇f . The unit normal vector is then defined as $\mathbf{n} = \nabla f/|\nabla f|$. For the bearing, the boundary is $f = y - h = 0$. Hence, the unit normal is given by

$$\mathbf{n} = \nabla(y - h)/|\nabla(y - h)| = \left(\frac{\partial}{\partial x}, \frac{\partial}{\partial y}, \frac{\partial}{\partial z} \right) (y - h)/|\nabla(y - h)| = (-h', 1, 0)/(1 + h'^2)^{1/2}. \quad (10.19)$$

The normal force (above atmospheric pressure) is

$$\int_0^L \hat{\mathbf{y}} \cdot \mathbf{T} \cdot \mathbf{n} - p_0 \, dx = \int_0^L p - p_0 \, dx = \dots = \frac{6\mu U}{\alpha^2} \left[\log\left(\frac{H_2}{H_1}\right) - \frac{2(H_2 - H_1)}{H_1 + H_2} \right]. \quad (10.20)$$

Similarly, we can calculate the tangential force:

$$\int_0^L \hat{\mathbf{x}} \cdot \mathbf{T} \cdot \mathbf{n} \, dx = \int_0^L \mu \frac{\partial u}{\partial y} \, dx = \dots = \frac{4\mu U}{\alpha} \left[\log\left(\frac{H_2}{H_1}\right) - \frac{3(H_2 - H_1)}{2(H_1 + H_2)} \right]. \quad (10.21)$$

It would be a good exercise to check these! In the thin film limit $|h'| = \alpha \ll 1$, the normal force is much larger than the tangential force, and hence this is a low friction bearing.

10.2.2 Cylinder approaching a wall

The second squeeze flow problem we will consider is a cylinder approaching a wall. We will carry out a similar procedure to the previous problem. Figure 10.5 shows the geometry of the problem. A cylinder of radius a falls vertically towards a horizontal plane with minimum gap $d(t)$ between the cylinder and the plane, where $d \ll a$ in the thin film limit. There are non-slip boundary conditions on the cylinder and on the plane.

Geometry The height of the fluid underneath the cylinder in the limit of $\theta \ll 1$ ($x/a = \sin\theta \simeq \theta$, $\cos\theta \simeq 1 - \theta^2/2$) is

$$h(x) = d + a(1 - \cos\theta) \simeq d + \frac{a\theta^2}{2} \simeq d + \frac{x^2}{2a} = d \left(1 + \frac{x^2}{2ad} \right). \quad (10.22)$$

This expression for the height gives the horizontal lengthscale in the problem $L \sim \sqrt{ad}$. This lengthscale is much smaller than the radius of the cylinder ($\sqrt{ad} \ll a$) so is consistent with the approximation of $\theta \ll 1$. This

lengthscale is also much larger than the minimum gap ($\sqrt{ad} \gg d$) so the flow is in the thin film limit and can be approximated as unidirectional.

Unidirectional flow Following the same method as for the thrust bearing, we can write the unidirectional flow horizontal velocity as

$$u = -\frac{1}{2\mu} \frac{dp}{dx} y(h-y). \quad (10.23)$$

Mass conservation The total volume flux (per unit z -width) is given by

$$Q = \int_0^h u \, dy = -\frac{h^3}{12\mu} \frac{dp}{dx} \quad (10.24)$$

Since the vertical velocity of the cylinder is $-\dot{d}$ we know the volume leaving a region $[0, x]$ per unit time is $-\dot{d}x$ [where $-d/dt(\int_0^x h(u, t) \, du) = -\dot{d}x$]. This must be equivalent to the volume flux. Hence, $Q = -\dot{d}x$ and

$$\frac{dp}{dx} = \frac{12\mu\dot{d}}{d^3} \frac{x}{(1 + \frac{x^2}{2ad})^3} \Rightarrow p(x) = p_0 - \frac{6\mu\dot{d}a}{d^2(1 + \frac{x^2}{2ad})^2}, \quad (10.25)$$

using the boundary condition $p \rightarrow p_0$ and $x \rightarrow \infty$.

Forces As in the case of the thrust bearing, the normal force per unit- z width (above atmospheric pressure) is

$$F = \int_{-\infty}^{\infty} p - p_0 \, dx = -\frac{6\mu\dot{d}a}{d^2} \sqrt{2ad} \int_{-\infty}^{\infty} \frac{1}{(1 + X^2)^2} \, dX = -\frac{6\mu\dot{d}a}{d^2} \sqrt{2ad} \frac{\pi}{2} = -3\sqrt{2}\pi\mu\dot{d} \left(\frac{a}{d}\right)^{3/2}. \quad (10.26)$$

If the cylinder is sedimenting under gravity we know that $F = -mg = \text{constant}$. Substituting this in we find

$$\dot{d} \sim d^{3/2} \Rightarrow d \sim t^{-2}. \quad (10.27)$$

Hence, the cylinder does not reach the wall in finite time.

10.3 Free surface flow

In the previous two problems we have considered the squeeze flow between two surfaces where the boundary condition on each surface is no-slip (i.e. the velocity parallel, or approximately parallel, to the surface is zero). In this next section, we will consider free surface flows where we remove one surface so the fluid is ‘free’ to move and its location needs to be determined as part of the problem. In particular, we will consider the shape of a drop on a horizontal plane controlled by either capillary or gravitational forces. To understand when these forces are applicable we will first introduce the idea of surface tension.

10.3.1 Surface Tension

Surface tension is a property of a free surface which appears due to the asymmetry of intermolecular forces acting in the interfacial region (typically of nanometric width). As one goes to smaller length scales, surface forces ($\sim L^2$) begin to dominate volume forces ($\sim L^3$). In particular, the surface tension force typically begins to dominate gravity when the length scale goes below millimetres-cm.

In the general case, for a free surface between a viscous liquid and a second viscous fluid (gas or liquid), if we assume that the velocity is continuous across the interface, there are 4 boundary conditions required for the 4 unknowns (3 velocities, which are not fixed, and 1 variable representing the free surface shape). These are provided by kinematic and dynamic boundary conditions.

Kinematic Boundary Condition Consider a free surface given in implicit form as $f(\mathbf{x}, t) = 0$ with $f < 0$ corresponding to fluid 1 and $f > 0$ corresponding to fluid 2. The free surface moves with the velocity of the fluid, so that fluid particles which begin on the free surface remain there. In other words, the surface ‘follows the fluid’. This means that we have conservation of f along the fluid paths of the surface particles, i.e. the material derivative of f is zero:

$$D_t f = (\partial_t + (\mathbf{u} \cdot \nabla)) f(\mathbf{x}, t) = 0. \quad (10.28)$$

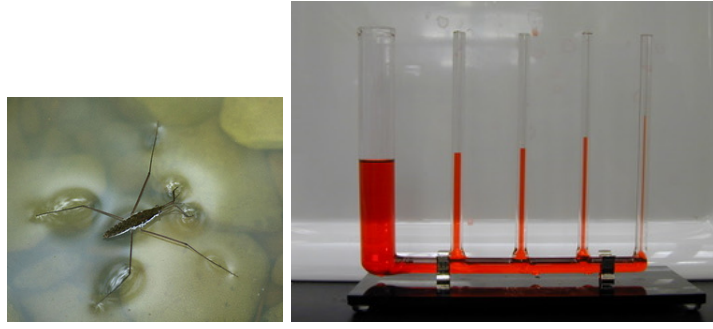


Figure 10.6: The tension of a liquid's surface allows water striders to 'walk on water' and causes liquids to rise up narrow gaps, through capillary action (here there is a liquid-solid surface tension also).

E.g. For a two-dimensional flow, suppose the free surface is defined as $y = h(x, t)$. Then $f(x, y, t) = y - h(x, t)$. At the free surface we have $f = 0$ and a unit normal vector $\mathbf{n} = (-\partial_x h, 1)/\sqrt{1 + (\partial_x h)^2}$ which point out of fluid 1. For $f(x, y, t) = y - h(x, t)$ so that $\nabla f = (-\partial_x h, 1)$ we find that

$$-\partial_t h + (u\partial_x + v\partial_y)(y - h(x, t)) = 0 \quad \text{so that} \quad \partial_t h + u\partial_x h = v. \quad (10.29)$$

Dynamic Boundary Condition To obtain a dynamic boundary condition, one applies Newton's II Law to the surface (an interface) separating the two fluids. Because there is no mass to the surface ($m\mathbf{a} = \mathbf{0}$ and external body forces are negligible), the forces acting on the surface from either side, i.e. caused by the stresses from the two fluids, must balance with any forces that occur from inside the interface.

To calculate the forces from inside the interface we will be interested in surface tension. Surface tension acts like an elastic membrane on the surface of a liquid and forces it to attempt to minimise its area (crudely, this is because it is energetically favourable for molecules to be in the bulk of the liquid, rather than at its surface). This force is responsible for a whole host of effects ranging from the suspension of small objects (e.g. water striders) through to the breakup of liquid jets (e.g. from a tap in a kitchen), which occurs when the liquid can reduce its surface area by forming a series of spheres (drops) rather than one cylinder (the jet), see figure 10.6. Problems involving surface tension are known as capillary flows.

The surface tension force γ (taken to be constant here), per unit length of line, is directed tangentially along the surface which is parameterised by coordinates (s_1, s_2) with tangent vectors in these directions $(\mathbf{t}_1, \mathbf{t}_2)$. Our control volume will have 'lower edge' at (s_{10}, s_{20}) and now has a surface tension force tugging at all four ends in the tangential direction.

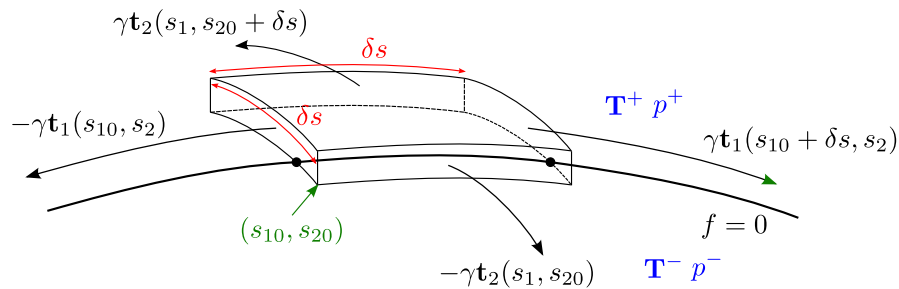


Figure 10.7: Forces acting on a control volume located at the interface. The stress from the two liquids act on the faces of the volume, which have area δs^2 , and the surface tension, which acts on acts on a line, tugs on the four ends of length δs (the height of the control volume is considered negligible). The interface is parameterised by coordinates (s_1, s_2) and the control volume's 'lower corner' is at (s_{10}, s_{20}) .

Consider a control volume of length and width along the interface equal to δs whose height is negligible compared to δs , see figure 10.7. This gives a force balance of

$$\delta s^2 \mathbf{T}^+ \cdot \mathbf{n} + \delta s^2 \mathbf{T}^- \cdot (-\mathbf{n}) + \gamma \delta s (\mathbf{t}_1(s_{10} + \delta s, s_2) - \mathbf{t}_1(s_{10}, s_2)) + \gamma \delta s (\mathbf{t}_2(s_1, s_{20} + \delta s) - \mathbf{t}_2(s_1, s_{20})) = \mathbf{0}$$

at $f = 0$. Dividing through by δs^2 and taking the limit $\delta s \rightarrow 0$ we find that

$$(\mathbf{T}^+ - \mathbf{T}^-) \cdot \mathbf{n} = [\mathbf{T} \cdot \mathbf{n}]_+^- = -\gamma \left(\frac{\partial \mathbf{t}_1}{\partial s_1} + \frac{\partial \mathbf{t}_2}{\partial s_2} \right) \equiv \gamma \kappa \mathbf{n} \quad \text{at} \quad f = 0. \quad (10.30)$$

where we have defined the curvature of the interface κ using

$$\kappa \mathbf{n} = - \left(\frac{\partial \mathbf{t}_1}{\partial s_1} + \frac{\partial \mathbf{t}_2}{\partial s_2} \right) \quad \text{or} \quad \kappa = [(\mathbf{I} - \mathbf{nn}) \cdot \nabla] \cdot \mathbf{n} \equiv \nabla_s \cdot \mathbf{n}. \quad (10.31)$$

To arrive at this expression we know that $\mathbf{t}_1 \cdot \mathbf{n} = 0$ and $\mathbf{t}_2 \cdot \mathbf{n} = 0$. Differentiating with respect to interface coordinates (s_1, s_2) gives

$$\frac{\partial \mathbf{t}_1}{\partial s_1} \cdot \mathbf{n} + \mathbf{t}_1 \cdot \frac{\partial \mathbf{n}}{\partial s_1} = 0 \quad \text{and} \quad \frac{\partial \mathbf{t}_2}{\partial s_2} \cdot \mathbf{n} + \mathbf{t}_2 \cdot \frac{\partial \mathbf{n}}{\partial s_2} = 0 \quad (10.32)$$

$$\Rightarrow \quad \kappa = - \left(\frac{\partial \mathbf{t}_1}{\partial s_1} + \frac{\partial \mathbf{t}_2}{\partial s_2} \right) \cdot \mathbf{n} = \mathbf{t}_1 \cdot \frac{\partial \mathbf{n}}{\partial s_1} + \mathbf{t}_2 \cdot \frac{\partial \mathbf{n}}{\partial s_2} = \nabla_s \cdot \mathbf{n}. \quad (10.33)$$

This can be simplified further by noting that $\mathbf{n} \cdot (\mathbf{n} \cdot \nabla) \mathbf{n} = 0$. Hence, the curvature can be written as

$$\kappa = \nabla_s \cdot \mathbf{n} = \nabla \cdot \mathbf{n}. \quad (10.34)$$

10.3.2 Bond number

We have seen from equation (10.30) that the stresses tangential to the interface are continuous, whereas the normal stress has a jump caused by the surface tension force $\gamma\kappa$. Hence, the pressure generated by surface tension is of the order γ/L , where L is a characteristic lengthscale in the problem which is approximately the radius of curvature of our interface. Therefore, capillary forces will be important when this is comparable to the pressure generated by gravitational forces, i.e. the hydrostatic pressure $\rho g L$ which occurs when

$$Bo = \frac{\rho g L^2}{\gamma} = 1 \quad \text{i.e. when} \quad L_\gamma = \sqrt{\gamma/(\rho g)}, \quad (10.35)$$

where L_γ is known as the capillary length and Bo is the Bond number. For water in air, where $\gamma = 0.07$ N/m, we have $L_\gamma = 3$ mm. Therefore, for large scale flows, such as sea waves, surface tension has no effect, but for small scale flows, such as those encountered in micro and nanofluidics, its importance far outweighs that of gravity.

10.3.3 Capillary number

In many cases, we are interested in knowing the shape of a liquid drop or bubble whose flow has negligible force in comparison to the surface tension forces. In the latter case, for low Reynolds number flows, where viscous forces dominate inertial ones, looking at the dynamic boundary condition we can see that the viscous force has magnitude $\mu U/L$ whilst the surface tension force is γ/L . The ratio of these forces gives the capillary number:

$$Ca = \frac{\mu U}{\gamma} \quad (10.36)$$

and when $Ca \ll 1$ the flow within the drop has a negligible effect on the free surface, so that the shape can be calculated independently of the flow (a huge simplification).

10.3.4 Capillary drop

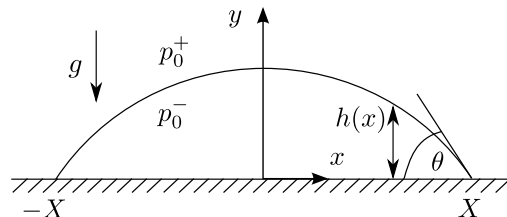


Figure 10.8: Two-dimensional capillary drop

Let's consider a liquid drop sat on a horizontal surface. For simplicity, let's consider a two-dimensional drop pinned at $x = \pm X$ where $h(\pm X, t) = 0$, see figure 10.8. In the limit of small capillary number $Ca \ll 1$, we can neglect the stress in the drop and calculate the shape of the drop from the dynamic boundary condition:

$$p^- - p^+ = \gamma \nabla \cdot \mathbf{n} \quad \text{at} \quad f = 0. \quad (10.37)$$

This is known as the *Young-Laplace equation*. We can parametrise the free surface in terms of a height function $y = h(x)$, so that $f = y - h(x, t)$, see figure 10.8. Then

$$\mathbf{n} = \frac{(-h_x, 1)}{\sqrt{(1 + h_x^2)}} \quad \text{and} \quad \nabla \cdot \mathbf{n} = \frac{\partial n_x}{\partial x} + \frac{\partial n_y}{\partial y} = -\frac{h_{xx}}{(1 + h_x^2)^{3/2}}. \quad (10.38)$$

From our y -momentum equation we find the pressure in the fluid is hydrostatic $p^- = p_0^- - \rho g y$. We assume the ambient fluid has a uniform pressure $p^+ = p_0^+$. Substituting these into the dynamic boundary condition (10.37) gives

$$-P - \rho g h = \gamma \nabla \cdot \mathbf{n} \quad \text{at} \quad f = 0. \quad (10.39)$$

where $P = p_0^+ - p_0^-$ is the (constant) pressure drop across the interface. Hence,

$$-P - \rho g h = -\frac{\gamma h_{xx}}{(1 + h_x^2)^{3/2}} \quad \text{at} \quad y = h(x, t). \quad (10.40)$$

This is a second order PDE for h and hence we must specify a boundary condition on h or its derivative at each end of the free surface. On top of this one either needs to specify the pressure drop P or, more often, the volume of the liquid which can then be used to find P .

In the lubrication limit $h_x \ll 1$ for small bond numbers $Bo \ll 1$, this reduces to

$$P = \gamma \frac{d^2 h}{dx^2} \quad (10.41)$$

with solution a parabola

$$h = \frac{-P}{2\gamma} (X^2 - x^2), \quad (10.42)$$

where we have used the pinned boundary condition $h(\pm X, t) = 0$. We see that for meaningful solutions we need $P < 0$ as P represents the pressure in the gas minus the pressure in the liquid (which we expect to be higher for a drop, due to surface tension). If we calculate the volume of the drop V we can see how the pressure and volume of the drop are related:

$$V = 2 \int_0^X \frac{-P}{2\gamma} (X^2 - x^2) dx = \frac{-2PX^3}{3\gamma} \quad \Rightarrow \quad -P = \frac{3\gamma V}{2X^3}. \quad (10.43)$$

In this solution we assumed the drop was pinned at points $x = \pm X$. This is known as a *pinned contact line*. An alternative boundary condition would be to *prescribe the contact angle* θ , the angle at which the free surface meets the horizontal plane, see figure 10.8. This then gives a boundary condition on the gradient $h_x = \pm \tan \theta$ at $x = \pm X$. In this case the position of the contact line would be found as part of the solution.

The prescribed contact angle will depend on the liquid-solid-gas combination in question: if the solid is 'wetable' (aka hydrophilic for water) this angle will be small (i.e. close to zero), so the drop spreads out a lot (e.g. water on glass), whereas if the angle is high (close to 180°) then the solid is non-wetable (aka hydrophobic) and the drop beads up (e.g. water on a lotus leaf).

10.3.5 Gravitational spreading

When the lengthscale of the liquid drop becomes large, gravitational forces begin to dominate over capillary forces (large Bond number) and viscous forces begin to dominate over surface tension (large capillary number). We can therefore neglect the jump in the normal stress at the free surface but now need to calculate the flow within the fluid. Let's consider the shape of an axisymmetric drop on a horizontal surface under the influence of gravity, or equivalently, let's consider the axisymmetric, gravitational spreading of a thin film layer on a horizontal surface, see figure 10.9.

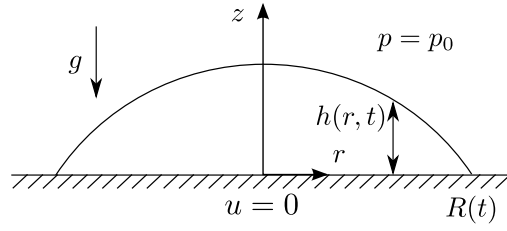


Figure 10.9: Axisymmetric spreading of a thin film

Geometry Unlike the squeeze flow problems, the geometry is unknown and will be determined as part of the solution. In addition, we are now in a cylindrical polar coordinate system. We write the surface of the thin-film as

$$z = h(r, t), \quad (10.44)$$

where z is the vertical coordinate, and r in the radial coordinate parallel to the horizontal plane.

Unidirectional flow In the thin film limit $|\partial h/\partial r| \ll 1$ so the flow is predominantly in the r direction. We can write the velocity as $\mathbf{u} = (u_r, u_\theta, u_z) = (u, 0, 0)$. The r - and z -momentum equations are then

$$0 = -\frac{\partial p}{\partial r} + \mu \frac{\partial^2 u}{\partial z^2} \quad \text{and} \quad 0 = -\frac{\partial p}{\partial z} - \rho g. \quad (10.45)$$

[Note, here we have taken the lubrication approximation of the Stokes equations written in cylindrical polar coordinates. In this case, the two-dimensional version is the same if we replace $r \rightarrow x$ and $z \rightarrow y$.] We have also now introduced body force $\mathbf{f} = -\rho g \hat{z}$. Integrating the z -momentum equation and applying boundary condition $p(h, t) = p_0$ gives

$$p = p_0 + \rho g(h - z). \quad (10.46)$$

Hence, the pressure in the fluid film is hydrostatic. Substituting this into the r -momentum equation we have

$$\mu \frac{\partial^2 u}{\partial z^2} = \rho g \frac{\partial h}{\partial r}. \quad (10.47)$$

The right-hand side is independent of z so the flow is driven by the slope of the free-surface. The boundary conditions on the no-slip underlying plane and the free surface are:

$$u|_{z=0} = 0 \quad \text{and} \quad \mu \frac{\partial u}{\partial z} \Big|_{z=h} = 0. \quad (10.48)$$

The second condition here is the dynamic boundary condition. Because we are considering large capillary numbers there is no jump in stress at the boundary (and the ambient fluid is assumed to have a negligible viscosity). Hence, we find the shear stress must be zero at the free surface.

Finally, integrating the momentum equation and applying the boundary conditions gives radial velocity profile

$$u = -\frac{\rho g}{2\mu} \frac{\partial h}{\partial r} z(2h - z). \quad (10.49)$$

Mass conservation For mass conservation we consider a cylindrical annulus from $r \rightarrow r + \delta r$, see figure 10.10. The volume of fluid entering the annulus at radius r per unit time is $Q(r)$, where Q is the radial volume flux. Similarly, the volume of fluid leaving the annulus at radius $r + \delta r$ is $Q(r + \delta r)$. In addition, because the top surface is able to move volume can also leave the annulus vertically at a rate per unit time of $(2\pi r \delta r)w = (2\pi r \delta r)\partial h/\partial t$. Here, I have used kinematic boundary condition $\partial h/\partial t = w$, which is valid when $\partial h/\partial r \ll 1$. Equating these volumes to ensure volume conservation gives

$$(2\pi r \delta r) \frac{\partial h}{\partial t} + Q(r + \delta r) = Q(r) \quad \Rightarrow \quad 2\pi r \frac{\partial h}{\partial t} + \frac{\partial Q}{\partial r} = 0 \quad \text{as} \quad \delta r \rightarrow 0. \quad (10.50)$$

[Note, the $2\pi r$ is present because we need to think about the volume flux in to and out of the entire annulus. If we were in a two-dimensional geometry, we could ignore this factor and then replace $r \rightarrow x$.] As before, we can calculate the volume flux by considering the flux out of a cylinder of radius r :

$$Q(r) = \int_0^{2\pi} \int_0^h u r \, dz \, d\theta = 2\pi r \int_0^h u \, dz = -\frac{2\pi g}{3\nu} h^3 r \frac{\partial h}{\partial r}, \quad (10.51)$$

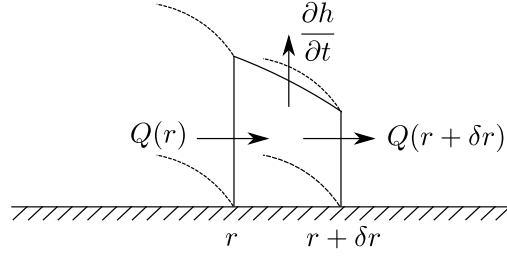


Figure 10.10: Volume flux in to and out of a cylindrical annulus

where we have used surface element $dS = r dz d\theta$ in a surface of constant radius r . Substituting this flux into the mass conservation equation gives

$$\frac{\partial h}{\partial t} = \frac{g}{3\nu} \frac{1}{r} \frac{\partial}{\partial r} \left(r h^3 \frac{\partial h}{\partial r} \right). \quad (10.52)$$

We now need to solve this Partial Differential Equation (PDE) for the free boundary $z = h$. As an aside, let's integrate the PDE in r between 0 and the boundary $r = R(t)$ where $h(R, t) = 0$ (it'll be clear why in a moment):

$$\int_0^{R(t)} r \frac{\partial h}{\partial t} dr = \int_0^{R(t)} \frac{g}{3\nu} \frac{\partial}{\partial r} \left(r h^3 \frac{\partial h}{\partial r} \right) dr, \quad (10.53)$$

$$\frac{d}{dt} \int_0^{R(t)} r h dr - \underbrace{\dot{R}(t) h r}_{=0} \Big|_{r=R} = \underbrace{\left[\frac{g}{3\nu} r h^3 \frac{\partial h}{\partial r} \right]_0}_{=0}^{R(t)}. \quad (10.54)$$

The second term on the left-hand side is zero because the film has zero height at the edge, $h(R, t) = 0$. The right-hand side is zero because the flux at the centre and the edge is zero, $Q(0) = Q(R) = 0$. Therefore, the volume of the drop is constant:

$$V = \int_0^{2\pi} \int_0^{R(t)} \int_0^{h(r,t)} r dz dr d\theta = \int_0^{2\pi} \int_0^{R(t)} r h dr d\theta = 2\pi \int_0^{R(t)} r h dr = \text{constant}, \quad (10.55)$$

where we have used volume element $dV = r dz dr d\theta$ in cylindrical polar coordinates. If instead, we were able to introduce fluid at the centre of the flow with some non-zero volume flux we would have condition $Q \rightarrow Q_0$ as $r \rightarrow 0$ and $V = Q_0 t$.

Solving for the free boundary

We would like to solve the following PDE (non-linear diffusion equation) subject to the global constraint that the volume is constant:

$$\frac{\partial h}{\partial t} = \frac{g}{3\nu} \frac{1}{r} \frac{\partial}{\partial r} \left(r h^3 \frac{\partial h}{\partial r} \right), \quad h(R, t) = 0, \quad \text{and} \quad V = 2\pi \int_0^{R(t)} r h dr. \quad (10.56)$$

Scaling the equation of motion and global mass conservation using characteristic height, radial and time scales H, R and T gives

$$\frac{H}{T} \sim \frac{gH^4}{\nu R^2} \quad \text{and} \quad V \sim hR^2, \quad (10.57)$$

which can be rearranged to

$$H \sim \left(\frac{\nu V}{gT} \right)^{1/4} \quad \text{and} \quad R \sim \left(\frac{gV^3 T}{\nu} \right)^{1/8}. \quad (10.58)$$

Since there are no more scales in the problem (assuming the initial condition was a sufficiently long ago to be irrelevant) it suggests we such look for a *similarity solution* of the form

$$h(r, t) = (\nu V / g t)^{1/4} H(\eta) \quad \text{where} \quad \eta \equiv r / (g V^3 t / \nu)^{1/8} \quad (10.59)$$

with the edge of the film at $\eta_N = R / (g V^3 t / \nu)^{1/8}$. These solutions are *self-similar* which means that by appropriately scaling the radius and height of the film by a power of t the time evolution of the current falls

onto a universal curve (we'll plot the solution up later to show this more clearly). Let's substitute this ansatz into the PDE and constraints. With some algebra we arrive at:

$$-\frac{1}{4}H - \frac{1}{8}\eta H' = \frac{1}{3\eta}(\eta H^3 H')', \quad H(\eta_N) = 0, \quad \text{and} \quad 1 = 2\pi \int_0^{\eta_N} \eta H \, d\eta, \quad (10.60)$$

where the prime denotes differentiation w.r.t η . The power of this type of solution is that we've turned a PDE into an ODE for $H(\eta)$ which is significantly easier to solve. We can now make progress with the ODE as follows:

$$-\frac{1}{8}(2\eta H + \eta^2 H') = \frac{1}{3}(\eta H^3 H')' \quad (10.61)$$

$$-\frac{1}{8}(\eta^2 H)' = \frac{1}{3}(\eta H^3 H')' \quad (10.62)$$

$$-\frac{1}{8}\eta^2 H = \frac{1}{3}\eta H^3 H' + \underbrace{\text{const.}}_{=0} \quad (10.63)$$

since we want $H(\eta_N) = 0$. Integrating again we get

$$\frac{1}{9}H^3 = \frac{1}{16}(\eta_N^2 - \eta^2). \quad (10.64)$$

Finally, applying our volume constraint we can determine η_N and hence solution

$$H = \left(\frac{9}{16}(\eta_N^2 - \eta^2) \right)^{1/3} \quad \text{where} \quad \eta_N = \left(\frac{2^{10}}{3^5 \pi^3} \right)^{1/8}, \quad (10.65)$$

or equivalently

$$h = \left(\frac{\nu V}{gt} \right)^{1/4} \left(\frac{9\eta_N^2}{16} \left(1 - \frac{r^2}{R^2} \right) \right)^{1/3}, \quad R(t) = \eta_N \left(\frac{gV^3 t}{\nu} \right)^{1/8}. \quad (10.66)$$

Figure 10.11 plots the solution to demonstrate the self-similar behaviour.

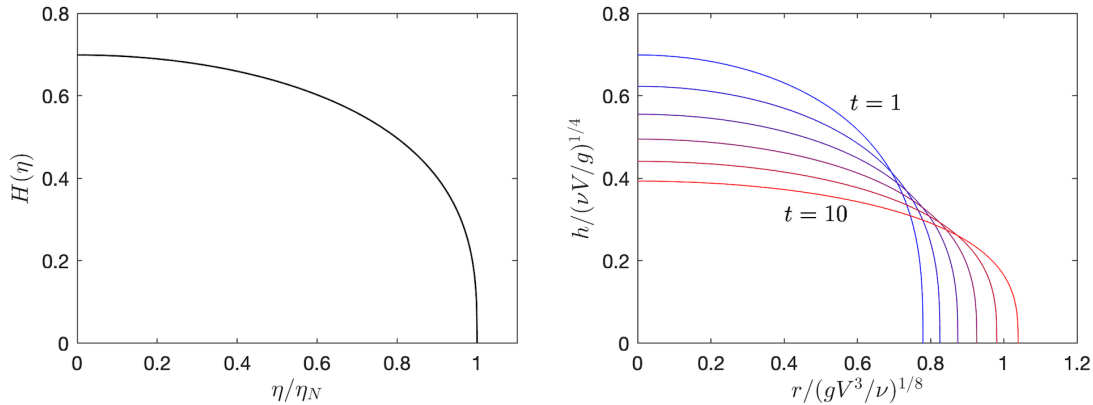


Figure 10.11: Height versus radius in similarity variables H and η and rescaled variables h and r for $1 \leq t \leq 10$ (increasing time from blue to red).

Shape of the nose

To investigate the shape of the nose we let $h = A(R - r)^\alpha$. Substituting into the governing equation when $r \simeq R$ gives

$$A\alpha(R - r)^{\alpha-1} \dot{R} = \frac{g}{3\nu} \frac{1}{R} \frac{\partial}{\partial r} (RA^3(R - r)^{3\alpha} A\alpha(-)(R - r)^{\alpha-1}) \quad (10.67)$$

$$= \frac{g}{3\nu} A^4 \alpha(4\alpha - 1)(R - r)^{4\alpha-2}. \quad (10.68)$$

Matching the powers of $R - r$ gives $\alpha = 1/3$. The shape of the nose is then $h = A(R - r)^{1/3}$. The gradient $\partial h / \partial r$ is therefore singular at the nose, but not too singular that the flux boundary condition $Q(r \rightarrow R) \rightarrow 0$ is still satisfied.

10.3.6 Gravitational spreading down an inclined plane

Let's now consider the shape of a two-dimensional drop spreading down an inclined plane of slope θ . x is the downslope coordinate and y is the vertical coordinate perpendicular to the slope. The body force is then $\mathbf{f} = \rho g(\sin \theta, -\cos \theta)$. The fluid is released from a fixed point such that $h(0, t) = 0$ and the ambient has constant pressure p_0 .

The Lubrication approximation is then

$$0 = -\frac{\partial p}{\partial x} + \mu \frac{\partial^2 u}{\partial y^2} + \rho g \sin \theta, \quad 0 = -\frac{\partial p}{\partial y} - \rho g \cos \theta. \quad (10.69)$$

Integrating the y -momentum equation gives hydrostatic pressure $p = p_0 + \rho g \cos \theta (h - y)$. Calculating the velocity field, integrating across the depth to get the volume flux, and applying mass conservation, we arrive at evolution equation

$$\frac{\partial h}{\partial t} + \frac{g \sin \theta}{3\nu} \frac{\partial h^3}{\partial x} = \frac{g \cos \theta}{3\nu} \frac{\partial}{\partial x} \left(h^3 \frac{\partial h}{\partial x} \right). \quad (10.70)$$

A similarity solution does not exist for the full governing equation. Instead we will consider one particular limit.

Problem: Let's consider a constant volume release A (per cross-slope distance) of viscous fluid at $x = 0$ such that $h(0, t) = 0$. After a long time the nose (or front) of the current has travelled a distance $X_N(t) \gg (A \cot \theta)^{1/2}$. We want to find a similarity solution for $h(x, t)$. The volume constraint can be written as

$$A = \int_0^{X_N} h \, dx \quad \Rightarrow \quad A \sim HX, \quad H \sim \frac{A}{X}. \quad (10.71)$$

Scaling the evolution equation to look for the dominant terms gives

$$\frac{H}{T} : \frac{g \sin \theta}{3\nu} \frac{H^3}{X} : \frac{g \cos \theta}{3\nu} \frac{H^4}{X^2} \quad (10.72)$$

$$\frac{1}{T} : \frac{g \sin \theta}{3\nu} \frac{A^2}{X^3} : \frac{g \cos \theta}{3\nu} \frac{A^3}{X^5} \quad (10.73)$$

$$\frac{3\nu}{g \sin \theta} \frac{X^5}{A^2 T} : X^2 : A \cot \theta \quad (10.74)$$

Looking at the relative size of the terms, for $X_N(t) \gg (A \cot \theta)^{1/2}$, we can neglect the RHS of the evolution equation. The system we want to solve is then

$$\frac{\partial h}{\partial t} + \frac{g \sin \theta}{3\nu} \frac{\partial h^3}{\partial x} = 0, \quad A = \int_0^{X_N} h \, dx, \quad h(0, t) = 0. \quad (10.75)$$

Scaling the remainder of the equations suggest the following scales for the vertical and horizontal coordinates

$$H \sim \left(\frac{\nu A}{g \sin \theta T} \right)^{1/3} \quad \text{and} \quad X \sim \left(\frac{g \sin \theta A^2 T}{\nu} \right)^{1/3}. \quad (10.76)$$

Given these scales we will look for a similarity solution of the form

$$h = \left(\frac{\nu A}{g \sin \theta t} \right)^{1/3} H(\eta), \quad \eta = \frac{x}{\left(\frac{g \sin \theta A^2 t}{\nu} \right)^{1/3}}. \quad (10.77)$$

The governing equations then become

$$-\frac{1}{3}H - \frac{1}{3}\eta H' + \frac{1}{3}(H^3)' = 0, \quad 1 = \int_0^{\eta_N} H \, d\eta, \quad H(0) = 0. \quad (10.78)$$

Integrating gives $H = \eta^{1/2}$ we can then determine the nose position

$$1 = \int_0^{\eta_N} \eta^{1/2} \, d\eta = \frac{2}{3} \eta_N^{3/2} \quad \Rightarrow \quad \eta_N = \left(\frac{3}{2} \right)^{2/3}. \quad (10.79)$$

The similarity solution is then

$$h = \left(\frac{\nu A}{g \sin \theta t} \right)^{1/3} \left[\frac{x}{\left(\frac{g \sin \theta A^2 t}{\nu} \right)^{1/3}} \right]^{1/2} = \left(\frac{\nu}{g \sin \theta} \right)^{1/2} \frac{x^{1/2}}{t^{1/2}}, \quad X_N(t) = \left(\frac{3}{2} \right)^{2/3} \left(\frac{g \sin \theta A^2 t}{\nu} \right)^{1/3}. \quad (10.80)$$

We can see from the similarity solution that the thickness is finite at the front $h(X_N, t) = h_N \neq 0$. This is because we have neglected a term in the evolution equation which becomes important when you are near the front. To find the shape of the front (how this jump in the thickness is rounded off) we can substitute in $h = B(X_N - x)^\beta$ into the evolution equation. This gives two possible values for $\beta = 1, 1/3$ (assuming the neglected term is one of the scales). We know we need to match onto the finite thickness height so must have a cube-root singularity at the nose. This just says that at the nose, the first term on the LHS and the term on the RHS dominate. Alternatively, we could pose ansatz $h = h_N f(X_N - x)$ where f has some unknown functional form to be determined and h_N is the thickness at the front and solve for f using the full equation.

Chapter 11

Complex Fluids and Non-Newtonian Rheology

11.1 Constitutive laws

Up until now, we have considered Newtonian fluids with a linear relationship between the stress and rate of deformation in the fluid. For fluids consisting of small molecules, like water, this approximation works very well, even in turbulent flows with high flow rates. In realistic Newtonian flows, the separation of length and time scales mean the typical intermolecular distances or velocity distributions of individual constituents are the same whether the flow is turbulent or at rest. Hence, the energy dissipation in the fluid, which is represented by viscosity in the Newtonian constitutive law, is not affected by the flow.

When the applied flows are capable of altering the local microstructure of the fluid the classical Newtonian approximation might fail to provide an adequate mathematical model of the dynamics. For example, this is the case in solutions of colloidal particles, long flexible polymers, wormlike micelles, and similar complex fluids. These particles are significantly larger than individual molecules of typical Newtonian fluids, and the time scales of stress relaxation in these complex fluids are significantly longer than in their Newtonian counterparts. One can use the longest relaxation time λ to form a dimensionless group

$$\text{Wi} = \lambda \dot{\gamma}, \quad \dot{\gamma} = \sqrt{\frac{1}{2} \Sigma_{jk} \dot{\gamma}_{jk}^2}, \quad (11.1)$$

the Weissenberg number. Here the shear rate $\dot{\gamma}$ is an invariant measure of the rate of strain in the fluid (we will talk about this more in detail below).

For small velocity gradients, $\text{Wi} \ll 1$, complex fluids obey the linear constitutive law, and flow like Newtonian fluids at the same Reynolds number. When the Weissenberg number is comparable to or larger than unity, complex fluids exhibit non-Newtonian behaviour and obey complicated constitutive models, often involving non-linear dependence of the local stress on the velocity gradient and the deformation history of the fluid. In this chapter we will first consider the simplest extension of a Newtonian description in which the flow only influences the instantaneous viscosity of the fluid. We will then discuss a general theory dealing with history-dependent properties of viscoelastic fluids.

11.1.1 Newtonian fluid

To begin with, let's recap what we know for Newtonian fluids. The fluid is Newtonian if the relationship between the rate of deformation ($\gamma_{ij} = \partial u_i / \partial x_j + \partial u_j / \partial x_i$) and the stress \mathbf{T} is local, linear, instantaneous and isotropic. If the fluid is also incompressible, the Newtonian constitutive law is

$$\mathbf{T} = -p\mathbf{I} + \mu(\nabla\mathbf{u} + \nabla\mathbf{u}^T) \equiv -p\mathbf{I} + \underbrace{\mu\dot{\boldsymbol{\gamma}}}_{\boldsymbol{\tau}}, \quad (11.2)$$

where μ is constant and $\boldsymbol{\tau}$ is the deviatoric stress tensor and represents the traceless ($\nabla \cdot \mathbf{u} = 0$) part of the stress tensor, while the pressure is the isotropic part.

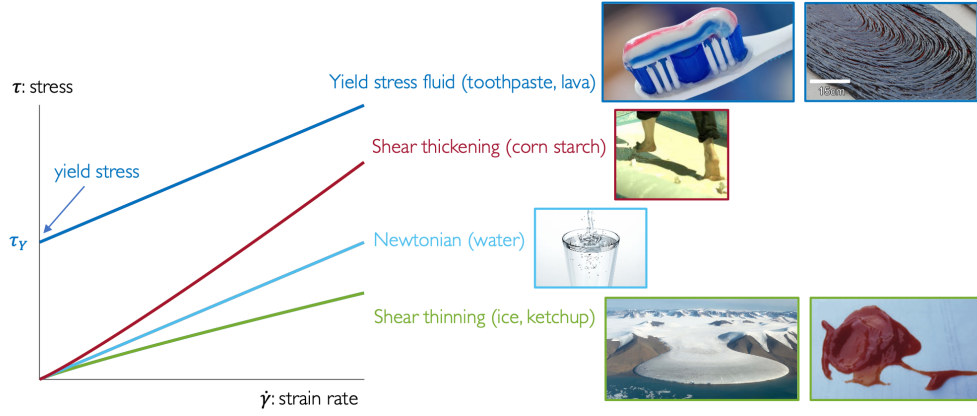


Figure 11.1: 1D constitutive laws for Newtonian, power-law and yield stress fluids with typical examples.

11.1.2 Generalised Newtonian fluid

A generalised Newtonian fluid assumes that the applied flow only changes the energy dissipation in the fluid, represented by the viscosity, but does not change the tensorial structure of the Newtonian model. The generalised constitutive law is given by

$$\mathbf{T} = -p\mathbf{I} + \mu(\dot{\boldsymbol{\gamma}})\dot{\boldsymbol{\gamma}}, \quad (11.3)$$

where $\mu(\dot{\boldsymbol{\gamma}})$ is the viscosity now dependent on the fluid flow. To ensure that the viscosity does not change under a coordinate transformation, which would be unphysical, the viscosity can only depend on invariants of the strain-rate tensor $\dot{\boldsymbol{\gamma}}$. The second tensorial invariant is the lowest non-trivial invariant, so we may write

$$\mathbf{T} = -p\mathbf{I} + \mu(\dot{\boldsymbol{\gamma}})\dot{\boldsymbol{\gamma}}, \quad \dot{\boldsymbol{\gamma}} = \sqrt{\frac{1}{2}\sum_{jk}\dot{\gamma}_{jk}^2}. \quad (11.4)$$

Power-law fluid

For a power-law fluid the viscosity is given by

$$\mu(\dot{\boldsymbol{\gamma}}) = \hat{\mu}|\dot{\boldsymbol{\gamma}}|^{n-1}. \quad (11.5)$$

When $n = 1$ this reduces to a Newtonian fluid. When $n < 1$ the fluid is *shear-thinning* and the effective viscosity decreases with the rate of deformation; when $n > 1$ the fluid is *shear-thickening* and the effective viscosity increases with the rate of deformation. Figure 11.1 gives some examples of these fluids. Note, the units of $\hat{\mu}$ are PT^n (P -pressure, T -time). The constitutive law for a power-law fluid is then written as

$$\boldsymbol{\tau} = \hat{\mu}|\dot{\boldsymbol{\gamma}}|^{n-1}\dot{\boldsymbol{\gamma}}. \quad (11.6)$$

Yield stress fluid

Yield stress fluids incorporate both solid-like and fluid like behaviour. They are characterised in terms of a yield stress τ_Y . When the stress is below this yield stress there is no deformation, $\dot{\boldsymbol{\gamma}} = \mathbf{0}$. When the stress is above this yield stress the fluid flows with some viscosity dependent on the strain-rate invariant.

For example, a *Bingham fluid* has constitutive law

$$\boldsymbol{\tau} = \left(\frac{\tau_Y}{\dot{\boldsymbol{\gamma}}} + \mu\right)\dot{\boldsymbol{\gamma}}, \quad \tau = \sqrt{\frac{1}{2}\sum_{jk}\tau_{jk}^2} > \tau_Y, \quad (11.7)$$

and $\dot{\boldsymbol{\gamma}} = \mathbf{0}$ otherwise, where μ is a constant viscosity. Note, τ is the second invariant of the deviatoric stress tensor $\boldsymbol{\tau}$. This is chosen to decide whether the fluid is yielded or not as it does not change under a coordinate transformation and the first invariant is zero.

A *Herschel-Bulkley fluid* has constitutive law

$$\boldsymbol{\tau} = \left(\frac{\tau_Y}{\dot{\boldsymbol{\gamma}}} + K|\dot{\boldsymbol{\gamma}}|^{n-1}\right)\dot{\boldsymbol{\gamma}}, \quad \tau = \sqrt{\frac{1}{2}\sum_{jk}\tau_{jk}^2} > \tau_Y, \quad (11.8)$$

and $\dot{\boldsymbol{\gamma}} = \mathbf{0}$ otherwise, where K is the consistency with units PT^n and n is the power-law index.

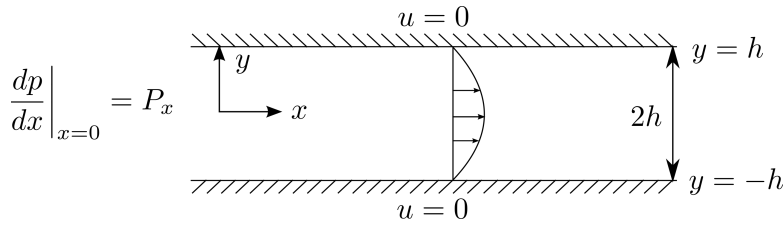


Figure 11.2: Sketch of Poiseuille flow through a two-dimensional pipe.

11.2 Poiseuille flow

As a simple example, we will consider Poiseuille flow through a two-dimensional pipe. Figure 11.2 shows the set up of a pipe with pressure gradient P_x driving the flow at one end $x = 0$. x is the along pipe coordinate; y in the across pipe coordinate with $-h \leq y \leq h$. The velocity $\mathbf{u} = (u, v)$ then satisfies the following conservation of momentum and mass equations:

$$\rho \left(\frac{\partial u}{\partial t} + u \frac{\partial u}{\partial x} + v \frac{\partial u}{\partial y} \right) = \frac{\partial T_{xx}}{\partial x} + \frac{\partial T_{xy}}{\partial y} \quad (11.9)$$

$$\rho \left(\frac{\partial v}{\partial t} + u \frac{\partial v}{\partial x} + v \frac{\partial v}{\partial y} \right) = \frac{\partial T_{xy}}{\partial x} + \frac{\partial T_{yy}}{\partial y} \quad (11.10)$$

$$\frac{\partial u}{\partial x} + \frac{\partial v}{\partial y} = 0. \quad (11.11)$$

We look for steady solutions where the flow is all in the x -direction and only varies in y such that $\mathbf{u} = (U(y), 0)$. Mass conservation is automatically satisfied and the momentum equations reduce to

$$0 = \frac{\partial T_{xx}}{\partial x} + \frac{\partial T_{xy}}{\partial y} \quad (11.12)$$

$$0 = \frac{\partial T_{xy}}{\partial x} + \frac{\partial T_{yy}}{\partial y}. \quad (11.13)$$

The only non-zero component of the strain-rate tensor is $\dot{\gamma}_{xy} = dU/dy$, and hence $\dot{\gamma} = |dU/dy|$. The stress components are therefore

$$T_{xx} = T_{yy} = -p, \quad T_{xy} = \tau_{xy} \quad \Rightarrow \quad 0 = -\frac{\partial p}{\partial x} + \frac{\partial \tau_{xy}}{\partial y} \quad \text{and} \quad 0 = -\frac{\partial p}{\partial y}. \quad (11.14)$$

Hence, p is only a function x . Since τ_{xy} is only a function of y , p must also be linear in x :

$$p = p_0 - P_x x \quad \Rightarrow \quad -P_x = \frac{d\tau_{xy}}{dy}. \quad (11.15)$$

We have yet to consider the rheology of the fluid which we will need to do to solve for the flow field.

Newtonian fluid

For a Newtonian fluid,

$$\tau_{xy} = \mu \dot{\gamma}_{xy} = \mu \frac{dU}{dy}. \quad (11.16)$$

Substituting this into (11.15) gives a second order ODE for U subject to two boundary conditions: no-slip on the walls $U(\pm h) = 0$. Solving for the velocity we find

$$U(y) = \frac{P_x}{2\mu} (h^2 - y^2). \quad (11.17)$$

Power-law fluid

For a power-law fluid, we have

$$\tau_{xy} = \hat{\mu} \left| \frac{dU}{dy} \right|^{n-1} \frac{dU}{dy}. \quad (11.18)$$

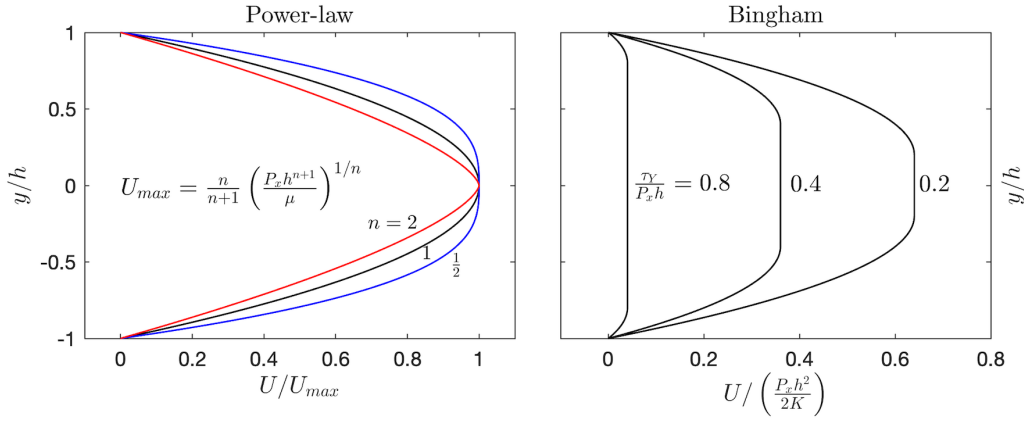


Figure 11.3: Velocity profile for Power-law and Bingham constitutive laws.

Substituting this into (11.15) again gives a second order ODE for U subject to two boundary conditions: no-slip on the walls $U(\pm h) = 0$. We have

$$\hat{\mu} \left| \frac{dU}{dy} \right|^{n-1} \frac{dU}{dy} = -P_x y + A. \quad (11.19)$$

By symmetry, we know $A = 0$. Upon integrating we find velocity

$$U(y) = \frac{n}{n+1} \left(\frac{P_x}{\hat{\mu}} \right)^{1/n} \left[h^{(n+1)/n} - |y|^{(n+1)/n} \right]. \quad (11.20)$$

Note, you need to be careful of signs here, in particular it's useful to know that $\text{sgn}(dU/dy) = -\text{sgn}(y)$.

Bingham fluid

For a Bingham fluid, we have

$$\tau_{xy} = \left(\frac{\tau_Y}{\dot{\gamma}} + K \right) \dot{\gamma}_{xy} = \tau_Y \text{sgn} \left(\frac{dU}{dy} \right) + K \frac{dU}{dy} = -P_x y \quad \text{for } \tau = |\tau_{xy}| > \tau_Y \quad (11.21)$$

The yield condition is equivalent to $|y| > \tau_Y/P_x$. Hence, we need to solve for U in three different regions:

1. $\tau_Y/P_x < y < h$ where $dU/dy < 0$. This then gives

$$-\tau_Y + K \frac{dU}{dy} = -P_x y \quad \Rightarrow \quad U(y) = \frac{P_x}{2K} (h^2 - y^2) - \frac{\tau_Y}{K} (h - y). \quad (11.22)$$

2. $-h < y < -\tau_Y/P_x$ where $dU/dy > 0$. This then gives

$$\tau_Y + K \frac{dU}{dy} = -P_x y \quad \Rightarrow \quad U(y) = \frac{P_x}{2K} (h^2 - y^2) - \frac{\tau_Y}{K} (h + y). \quad (11.23)$$

3. $-\tau_Y/P_x < y < \tau_Y/P_x$ where $dU/dy = 0$. By matching onto the velocities either side of the unyielded region ($|\tau_{xy}| < \tau_Y$) we find plug velocity

$$U(y) = U_p = \frac{P_x h^2}{2K} \left[1 - \frac{\tau_Y}{P_x h} \right]^2 \quad (11.24)$$

which is constant. Figure 11.3 plots the velocity profiles for Power-law and Bingham fluids. The central region is *unyielded* and flows in a solid plug. When $\tau_Y/P_x h = 1$ the whole flow is unyielded and the plug velocity is zero i.e. the pressure gradient is not sufficient to get the flow to yield. Yield surfaces divide the unyielded and yielded parts of the flow. In this case the yield surfaces are given by $|y| = Y \equiv \tau_Y/P_x$.

11.3 Taylor-Couette flow

A second example is a Taylor-Couette device where we have fluid between two concentric cylinders. The inner cylinder at $r = a$ is fixed and the outer cylinder at $r = b$ rotates at a constant rotation rate Ω , see figure 11.4.

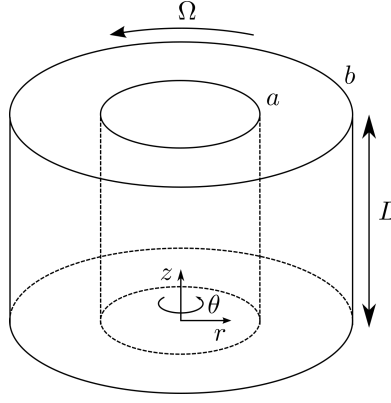


Figure 11.4: Sketch of Taylor-Couette flow between two concentric cylinders.

For an axisymmetric steady flow, the velocity has the form $\mathbf{u} = (0, u_\theta(r), 0)$. The only non-zero strain-rate component is $\dot{\gamma}_{r\theta}$, and hence $T_{r\theta} = \tau_{r\theta}$ is the only non-zero deviatoric stress component. In cylindrical polar coordinates, the strain rate tensor and conservation of momentum in the azimuthal direction are given by

$$\dot{\gamma}_{r\theta} = \frac{du_\theta}{dr} - \frac{u_\theta}{r} = r \frac{d}{dr} \left(\frac{u_\theta}{r} \right), \quad \frac{d}{dr} (\tau_{r\theta}) + \frac{2}{r} \tau_{r\theta} = \frac{1}{r^2} \frac{d}{dr} (r^2 \tau_{r\theta}) = 0. \quad (11.25)$$

N.B. Mass conservation is automatically satisfied by the form of the assumed velocity field. This can be integrated to give stress

$$\tau_{r\theta} = \frac{A}{r^2}, \quad (11.26)$$

for some constant A .

Bingham fluid

For a Bingham fluid, the constitutive law is

$$\tau_{r\theta} = \begin{cases} \left(\frac{\tau_Y}{|\dot{\gamma}_{r\theta}|} + \mu \right) \dot{\gamma}_{r\theta} = \tau_Y + \mu \dot{\gamma}_{r\theta}, & \tau_{r\theta} > \tau_Y \\ \dot{\gamma}_{r\theta} = 0, & \tau_{r\theta} < \tau_Y, \end{cases} \quad (11.27)$$

where $\dot{\gamma}_{r\theta} > 0$ because the inner cylinder is held fixed and the outer cylinder is rotating with rotation rate $\Omega > 0$. Substituting this into (11.26), in the yielded region, $a < r < r_Y$, we have

$$\frac{A}{r^2} - \tau_Y = \mu \dot{\gamma}_{r\theta} = \mu r \frac{d}{dr} \left(\frac{u_\theta}{r} \right), \quad \frac{A}{r_Y^2} - \tau_Y = 0 \quad (11.28)$$

and in the unyielded region $r_Y < r < b$ we have

$$\dot{\gamma}_{r\theta} = 0 \quad \Rightarrow \quad \frac{u_\theta}{r} = \Omega. \quad (11.29)$$

Upon integrating and applying boundary condition $u_\theta(a) = 0$ we find

$$\frac{u_\theta}{r} = \begin{cases} \frac{\tau_Y r_Y^2}{2\mu} \left(\frac{1}{a^2} - \frac{1}{r^2} \right) - \frac{\tau_Y}{\mu} \ln \left(\frac{r}{a} \right) & a < r < r_Y \\ \Omega & r_Y < r < b, \end{cases} \quad (11.30)$$

where matching at yield surface gives relationship between the rotation rate and r_Y

$$\Omega = \frac{\tau_Y r_Y^2}{2\mu} \left(\frac{1}{a^2} - \frac{1}{r_Y^2} \right) - \frac{\tau_Y}{\mu} \ln \left(\frac{r_Y}{a} \right). \quad (11.31)$$

Here, we have assumed that we can rotate the outer cylinder with some fixed rotation rate Ω and cause it to yield irrespective of how large the yield stress of the Bingham fluid is. In reality, we will apply some torque $\mathbf{G} = G\hat{\mathbf{z}}$ to the outer cylinder and the rotation rate will depend on the magnitude of the torque, the rheology of the fluid, and the size of the cylinder. The torque on the outer cylinder is defined as

$$\mathbf{G} = \int \mathbf{r} \times (\mathbf{T} \cdot \hat{\mathbf{n}}) dA = \int \mathbf{r} \times (\mathbf{T} \cdot \hat{\mathbf{n}}) b d\theta dz, \quad (11.32)$$

where we have used surface element $dA = r d\theta dz$. We know that on the outer cylinder $\mathbf{r} = (b, 0, 0) = b\hat{\mathbf{r}}$, $\mathbf{T} \cdot \hat{\mathbf{n}} = (0, \tau_{r\theta}|_b, 0) = \tau_{r\theta}|_b \hat{\boldsymbol{\theta}}$ and $\hat{\mathbf{r}} \times \hat{\boldsymbol{\theta}} = \hat{\mathbf{z}}$. Hence,

$$\mathbf{G} = \hat{\mathbf{z}} \int_0^L \int_0^{2\pi} \tau_{r\theta}|_b b^2 d\theta dz = 2\pi L b^2 \tau_{r\theta}|_b \hat{\mathbf{z}} \quad \Rightarrow \quad \tau_{r\theta}|_b = \frac{G}{2\pi L b^2}. \quad (11.33)$$

Comparing this with the stress $\tau_{r\theta} = \tau_Y r_Y^2 / r^2$ calculated above, we find a relationship between the yield surface and the magnitude of the torque G

$$\tau_{r\theta}|_b = \tau_Y r_Y^2 / b^2 = \frac{G}{2\pi L b^2} \quad \Rightarrow \quad r_Y = \sqrt{\frac{G}{2\pi L \tau_Y}}. \quad (11.34)$$

If $a < \sqrt{G/2\pi L \tau_Y} < b$, then we have the velocity structure as calculated above with a yield surface within the domain. If $\sqrt{G/2\pi L \tau_Y} < a$ then the fluid is unyielded everywhere and performs solid body rotation. (N.B. if solid body rotation does occur everywhere then the rotation rate at the inner cylinder is also $\Omega > 0$, which does not satisfy the fixed boundary condition there. Instead there must be a yielded boundary layer near the inner wall). If $\sqrt{G/2\pi L \tau_Y} > b$, the fluid is yielded everywhere.

11.4 Viscoelastic fluids

When experiments are done with polymeric fluids it is observed that the response to the shear rate is not always reproducible even if the same stress is reached. In this case, it takes time for the fluid to adjust to the flow with fluid having some memory of its flow history. A polymeric fluid will not remember its history forever, but because the molecules can be stretched by the flow it has some memory until the molecules relax. These fluids incorporate the behaviours of viscous fluids (which are instantaneous and have no memory) and elastic solids (which remember everything). Their combination gives a *viscoelastic liquid* that has a memory that decays with time.

11.4.1 Maxwell fluid

Let's first look at a simple model of a viscoelastic fluid called a Maxwell fluid. Consider a shear deformation where adjacent layers of the material are shifted in the same direction along the planes relative to each other. The deformation can be described by the strain γ , which is approximately the total relative shift divided by the distance between the two layers assuming the displacement is small.

The shear stress τ for an elastic solid is given by Hooke's law

$$\tau_e = G\gamma_e, \quad (11.35)$$

where G is the shear modulus of the material. For a Newtonian fluid the constitutive law is

$$\tau_v = \mu_p \dot{\gamma}_v, \quad (11.36)$$

where μ_p is the constant Newtonian viscosity. Graphically we could depict these two elements as a spring and a dampner. Depending on how we connect them, we form a viscoelastic fluid or viscoelastic solid.

Combined in series To combine these two relations to describe the total stress in terms of the total deformation we consider the elastic and viscous elements working in series such that the deformation is distributed ($\gamma = \gamma_e + \gamma_v$) but the stress is the same ($\tau = \tau_e = \tau_v$). Initially, the displacement is taken up by the spring and the dampner, but the displacement of the spring can be redistributed onto the dampner, resulting in the absence of stress at long times. Rearranging these equations we obtain

$$\tau + \frac{\mu}{G} \dot{\tau} = \mu \dot{\gamma}. \quad (11.37)$$

This is the constitutive law for a *Maxwell fluid*, which is a viscoelastic fluid.

Combined in parallel Combining these two relations in parallel, the stress is now distributed ($\tau = \tau_e + \tau_v$) but the deformation is the same ($\gamma = \gamma_e = \gamma_v$). In this parallel connection, unlike the previous case, the system remains under stress so long as $\dot{\gamma} \neq 0$. Rearranging these equations we obtain

$$\tau = G\gamma + \mu \dot{\gamma}. \quad (11.38)$$

This is the constitutive law for a *Kelvin-Voigt solid*, which is a viscoelastic solid. In this course, we will be focusing on viscoelastic fluids so we will return to the Maxwell model.

The 1D Maxwell model $\tau + \lambda \dot{\tau} = \mu \dot{\gamma}$, where $\lambda = \mu/G$, can be solved to give

$$\frac{d}{dt} \left(e^{t/\lambda} \tau \right) = \frac{\mu \dot{\gamma}}{\lambda} e^{t/\lambda} \Rightarrow \tau(t) = \frac{\mu}{\lambda} \int_{-\infty}^t \dot{\gamma}(t') e^{-(t-t')/\lambda} dt'. \quad (11.39)$$

The parameter λ is the Maxwell relaxation time. Looking at the expression for the stress response, we see that the stress created by a stepwise deformation relaxes exponentially on a time scale λ (viscous-fluid-like property). Whereas, on short times $\tau(t) \sim \mu \gamma(t)/\lambda$ and the material behaves like a solid. For example, consider the stress response to a periodic deformation with frequency ω , where $\gamma = \gamma_0 \sin(\omega t)$, $\dot{\gamma} = \gamma_0 \omega \cos(\omega t)$. Substituting into the integral expression gives

$$\tau(t) = \frac{\mu \gamma_0 \omega}{\lambda} \int_{-\infty}^t \cos(\omega t') e^{-(t-t')/\lambda} dt' = \mu \gamma_0 \omega \frac{\cos(\omega t) + \lambda \omega \sin(\omega t)}{1 + (\lambda \omega)^2} \quad (11.40)$$

$$= \frac{\mu \dot{\gamma}}{1 + (\lambda \omega)^2} + \frac{G(\lambda \omega)^2 \gamma}{1 + (\lambda \omega)^2} = \tilde{\mu}(\omega) \dot{\gamma} + \tilde{G}(\omega) \gamma, \quad (11.41)$$

where $\tilde{\mu}(\omega)$, $\tilde{G}(\omega)$ are the frequency dependent viscosity and shear modulus. At short times ($\lambda \omega \gg 1$), $\tilde{G} \simeq G$ and the material behaves like a solid. Whereas, at long times ($\lambda \omega \ll 1$), $\tilde{\mu} \simeq \mu$ and the material behaves as a viscous fluid. The crossover between these two behaviors occurs when the time scale of deformation is the same as the time scale of relaxation, $\omega^{-1} \sim \lambda$.

Frame invariant? In three dimensional coordinates, the Maxwell fluid constitutive law can be written as

$$\boldsymbol{\tau} + \frac{\mu}{G} \dot{\boldsymbol{\tau}} = \mu \dot{\boldsymbol{\gamma}}. \quad (11.42)$$

As we saw with the generalised Newtonian fluids above, we require the constitutive law to be frame invariant. However, the time derivative of the stress $\boldsymbol{\tau}$ is not frame invariant. For example, if we move from a stationary lab frame to one moving with constant velocity \mathbf{u}_0 , we have

$$\frac{\partial \tau_{ij}}{\partial t}(\mathbf{x} + \mathbf{u}_0 t) = \frac{\partial \tau_{ij}}{\partial t} + \mathbf{u}_0 \cdot \nabla \tau_{ij}. \quad (11.43)$$

But clearly, adding a constant velocity to the fluid should not result in any additional velocity gradients or additional stresses. Hence, the Maxwell fluid is not frame invariant. This is because the time derivatives of individual components of the stress tensor do not form a tensor themselves. To deal with this, the ordinary time derivative needs to be replaced by another derivative.

11.4.2 Oldroyd B fluid

One version of a frame invariant derivative is the *upper convected derivative* defined as

$$\overset{\nabla}{\boldsymbol{\tau}}_p = \frac{\partial \boldsymbol{\tau}_p}{\partial t} + \mathbf{u} \cdot \nabla \boldsymbol{\tau}_p - (\nabla \mathbf{u})^T \cdot \boldsymbol{\tau}_p - \boldsymbol{\tau}_p \cdot (\nabla \mathbf{u}), \quad (11.44)$$

which transforms as a covariant tensor. N.B. there are other choices for a frame invariant derivative but we will only consider the upper convected derivative during this course. Rewriting the relationship between stress and strain-rate (11.42) using the upper convected derivative gives

$$\boldsymbol{\tau}_p + \frac{\mu_p}{G} \overset{\nabla}{\boldsymbol{\tau}}_p = \mu_p \dot{\boldsymbol{\gamma}} \quad (11.45)$$

to describe the polymeric stress which incorporates both viscous and elastic properties. The relaxation time of the fluid is defined as $\lambda = \mu_p/G$. For a polymeric fluid, there is an additional Newtonian contribution from the solvent viscosity μ_s . Hence, the total deviatoric stress tensor is written as

$$\boldsymbol{\tau} = \mu_s \dot{\boldsymbol{\gamma}} + \boldsymbol{\tau}_p. \quad (11.46)$$

This model is known as the *Oldroyd B model*. In the limit of vanishing deformation rates it describes a Newtonian fluid with viscosity $\mu = \mu_s + \mu_p$.

Oldroyd B Model:

$$\nabla \cdot \mathbf{u} = 0 \quad (11.47)$$

$$\rho \left(\frac{\partial \mathbf{u}}{\partial t} + \mathbf{u} \cdot \nabla \mathbf{u} \right) = \nabla \cdot \mathbf{T} \quad (11.48)$$

$$\mathbf{T} = -p\mathbf{I} + \boldsymbol{\tau} = -p^*\mathbf{I} + \mu_s \dot{\boldsymbol{\gamma}} + G\mathbf{A} \quad (11.49)$$

$$\overset{\nabla}{\mathbf{A}} = \frac{\partial \mathbf{A}}{\partial t} + \mathbf{u} \cdot \nabla \mathbf{A} - (\nabla \mathbf{u})^T \cdot \mathbf{A} - \mathbf{A} \cdot (\nabla \mathbf{u}) = -\frac{1}{\lambda}(\mathbf{A} - \mathbf{I}) \quad (11.50)$$

where

$$p^* = p + \frac{\mu_p}{\lambda}, \quad G = \frac{\mu_p}{\lambda} \quad \text{and} \quad \mathbf{A} = \frac{1}{G} [\boldsymbol{\tau} - \mu_s \dot{\boldsymbol{\gamma}} + G\mathbf{I}]. \quad (11.51)$$

Here, we have rewritten the Oldroyd B model in terms of variable \mathbf{A} ; a symmetric second rank tensor. This form of the model shows that \mathbf{A} tends towards its relaxed state $\mathbf{A} = \mathbf{I}$ at long times governed by long timescale λ at which point the polymer stress $\boldsymbol{\tau}_p$ vanishes. To understand the properties of Oldroyd B fluids let's see how it behaves in some simple fluid flows.

11.4.3 Shear flow

First consider a shear flow of the form

$$\mathbf{u} = (\dot{\gamma}y, 0, 0), \quad (11.52)$$

which only depends on t ($\dot{\gamma} = \dot{\gamma}(t)$) and y so all variables must also only be functions of t and y . By construction this satisfies mass conservation. The momentum equation reduces to

$$\rho \frac{\partial \mathbf{u}}{\partial t} = \nabla \cdot \mathbf{T}, \quad (11.53)$$

where

$$\mathbf{T} = \begin{pmatrix} -p^* & 0 \\ 0 & -p^* \end{pmatrix} + \begin{pmatrix} 0 & \mu_s \dot{\gamma} \\ \mu_s \dot{\gamma} & 0 \end{pmatrix} + G \begin{pmatrix} A_{xx} & A_{xy} \\ A_{xy} & A_{yy} \end{pmatrix}, \quad (11.54)$$

and

$$\frac{\partial}{\partial t} \mathbf{A} - \begin{pmatrix} \dot{\gamma} A_{xy} & \dot{\gamma} A_{yy} \\ 0 & 0 \end{pmatrix} - \begin{pmatrix} \dot{\gamma} A_{xy} & 0 \\ \dot{\gamma} A_{yy} & 0 \end{pmatrix} = -\frac{1}{\lambda} \begin{pmatrix} A_{xx} - 1 & A_{xy} \\ A_{xy} & A_{yy} - 1 \end{pmatrix} \quad (11.55)$$

Steady flow

If the strain rate $\dot{\gamma}$ is constant, the components of \mathbf{A} must also be independent of t . The components then satisfy

$$-2\dot{\gamma} A_{xy} = -\frac{1}{\lambda}(A_{xx} - 1) \quad (11.56)$$

$$-\dot{\gamma} A_{yy} = -\frac{1}{\lambda} A_{xy} \quad (11.57)$$

$$0 = -\frac{1}{\lambda}(A_{yy} - 1) \quad (11.58)$$

$$-\dot{\gamma} A_{yy} = -\frac{1}{\lambda} A_{xy}. \quad (11.59)$$

Hence the total stress is

$$\mathbf{T} = \begin{pmatrix} -p^* + G(1 + 2\lambda^2 \dot{\gamma}^2) & (\mu_s + G\lambda)\dot{\gamma} \\ (\mu_s + G\lambda)\dot{\gamma} & -p^* + G \end{pmatrix}, \quad (11.60)$$

$$= \begin{pmatrix} -p + 2G\lambda^2 \dot{\gamma}^2 & \mu\dot{\gamma} \\ \mu\dot{\gamma} & -p \end{pmatrix} \quad (11.61)$$

Compared with the Newtonian equivalent, adding polymers to the solvent causes the viscosity to increase from μ_s to $\mu = \mu_s + \mu_p$, and there is now a normal stress difference

$$T_{xx} - T_{yy} = 2G\lambda^2 \dot{\gamma}^2. \quad (11.62)$$

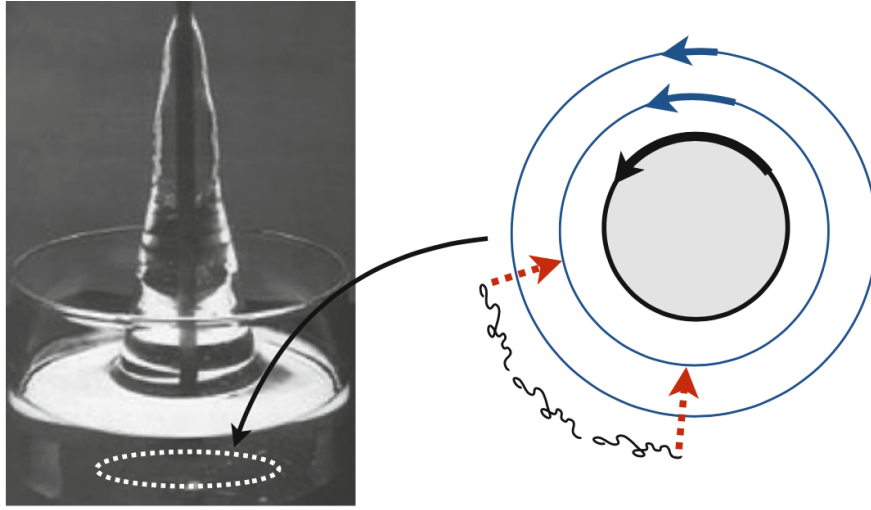


Figure 11.5: Rod climbing experiment. A rod rotates at the centre of a viscoelastic fluid. The normal stresses cause the fluid along streamlines to move inwards, and hence, by mass conservation, are forced to climb the rod. (Adapted from Morozov and Spagnolie, Introduction to Complex fluids.)

This acts in the opposite direction to pressure so is like a tension for stretched polymers along streamlines. This explains the famous rod-climbing experiments, see figure 11.5. A rod in the middle of an Oldroyd B fluid is rotated generating a shear flow in the azimuthal direction. The normal stress difference acts as a tension on the circular streamlines causing them to contract. By mass conservation, the fluid must instead move vertically, hence causing the fluid to climb up the rod.

11.4.4 Extensional flow

Now let's consider a two dimensional extensional flow of the form

$$\mathbf{u} = (\dot{\epsilon}x, -\dot{\epsilon}y), \quad (11.63)$$

where $\dot{\epsilon}$ is constant. Again, this automatically satisfies mass conservation. The strain-rate and stress tensors are

$$\dot{\gamma} = \begin{pmatrix} 2\dot{\epsilon} & 0 \\ 0 & -2\dot{\epsilon} \end{pmatrix} = 2\nabla\mathbf{u} = 2(\nabla\mathbf{u})^T, \quad (11.64)$$

$$\mathbf{T} = \begin{pmatrix} -p^* & 0 \\ 0 & -p^* \end{pmatrix} + \begin{pmatrix} 2\mu_s\dot{\epsilon} & 0 \\ 0 & -2\mu_s\dot{\epsilon} \end{pmatrix} + G \begin{pmatrix} A_{xx} & A_{xy} \\ A_{xy} & A_{yy} \end{pmatrix}. \quad (11.65)$$

with the components A_{ij} satisfying

$$-\dot{\epsilon} \begin{pmatrix} A_{xx} & A_{xy} \\ -A_{xy} & -A_{yy} \end{pmatrix} - \dot{\epsilon} \begin{pmatrix} A_{xx} & -A_{xy} \\ A_{xy} & -A_{yy} \end{pmatrix} = -\frac{1}{\lambda} \begin{pmatrix} A_{xx} - 1 & A_{xy} \\ A_{xy} & A_{yy} - 1 \end{pmatrix}. \quad (11.66)$$

Rearranging, we find

$$A_{xx} = \frac{1}{1 - 2\lambda\dot{\epsilon}}, \quad A_{xy} = 0, \quad A_{yy} = \frac{1}{1 + 2\lambda\dot{\epsilon}}. \quad (11.67)$$

The total stress is then

$$\mathbf{T} = \begin{pmatrix} -p^* + \frac{G}{1 - 4\lambda^2\dot{\epsilon}^2} + 2\mu_{ext}\dot{\epsilon} & 0 \\ 0 & -p^* + \frac{G}{1 - 4\lambda^2\dot{\epsilon}^2} - 2\mu_{ext}\dot{\epsilon} \end{pmatrix}, \quad (11.68)$$

where

$$\mu_{ext} = \mu_s + \frac{\lambda G}{1 - 4\lambda^2\dot{\epsilon}^2} = \mu_s + \frac{\mu_p}{1 - 4\lambda^2\dot{\epsilon}^2} \quad (11.69)$$

If we plot this viscosity as a function of the strain rate $\dot{\epsilon}$ (figure 11.6) we see that initially the viscosity increases (hence thickens, or strain hardens). But when $\dot{\epsilon} = 1/2\lambda$ the viscosity diverges and then is negative for larger values. This result is clearly unphysical. This happens because the Oldroyd B model is derived using Hooke's law which is infinitely extensible. To get around this a modification, a nonlinear spring law must be used.

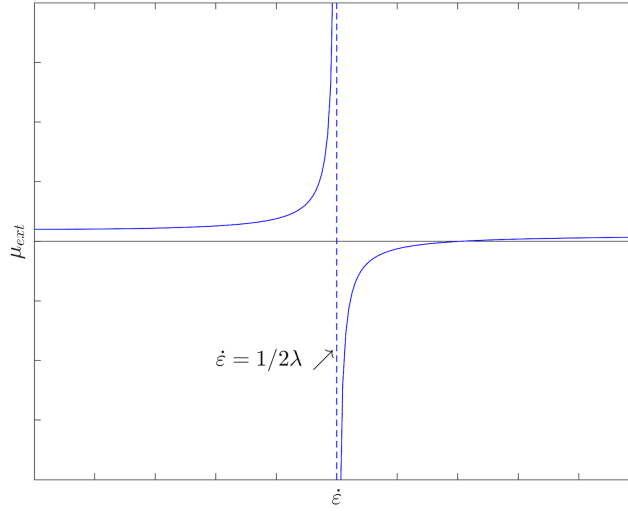


Figure 11.6: Plot of extensional viscosity for an Oldroyd B fluid against strain rate $\dot{\epsilon}$. At $\dot{\epsilon} = 1/2\lambda$ the viscosity diverges and is negative for larger values.

11.4.5 Weakly non-linear viscoelastic fluids

A weakly non-linear flow is a situation wherein the flow changes on time scales much longer than the relaxation time, λ , and therefore λ is in some sense small and can be used as an expansion parameter. It is generally a bad practice to perform a Taylor expansion in a dimensional variable; a better expansion parameter might be λ/T_0 , where T_0 is the typical time scale set by the flow.

From the Oldroyd B model we have

$$\boldsymbol{\tau} + \lambda \overset{\nabla}{\boldsymbol{\tau}} = \mu \left(\dot{\boldsymbol{\gamma}} + \lambda \frac{\mu_s}{\mu} \overset{\nabla}{\dot{\boldsymbol{\gamma}}} \right), \quad (11.70)$$

where $\mu = \mu_s + \mu_p$. Let P be a characteristic pressure scale, L a characteristic length scale, L/T_0 a characteristic velocity scale. The non-dimensional version of equation (11.70) is

$$\boldsymbol{\tau} + \epsilon \overset{\nabla}{\boldsymbol{\tau}} = \frac{\mu}{PT_0} \left(\dot{\boldsymbol{\gamma}} + \epsilon \frac{\mu_s}{\mu} \overset{\nabla}{\dot{\boldsymbol{\gamma}}} \right), \quad (11.71)$$

where $\epsilon = \lambda/T_0$. Expanding in this parameter, we may write

$$\boldsymbol{\tau} = \boldsymbol{\tau}^{(0)} + \epsilon \boldsymbol{\tau}^{(1)} + O(\epsilon^2). \quad (11.72)$$

Substituting this into the Oldroyd B model, we recover a Newtonian constitutive law to leading order,

$$\boldsymbol{\tau}^{(0)} = \frac{\mu}{PT_0} \dot{\boldsymbol{\gamma}}, \quad \text{and} \quad \boldsymbol{\tau}^{(1)} = -\overset{\nabla}{\boldsymbol{\tau}}^{(0)} + \frac{\mu_s}{PT_0} \overset{\nabla}{\dot{\boldsymbol{\gamma}}} = -\frac{\mu_p}{PT_0} \overset{\nabla}{\dot{\boldsymbol{\gamma}}}. \quad (11.73)$$

Putting the dimensions back in, we have

$$\boldsymbol{\tau} = \mu \dot{\boldsymbol{\gamma}} - \lambda \mu_p \overset{\nabla}{\dot{\boldsymbol{\gamma}}}. \quad (11.74)$$

This is an example of a *second-order fluid*.

Second-order fluid: The simplest class of equations for viscoelastic solutions involves the expression of the stress tensor as a sum of all admissible combinations of the velocity gradient tensor. Depending on the highest algebraic power of the velocity gradient tensor involved, they are called the *second-order fluid*, *third-order fluid*, etc. For example, the deviatoric stress of the second-order fluid is given by

$$\boldsymbol{\tau} = \mu \dot{\boldsymbol{\gamma}} + b_2 \overset{\nabla}{\dot{\boldsymbol{\gamma}}} + b_{11} \dot{\boldsymbol{\gamma}} \cdot \dot{\boldsymbol{\gamma}}, \quad (11.75)$$

where b_2, b_{11} are material constants.

Returning back to our Oldroyd B model, the weakly non-linear expansion is a second-order fluid with material parameters $b_2 = -\lambda \mu_p$, $b_{11} = 0$.

11.4.6 Rod climbing for a second-order fluid

For an Oldroyd B fluid we showed that there is a normal stress difference in a shear flow. In this section we will determine the steady free surface of a weakly non-linear second-order fluid caused by a rod of radius $r = a$ rotating at a frequency Ω in the fluid. Flow is purely in the azimuthal direction so we write $\mathbf{u} = (0, v(r), 0)$ in cylindrical polars.

The flow is weakly non-linear so to leading order, the fluid behaves like a Newtonian fluid where $\dot{\gamma}_{r\theta}$ is the only non-zero strain-rate component. In terms of the deviatoric stress components, taking P to be a characteristic stress scale, $\tau_{r\theta}(r) \sim O(P)$ and $\tau_{rr}(r), \tau_{\theta\theta}(r) \sim O(\epsilon P)$ with pressure $p(r, z) \sim O(P)$. The leading order momentum equations give

$$0 = \frac{\partial}{\partial r} (T_{r\theta}) + \frac{2}{r} T_{r\theta} = \frac{1}{r^2} \frac{\partial}{\partial r} (r^2 T_{r\theta}), \quad 0 = \frac{\partial T_{zz}}{\partial z} - \rho g. \quad (11.76)$$

We can use these to solve for the azimuthal component of the velocity. The leading order r-momentum equation gives $\partial p / \partial r = 0$. The r-momentum equation at order $O(\lambda/T_0)$ can be used to calculate the higher order components of the stress

$$0 = \frac{\partial T_{rr}}{\partial r} + \frac{T_{rr} - T_{\theta\theta}}{r}. \quad (11.77)$$

For the leading order balance, the fluid has a Newtonian constitutive law:

$$\dot{\gamma}_{r\theta} = r \frac{d}{dr} \left(\frac{v}{r} \right), \quad T_{r\theta} = \mu \dot{\gamma}_{r\theta} \quad \Rightarrow \quad T_{r\theta} = \frac{A}{r^2} = \frac{d}{dr} \left(\frac{v}{r} \right) \quad (11.78)$$

Integrating and applying boundary conditions $v(a) = \Omega a$, $v \rightarrow 0$ as $r \rightarrow \infty$, gives

$$v = \frac{\Omega a^2}{r}, \quad \dot{\gamma}_{r\theta} = r \frac{d}{dr} \left(\frac{v}{r} \right) = -\frac{2\Omega a^2}{r^2}. \quad (11.79)$$

The vertical component of the Stokes equation gives a hydrostatic balance

$$0 = \frac{\partial T_{zz}}{\partial z} - \rho g \quad \Rightarrow \quad p = \rho g (h(r) - z). \quad (11.80)$$

We now consider the second-order contribution to the stress. Using the second-order fluid model, we have

$$T_{r\theta} = \mu \dot{\gamma}_{r\theta}, \quad T_{rr} = -p + b_{11} \dot{\gamma}_{r\theta}^2, \quad T_{\theta\theta} = -p - 2b_2 \dot{\gamma}_{r\theta}^2 + b_{11} \dot{\gamma}_{r\theta}^2, \quad T_{zz} = -p. \quad (11.81)$$

since $(\overset{\nabla}{\dot{\gamma}})_{rr} = 0$, $(\overset{\nabla}{\dot{\gamma}})_{\theta\theta} = -2\dot{\gamma}_{r\theta}^2$. Substituting into the r-momentum balance gives

$$\frac{\partial T_{rr}}{\partial r} + \frac{2b_2 \dot{\gamma}_{r\theta}^2}{r} = 0 \quad \Rightarrow \quad -p + b_{11} \dot{\gamma}_{r\theta}^2 = \frac{b_2}{2} \dot{\gamma}_{r\theta}^2 + f(z) \quad (11.82)$$

$$- \rho g (h(r) - z) + (b_{11} - b_2/2) \dot{\gamma}_{r\theta}^2 = f(z). \quad (11.83)$$

Choosing $f(z) = \rho g z$, we arrive at

$$h(r) = \frac{1}{\rho g} \left(b_{11} - \frac{b_2}{2} \right) \dot{\gamma}_{r\theta}^2. \quad (11.84)$$

Referring back to the material parameters for the Oldroyd B model, we see the surface has height

$$h(r) = \frac{2\lambda\mu_p\Omega^2 a^4}{\rho g r^4}. \quad (11.85)$$

Hence, for an Oldroyd B model, rod climbing occurs.

11.4.7 Words of caution

1. The linear Maxwell model is not objective

The model is not frame invariant so none of the conclusions drawn from studying the model can be guaranteed to be physical.

2. Time-dependent flows in weakly non-linear viscoelastic fluids are unstable

Consider the second-order fluid model

$$\boldsymbol{\tau} = \mu \dot{\boldsymbol{\gamma}} + b_2 \overset{\nabla}{\dot{\boldsymbol{\gamma}}} + b_{11} \dot{\boldsymbol{\gamma}} \cdot \dot{\boldsymbol{\gamma}} \quad (11.86)$$

in a two-dimensional shear flow $\mathbf{u} = (u(y, t), 0)$ in a channel $0 \leq y \leq h$. From momentum balance we have

$$\rho \frac{\partial u}{\partial t} = \frac{\partial T_{xy}}{\partial y} \equiv \frac{\partial \tau_{xy}}{\partial y}. \quad (11.87)$$

From the constitutive law, the deviatoric stress τ_{xy} is

$$\tau_{xy} = \mu \frac{\partial u}{\partial y} + b_2 \frac{\partial}{\partial t} \frac{\partial u}{\partial y}. \quad (11.88)$$

These two can be combined to give

$$\rho \frac{\partial u}{\partial t} = \mu \frac{\partial^2 u}{\partial y^2} + b_2 \frac{\partial}{\partial t} \frac{\partial^2 u}{\partial y^2}. \quad (11.89)$$

Taking no-slip boundary conditions at the walls of a channel located at $y = 0$ and $y = h$, we write the flow velocity as a Fourier sine series:

$$u(y, t) = \sum_{m=1}^{\infty} u_m e^{\alpha_m t} \sin\left(\frac{m\pi y}{h}\right). \quad (11.90)$$

Substituting this into the above equation and rearranging, we find growth rates α_m

$$\alpha_m = -\frac{\mu}{b_2 + \frac{\rho h^2}{(m\pi)^2}}. \quad (11.91)$$

For polymer solutions b_2 is typically negative (recall its value based on the Oldroyd B model, $b_2 = -\lambda\mu_p$), so that α_m is positive for sufficiently large m . This implies that a steady shear flow of a second-order fluid is unstable to short-wavelength perturbations and cannot be realized. In the case of negligible inertia, achieved in the above by setting $\rho = 0$, this predicts that all Fourier modes are unstable. The implications of this result are profound: it shows that an approximation of slow flows, or, in other words, Taylor expansions of the stress in terms of the relaxation time cannot be used in time-dependent flows where any shear component would result locally in a linear instability and exponential growth of the stress. Hence, the second-order fluid and similar approximations should generally not be used to study time-dependent flows!

Chapter 12

Hydrodynamic Instability

Many steady lamina flows at high $Re \gg 1$ are unstable - they can often break down into turbulent-time-dependent flows with many spatial scales. The idea is to start with a steady base flow and add small perturbations. We will then look to see if these perturbations grow or decay. We will focus on linearised perturbations so ignore non-linear terms such as quadratic and higher orders. This is called a *linear stability analysis*. In particular, in this chapter we will consider two instabilities: the Kelvin-Helmholtz instability and the Rayleigh-Plateau instability. Low $Re \ll 1$ can also be unstable. We will show this by considering the viscous analogue of the Rayleigh-Plateau instability.

12.1 The Kelvin-Helmholtz Instability

In this section we consider the Kelvin-Helmholtz instability of plane-parallel shear flow. It is this instability that is responsible for patterns observed in clouds when two air volumes move past each other with different horizontal velocities, see figure 12.1.

Base state

Let's consider a plane-parallel shear flow with a velocity profile that has a tangential discontinuity:

$$\mathbf{u} = (U_1, 0) \quad \text{for } y > 0 \quad \text{and} \quad \mathbf{u} = (U_2, 0) \quad \text{for } y < 0, \quad (12.1)$$

see figure 12.2. We will ignore the thin viscous boundary layer which smoothes out the velocity discontinuity. The base state is a stationary solution of Euler's equation.

Perturbed state

We set up a perturbation to the system by perturbing the interface between the two layers. We are ignoring viscosity so the flow is inviscid. The initial condition is irrotational so the flow must be irrotational for all time. Hence, the perturbations will be of the form $\hat{\mathbf{u}} = \nabla\phi$ for potential flow:

$$\mathbf{u} = (U_1, 0) + \nabla\phi_1 \quad \text{for } y > \eta \quad \text{and} \quad \mathbf{u} = (U_2, 0) + \nabla\phi_2 \quad \text{for } y < \eta, \quad (12.2)$$

where $\eta(x, t)$ is the perturbed interface and the perturbed pressure is $p = p_0 + p_1$ for $y > \eta$ and $p = p_0 + p_2$ for



Figure 12.1: (a) Kelvin-Helmholtz instability marked by a cloud located at the interface of two air volumes moving with different horizontal velocities.

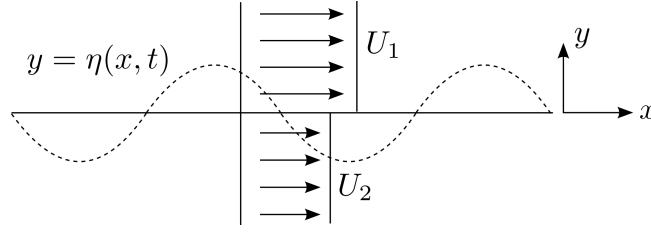


Figure 12.2: Sketch of a shear flow with a perturbation at the interface.

$y < \eta$. From mass conservation $\nabla \cdot \mathbf{u} = 0$ we have

$$\nabla^2 \phi_1 = 0 \quad \text{for } y > \eta \quad \text{and} \quad \nabla^2 \phi_2 = 0 \quad \text{for } y < \eta \quad (12.3)$$

There are boundary conditions at the interface and at infinity. At infinity we have the perturbations decaying and the pressure tending to a constant p_0 . Hence

$$\phi_1, \phi_2 \rightarrow 0 \quad \text{and} \quad p \rightarrow p_0 \quad \text{as } y \rightarrow \pm\infty. \quad (12.4)$$

At the interface we have kinematic and dynamic boundary conditions. Our kinematic boundary condition states that $y = \eta(x, t)$ remains a material surface, i.e. $D_t(\eta - y) = 0$:

$$\frac{\partial}{\partial t}(\eta - y) + (\mathbf{u} \cdot \nabla)(\eta - y) = 0 \quad (12.5)$$

$$\frac{\partial \eta}{\partial t} + \left(U + \frac{\partial \phi}{\partial x} \right) \frac{\partial \eta}{\partial x} - \frac{\partial \phi}{\partial y} = 0 \quad (12.6)$$

$$\frac{\partial \eta}{\partial t} + U \frac{\partial \eta}{\partial x} - \frac{\partial \phi}{\partial y} = 0 \quad \text{at } y = \eta, \quad (12.7)$$

where we have only kept terms linear in the perturbation variables. To simplify the boundary condition further we expand about the interface $y = \eta$ using Taylor series

$$\frac{\partial \phi}{\partial y} \Big|_{y=\eta} = \frac{\partial \phi}{\partial y} \Big|_{y=0} + \eta \frac{\partial^2 \phi}{\partial y^2} \Big|_{y=0} + \frac{1}{2} \eta^2 \frac{\partial^3 \phi}{\partial y^3} \Big|_{y=0} + \dots \quad (12.8)$$

We can ignore all but the first term as the others are quadratic or higher order. The two boundary conditions are then

$$\frac{\partial \eta}{\partial t} + U_1 \frac{\partial \eta}{\partial x} = \frac{\partial \phi_1}{\partial y} \Big|_{y=0^+} \quad (12.9)$$

$$\frac{\partial \eta}{\partial t} + U_2 \frac{\partial \eta}{\partial x} = \frac{\partial \phi_2}{\partial y} \Big|_{y=0^-}. \quad (12.10)$$

N.B. because of the discontinuity in the base state, the perturbation to the vertical velocity $\partial \phi / \partial y$ is not continuous at $y = 0$. The dynamic boundary condition for an inviscid flow gives that the pressure must be continuous at $y = \eta$, i.e. $p_1 = p_2$. To obtain the pressure at the interface we apply Bernoulli's equation for a time-dependent irrotational flow:

$$\rho \frac{\partial \phi}{\partial t} + \frac{1}{2} \rho |\mathbf{u}|^2 + p + \rho g y = f(t) \quad \text{at } y = \eta, \quad (12.11)$$

where $|\mathbf{u}|^2 = U^2 + 2U \partial \phi / \partial x + |\nabla \phi|^2$. After expanding about the interface $y = \eta$ using Taylor series, Bernoulli's equation gives

$$\frac{\partial \phi_1}{\partial t} + U_1 \frac{\partial \phi_1}{\partial x} = \frac{\partial \phi_2}{\partial t} + U_2 \frac{\partial \phi_2}{\partial x}. \quad (12.12)$$

N.B. we have assumed the density of the two layers is the same, $\rho_1 = \rho_2 = \rho$, we have taken $f(t) = \frac{1}{2} U_{1,2}^2 + p_0$ from the far field conditions, and we have ignored the influence of gravity.

The governing equations involve $\partial / \partial x$, $\partial / \partial t$ and no special values of x , t (unlike $\partial / \partial y$ with special value $y = 0$), so we can Fourier transform in x , t and look for perturbations of the form

$$e^{ikx + \sigma t}, \quad (12.13)$$

with wavenumber k (wavelength $2\pi/k$) and growth rate σ , which might be complex. $Re(\sigma) > 0$ gives growth and $Im(\sigma)$ gives propagation. Let the interface be of the form

$$\eta(x, t) = Ae^{ikx+\sigma t}, \quad (12.14)$$

with A constant, and velocity potentials

$$\phi_1 = \hat{\phi}_1(y)e^{ikx+\sigma t}, \quad \phi_2 = \hat{\phi}_2(y)e^{ikx+\sigma t}. \quad (12.15)$$

Substituting this form into Laplace's equation gives

$$\nabla^2 \phi = 0 \quad \Rightarrow \quad -k^2 \hat{\phi} e^{ikx+\sigma t} + \frac{\partial^2 \hat{\phi}}{\partial y^2} e^{ikx+\sigma t} = 0 \quad \Rightarrow \quad \hat{\phi} = e^{\pm ky}. \quad (12.16)$$

Applying boundary conditions at $\pm\infty$, the velocity potentials are then

$$\phi_1 = Be^{ikx+\sigma t} e^{-ky} \quad \text{for } y > \eta \quad \text{and} \quad \phi_2 = Ce^{ikx+\sigma t} e^{ky} \quad \text{for } y < \eta. \quad (12.17)$$

Using kinematic conditions (12.9-12.10) and dynamic boundary condition (12.12) we have three equations involving A , B , C and σ as a function of the wavenumber k :

$$(\sigma + ikU_1)A = -kB \quad (12.18)$$

$$(\sigma + ikU_2)A = kC \quad (12.19)$$

$$(\sigma + ikU_1)B = (\sigma + ikU_2)C \quad (12.20)$$

$$\Rightarrow \quad \sigma = -\frac{ik(U_1 + U_2)}{2} \pm \frac{k(U_1 - U_2)}{2}. \quad (12.21)$$

Hence, the disturbance varies as

$$\underbrace{e^{ik[x - \frac{1}{2}(U_1 + U_2)t]}}_{(1)} \underbrace{e^{\pm \frac{k}{2}(U_1 - U_2)t}}_{(2)}, \quad (12.22)$$

1. disturbance propagates at the average velocity
2. decaying and growing mode \Rightarrow flow is unstable because there is some growing disturbance

12.2 The Rayleigh-Plateau Instability

In this section we consider the Rayleigh-Plateau instability of a cylinder of inviscid fluid bounded by surface tension. It is this instability that is responsible for the break up of a water thread falling from a kitchen tap, see figure 12.3.

Base state

For the equilibrium base state we have an infinitely long quiescent ($\mathbf{u} = (u_r, u_\theta, u_z) = (0, 0, 0)$) inviscid cylinder of radius of R_0 , density ρ and surface tension γ , see figure 12.3. For simplicity we will ignore the influence of gravity. The pressure in the cylinder is constant given by p_0 . The kinematic boundary condition at the free surface $f = r - R_0 = 0$, $\mathbf{n} = (1, 0, 0)$, is

$$D_t f = (\partial_t + (\mathbf{u} \cdot \nabla)) f(\mathbf{x}, t) = 0 \quad \Rightarrow \quad \partial_t(R_0) = 0 \quad \Rightarrow \quad R_0 = \text{const} \quad (12.23)$$

and the dynamic boundary condition is

$$[\mathbf{T} \cdot \mathbf{n}]_+^+ = \gamma (\nabla \cdot \mathbf{n}) \mathbf{n} \quad \Rightarrow \quad p_0 \mathbf{n} = \frac{\gamma}{R_0} \mathbf{n} \quad \Rightarrow \quad p_0 = \frac{\gamma}{R_0}, \quad (12.24)$$

where $(\nabla \cdot \mathbf{n}) = 1/r$.

Perturbed state

We consider small axisymmetric perturbations to the cylinder of the form

$$R = R_0 + \epsilon \tilde{R} e^{\sigma t + ikz}, \quad (12.25)$$

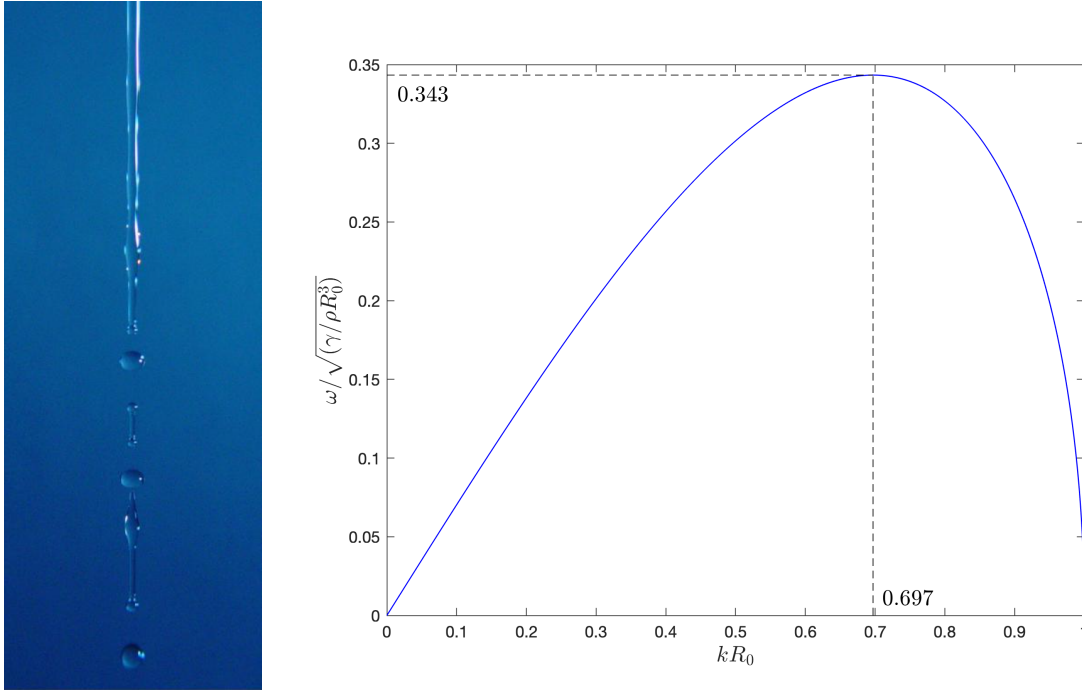


Figure 12.3: (a) Surface tension instability of an inviscid thread falling under gravity. (b) Plot of growth rate $\sigma/\sqrt{(\gamma/\rho R_0^3)}$ against wavenumber kR_0 .

where σ is the growth rate of the instability, and k is the wavenumber along the cylinder (z -direction) and the amplitude $\epsilon \ll R_0$. In addition, we write perturbations to the velocities and pressure in the form

$$(u_r, u_z, p) = (0, 0, p_0) + \epsilon(\tilde{u}_r(r), \tilde{u}_z(r), \tilde{p}(r))e^{\sigma t + ikz}, \quad (12.26)$$

Because the perturbation is small relative to the base state, the governing equations can be linearised. Substituting these perturbation fields into the conservation of momentum equations and only keeping terms of $O(\epsilon)$ we have

$$\rho \frac{\partial u_r}{\partial t} = -\frac{\partial p}{\partial r}, \quad (12.27)$$

$$\rho \frac{\partial u_z}{\partial t} = -\frac{\partial p}{\partial z}, \quad (12.28)$$

where we have neglected non-linear terms $\mathbf{u} \cdot \nabla \mathbf{u} \sim O(\epsilon^2)$. N.B. for an inviscid cylinder $\mu = 0$. In a similar manner, mass conservation gives

$$\frac{1}{r} \frac{\partial}{\partial r} (u_r r) + \frac{\partial u_z}{\partial z} = 0. \quad (12.29)$$

Substituting the form of the perturbation (12.26) into these equations gives a set of coupled ODEs for $(\tilde{u}_r, \tilde{u}_z, \tilde{p})$

$$\rho \sigma \tilde{u}_r = -\frac{d\tilde{p}}{dr} \quad (12.30)$$

$$\rho \sigma \tilde{u}_z = -ik\tilde{p} \quad (12.31)$$

$$\frac{d\tilde{u}_r}{dr} + \frac{\tilde{u}_r}{r} + ik\tilde{u}_z = 0. \quad (12.32)$$

Rearranging these equations gives a second order ODE for \tilde{u}_r :

$$r^2 \frac{d^2 \tilde{u}_r}{dr^2} + r \frac{d\tilde{u}_r}{dr} - (1 + (kr)^2) \tilde{u}_r = 0. \quad (12.33)$$

This corresponds to the modified Bessel Equation of order 1, whose solutions may be written in terms of the modified Bessel functions of the first and second kind, respectively, $I_1(kr)$ and $K_1(kr)$.

A quick note on *modified Bessel functions*. $I_\alpha(x)$ and $K_\alpha(x)$ are the two linearly independent solutions to the modified Bessel's equation

$$x^2 \frac{d^2 y}{dx^2} + x \frac{dy}{dx} - (x^2 + \alpha^2)y = 0. \quad (12.34)$$

I_α and K_α are exponentially growing and decaying functions, respectively, with properties $I_\alpha(x), K_\alpha(x) > 0$ for $x > 0$, $I_\alpha \rightarrow 0$ as $x \rightarrow 0$ for $\alpha > 0$ and $K_\alpha \rightarrow \infty$ diverges as $x \rightarrow 0$. I_α also has the property that $I'_0(x) = I_1(x)$ and $(xI_1(x))' = xI_0(x)$.

Since we want a well-behaved solution at $r = 0$ we have

$$\tilde{u}_r = AI_1(kr), \quad (12.35)$$

where A is a constant to be determined using boundary conditions. Using the properties of the modified Bessel functions as stated above, we can also write

$$\tilde{p} = -\frac{A\rho\sigma}{k}I_0(kr) \quad \text{and} \quad \tilde{u}_z = -\frac{ik}{\rho\sigma}\tilde{p}. \quad (12.36)$$

We can now apply the kinematic and dynamic boundary conditions to the perturbed system. The linearised kinematic boundary condition gives

$$u_r|_{r=R_0} = R_t \quad \Rightarrow \quad A = \frac{\tilde{R}\sigma}{I_1(kR_0)}. \quad (12.37)$$

Similarly, for the linearised dynamic boundary condition

$$\hat{\mathbf{n}} = \frac{\nabla(r-R)}{|\nabla(r-R)|} \simeq (1, 0, -\epsilon\tilde{R}ike^{\sigma t+ikz}) \quad \Rightarrow \quad \nabla \cdot \hat{\mathbf{n}}|_{r=R_0} \simeq \frac{1}{R_0} - \frac{\epsilon\tilde{R}}{R_0^2}(1-k^2R_0^2)e^{\sigma t+ikz} \quad (12.38)$$

$$p_0 + \epsilon\tilde{p}|_{r=R_0}e^{\sigma t+ikz} = \gamma \left(\frac{1}{R_0} - \frac{\epsilon\tilde{R}}{R_0^2}(1-k^2R_0^2)e^{\sigma t+ikz} \right) \quad \Rightarrow \quad \tilde{p}|_{r=R_0} = -\frac{\tilde{R}\gamma}{R_0^2}(1-k^2R_0^2). \quad (12.39)$$

Substituting in the solution for the perturbed pressure gives a *dispersion relation* for the growth rate σ :

$$\sigma^2 = \frac{k\gamma}{\rho R_0^2} \frac{I_1(kR_0)}{I_0(kR_0)} (1-k^2R_0^2) = \frac{kR_0\gamma}{\rho R_0^3} \frac{I_1(kR_0)}{I_0(kR_0)} (1-k^2R_0^2) \quad (12.40)$$

For the perturbation to grow we require the growth rate to be real (and positive). This is only the case when $kR_0 < 1$, since $I_1(kR_0), I_0(kR_0) > 0$. Hence, the cylinder needs to be thinner than $1/k$ for the mode with wavenumber k to be unstable. In other words, the cylinder is unstable to disturbances whose wavelengths exceed the circumference of the cylinder. There exists a maximum growth rate in the interval $0 < kR_0 < 1$, see figure 12.3. Numerically, we find this occurs when

$$kR_0 \simeq 0.697, \quad \lambda_{max} \simeq 9.02R_0, \quad (12.41)$$

where λ_{max} is the corresponding wavelength that grows most quickly. This corresponds to a timescale of breakup of

$$t \sim \frac{1}{\sigma_{max}} \simeq 2.91 \sqrt{\frac{\rho R_0^3}{\gamma}}. \quad (12.42)$$

12.3 The Rayleigh Instability

In this section we consider the Rayleigh instability of a cylinder of viscous fluid bounded by surface tension.

Base state

The base state is the same as in the inviscid case, with an infinitely long quiescent cylinder ($\mathbf{u} = (u_r, u_\theta, u_z) = (0, 0, 0)$) of constant radius R_0 , density ρ , viscosity μ , surface tension γ and pressure $p_0 = \gamma/R_0$.

Perturbed state

We consider small axisymmetric perturbations to the cylinder of the form

$$R = R_0 + \epsilon\tilde{R}e^{\sigma t+ikz}, \quad (12.43)$$

where σ is the growth rate of the instability, and k is the wavenumber along the cylinder (z -direction) and the amplitude $\epsilon \ll R_0$. In addition, we write perturbations to the velocities and pressure in the form

$$(u_r, u_z, p) = (0, 0, p_0) + \epsilon(\tilde{u}_r(r), \tilde{u}_z(r), \tilde{p}(r))e^{\sigma t + ikz}. \quad (12.44)$$

The kinematic condition gives $\tilde{u}_r|_{r=R_0} = \sigma \tilde{R}$, with curvature

$$\nabla \cdot \hat{\mathbf{n}}|_{r=R_0} \simeq \frac{1}{R_0} - \frac{\epsilon \tilde{R}}{R_0^2}(1 - k^2 R_0^2)e^{\sigma t + ikz}. \quad (12.45)$$

Looking at final term in the curvature, we can see that the thread is stabilised by axial curvature, and destabilised by azimuthal curvature. Balancing these two terms shows that the system is unstable to long wavelengths $k^2 R_0^2 < 1$. From the dynamic boundary condition we have a balance of tangential and normal stress at the interface. For the tangential stress $[\mathbf{n} \times \mathbf{T} \cdot \mathbf{n}]_{\pm}^{\pm} = \mathbf{0}$ we get

$$\frac{\partial u_r}{\partial z} + \frac{\partial u_z}{\partial r} = 0 \quad \Rightarrow \quad ik\tilde{u}_r + \frac{d\tilde{u}_z}{dr}, \quad (12.46)$$

on $r = R_0$. For the normal stress $[\mathbf{n} \cdot \mathbf{T} \cdot \mathbf{n}]_{\pm}^{\pm} = \gamma(\nabla \cdot \mathbf{n})$ we get

$$-p + 2\mu \frac{\partial u_r}{\partial r} = \gamma(\nabla \cdot \mathbf{n}) \quad \Rightarrow \quad -\tilde{p} + 2\mu \frac{\partial \tilde{u}_r}{\partial r} = \frac{\gamma \tilde{R}}{R_0^2}(1 - k^2 R_0^2) \quad (12.47)$$

on $r = R_0$.

Governing equations

To solve for the Stokes flow inside the cylinder we want axisymmetric harmonic functions $\propto e^{ikz}$. Using the Papkovitch-Neuber representation, we write harmonic functions

$$\chi = \hat{\chi}(r)e^{ikz + \sigma t}, \quad \Phi = \hat{\Phi}e^{ikz + \sigma t} = (\hat{\Phi}_r(r), 0, \hat{\Phi}_z(r))e^{ikz + \sigma t}. \quad (12.48)$$

$$\nabla^2 \chi = 0 \quad \Rightarrow \quad r^2 \frac{d^2 \hat{\chi}}{dr^2} + r \frac{d\hat{\chi}}{dr} - k^2 r^2 \hat{\chi} = 0. \quad (12.49)$$

You will recognise this as the modified Bessel's Equation of order 0. We want the solution to be well-behaved at $r = 0$ so $\hat{\chi}/2\mu = AI_0(kr)$. Similarly, we have

$$\nabla^2 \Phi = \mathbf{0} \quad \Rightarrow \quad \nabla^2(\hat{\Phi}_r e^{ikz + \sigma t}) - \hat{\Phi}_r e^{ikz + \sigma t}/r^2 = 0, \quad \nabla^2(\hat{\Phi}_z e^{ikz + \sigma t}) = 0. \quad (12.50)$$

Therefore, we have $\hat{\Phi}_r/2\mu = BI_1(kr)$ and $\hat{\Phi}_z/2\mu = BI_0(kr)$. We set $C = 0$ otherwise $\nabla(\mathbf{x} \cdot \Phi)$ has a term $\propto z$. Substituting into the PN representation we have

$$2\mu \mathbf{u} = \nabla(\mathbf{x} \cdot \Phi + \chi) - 2\Phi \quad (12.51)$$

$$= \nabla(r\hat{\Phi}_r e^{ikz + \sigma t} + \hat{\chi}e^{ikz + \sigma t}) - 2\Phi e^{ikz + \sigma t} \quad (12.52)$$

$$2\mu \tilde{u}_r = (r\hat{\Phi}_r + \hat{\chi})' - 2\hat{\Phi}_r \quad (12.53)$$

$$\tilde{u}_r = [BrI_1(kr) + AI_0(kr)]' - 2BI_1(kr) \quad (12.54)$$

$$= AkI_1(kr) + BkrI_0(kr) - 2BI_1(kr) \quad (12.55)$$

$$2\mu \tilde{u}_z = (r\hat{\Phi}_r + \hat{\chi})ik \quad (12.56)$$

$$\tilde{u}_z = (BrI_1(kr) + AI_0(kr))ik, \quad (12.57)$$

together with the pressure

$$p = \nabla \cdot \Phi \quad \Rightarrow \quad \tilde{p} = \frac{1}{r} \frac{d}{dr} (r\hat{\Phi}_r) = \frac{2\mu B}{r} (rI_1(kr))' = 2\mu BI_0(kr), \quad (12.58)$$

where we have used properties $I_0'(x) = I_1(x)$ and $(xI_1(x))' = xI_0(x)$. Substituting the form of the pressure, radial and vertical velocity into the kinematic, and dynamic boundary conditions (tangential and normal stress balance) gives dispersion relation

$$\sigma = \frac{\gamma}{2\mu R_0}(1 - k^2 R_0^2) \frac{[I_1(kR_0)]^2}{k^2 R_0^2 [I_0(kR_0)]^2 - (1 + k^2 R_0^2) [I_1(kR_0)]^2} \quad (12.59)$$

(Lord Rayleigh, 1892). Expanding around $x = 0$ ($I_0(x) \sim 1 - x^2/4$, $I_1(x) \sim x/2 + x^3/16$), we see that the most unstable disturbance is at $k = 0$, where $\sigma = \gamma/6\mu R_0$, infinite wavelength since this minimises the internal deformation. From the form of the dispersion relation we can see that the viscosity does not influence which wavelengths will be unstable, only acts to change the magnitude of the growth rate.

To understand when inertia can be neglected we will go through a scaling argument. To do so we will consider $kR_0 = O(1)$ so the wavelength scales like the radius of the cylinder and there is only one length scale in the problem. Taking velocity scale U , lengthscale R_0 and timescale $1/\sigma$, we have

$$\frac{\mu U}{R_0} \sim p \sim \frac{\gamma}{R_0}, U \sim R_0 \sigma, \sigma \sim \frac{\gamma}{\mu R_0}. \quad (12.60)$$

Balancing terms in Navier-Stokes equations, we can neglect inertia provided

$$\frac{\rho U}{T} \ll \frac{\mu U}{R_0^2} \quad \Rightarrow \quad \frac{\rho \gamma R_0}{\mu^2} \ll 1. \quad (12.61)$$

From this, we can define Ohnesorge number $Oh = \mu/\sqrt{\rho\gamma R_0}$ that relates viscous forces to inertial and surface forces. For low Oh (inertial), the time scale of breakup is $t_{breakup} \sim (\rho R_0^3/\gamma)^{1/2}$. At high Oh (viscous), the time scale of breakup is $t_{breakup} \sim \mu R_0/\gamma$.

Chapter 13

Linear waves and instabilities

13.1 Interfacial waves and instabilities

This chapter presents a unified treatment of gravity-capillary wave, Rayleigh-Taylor instability and Kelvin-Helmholtz instability.

Consider an infinitely deep pool of static water below an infinite atmosphere of air, with the wind blowing at speed U . (Here water and air should be considered merely as labels for the two fluids; the analysis applies equally well to any two immiscible fluids.) Gravity g acts along the negative y -axis of the two-dimensional Cartesian coordinate system, pointing towards water. The interface, which is taken along the x -axis, is perpendicular to gravity and has surface tension σ . While the interface is initially flat, at $t = 0$ the action of an impulsive conservative force perturbs the interface shape to the curve given by $y = h(x, t)$ and sets up a flow in the two fluids. This analysis is about the subsequent development of the interface shape and the accompanying flow. Figure 13.1 shows the configuration schematically. Water has density ρ_w and the air has density ρ_a . Both fluids are assumed to be inviscid and incompressible.

13.1.1 The governing equations

The equations governing the flow and interface shape are as follows. Because both the static water and uniformly flowing air initially lack vorticity, and viscosity and non-conservative forces needed for generating vorticity in the flow are absent, the flow remains irrotational in both fluids.

1. **Air:** The fluid velocity \mathbf{u}_a , the velocity potential ϕ_a and the fluid pressure p_a satisfy

$$\mathbf{u}_a = \nabla\phi_a, \quad \text{and} \quad \nabla \cdot \mathbf{u}_a = 0 \quad \rightarrow \quad \nabla^2\phi_a = 0, \quad (13.1a)$$

$$\rho_a \left(\frac{\partial\phi_a}{\partial t} + \frac{1}{2}|\nabla\phi_a|^2 \right) + p_a + \rho_a g y = c = \text{a constant}, \quad (13.1b)$$

where (13.1a) represents conservation of mass and (13.1b) conservation of momentum in the form of Bernoulli equation for unsteady potential flow, as described in (5.11) from §5.2.2.

2. **Water:** Denoting the water velocity, velocity potential and pressure by \mathbf{u}_w , ϕ_w and p_w , the equations governing its flow analogous to the ones in the air are

$$\mathbf{u}_w = \nabla\phi_w, \quad \text{and} \quad \nabla \cdot \mathbf{u}_w = 0 \quad \rightarrow \quad \nabla^2\phi_w = 0, \quad (13.2a)$$

$$\rho_w \left(\frac{\partial\phi_w}{\partial t} + \frac{1}{2}|\nabla\phi_w|^2 \right) + p_w + \rho_w g y = d = \text{another constant}. \quad (13.2b)$$

3. **Dynamic boundary condition:** At the interface, the force per unit area exerted from the two fluids must add up to the unbalanced force due to Laplace pressure (Refer to: Chapter on surface tension) on the interface. Mathematically, this amounts to the boundary condition at $y = h$ as

$$p_a = p_w + \sigma\kappa, \quad \text{where} \quad \kappa = \left(\frac{\partial^2 h / \partial x^2}{1 + (\partial h / \partial x)^2} \right) = \text{interface mean curvature}. \quad (13.3)$$

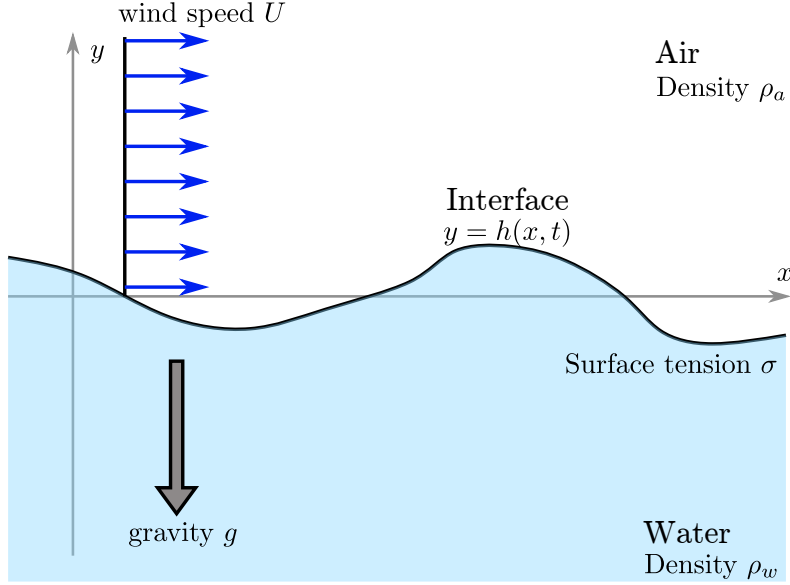


Figure 13.1: Schematic showing two infinitely deep layers of air and water with an interface.

This condition imposes momentum balance over the interface and ensures that forces are transmitted appropriately across it.

4. **Kinematic boundary condition:** The interface moves with the fluid(s) or, in other words, the interface is a “material property”. The corresponding mathematical statement is

$$\frac{D}{Dt}(h(x, t) - y) = 0.$$

When the material derivative is expanded and the velocity of the two fluids is substituted, the kinematic boundary condition becomes

$$\frac{\partial h}{\partial t} + \frac{\partial \phi_a}{\partial x} \frac{\partial h}{\partial x} = \frac{\partial \phi_a}{\partial y} \quad \text{at } y = h, \quad \text{and} \quad (13.4a)$$

$$\frac{\partial h}{\partial t} + \frac{\partial \phi_w}{\partial x} \frac{\partial h}{\partial x} = \frac{\partial \phi_w}{\partial y} \quad \text{at } y = h, \quad (13.4b)$$

where (13.4a) uses the air velocity and (13.4b) uses the water velocity.

Equations (13.1-13.4) constitute the governing equations for the air-water-interface dynamics.

13.1.2 Steady state and linearization

A trivial steady state satisfies of the governing equations:

$$\mathbf{u}_a = U\mathbf{e}_x, \quad \phi_a = Ux, \quad p_a = c - \rho_a g y - \frac{1}{2}\rho_a U^2, \quad (13.5a)$$

$$\mathbf{u}_w = \mathbf{0}, \quad \phi_w = 0, \quad p_w = d - \rho_w g y, \quad (13.5b)$$

$$h(x, t) = 0. \quad (13.5c)$$

This flow corresponds to a uniform flow in the air, no flow in the water and a flat interface. The configuration is perturbed slightly as

$$\mathbf{u}_a = U\mathbf{e}_x + \epsilon\mathbf{u}'_a, \quad \phi_a = Ux + \epsilon\phi'_a, \quad p_a = \epsilon p'_a + c - \rho_a g y - \frac{1}{2}\rho_a U^2, \quad (13.6a)$$

$$\mathbf{u}_w = \mathbf{0} + \epsilon\mathbf{u}'_w, \quad \phi_w = 0 + \epsilon\phi'_w, \quad p_w = \epsilon p'_w + d - \rho_w g y, \quad (13.6b)$$

$$h(x, t) = 0 + \epsilon h'(x, t). \quad (13.6c)$$

Here ϵ parameterizes the size of the perturbation, and the functions decorated with a prime denote a perturbation to the unprimed version of the function. This transformation of the dependent variables adds little to the analysis by itself, except when the size of the perturbation is assumed to be small. Mathematically, this assumption implies a vanishingly small ϵ and leads to the process of linearization as follows.

Substituting (13.6) in the governing equations (13.1-13.4) and canceling a factor of ϵ , and dropping the prime decoration leads to

$$\mathbf{u}_a = \nabla \phi_a, \quad \text{and} \quad \nabla \cdot \mathbf{u}_a = 0 \quad \rightarrow \quad \nabla^2 \phi_a = 0, \quad (13.7a)$$

$$\rho_a \left(\frac{\partial \phi_a}{\partial t} + U \frac{\partial \phi_a}{\partial x} + \frac{\epsilon}{2} |\nabla \phi_a|^2 \right) + p_a = 0 \quad \text{at} \quad y = \epsilon h, \quad (13.7b)$$

from (13.1),

$$\mathbf{u}_w = \nabla \phi_w, \quad \text{and} \quad \nabla \cdot \mathbf{u}_w = 0 \quad \rightarrow \quad \nabla^2 \phi_w = 0, \quad (13.8a)$$

$$\rho_w \left(\frac{\partial \phi_w}{\partial t} + \frac{\epsilon}{2} |\nabla \phi_w|^2 \right) + p_w + \rho_w g h = 0 \quad \text{at} \quad y = \epsilon h, \quad (13.8b)$$

from (13.2),

$$p_a - \rho_a g h = p_w - \rho_w g h + \sigma \frac{\partial^2 h / \partial x^2}{(1 + \epsilon^2 (\partial h / \partial x)^2)^{3/2}} \quad \text{at} \quad y = \epsilon h, \quad (13.9)$$

from (13.3), and

$$\frac{\partial h}{\partial t} + U \frac{\partial h}{\partial x} + \epsilon \frac{\partial \phi_a}{\partial x} \frac{\partial h}{\partial x} = \frac{\partial \phi_a}{\partial y} \quad \text{at} \quad y = \epsilon h, \quad \text{and} \quad (13.10a)$$

$$\frac{\partial h}{\partial t} + \epsilon \frac{\partial \phi_w}{\partial x} \frac{\partial h}{\partial x} = \frac{\partial \phi_w}{\partial y} \quad \text{at} \quad y = \epsilon h, \quad (13.10b)$$

from (13.4). Equations (13.7-13.10) are in every way equivalent to (13.1-13.4) so far. Now we apply the defining step of linearization, the limit of vanishingly small ϵ . Substituting this limit into (13.7-13.10) yields

$$\mathbf{u}_a = \nabla \phi_a, \quad \text{and} \quad \nabla \cdot \mathbf{u}_a = 0 \quad \rightarrow \quad \nabla^2 \phi_a = 0, \quad (13.11a)$$

$$\rho_a \left(\frac{\partial \phi_a}{\partial t} + U \frac{\partial \phi_a}{\partial x} \right) + p_a = 0 \quad \text{at} \quad y = 0, \quad (13.11b)$$

from (13.7),

$$\mathbf{u}_w = \nabla \phi_w, \quad \text{and} \quad \nabla \cdot \mathbf{u}_w = 0 \quad \rightarrow \quad \nabla^2 \phi_w = 0, \quad (13.12a)$$

$$\rho_w \left(\frac{\partial \phi_w}{\partial t} \right) + p_w = 0 \quad \text{at} \quad y = 0, \quad (13.12b)$$

from (13.8),

$$p_a - \rho_a g h = p_w - \rho_w g h + \sigma \frac{\partial^2 h}{\partial x^2} \quad \text{at} \quad y = 0, \quad (13.13)$$

from (13.9), and

$$\frac{\partial h}{\partial t} + U \frac{\partial h}{\partial x} = \frac{\partial \phi_a}{\partial y} \quad \text{at} \quad y = 0 \quad \text{and} \quad (13.14a)$$

$$\frac{\partial h}{\partial t} = \frac{\partial \phi_w}{\partial y} \quad \text{at} \quad y = 0, \quad (13.14b)$$

from (13.10). A defining feature of the resulting (13.11-13.14) is that they are linear in the dependent variables. Hence this process of making infinitesimally small amplitude perturbations is called linearization. Also note, how the boundary conditions are now imposed at $y = 0$ instead of the exact interface location $y = \epsilon h$.

13.1.3 Fourier transform

The most convenient way to interpret the linear equations (13.11-13.14) is to identify the directions along which translational invariance applies and perform a Fourier transform along them. In this case, the physical system

and the corresponding mathematical model given by (13.11-13.14) is translationally invariant along x (but not y because of the presence of the interface). A shift of the origin along x does not change the equations, but a shift along y does through a change in the nominal position of the interface. Thus, we will perform a Fourier transform of (13.11-13.14) along the x axis.

For this purpose, let us define the transformed variable $\hat{\phi}$ decorated by a caret for the untransformed undecorated variable ϕ

$$\hat{\phi}(k, y, t) = \frac{1}{2\pi} \int_{-\infty}^{\infty} \phi(x, y, t) e^{-ikx} dx, \quad \text{and} \quad (13.15a)$$

$$\phi(x, y, t) = \int_{-\infty}^{\infty} \hat{\phi}(k, y, t) e^{ikx} dk. \quad (13.15b)$$

Here (13.15a) is the forward Fourier transform and (13.15b) is the inverse transform. The transform is a function of the variable k , which is called the wave number. And interpretation of (13.15b) is that the function in the physical space $\phi(x, y, t)$ is being written as a linear combination of the sinusoids, i.e. e^{ikx} , of wavenumber k (equivalently wavelength $2\pi/k$) with amplitude $\hat{\phi}(k, y, t)$. Thus the forward transform (13.15a) decomposes a given function into its components and deduces the amplitude of the sinusoid with wavelength $2\pi/k$. The amplitudes are in general complex, which accounts for the sine and the cosine part of the sinusoid. However, because the variable $\phi(x, y, t)$ in the physical space is real, the Fourier transformed amplitude $\hat{\phi}(k, y, t)$ satisfies $\hat{\phi}(-k, y, t) = \hat{\phi}^*(k, y, t)$, where the asterisk denotes complex conjugation.

A property of the Fourier transform used in this analysis is the relation between the Fourier transform of functions and its derivatives. It may be readily verified using integration by parts that

$$ik\hat{\phi}(k, y, t) = \frac{1}{2\pi} \int_{-\infty}^{\infty} \frac{\partial\phi(x, y, t)}{\partial x} e^{-ikx} dx. \quad (13.16)$$

Loosely speaking, differentiation with respect to x in the real space is converted to a factor of ik in Fourier transformed space.

Fourier transform of (13.11-13.14) and dropping the caret decoration yields

$$u_a = ik\phi_a, \quad v_a = \frac{\partial\phi_a}{\partial y}, \quad \text{and} \quad iku_a + \frac{\partial v_a}{\partial y} = 0 \quad \rightarrow \quad \left(\frac{\partial^2}{\partial y^2} - k^2 \right) \phi_a = 0, \quad (13.17a)$$

$$\rho_a \left(\frac{\partial\phi_a}{\partial t} + ikU\phi_a \right) + p_a = 0 \quad \text{at} \quad y = 0, \quad (13.17b)$$

from (13.11),

$$u_w = ik\phi_w, \quad v_w = \frac{\partial\phi_w}{\partial y}, \quad \text{and} \quad iku_w + \frac{\partial v_w}{\partial y} = 0 \quad \rightarrow \quad \left(\frac{\partial^2}{\partial y^2} - k^2 \right) \phi_w = 0, \quad (13.18a)$$

$$\rho_w \frac{\partial\phi_w}{\partial t} + p_w = 0 \quad \text{at} \quad y = 0, \quad (13.18b)$$

from (13.12),

$$p_a - \rho_a g h = p_w - \rho_w h g - \sigma k^2 h \quad \text{at} \quad y = 0, \quad (13.19)$$

from (13.13), and

$$\frac{\partial h}{\partial t} + ikUh = \frac{\partial\phi_a}{\partial y} \quad \text{at} \quad y = 0 \quad \text{and} \quad (13.20a)$$

$$\frac{\partial h}{\partial t} = \frac{\partial\phi_w}{\partial y} \quad \text{at} \quad y = 0, \quad (13.20b)$$

from (13.14). Equations (13.17-13.20) are the Fourier transformed versions governing the evolution of the perturbation. Notably, the amplitudes ϕ_a , ϕ_w , p_a , p_w and h with wavenumber k evolve independently of other wavenumbers, as inferred from the fact that (13.17-13.20) do not couple the wavenumber k to any other wavenumber. This demonstrates that a sinusoidal perturbation with wavenumber k evolves in time independently of every other wavenumber that may comprise the general perturbation. Because the most general perturbation can always be decomposed into its constituent sinusoids using the Fourier transform, each wavenumber then evolved in time independently, and later recomposed using the inverse Fourier transform. Thus, it suffices to study the evolution of each wavenumber separately.

(Sinusoids are normal modes – i.e. shape functions which decouple a linear operator – for translationally invariant systems. If the system of interest is not translationally invariant, the normal modes for that system may be deduced by solving for the eigenfunctions of the underlying linear operator. Because the process of investigating the evolution of small perturbation leads to linear equations, determining normal modes of the underlying linear operators are a common operation in the analysis of waves and instabilities.)

13.1.4 Solution to Laplace equation

The solution to (13.17a) for ϕ_a and (13.18a) for ϕ_w is

$$\phi_a = Ae^{-|k|y} + Be^{|k|y} \quad \text{for } y > 0 \text{ and} \quad (13.21a)$$

$$\phi_w = Ce^{|k|y} + De^{-|k|y} \quad \text{for } y < 0, \quad (13.21b)$$

where A , B , C and D are constants of integration, themselves functions of k and t . Now we apply the conditions of stagnancy deep into the water layer, and uniform flow high up into the air layer. This implies that the perturbation to velocity perturbations decay as $|y| \rightarrow \infty$. This is achieved by setting the constants $B = D = 0$. The remaining constants A and C are determined by the boundary conditions on the interface $y = 0$. Substituting in (13.17-13.20) then yields a set of five coupled equations for A , C , p_a , p_w and h as

$$p_a = -\rho_a \left(\frac{\partial}{\partial t} + ikU \right) A, \quad (13.22a)$$

$$p_w = -\rho_w \frac{\partial C}{\partial t}, \quad (13.22b)$$

$$p_a - p_w = -(\rho_w - \rho_a)gh - \sigma k^2 h, \quad (13.22c)$$

$$\left(\frac{\partial}{\partial t} + ikU \right) h = -|k|A, \quad (13.22d)$$

$$\frac{\partial h}{\partial t} = |k|C. \quad (13.22e)$$

Eliminating all the variables in favour of h yields the master equation for our analysis

$$\rho_w \frac{\partial^2 h}{\partial t^2} + \rho_a \left(\frac{\partial}{\partial t} + ikU \right)^2 h + [(\rho_w - \rho_a)g|k| + \sigma|k|^3] h = 0. \quad (13.23)$$

Special cases of this equation demonstrate the various phenomena of waves and instabilities that interest us.

13.2 Waves and instabilities

We will start with deep water gravity waves to illustrate the solution and the use of the master equation (13.23).

13.2.1 Deep water gravity waves

Here we set the wind speed $U = 0$ and the surface tension $\sigma = 0$. Doing so reduces (13.23) to

$$\underbrace{(\rho_w + \rho_a) \frac{\partial^2 h}{\partial t^2}}_{\text{Composite inertia}} + \underbrace{(\rho_w - \rho_a)g|k|h}_{\text{gravitational restoring force}} = 0. \quad (13.24)$$

This is a second order constant coefficient ordinary differential equation, which has the solution

$$h = Ee^{i\omega t} + Fe^{-i\omega t}, \quad \text{where } \omega = \omega_{\text{grav}}(k) = \left[\left(\frac{\rho_w - \rho_a}{\rho_w + \rho_a} \right) g|k| \right]^{1/2}, \quad (13.25)$$

where E and F are constants of integration, possibly functions of k . Inverting the Fourier transform for h and restoring the prime notation from 13.6 for the perturbation yields

$$h'(x, t) = \underbrace{\int_{-\infty}^{\infty}}_{\text{linear combination}} E(k) \underbrace{e^{i(kx+\omega t)}}_{\text{backward wave}} + F(k) \underbrace{e^{i(kx-\omega t)}}_{\text{forward wave}} dk. \quad (13.26)$$

As the labels indicate, the term proportional to E and F represent backward and forward propagating sinusoidal waves, respectively, and the integral in the inverse Fourier transform may be interpreted as forming a linear combination of sinusoids with all wavenumbers. The functions $E(k)$ and $F(k)$ may be determined using knowledge of the initial conditions, say $h(x, t = 0)$ and $\frac{\partial h}{\partial t}(x, t = 0)$.

In other words, $E(k)$ and $F(k)$ are the amplitudes of the sinusoids that compose the initial condition. The sinusoids evolve independent of each other, which amounts to them propagating without changing shape. The phase speed of wave propagation $c(k)$ depends on the wavenumber and is given by

$$c_{\text{grav}}(k) = \frac{\omega(k)}{k} = \left[\left(\frac{\rho_w - \rho_a}{\rho_w + \rho_a} \right) \frac{g}{|k|} \right]^{1/2}. \quad (13.27)$$

The relation $c(k)$, or equivalently $\omega(k)$, is known as the dispersion relation because it quantifies how waves of different wavenumbers that make the initial condition disperse. At any subsequent time, the shape of the interface can be reconstructed by linearly combining the translated sinusoids. These are the dynamics of small amplitude waves, specifically in this case the deep-water gravity waves. These waves are dispersive because different wavenumbers propagate at different speeds. In particular, the phase speed decreases with increasing $|k|$, as shown in Figure 13.2.

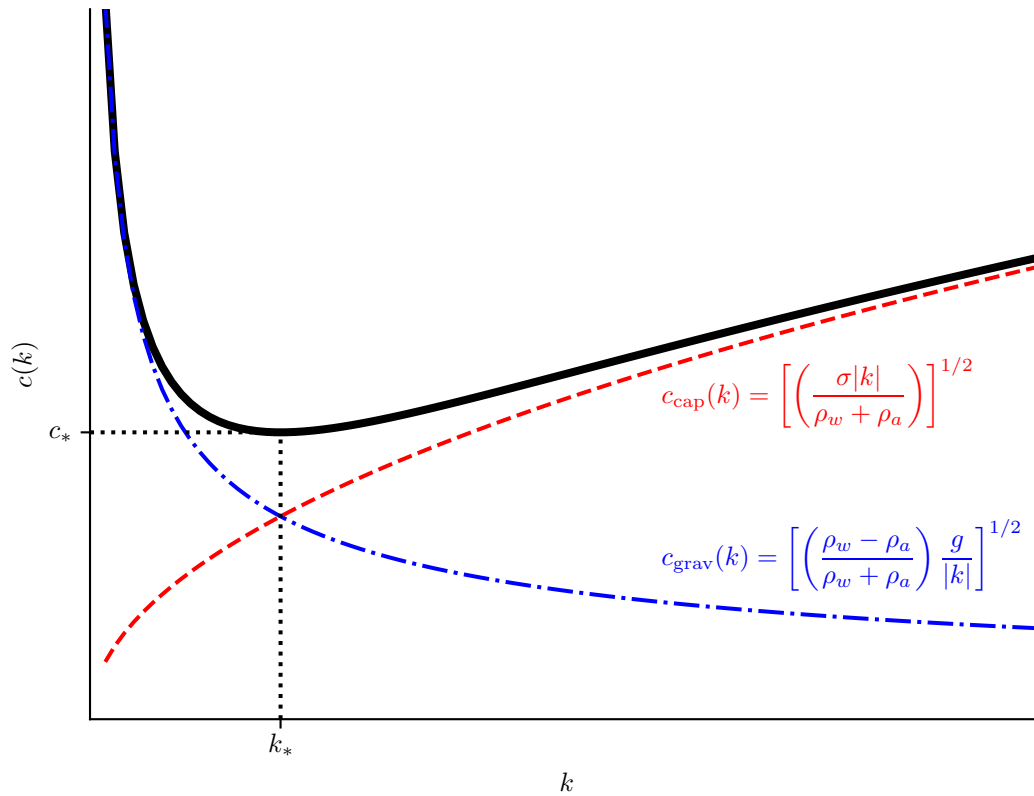


Figure 13.2: Dispersion relation for gravity, capillary and gravity-capillary waves.

A simple dimensional argument rationalizes the propagation speed of deep-water gravity waves. For a sinusoidal wave with amplitude h and wavelength $\lambda = 2\pi/k$, the excess weight of the fluid above the interface and the buoyancy below the interface (wavy shaded region in Figure 13.3) scales as $(\rho_w - \rho_a)g\lambda h$ per unit distance perpendicular to the plane of the page. This unbalanced force drives motion in the surrounding fluid, the motion permeates a distance of $\mathcal{O}(\lambda)$ perpendicular to the interface, decaying further away from it, as shown by the translucent region in Figure 13.3. Thus, the mass of the accelerated fluid scales as $(\rho_a + \rho_w)\lambda^2$ per unit width perpendicular to the plane of the page. The acceleration of this mass caused by the unbalanced force scales as h/T^2 , where T is the time-scale over which motion occurs, which is to be determined. Balancing this

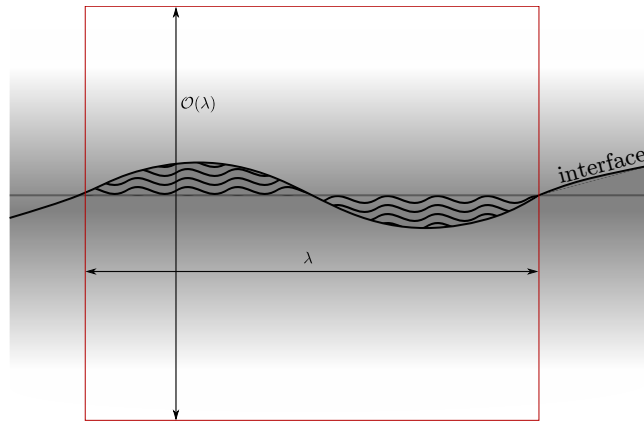


Figure 13.3: A sketch explaining the dimensional rationalization for the dispersion relation (13.27). The wavy shaded region shows the excess fluid weight or buoyant force. The extent of the motion of the fluid arising from the wave propagation is shown in red square. The motion decays away from the interface as shown by the gray shading.

mass times the acceleration with the unbalanced force yields

$$(\rho_a + \rho_w)\lambda^2 \times \frac{h}{T^2} \sim (\rho_w - \rho_a)g\lambda h \implies c \propto \frac{1}{T} \sim \left[\left(\frac{\rho_w - \rho_a}{\rho_w + \rho_a} \right) \frac{g}{\lambda} \right]^{1/2}. \quad (13.28)$$

In other words, the wave period scales inversely with $\lambda^{1/2}$ because the accelerated mass scales with λ^2 but the driving force scales proportional to λ . The dimensional dependence on the difference and sum of the density is also rationalized in this simple analysis.

13.2.2 Capillary and gravity-capillary waves

In this case, we set $U = 0$ for deep water gravity-capillary waves, and $g = 0$ in addition for capillary waves. Repeating the analysis of §13.2.1, yields

$$\omega(k) = \left[\left(\frac{(\rho_w - \rho_a)g|k| + \sigma|k|^3}{\rho_w + \rho_a} \right) \right]^{1/2} \quad \text{and} \quad c(k) = \left(\frac{(\rho_w - \rho_a)\frac{g}{|k|} + \sigma|k|}{\rho_w + \rho_a} \right)^{1/2}, \quad (13.29)$$

for the gravity-capillary waves. In the capillary limit, these expressions become

$$\omega_{\text{cap}}(k) = \left(\frac{\sigma|k|^3}{\rho_w + \rho_a} \right)^{1/2} \quad \text{and} \quad c_{\text{cap}}(k) = \left(\frac{\sigma|k|}{\rho_w + \rho_a} \right)^{1/2}. \quad (13.30)$$

A dimensional analysis interpretation of (13.30) proceeds on the same lines as the derivation of (13.28) except for the restoring force of gravity $(\rho_w - \rho_a)g\lambda$ being replaced by the Laplace pressure acting over length λ , i.e. $(\sigma h/\lambda^2) \times \lambda$. For capillary waves, the phase speed increases with the wavenumber $|k|$, as shown in Figure 13.2.

Now we turn to some salient features of gravity-capillary waves as characterized by the dispersion relation. The expressions for the phase speeds of wave propagation for gravity, capillary, and gravity-capillary waves are plotted in Figure 13.2. The combination of gravity and capillary forces acting on the interface has complementary effect on the dispersion relation for long and short waves. On the one hand, the force of capillarity is strong for short waves, i.e. waves with short wavelength corresponding to large k , and therefore the gravity-capillary dispersion relation approaches that of capillary waves in the large- k limit. In this regime, $c(k)$ increases with k . On the other hand, the gravitational restoring force dominates for long wave, i.e. waves with long wavelengths corresponding to small k , and the gravity-capillary dispersion relation approaches that of gravity waves in that limit. In this regime, $c(k)$ decreases with k . For intermediate values of k , the gravity-capillary phase speed has a minimum, which can be found by setting

$$\frac{d}{d|k|}(c(k)^2) = \frac{1}{(\rho_w + \rho_a)} \left[\sigma - \frac{(\rho_w - \rho_a)g}{|k|^2} \right] = 0 \implies |k| = k_* = \left[\frac{(\rho_w - \rho_a)g}{\sigma} \right]^{1/2}, \quad (13.31)$$

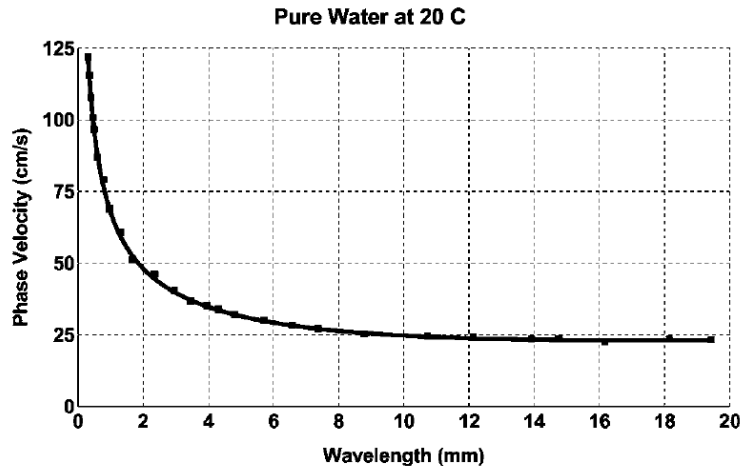


Figure 13.4: Experimentally measured dispersion relation for the air-water interface compared with theory. The black dots are experimentally measured values of phase speed of sinusoidal waves and the solid curve is from (13.29) with values substituted for the air-water interface at 20° C. Reproduced from Behroozi and Perkins, American Journal of Physics, 74(11), pp. 957-961 with the permission of the American Association of Physics Teachers.

for which

$$c(k_*) = c_* = \frac{[4(\rho_w - \rho_a)g\sigma]^{1/4}}{(\rho_w + \rho_a)^{1/2}}. \quad (13.32)$$

To get a sense of what this calculations represent, let us substitute some numbers into the expressions. The density of water $\rho_w = 10^3 \text{ kg/m}^3$ is much greater than the density of air $\rho_a = 1.2 \text{ kg/m}^3$, so $\rho_w \pm \rho_a \approx \rho_w$. Gravity $g = 9.8 \text{ m/s}^2$ and surface tension $\sigma = 72 \times 10^{-3} \text{ N/m}$. The slowest propagating wave corresponds to wavenumber

$$k_* = \left[\frac{(\rho_w - \rho_a)g}{\sigma} \right]^{1/2} \approx 368 \text{ m}^{-1}. \quad (13.33)$$

This corresponds to a wavelength of

$$\lambda_* = \frac{2\pi}{k_*} = 1.7 \text{ cm}. \quad (13.34)$$

Waves on the ocean surface with wavelength much larger than λ_* are gravity waves governed by the part of the dispersion relation that approximates (13.27), whereas waves with wavelength much shorter than λ_* are governed by (13.30) dominated by capillarity. The speed of the slowest propagating wave is

$$c_* = 23 \text{ cm/s}. \quad (13.35)$$

We shall refer to these numerical values later in this chapter.

Even though the mathematical analysis so far has been based on vanishingly small perturbation amplitude, the results of this theory apply quite well to practical situations where the amplitude of the waves is small compared to its wavelength, as shown in Figure 13.4. However, it is not merely the applicability of the analysis to the corresponding physical system that is of value, but also the fundamental concepts of wave propagation and the insight into the physical processes, which cannot be gained purely from an experimental approach. This insight ties into the subsequent analysis on instabilities and thus provides a more complete picture of the underlying physics than possible from analyses of the phenomena considered separately.

13.2.3 Rayleigh-Taylor instability

We now turn to the mechanism of overturning of the interface when the fluid above is heavier than the fluid below. The situation is analogous to balancing an inverted pendulum. While theoretically a pendulum may

be balanced in an inverted configuration by having the point of support *exactly* below the centre of gravity of the pendulum, it is practically impossible to achieve it. The smallest, even infinitesimal, perturbation from a systematic or a random source in the environment, pushes the pendulum out of balance and the ensuing dynamics naturally pushes it further away from the equilibrium. A similar dynamics occurs when attempting to balance a semi-infinite layer of heavier fluid on top of a semi-infinite layer of lighter fluid. While the governing equations allow such a static equilibrium to exist, even an infinitesimal perturbation away from this equilibrium drives the interface away from its flat shape. The resulting fluid flow causes an overturning of the interface, causing the heavier fluid to flow downwards and pushes the lighter fluid upwards. The mechanism of this dynamics is termed as the Rayleigh-Taylor instability, after Lord Rayleigh and Geoffrey Ingram Taylor, who first presented the essential aspects of the dynamics.

A simple way to represent heavy fluid on top of light is to transform $g \rightarrow -g$ and set $U = 0$ in (13.23). (Equivalently, we can switch ρ_w and ρ_a , the only parameters that depend on the fluids.)

$$(\rho_w + \rho_a) \frac{\partial^2 h}{\partial t^2} + [\sigma |k|^3 - (\rho_w - \rho_a)g|k|] h = 0. \quad (13.36)$$

The corresponding dispersion relation

$$\omega(k) = \left[\left(\frac{\sigma |k|^3 - (\rho_w - \rho_a)g|k|}{\rho_w + \rho_a} \right) \right]^{1/2} \quad \text{and} \quad c(k) = \left[\frac{\sigma |k| - (\rho_w - \rho_a) \frac{g}{|k|}}{\rho_w + \rho_a} \right]^{1/2}. \quad (13.37)$$

Equation (13.37) only differs from (13.29) by a negative sign, which changes the qualitative character of the dynamics. For short waves, $|k| > k_*$, the numerator inside the square-root for $\omega(k)$ is positive, and the wave-propagation character of the dynamics is preserved just as for gravity-capillary waves, albeit with a modified wave speed. But for long waves, $|k| < k_*$, the numerator is negative and $\omega(k)$ is purely imaginary. This implies that the oscillatory behaviour of $e^{\pm i\omega t}$ in (13.25) changes to exponential growth or decay, and the wave propagation at constant speed in (13.26) changes to exponential growth or decay of sinusoids.

We will now interpret the mathematical analysis in term of its physical mechanics. According to hydrodynamic stability theory, perturbations are unavoidable in any physical system. When such a perturbation is forced on the interface, it can be decomposed into the normal modes of the system. As described in (13.26), $\epsilon E(k)$ and $\epsilon F(k)$ are the infinitesimally small amplitudes of sinusoids with wavenumber k comprising the initial perturbation to the interface shape. Each of these modes evolve independently. If ω is purely imaginary, $e^{i\omega t}$ decays exponentially, so the sinusoid proportional to $F(k)$ decays exponentially, and thus its magnitude remains infinitesimal. But $e^{-i\omega t}$ grows exponentially, so the sinusoid proportional to $E(k)$ grows in magnitude, at least until the perturbation is no longer infinitesimal. Generically, perturbations forced randomly by the environment contain all normal modes of the system. Most of them are expected to decay, but if even a single mode grows exponentially, this growth continues until the flat interface shape is disrupted. The shape of the interface then more and more closely resembles the shape of the fastest growing mode. Therefore, the analysis of hydrodynamic stability reduces to the determination of growing normal modes.

For Rayleigh-Taylor instability, the exponential growth rate is given by

$$i\omega = \left[\left(\frac{(\rho_w - \rho_a)g|k| - \sigma |k|^3}{\rho_w + \rho_a} \right) \right]^{1/2}, \quad 0 \leq k \leq k_*. \quad (13.38)$$

The growth rate is zero at $k = 0$ and $k = k_*$, and positive in between. The growth is fastest for wavenumber given by

$$|k| = \left[\frac{(\rho_w - \rho_a)g}{3\sigma} \right]^{1/2} = \frac{k_*}{\sqrt{3}}. \quad (13.39)$$

This is the fastest growing mode.

Physically, a depression in the interface displaces heavy fluid downwards with lighter fluid surrounding it. The lighter fluid does not provide sufficient buoyancy to compensate for the weight of the heavy fluid. Similarly, if a parcel of the lighter fluid is displaced upwards, the buoyant force on it exceeds its weight. The imbalance in both these situations continues to push the heavier fluid downward and the lighter fluid upwards. For short waves, the tension in the surface provides sufficient restoring force to overcome the driving force of gravity, but the process runs away for long waves overturning the interface. The dimensional analysis version of Rayleigh-Taylor closely parallels that of gravity-capillary waves, except gravity provides a driving force destabilizing this static flat interface instead of a restoring force. This is the physical mechanism of the Rayleigh-Taylor instability.

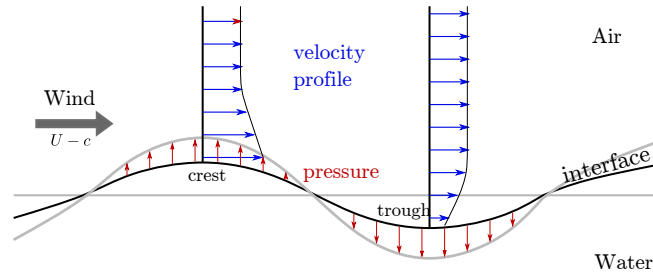


Figure 13.5: Instability mechanism for Kelvin-Helmholtz instability. In the reference frame of the wave, the wind speed is $U - c$. The air flowing over the crests speed up because it has to flow through smaller space than in the absence of the wave (blue arrows). By the Bernoulli principle, the air pressure there drops and pulls the interface further away from the flat shape (red arrows). Similarly, through the troughs, the flow slows down and the pressure rises, further pushing the troughs to become deeper.

13.2.4 Kelvin-Helmholtz instability

In this case, we restore the blowing wind and retain every variable in (13.23). The interpretation is facilitated by the substitution $(\rho_w - \rho_a)g|k| + \sigma|k|^3 = (\rho_w + \rho_a)c^2k^2$ from (13.29), which leads to the form of (13.23) as

$$\rho_w \frac{\partial^2 h}{\partial t^2} + \rho_a \left(\frac{\partial h}{\partial t} + ikU \right)^2 h + (\rho_w + \rho_a)c^2k^2 h = 0. \quad (13.40)$$

The dispersion relation for this equation is the solution of

$$\rho_w \omega^2 + \rho_a (\omega + kU)^2 = (\rho_w + \rho_a)c^2k^2. \quad (13.41)$$

This is a quadratic equation for ω , which has the solution

$$\frac{\omega}{k} = -\frac{\rho_a U}{\rho_w + \rho_a} \pm \sqrt{c^2 - \frac{U^2 \rho_w \rho_a}{(\rho_w + \rho_a)^2}}. \quad (13.42)$$

The variable ω is real for small U if discriminant inside the square-root is positive, and sinusoids propagate at a constant speed ω/k . However, for

$$U > U_{\text{cr}}(k) = (f + f^{-1})c(k), \quad f = \sqrt{\frac{\rho_w}{\rho_a}}, \quad (13.43)$$

the discriminant is negative, ω is complex, and sinusoids grow exponentially. Here $U_{\text{cr}}(k)$ is the critical wind speed, which when exceeded perturbation to the interface with wavenumber k is amplified by the wind. The smallest value for U_{cr} that leads to amplification of any wavenumber occurs for $k = k_*$, where $c(k)$ has its minimum value of c_* . This analysis makes the following physical prediction: on a windy day as the gusts pick up, the first appearance of ripples spontaneously appearing on the interface corresponds to a wavenumber $k = k_*$, wavelength $\lambda = \lambda_*$ at a wind-speed

$$U = U_{\text{cr}}(k_*) = \left(f + \frac{1}{f} \right) c_*. \quad (13.44)$$

For the air-water interface, using $\rho_a \ll \rho_w$, this speed is

$$U \approx \frac{(4\rho_w g \sigma)^{1/4}}{\rho_a^{1/2}} = 6.7 \text{ m/s}. \quad (13.45)$$

To physically understand the mechanism underlying this mathematical analysis of exponential growth, we go back to the expression for the air pressure in (13.22a) and (13.22d). Writing the air pressure in terms of interface perturbation gives

$$p_a = \frac{\rho_a}{|k|} \left(\frac{\partial}{\partial t} + ikU \right)^2 h. \quad (13.46)$$

To imagine the influence of the blowing wind on a propagating wave, we substitute $h \propto ae^{i(kx-ckt)}$ (here c is the speed of propagation of the sinusoid and a its amplitude) to yield the air pressure to be

$$p_a \propto -\rho_a |k| (U - c)^2 ae^{i(kx-ckt)}. \quad (13.47)$$

When air flows over the crests of the waves, it has to squeeze through a narrower space because of the presence of the crest, which reduces the space available for the air to flow. This results in a speeding up when flowing over the crests, as shown in Figure 13.5. Similarly, the wind slows down when flowing through the troughs, also shown in Figure 13.5. By the Bernoulli equation, the pressure is lower where the speed is faster, i.e. the crests, and higher where the speed is slower, i.e. the troughs. This influence of the air pressure out-of-phase with the waveform acts to amplify the interface waveform and drives the instability.

It so happens that the neglect of viscosity is tolerable for the waves and the Rayleigh-Taylor instability. However, the uniform wind speed violates the no-slip condition on the interface. The presence of viscosity smoothes this profile, and the effect of this modified velocity profile needs to be accounted for in the stability analysis. This is the subject for further research for the keen student.